Evidence-Based Complementary and Alternative Medicine

Conference Issue: Biomedical Informatics Research for Integrative Medicine

Lead Guest Editor: Zhaohui Liang
Guest Editors: Huiru Zheng, Guo Zheng Li, and Xiaohua Hu

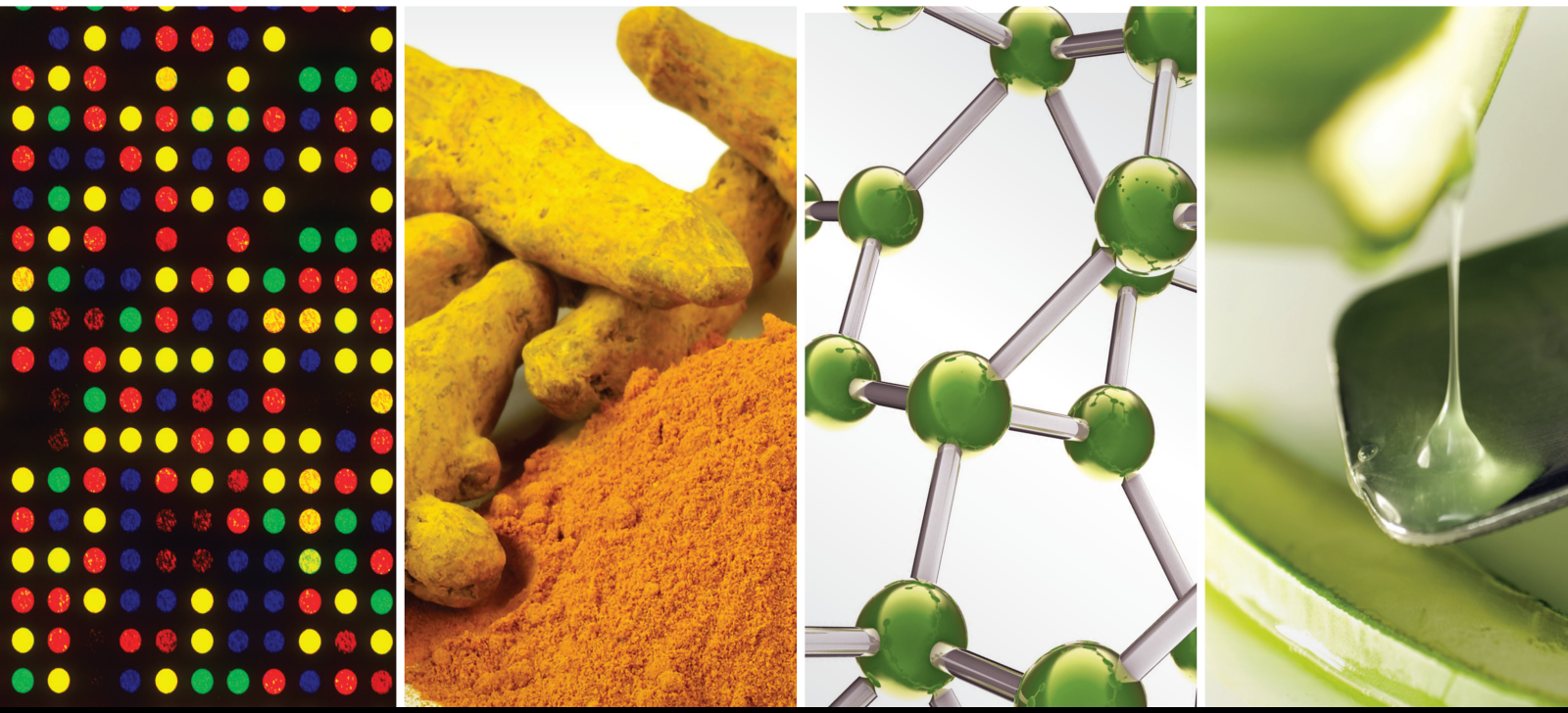

Conference Issue: Biomedical Informatics Research for Integrative Medicine

Evidence-Based Complementary and Alternative Medicine

Conference Issue: Biomedical Informatics Research for Integrative Medicine

Lead Guest Editor: Zhaohui Liang
Guest Editors: Huiru Zheng, Guo Zheng Li, and Xiaohua Hu

Chief Editor

Associate Editors

Academic Editors

Contents

Hindawi
Evidence-Based Complementary and Alternative Medicine
Volume 2022, Article ID 7303393, 7 pages
https://doi.org/10.1155/2022/7303393

Review Article

Complementary and Alternative Medicine for Long COVID: Scoping Review and Bibliometric Analysis

Tae-Hun Kim,[1] **Sae-Rom Jeon**,[1] **Jung Won Kang**,[2] **and Sunoh Kwon**[3]

[1]*Korean Medicine Clinical Trial Center, Korean Medicine Hospital, Kyung Hee University, 23 Kyungheedae-ro, Dongdaemun-gu, Seoul 02447, Republic of Korea*
[2]*Department of Acupuncture & Moxibustion, College of Korean Medicine, Kyung Hee University, 23 Kyungheedae-ro, Dongdaemun-gu, Seoul 02447, Republic of Korea*
[3]*Korean Medicine Convergence Research Division, Korea Institute of Oriental Medicine, Daejeon 34054, Republic of Korea*

Correspondence should be addressed to Sunoh Kwon; sunohkwon@kiom.re.kr

Received 3 February 2022; Accepted 1 July 2022; Published 4 August 2022

Academic Editor: Zhaohui Liang

Prolonged symptoms after the clearance of acute coronavirus disease 2019 (COVID-19) infection, termed long COVID, are an emerging threat to the post-COVID-19 era. Complementary and alternative medicine (CAM) interventions may play a significant role in the management of long COVID. The present study aimed to identify published studies on the use of CAM interventions for long COVID and provide an overview of the research status using bibliometric analysis. The present scoping review searched MEDLINE, Embase, and Cochrane Library from inception until November 2021 and identified published studies on CAM interventions for long COVID. A narrative analysis of the study types and effectiveness and safety of the CAM interventions are presented and a bibliometric analysis of citation information and references of the included publications were analyzed using the Bibliometrix package for R. An electronic database search identified 16 publications (2 clinical studies and 14 study protocols of systematic reviews or clinical studies) that were included in the present study. Dyspnea or pulmonary dysfunction, quality of life, olfactory dysfunction, and psychological symptoms after COVID-19 infection were assessed in the included publications. The two clinical studies suggested that Chinese herbal medications were effective in relieving symptoms of pulmonary dysfunction. Bibliometric analysis revealed the current trend of research publication in this area was driven by study protocols written by Chinese, Korean, and Indian authors. Thus, the present scoping review and bibliometric analysis revealed that there are few studies published about the use of CAM for long COVID and long-term management for COVID-19 survivors. Original studies on CAM interventions, including randomized controlled trials and systematic reviews, are required to actively support evidence for their use in the management of long COVID. PROSPERO registration: this trial is registered with CRD42021281526.

1. Introduction

Since the first report of the coronavirus disease 2019 case (COVID-19) in 2019, the impact of the pandemic has continued for more than 2 years worldwide. Although the number of people vaccinated has greatly increased, the number of new COVID-19 cases is still increasing due to factors, such as the delta and omicron variants [1]. However, a new health problem that is different from the acute increase of new confirmed cases is emerging, namely long COVID, which is defined as prolonged symptoms after the clearance of acute COVID-19 infection [2]. The number of patients experiencing long COVID is significant and is expected to increase as the COVID-19 pandemic continues. It is important to prepare for the post-COVID-19 era, and the healthcare strategy for long COVID patients is critical.

Several organs and systems are speculated to be involved in long COVID, and the spectrum of symptoms ranges widely, from dyspnea, sequelae of lung inflammation due to severe acute respiratory syndrome coronavirus 2 infection to "brain fog" and cognitive impairment due to chronic damage of the central nervous system [2]. The symptoms of long COVID are diverse, and the mechanisms involved remain unclear, making it difficult to establish a treatment

strategy for these patients [2]. Many countries have adopted complementary and alternative medicine (CAM) in their healthcare services during the COVID-19 pandemic [3–5], and surveys from different regions have reported a significant number of individuals using CAM interventions as a means to boost immunity and prevent acute COVID-19 infection [6, 7]. CAM interventions are expected to play a significant role in the management of long COVID. Therefore, understanding the efficacy and safety of CAM interventions is urgent and necessary for their implementation.

The present study comprised a scoping review and bibliometric analysis to explore the status of research evidence for the use of CAM interventions for long COVID. The study objectives were to identify publications and evidence for various CAM interventions for the treatment of long COVID and long-term management of survivors of COVID-19 infection. Furthermore, the current research status of long COVID was overviewed using bibliometric analysis.

2. Materials and Methods

2.1. Search and Selection of Published Articles. Core medical databases, including MEDLINE, Embase, and Cochrane Library, were searched from their inception until November 2021 to identify publications related to long COVID and long-term management using CAM interventions for COVID-19 survivors. The following PICO components were used for the literature searches:

Population: patients with long COVID symptoms, such as fatigue, mild cognitive dysfunction, anosmia, dysgeusia, and other pulmonary dysfunction or neurological or psychological problems after recovery from acute COVID-19 infection.

Intervention: any type of CAM intervention, including traditional medicine, mind-body therapy, homeopathy, and dietary supplements. Limitations were not imposed on the type of comparators and outcomes of the included publications.

Publication type: any type of publication, including systematic reviews (SRs), randomized controlled trials (RCTs), and observational studies, as well as study protocols were included for human studies.

The search strategy for each database was developed according to the specific features of each database using the keywords "CAM interventions," "long COVID," and "related symptoms" (Supplementary File 1). The titles and abstracts of the publications were independently reviewed by two authors (S-RK and T-HK), and hard copies of potential articles were assessed for selection. Decisions about selection of the publications were made in the following discussion.

2.2. Data Extraction. In the present scoping review, data of publications, including condition, type of publication, type of the study, number of patients, country of the authors, intervention types, and description of interventions (frequency, duration, potential effectiveness, and safety) were extracted from the included publications. To conduct a more productive analysis, we searched the Web of Science (WoS) database for each study which was located through MEDLINE, Embase, and Cochrane Library database searching. Bibliometric analyses were conducted by retrieving citation information and references of the included articles in the WoS database format. Citation information included keywords plus, which is a specific index term for each publication defined by the WoS [8]. Two authors (S-RK and T-HK) independently extracted data, and the third author (SOK) made a final decision about instances of disagreement.

2.3. Bibliometric Analysis. Bibliometric analyses were conducted by narratively analyzing information about the included publications. Relevant sources (journals), top 20 authors, relevant institutions, country of the corresponding author, country contribution, keywords, and title words were narratively analyzed. The current research trend was identified using a three-field plot, which links the title, authors, and country of the corresponding author in all included publications. Word cloud, which shows the most relevant keywords of the publication, was also used. Trends in publications by year of publication were not analyzed because the COVID-19 pandemic occurred after 2019. The degree of collaboration, which can be calculated as the ratio of multiauthored articles to the sum of single and multiauthored articles, was suggested for identifying how active research collaboration was during the last two years. To access the pattern of co-authorship, we calculated the co-authorship index (CAI). In addition to this, the collaborative coefficient (CC) was calculated for assessing dominant patterns of single-authored or multiauthored publications [9]. We analyzed publication data using the Bibliometrix package for *R* (version 3.1).

3. Results

3.1. Summary of the Included Publications. The electronic database searches identified 16 publications, including two clinical studies [10, 11] and 14 study protocols of SRs or clinical studies (Figure 1) [12–25]. Among the 13 published protocols, most were protocols for SRs and meta-analyses and only two were RCT protocols [15, 23]. Dyspnea or pulmonary dysfunction were the target conditions of the protocols in five publications [12, 15, 20, 23, 24], and the quality of life assessment was present in six publications [13, 16, 18, 21, 22, 25]. Olfactory dysfunction [17] or psychological symptoms [14] were assessed in one study each. Various symptoms were targeted in one publication (Table 1) [26]. Among the two clinical studies, one was a prospective case-control study [10], and the other was a single case report [11]; both assessed the clinical effects of Chinese herbal medicine (CHM) decoctions for lung inflammation. In these two studies, CHM was reported to be effective in relieving symptoms of pulmonary dysfunction in patients after COVID-19 infection [10, 11].

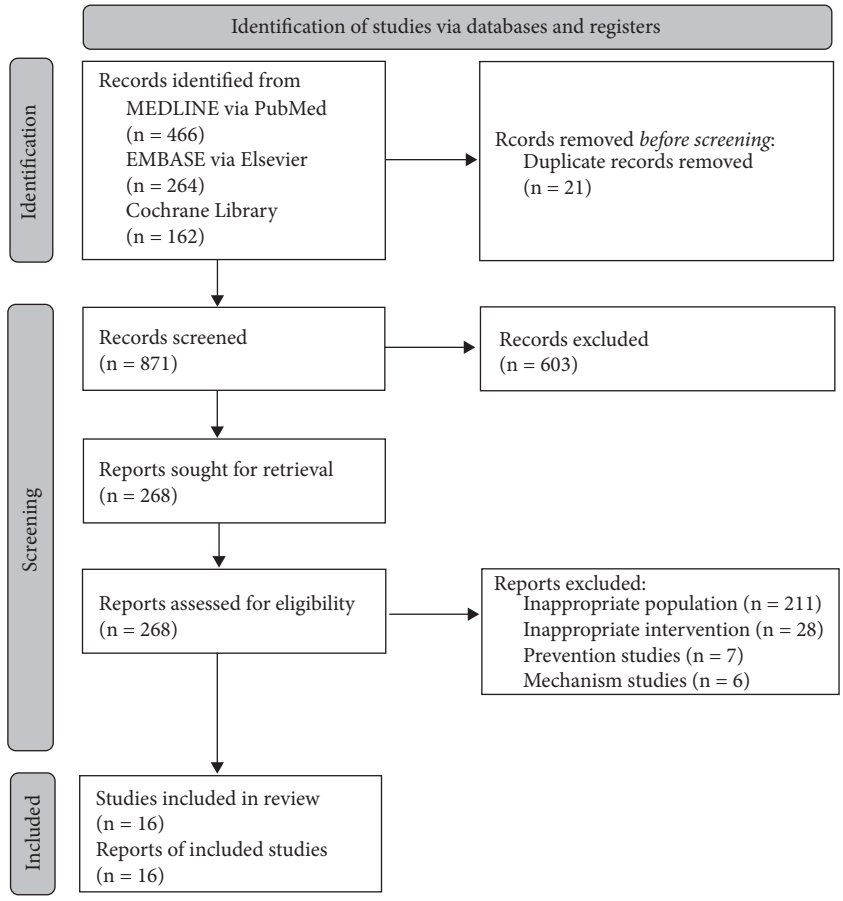

Figure 1: Study flow diagram.

3.2. Bibliometric Analysis. The 16 publications included in the analysis were published between 2020 and 2021, with an average of 0.438 years from publication as of November 2021. The average number of citations per document was 1.125. There were 33 extracted keywords plus and 42 authors' keywords. A total of 101 authors were included in all the publications, with an average of 6.31 authors per publication (Supplementary File 2). Evaluation of publication sources revealed "Medicine" as the journal most frequently published in ($n = 12$), followed by "Chinese Journal of Integrative Medicine" ($n = 1$), "Infectious Diseases of Poverty" ($n = 1$), "Journal of Integrative Medicine" ($n = 1$), and "Trials" ($n = 1$) (Supplementary File 3). The authors with the most publications were Chen Y ($n = 3$), Chi WX ($n = 3$), Luo ZY ($n = 3$), Wang LN ($n = 3$), Wen DP ($n = 3$), and Zhu XY ($n = 3$) (Table 2). The most common author affiliations were "Beijing University of Chinese Medicine" ($n = 7$), "Chengdu University of Traditional Chinese Medicine" ($n = 5$), "Capital Medical University" ($n = 4$), "Tianjin University of Traditional Chinese Medicine" ($n = 4$), "Beijing University" ($n = 3$), "Dongguk University" ($n = 3$), "Hospital of Chengdu University of Traditional Chinese Medicine" ($n = 3$), "Shandong University of Traditional Chinese Medicine" ($n = 3$), and "Shanghai University of Traditional Chinese Medicine" ($n = 3$) (Supplementary File 4). China was the most common author country, and most studies were published in China ($n = 14$), whereas the Republic of Korea and India had only one publication each (Supplementary File 5).

Analysis of the keywords revealed that "COVID-19" ($n = 10$) and "systematic review" ($n = 10$) were the most frequently used and "Tai Chi" ($n = 3$), "acupuncture" ($n = 2$), and "Traditional Chinese medicine" ($n = 2$) were the most frequently used keywords for the intervention (Supplementary File 6). Furthermore, "protocol" ($n = 13$), "review" ($n = 12$), "systematic" ($n = 12$), "COVID" ($n = 11$), "patients" ($n = 10$), and "meta-analysis" ($n = (9)$ were the most frequently used title words (Supplementary File 7). The three-field plot indicated that the current trend of research published in this area was driven by study protocols written by Chinese, Korean, and Indian authors (Supplementary File 8). Word cloud analysis showed that protocols for long COVID symptoms and CAM interventions were positioned in the center of the keywords in the included publications (Supplementary File 9).

Between 2020 and 2021, the degree of collaboration was calculated to be 1, which means that all the published articles had multiauthors and there was no single-authored article. The CAI was 100 which implied that the pattern of co-authorship of the included literature between 2020 and 2021 was similar to that of the world average. The CC was calculated to be 0.8607, which suggested that multiauthored publications were dominant in this research area.

Table 1: Summary of the included studies.

Study ID	Target condition or outcomes	Type of the study (review, RCT, observational study, case report)	Number of patients	Country	Intervention type	Frequency and duration of the treatment	Summary of the effectiveness (quote)	Summary of the safety (quote)
					Clinical studies			
Li et al. [10]	Lung inflammation after COVID-19 infection	Prospective case-control study	96 (CM: 64/control: 32)	China	CHM decoction	CHM decoction 150 ml twice a day for 28 days	"Patients with COVID-19 in convalescence had symptoms and lung inflammation after hospital discharge and recovered with time prolonging. CM could improve lung inflammation for early recovery."	NR
Zhi et al. [11]	Lung inflammation and pulmonary fibrosis after COVID-19 infection	Case report	1 case	China	CHM decoction	CHM decoction 150 ml three times a day for one month	"After one-month of oral treatment with traditional Chinese medicine decoction, without using other drugs, the lung inflammatory exudate, pulmonary fibrosis, and the quality of life of a 61-year-old female patient with coronavirus disease 2019 (COVID-19) were significantly improved."	No adverse events occurred
					Study protocols			
Chi et al. [12]	Dyspnea after ventilator weaning in the patients recovering from COVID-19 infection	Protocol for the systematic review and meta-analysis	NA	China	Acupuncture	NR	NA	NA
Ding et al. [13]	Quality of life in the patients recovering from COVID-19 infection	Protocol for the systematic review and meta-analysis	NA	China	Dance-based mind-motor activities including Tai chi, Baduanjin, Qigong, Yijinjing, Daoyin, and Tango dance program	NR	NA	NA
Kim et al. [14]	Psychological sequelae in the patients recovering from COVID-19 infection	Protocol for systematic review and meta-analysis	NA	Republic of Korea	THM	NR	NA	NA
Lu et al. [15]	Pulmonary fibrosis in the patients recovering from COVID-19 infection	Protocol for RCT	514 (TCM: 257/ Placebo: 257)	China	TCM herbal granule	TCM herbal granule three times a day for 12 months	NA	NA
Luo et al. [16]	Quality of life in the elderly patients recovering from COVID-19 infection	Protocol for the systematic review and meta-analysis	NA	China	Tai Chi such as Yang's Tai Chi, Chen's Tai Chi and other types of Tai Chi	NR	NA	NA

Table 1: Continued.

Study ID	Target condition or outcomes	Type of the study (review, RCT, observational study, case report)	Number of patients	Country	Intervention type	Frequency and duration of the treatment	Summary of the effectiveness (quote)	Summary of the safety (quote)
Ma et al. [17]	Olfactory dysfunction induced by viral infection	Protocol for the systematic review and meta-analysis	NA	China	TCM interventions including TCM decoction, acupuncture, moxibustion, massage and cupping	NR	NA	NA
Ma et al. [18]	Quality of life in the patients recovering from COVID-19 infection	Protocol for the systematic review and meta-analysis	NA	China	Baduanjin exercise	NR	NA	NA
Shi et al. [19]	Various symptoms in the patients recovering from COVID-19 infection	Protocol for the systematic review and meta-analysis	NA	China	Tai Chi	NR	NA	NA
Sun et al. [20]	Lung ventilation function in the patients recovering from COVID-19 infection	Protocol for the systematic review and meta-analysis	NA	China	CHM	NR	NA	NA
Wang et al. [21]	Quality of life in the patients recovering from COVID-19 infection	Protocol for the systematic review and meta-analysis	NA	China	Meditative movements such as Tai Chi or qigong or Tai Chi combined with qigong or yoga	NR	NA	NA
Wen et al. [25]	Quality of life in the patients recovering from COVID-19 infection	Protocol for the systematic review and meta-analysis	NA	China	Acupuncture	NR	NA	NA
Wu et al. [22]	Quality of life in the patients recovering from COVID-19 infection	Protocol for the systematic review and meta-analysis	NA	China	Massage including tuina and manipulation	NR	NA	NA
Yadav et al. [23]	Pulmonary function in the patients recovering from COVID-19 infection	Protocol for RCT	110 (55/55)	India	Ayurveda and yoga	Ayurveda interventions including Agastya Haritaki 6 g and Ashwagandha tablet 500 mg twice daily and two sessions of yoga (morning 30 minutes and evening 15 minutes) daily for 90 days	NA	NA
Zhu et al. [24]	Pulmonary function in the patients recovering from COVID-19 infection	Protocol for the systematic review and meta-analysis	NA	China	Tai Chi such as Yang's Tai Chi, Chen's Tai Chi and other types of Tai Chi	NR	NA	NA

CHM: Chinese herbal medicine; NA: not applicable; NR: not reported; RCT: randomized controlled trial; TCM: traditional Chinese medicine; THM: traditional herbal medicine.

Table 2: Top 20 relevant authors.

Authors	Articles
CHEN Y	3
CHI WX	3
LUO ZY	3
WANG LN	3
WEN DP	3
ZHU XY	3
DONG YT	2
HUANG J	2
LI HY	2
LI L	2
WU L	2
ZHANG J	2
ZHANG Y	2
CHEN H	1
CHEN HJ	1
CHEN XC	1
CHENG PY	1
CHENG XX	1
CHOI J	1
DAI SX	1

4. Discussion

The present scoping review and bibliometric analysis revealed a lack of published studies about use of CAM on long COVID and long-term management of COVID-19 survivors. Only 16 publications were available, including two observational studies that examined the effects of CHM treatment for recovery from lung inflammation after acute COVID-19 infection and 14 protocols for RCTs and SRs. In addition, the clinical effectiveness of CHM decoctions for lung inflammation was found to be suggested as limited evidence. Most prevalent and severe long COVID symptoms including brain fog, fatigue, and olfactory dysfunctions were not tested or were not evaluated, which suggested that urgent evaluation would be necessary for this area. From the bibliometric analysis, we found that China was the most active country where most research literature has been published already. The most frequently published journal was "Medicine," which may be because it publishes original research protocols. Several indicators for co-authorship suggested that multiauthored publication was dominant between 2020 and 2021. Frequently tested interventions were CHM, acupuncture, and Tai Chi. These results indicate that research on CAM interventions for long COVID by Chinese researchers has focused on TCM interventions. Furthermore, pulmonary rehabilitation and improvement of quality of life were reported to be the main target of the CAM interventions assessed in these publications. In addition to this, the current research trend in this area was mainly driven by Chinese, Korean, and Indian authors, and the main publication types were protocols of RCTs or SRs for long COVID symptoms. This suggests that more time will be required until the evidence for CAM treatments to handle these long COVID symptoms to be prepared.

The present study has some limitations. First, only a small number of publications are currently available; therefore, any evidence for the effectiveness and safety of CAM interventions for long COVID cannot be suggested in the present study. Long COVID includes a range of symptoms; however, the publications included in the present study only covered a limited number of symptoms. RCTs and SRs for various symptoms of long COVID are required in the future. Second, most of the publications used protocols that may reflect the current research status. However, we did not assess the registry for clinical trials and SRs, which contained research protocols. The primary objectives of the present study were to assess the publication status of this research area and conduct a bibliometric analysis; therefore, we did not include a search of the registries. Future studies should include clinical trials and SR registries to include more diverse studies. Third, there could be publication bias due to the limited searching strategy of this study. We only assessed core databases, and there may be more studies that have been published in local databases. These points need to be considered when interpreting the results of our study.

Long COVID is an emerging health problem, and the socioeconomic burden of this condition is expected to be severe [2]. Therefore, an appropriate therapeutic plan needs to be prepared for the post-COVID-19 era. The use of CAM interventions for various diseases and conditions is increasing worldwide; however, the evidence supporting their appropriate use remains insufficient [27]. As COVID-19 and long COVID are new health problems, there is a lack of evidence in the field of CAM. Considering that CAM interventions are expected to be used frequently for long COVID, the substantial gap between knowledge and practice should be resolved through rigorous clinical studies and RCTs.

In conclusion, there is a lack of published studies about the effectiveness and safety of CAM interventions for long COVID. Original studies on CAM interventions, including RCTs and SRs, are required in the future to provide evidence for their use in this condition.

Data Availability

All data of this study are included in the appendix file.

Conflicts of Interest

The authors declare that there are no conflicts of interest regarding the publication of this article.

Authors' Contributions

T-HK, S-RJ, SK, and JWK conceived the study design. T-HK, S-RJ, SK, and JWK conducted the literature searching and bibliometric analysis. T-HK, S-RJ, SK, and JWK wrote the final draft of this manuscript.

Acknowledgments

This study was supported by the Korea Institute of Oriental Medicine (KSN2022220).

Supplementary Materials

Supplementary file 1. Search strategies used in each database. *Supplementary file 2.* The main information of the included publications. *Supplementary file 3.* Most relevant sources (journals). *Supplementary file 4.* Most relevant affiliations of the authors. *Supplementary file 5.* Country scientific contribution. *Supplementary file 6.* Authors' keywords which were used in more than two articles. *Supplementary file 7.* Words of titles which were used in more than two articles. *Supplementary file 8.* Three field plots (title-author-country). *Supplementary file 9.* Word cloud. (*Supplementary Materials*)

References

[1] WHO, "Coronavirus (COVID-19) Dashboard," 2022, https://covid19.who.int, lastly.

[2] H. Crook, S. Raza, J. Nowell, M. Young, and P. Edison, "Long covid-mechanisms, risk factors, and management," *BMJ*, vol. 374, 2021.

[3] B.-J. Lee, J. A. Lee, K.-I. Kim, J.-Y. Choi, and H.-J. Jung, "A consensus guideline of herbal medicine for coronavirus disease 2019," *Integrative Medicine Research*, vol. 9, no. 3, Article ID 100470, 2019.

[4] N. Liang, Y. Ma, J. Wang et al., "Traditional Chinese Medicine guidelines for coronavirus disease 2019," *Journal of Traditional Chinese Medicine*, vol. 40, no. 6, pp. 891–896, 2020.

[5] R. D. Pandit and R. K. Singh, "COVID-19 Ayurveda treatment protocol of governments of Nepal and India: a review and perspective," *Applied Science and Technology Annals*, vol. 1, no. 1, pp. 72–80, 2020.

[6] A. A. Alotiby and L. N. Al-Harbi, "Prevalence of using herbs and natural products as a protective measure during the COVID-19 pandemic among the Saudi population: an online cross-sectional survey," *Saudi Pharmaceutical Journal*, vol. 29, no. 5, pp. 410–417, 2021.

[7] J. Green, J. Huberty, M. Puzia, and C. Stecher, "The effect of meditation and physical activity on the mental health impact of COVID-19-related stress and attention to news among mobile app users in the United States: cross-sectional survey," *JMIR Mental Health*, vol. 8, no. 4, Article ID e28479, 2021.

[8] M. Aria and C. Cuccurullo, "Bibliometrix: an R-tool for comprehensive science mapping analysis," *Journal of Informetrics*, vol. 11, no. 4, pp. 959–975, 2017.

[9] B. Elango, "A Bibliometric analysis of authorship and collaboration trend in nature nanotechnology," *Journal of Applied Informatics and Technology*, vol. 1, no. 1, pp. 56–63, 2018.

[10] L. Li, C.-Y. Gou, X.-M. Li et al., "Effects of Chinese medicine on symptoms, syndrome evolution, and lung inflammation absorption in COVID-19 convalescent patients during 84-day follow-up after hospital discharge: a prospective cohort and nested case-control study," *Chinese Journal of Integrative Medicine*, vol. 27, no. 4, pp. 245–251, 2021.

[11] N. Zhi, Q. Mo, S. Yang et al., "Treatment of pulmonary fibrosis in one convalescent patient with corona virus disease 2019 by oral traditional Chinese medicine decoction: a case report," *Journal of Integrative Medicine*, vol. 19, no. 2, pp. 185–190, 2021.

[12] W. Chi, Y. Chen, L. Wang, Z. Luo, Y. Zhang, and X. Zhu, "Acupuncture for COVID-19 patient after ventilator weaning," *Medicine*, vol. 99, no. 50, Article ID e23602, 2020.

[13] Y. Ding, C. Guo, S. Yu et al., "The effect of dance-based mind-motor activities on the quality of life in the patients recovering from COVID-19," *Medicine*, vol. 100, no. 11, Article ID e25102, 2021.

[14] E. Kim, J. Choi, S. Y. Min, J. H. Kim, and A. Jeong, "Efficacy of traditional herbal medicine for psychological sequelae in COVID-19 survivors," *Medicine*, vol. 100, no. 20, Article ID e25609, 2021.

[15] Z. H Lu, C. L. Yang, G. G. Yang et al., "Efficacy of the combination of modern medicine and traditional Chinese medicine in pulmonary fibrosis arising as a sequelae in convalescent COVID-19 patients: a randomized multicenter trial," *Infectious Diseases of Poverty*, vol. 10, no. 1, 2021.

[16] Z. Luo, Y. Chen, L. Wang, W. Chi, X. Cheng, and X. Zhu, "The effect of Tai Chi on the quality of life in the elderly patients recovering from coronavirus disease 2019," *Medicine*, vol. 99, no. 49, Article ID e23509, 2020.

[17] F. Ma, H. Zhang, B. Li et al., "The effect of traditional Chinese medicine treatment for post-viral olfactory dysfunction," *Medicine*, vol. 100, no. 16, Article ID e25536, 2021.

[18] Q. Ma, Z. Yang, F. Zhu, H. Chen, H. Yang, and S. Wang, "The effect of Baduanjin exercise on the quality of life in patients recovering from COVID-19," *Medicine*, vol. 99, no. 37, Article ID e22229, 2020.

[19] Y. Shi, D. Wen, H. Wang et al., "Tai Chi for coronavirus disease 2019 in recovery period," *Medicine*, vol. 99, no. 32, Article ID e21459, 2020.

[20] Y. M. Sun, J.-Y. Liu, R. Sun, J. Zhang, M.-L. Xiao, and G.-P. Li, "The long-term consequences of Corona Virus Disease 2019 patients receiving Chinese herbal medicine treatments in acute phase," *Medicine*, vol. 100, no. 29, Article ID e26677, 2021.

[21] Y. Wang, G. Luo, M. Shen et al., "The effect of meditative movement on the quality of life in patients recovering from COVID-19," *Medicine*, vol. 99, no. 47, Article ID e23225, 2020.

[22] L. Wu, Y. Dong, J. Li et al., "The effect of massage on the quality of life in patients recovering from COVID-19: a systematic review protocol," *Medicine (Baltimore)*, vol. 99, 2020.

[23] B. Yadav, A. Rai, P. S. Mundada et al., "Safety and efficacy of Ayurvedic interventions and Yoga on long term effects of COVID-19: a structured summary of a study protocol for a randomized controlled trial," *Trials*, vol. 22, 2021.

[24] X. Zhu, Z. Luo, Y. Chen et al., "Tai Chi for the elderly patients with COVID-19 in recovery period," *Medicine*, vol. 100, no. 3, Article ID e24111, 2021.

[25] D. Wen, L. Wu, Y. Dong et al., "The effect of acupuncture on the quality of life of patients recovering from COVID-19," *Medicine*, vol. 99, no. 30, Article ID e20780, 2020.

[26] S. Shi, F. Wang, J. Li et al., "The effect of Chinese herbal medicine on digestive system and liver functions should not be neglected in COVID-19: an updated systematic review and meta-analysis," *IUBMB Life*, vol. 73, no. 5, pp. 739–760, 2021.

[27] F. H. Fischer, G. Lewith, C. M. Witt et al., "High prevalence but limited evidence in complementary and alternative medicine: guidelines for future research," *BMC Complementary and Alternative Medicine*, vol. 14, no. 1, 2014.

Hindawi
Evidence-Based Complementary and Alternative Medicine
Volume 2022, Article ID 4172531, 18 pages
https://doi.org/10.1155/2022/4172531

Research Article

Comprehensive Computational Analysis of Honokiol Targets for Cell Cycle Inhibition and Immunotherapy in Metastatic Breast Cancer Stem Cells

Skolastika Skolastika,[1] **Naufa Hanif**,[2] **Muthi Ikawati**,[1,2] **and Adam Hermawan**[1,2]

[1]*Laboratory of Macromolecular Engineering, Department of Pharmaceutical Chemistry, Faculty of Pharmacy, Universitas Gadjah Mada Sekip Utara II, 55281 Yogyakarta, Indonesia*
[2]*Cancer Chemoprevention Research Center, Faculty of Pharmacy, Universitas Gadjah Mada Sekip Utara II, 55281 Yogyakarta, Indonesia*

Correspondence should be addressed to Adam Hermawan; adam_apt@ugm.ac.id

Received 19 January 2022; Accepted 12 April 2022; Published 8 July 2022

Academic Editor: Zhaohui Liang

Breast cancer stem cells (BCSCs) play a critical role in chemoresistance, metastasis, and poor prognosis of breast cancer. BCSCs are mostly dormant, and therefore, activating them and modulating the cell cycle are important for successful therapy against BCSCs. The tumor microenvironment (TME) promotes BCSC survival and cancer progression, and targeting the TME can aid in successful immunotherapy. Honokiol (HNK), a bioactive polyphenol isolated from the bark and seed pods of *Magnolia spp*., is known to exert anticancer effects, such as inducing cell cycle arrest, inhibiting metastasis, and overcoming immunotherapy resistance in breast cancer cells. However, the molecular mechanisms of action of HNK in BCSCs, as well as its effects on the cell cycle, remain unclear. This study aimed to explore the potential targets and molecular mechanisms of HNK on metastatic BCSC (mBCSC)-cell cycle arrest and the impact of the TME. Using bioinformatics analyses, we predicted HNK protein targets from several databases and retrieved the genes differentially expressed in mBCSCs from the GEO database. The intersection between the differentially expressed genes (DEGs) and the HNK-targets was determined using a Venn diagram, and the results were analyzed using a protein-protein interaction network, hub gene selection, gene ontology and Kyoto Encyclopedia of Genes and Genomes pathway enrichment analyses, genetic alteration analysis, survival rate, and immune cell infiltration levels. Finally, the interaction between HNK and two HNK-targets regulating the cell cycle was analyzed using molecular docking analysis. The identified potential therapeutic targets of HNK (PTTH) included *CCND1*, *SIRT2*, *AURKB*, *VEGFA*, *HDAC1*, *CASP9*, *HSP90AA1*, and *HSP90AB1*, which can potentially inhibit the cell cycle of mBCSCs. Moreover, our results showed that PTTH could modulate the PI3K/Akt/mTOR and HIF1/NFkB/pathways. Overall, these findings highlight the potential of HNK as an immunotherapeutic agent for mBCSCs by modulating the tumor immune environment.

1. Introduction

Breast cancer was the most prevalent cancer in 2020 (in terms of new cases) and the leading cause of cancer-related deaths among females [1]. According to the World Health Organization, breast cancer has the highest incidence rate in Indonesia, with a mortality rate of 22,692 cases per year [1]. By 2040, the incidence is predicted to reach 89,512 cases [1]. Chemotherapy, along with surgery, radiation, and mastectomy, is the most common treatment [2]. Chemoresistance, or the insensitivity of cancer cells to drug therapy, is a major factor in the failure of chemotherapy against breast cancer.

Breast cancer stem cells (BCSCs) are one of the main factors driving chemoresistance, thereby contributing to poor prognosis and clinical outcomes [3–5]. BCSCs can develop into many cell types and repopulate heterogeneous tumors following conventional chemotherapy or

radiotherapy [4, 6]. BCSCs are mostly dormant and therefore activating dormant cells, and modulating the cell cycle is important for achieving successful BCSCs therapy [7]. Recurrent tumors are highly aggressive, potentially cross-drug resistant, highly metastatic, and have a poor prognosis. A previous study demonstrated that immune cells such as CD8+ lymphocytes induce epithelial to mesenchymal transition of BCSCs [8] Moreover, the tumor microenvironment (TME) promotes BCSC survival and cancer progression [9], and hence it can prevent the success of immunotherapy [10] The use of combination therapy, in which both chemotherapy and natural compounds are used to target metastatic BCSCs (mBCSCs), could be a successful approach to overcome chemoresistance and achieve clinical success in treating breast cancer.

Honokiol (HNK; 3,5-di-(2-propenyl)-1,1′-biphenyl-2,2′-diol, Figure 1(a)) is a bioactive polyphenol isolated from the bark and seed pods of *Magnolia spp*., that is widely used in traditional Asian medicine [11]. HNK controls various intracellular signaling pathways involved in cancer, including those related to nuclear factor kappa B (NF-κB), signal transducers and activators of transcription 3 (STAT3), epidermal growth factor receptor (EGFR), and mammalian targets of rapamycin (mTOR) [12]. HNK-mediated cell cycle arrest is achieved via the downregulation of cyclin D1, an inhibition of cyclin E1, cyclin-dependent kinase 2, cyclin-dependent kinase 4, cMYC, and RB, CSK/EGFR signaling, and the upregulation of p27 and p21 [13, 14]. HNK has shown to inhibit matrix metalloproteinases, thereby reducing cell migration, invasion, and metastasis, while also regulating VEGFR signally, exerting an anti-angiogenic effect [15, 16]. In addition, HNK has been reported to successfully inhibit the pluripotency factors POU5F1, Nanog, and SOX2, and to abolish the BCSC-like phenotype [17–20] (p11). Moreover, HNK decreases drug resistance by inhibiting P-gp regulation and by enhancing apoptosis [21]. In addition, HNK also inhibits the PI3K/mTOR pathway, contributing to circumventing immunotherapeutic resistance in glioma and breast cancer cells [22]. Even though increasing research has evaluated the effects of HNK in the cell cycle, BCSCs, and metastasis, the molecular mechanisms underlying its effects on metastatic BCSC cell cycle axis and immunotherapy have not been elucidated.

This study aimed to explore the molecular mechanisms underlying HNK-mediated mBCSC-cell cycle arrest, as well as to assess the impact of this compound on the immune environment using bioinformatics studies.

2. Materials and Methods

2.1. Data Collection and Differentially Expressed Genes' (DEGs) Identification. Proteins that interact with HNK were searched using STITCH (https://stitch.embl.de), [23]. Swisstargetprediction (https://www.swisstargetprediction.ch), [24] canSAR Black (https://cansarblack.icr.ac.uk/) [25], and SEA (https://sea.bkslab.org/) [26]. The retrieved proteins were considered as HNK-mediated proteins (HMPs) and were included in the subsequent analyses. The microarray data of metastatic breast cancer stem cells were collected from the GEO database (https://www.ncbi.nlm.nih.gov/geo) using keywords such as metastatic breast cancer stem cells, and *Homo sapiens*. The inclusion criteria were: use of patient samples or patient-derived xenografts; focus on metastatic breast cancer; characterization of breast cancer stem cells; and clear description of the identity of samples in the GSE datasets. The exclusion criteria included: use of breast cancer cell lines; no emphasis on metastatic breast cancer; no characterization of breast cancer stem cells; and ambiguity around the identity of samples in the GSE datasets. One GSE Dataset (GSE151191) was selected among the 62 datasets for this study (Supplementary Figure 1). GEO2R, a web-based interactive program (https://www.ncbi.nlm.nih.gov/geo/geo2r) that compares two groups of samples under the same conditions, was used to identify the DEGs between primary and metastatic tumors, on the basis of the following criteria for significance: $P < 0.05$ and log | Fold Change| > 1. Using [27], the overlapping proteins between the HMP and those encoded by the DEGs were identified and further analyzed using a protein-protein interaction (PPI) network.

2.2. Construction of the PPI Network. The PPI was constructed and displayed using STRING-DB v11.0 and Cytoscape software, respectively [28, 29]. Proteins included in the top-10 rank according to the Maximal Clique Centrality (MCC) score determined by the Cyto-Hubba plugin were considered hub genes [30].

The hub genes were subjected to GO and KEGG enrichment analyses using the tools [31] and WebGestalt [32]. Statistical significance was set at $P < 0.05$.

2.3. Genetic Alterations Analysis. The proteins nominated by GO and KEGG enrichment analyses and an in-depth literature study on the hub genes were used to determine the potential therapeutic targets of HNK (PTTH). In this study, genes encoding PTTH such as *CCND1*, *SIRT2*, *AURKB*, *VEGFA*, *HDAC1*, *CASP9*, *HSP90AA1*, and *HSP90AB1* were screened for genetic changes in all breast cancer studies available in the cBio-portal database ((https://www.cbioportal.org) [33]. The studies with the highest number of genetic changes were selected for analysis further connectivity.

2.4. Survival Rate and Immune Cell Infiltration Level. The online database Gene Expression Profiling Interactive Analysis (GEPIA, https://gepia.cancer-pku.cn) was utilized to analyze the contribution of PTTH to the overall survival (OS) [34]. Tumor Immune Estimation Resource (TIMER) (https://cistrome.shinyapps.io/timer/) was used to analyze the correlation between PTTH expression levels and immune cell infiltration level [35].

2.5. Validation of the mRNA and Protein Expression Levels of PTTH. The mRNA and protein expression levels of PTTH were determined using TNMPlot and Human Protein Atlas

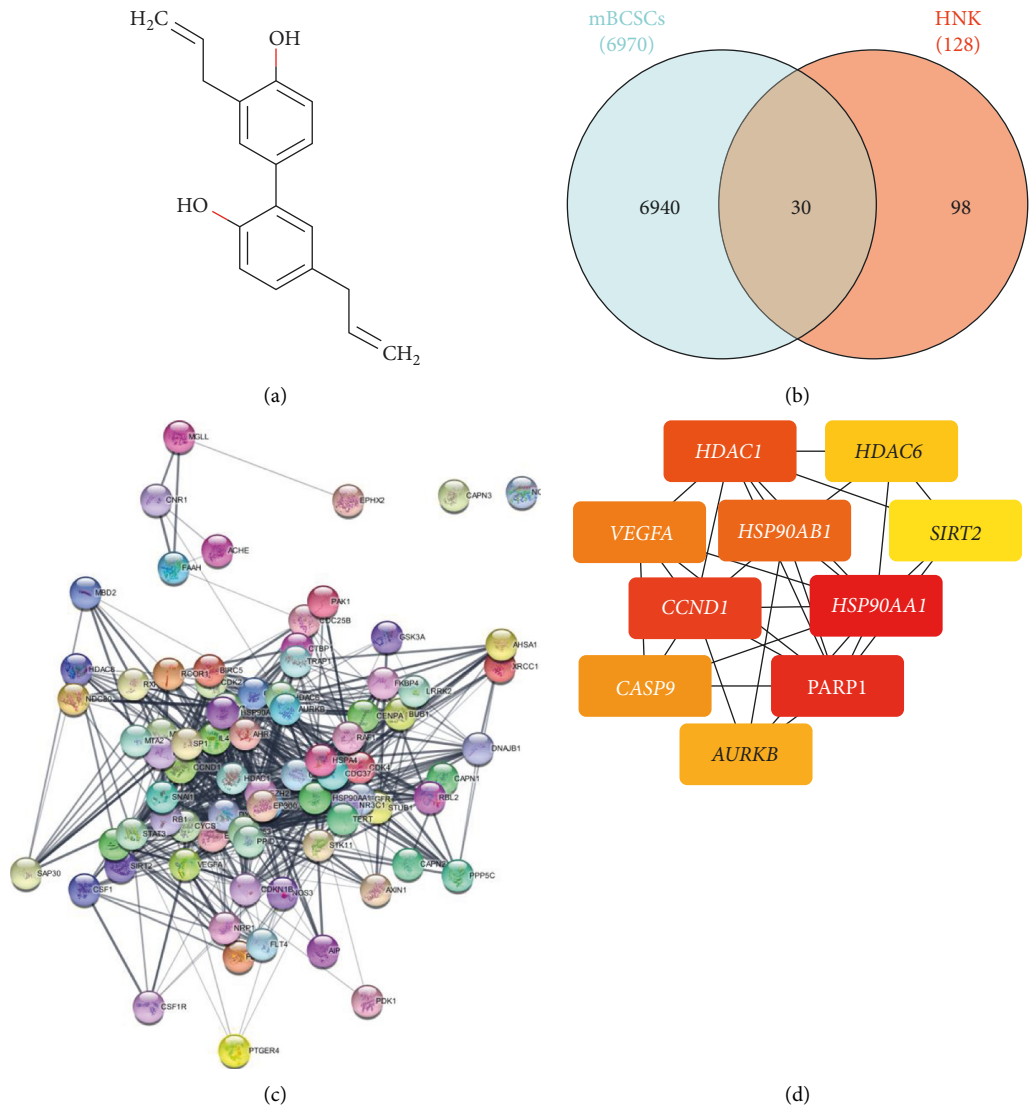

FIGURE 1: (a) Structure of honokiol. (b) Venn diagram of potential therapeutic targets of honokiol (PTTH) in breast cancer stem cells (BCSCs). (c) Protein-protein interaction (PPI) network of honokiol and the interacting proteins. (d) Top-10 hub genes determined according to the Maximal Clique Centrality (MCC) score.

(HPA). Differentially expressed genes and mRNA levels in tumor, normal, and metastatic tissues were analyzed using TNMplot (https://www.tnmplot.com/) [36], in which the database utilized data from GEO or RNA-seq libraries from The Cancer Genome Atlas (TCGA), Therapeutically Applicable Research to Generate Effective Treatments (TARGET), and The Genotype-Tissue Expression (GTEx). The protein expression levels were analyzed using the Human Protein Atlas (HPA) (https://www.proteinatlas.org/) [37], an online database that contains a wide range of transcriptomic and proteomic data from various tissues and cells.

2.6. Molecular Docking. To predict the binding properties of HNK to AURKB and RAC-1 through molecular docking, computational prediction was conducted on a Windows 10 operating system, Intel Core (TM) i5-10th Gen with 8 GB of RAM. MOE 2010 (licensed from Faculty of Pharmacy UGM) was used for docking simulation, RMSD-docking score calculation, and visualization interaction. The PDB IDs of the proteins AURKB and RAC-1 (3ZCW and 3TH5, respectively) were searched for in https://rcsb.org. The HNK structure was obtained from PubChem, subjected to conformational search, and minimized in the MOE using Energy Minimize Menu. For the docking simulation setting, London dG was used for both Rescoring 1 and Rescoring 2. Triangle Matcher was used for score function and placement setting, and Forcefield was used to refine the docking results from 30 retained settings. The results of this method will determine which conformation has the lowest binding interaction between the ligand and its receptor.

3. Results

3.1. DEG and HMP Identification. The DEGs are considered to be the molecular drivers and/or molecular biomarkers of

various phenotypes [38]. The identification of DEGs was carried out to determine the genes that act as biomolecular markers of metastatic breast cancer stem cells (mBCSCs). In total, 6,970 DEGs in the GSE 151191 dataset were found to be up/downregulated in metastatic breast cancer stem cells, according to the adjusted P value of <0.05, and a $|\log FC| \geq 1.0$ (Supplementary Table 1). Subsequently, proteins that interact directly and/or indirectly with HNK, referred to as HMPs, were identified. A total of 128 HMPs were retrieved from Swisstargetprediction, STITCH, canSAR Black, and SEA (Supplementary Table 2). Finally, 30 overlapping genes (OGs), including 18 upregulated and 12 downregulated genes, were identified to be both HMP and DEGs (Figure 1(b); Table 1).

3.2. PPI Network. To deepen our understanding of the interactions between the 30 OGs, we constructed a PPI network. The network contained 40 nodes and 134 edges, with an average node degree of 6.7, an average local clustering coefficient of 0.618, and a PPI enrichment value < 1.0e-16 (Figure 1(c)). Further analysis identified hub genes within the PPI network (Figure 1(d)), which included NAD-dependent deacetylase sirtuin 2 (SIRT2), cyclin D1 (CCND1), serine/threonine-protein kinase Aurora-B (AURKB), vascular endothelial growth factor A (VEGFA), histone deacetylase 1 (HDAC1), caspase 9 (CASP9), heat shock protein HSP 90-alpha (HSP90AA1), and heat shock protein HSP 90-beta (HSP90AB1) (Table 2).

3.3. GO and KEGG Pathway Enrichment Analysis. The functions of the OGs were further investigated using GO and KEGG pathway enrichment analyses. The biological processes in which these OGs were implicated are summarized in Figure 2(a). Among the identified biological processes, cell communication, metabolic process, cellular component organization, multicellular organismal process, developmental process, response to stimulus, and biological regulation are strongly linked to cancer progression. According to the enrichment analysis of cellular components, the OGs were abundant in the nucleus, cytosol, membrane-enclosed lumen, and protein-containing complex (Figure 2(a)). Finally, the OGs were enriched in the molecular function protein binding (Figure 2(a)). KEGG pathway enrichment analysis demonstrated that the OGs were particularly enriched in the PI3K-Akt signaling pathway, pathways associated with cancer, and the regulation of the cell cycle (Supplementary Table 3).

3.4. Genetics Alteration Analysis. Eight genes (*SIRT2*, *CCND1*, *AURKB*, *VEGFA*, *HDAC1*, *CASP9*, *HSP90AA1*, and *HSP90AB1*) that play an essential role in the growth and development of mBCSC were selected from hub genes and referred to as potential therapeutic targets of honokiol (PTTH). Genetic variation within these genes was analyzed using cBioportal. The breast cancer study with the highest number of genetic changes was selected for further analysis (Figure 2(b)). Oncoprint was used to determine the percentage of PTTH gene alterations in patients with mBC. Genetic alterations in PTTH ranged from 1.1% to 35% in the 180 patient samples analyzed (Figure 2(c)), with amplification being the most common gene alteration. The genes that were most frequently mutated were *CCND1* (35%), *HSP90AB1* (11%), and *VEGFA* (8%). Mutual exclusivity analysis showed that *VEGFA* mutations significantly co-occurred with *HSP90AB1* mutations (Table 3). Copy number alterations (CNAs) are particularly common in cancer and play a significant role in its development and progression. CNA status can be homozygously deleted (shallow deletion), heterozygously deleted (deep deletion), diploid, gained (amplification event with relatively few copies), or amplified (amplification event with many copies). CNAs analysis revealed that *SIRT2* mRNA expression was lower in shallow deletion cases and higher in amplification cases than in diploids (normal/without change) (Figure 2(d)). *HDAC1* and *HSP90AB1* mRNA expression was lower in cases with shallow deletions and higher in cases with gain. *HSP90AA1* mRNA expression was lower in patients with gain than in those with diploid gain. *CASP9* mRNA expression was lower in the gain than in the in shallow deletion cases, but not significantly different from that in diploid cases. All CNAs other than those mentioned were not differently expressed. Finally, the cBioportal pathway analysis showed that the cell cycle pathway is the main pathway that is disrupted by PTTH genetic alterations. Among the genes involved in the regulation of cell pathway, *CCND1*, encoding cyclin D1, was identified as PTTH (Figure 2(e)).

3.5. Survival Rate and Immune Cell Infiltration Level. To assess the clinical value of PTTH genes' expression levels, we examined whether they are associated with the OS or prognosis of patients with breast cancer. Low expression levels of *CASP9* and *HSP90AB1* were significantly associated with poor OS ($P < 0.05$) (Figure 3(a)). To understand the role of the immune microenvironment in the development and prognosis of patients with BRCA mutations, we analyzed the correlation between the expression levels of PTTH and immunocyte infiltration. The expression level of PTTH was either positively or negatively related to the infiltration level of different immune cells, indicating that PTTH modulated the immunologic microenvironment by influencing immune cell infiltration. The expression levels of *CCND1*, *VEGFA*, *AURKB*, *HDAC1*, *HSP90AA1*, and *HSP90AB1* were positively correlated with immune cell infiltration levels, whereas the expression levels of *SIRT2* and *CASP9* were negatively correlated with the tumor purity of BRCA (Figure 3(b)). Additionally, the B cells' infiltration level was positively correlated with the expression levels of *HSP90AB1* and *AURKB*, and negatively correlated with the expression level of *CCND1*. Moreover, we observed a positive correlation between CD8+ T cells' infiltration levels and *SIRT2*, *HDAC1*, *CASP9*, and *HSP90AA1* expression levels, and between CD4+ T cells' infiltration levels and *SIRT2*, *HDAC1*, and *CASP9* expression levels. However, CD4+ T cells' infiltration levels were negatively correlated with

Table 1: Potential therapeutic targets of honokiol (PTTH) in metastatic breast cancer stem cells (mBCSCs).

No.	Protein symbol	Protein name	Database
1	*CASP9*	Caspase 9	STITCH
2	IL4	Interleukin 4	STITCH
3	PDK1	Pyruvate dehydrogenase kinase isoform 1	Swisstargetprediction
4	*CCND1*	Cyclin D1	STITCH
5	CSF1R	Macrophage colony stimulating factor receptor	Swisstargetprediction
6	TRAP1	Heat shock protein 75 kDa, mitochondrial	Swisstargetprediction
7	VEGFA	Vascular endothelial growth factor A	STITCH
8	HDAC8	Histone deacetylase 8	Swisstargetprediction
9	CAPN1	Calpain 1	STITCH
10	PARP1	Poly (ADP-ribose) polymerase-1	Swisstargetprediction
11	MGLL	Monoglyceride lipase	Swisstargetprediction
12	NQO2	Quinone reductase 2	Swisstargetprediction
13	RXRA	Retinoid X receptor alpha	canSAR Black
14	CNR1	Cannabinoid receptor 1	Swisstargetprediction
15	*HSP90AB1*	Heat shock protein HSP 90-beta	Swisstargetprediction
16	AURKB	Serine/threonine-protein kinase Aurora-B	Swisstargetprediction
17	PTGER4	Prostanoid EP4 receptor	Swisstargetprediction
18	*HSP90AA1*	Heat shock protein HSP 90-alpha	Swisstargetprediction
19	DYRK1A	Dual-specificity tyrosine-phosphorylation regulated kinase 1A	Swisstargetprediction
20	GSK3A	Glycogen synthase kinase-3 alpha	Swisstargetprediction
21	ACHE	Acetylcholinesterase	Swisstargetprediction
22	PAK1	Serine/threonine-protein kinase PAK 1	Swisstargetprediction
23	FAAH	Anandamide amidohydrolase	Swisstargetprediction
24	CAPN2	Calpain 2	STITCH
25	CAPN3	Calpain 3	STITCH
26	*HDAC1*	Histone deacetylase 1	Swisstargetprediction
27	EPHX2	Epoxide hydratase	Swisstargetprediction
28	CDC25B	Dual specificity phosphatase Cdc25B	Swisstargetprediction
29	HDAC6	Histone deacetylase 6	Swisstargetprediction
30	SIRT2	NAD-dependent deacetylase sirtuin 2	Swisstargetprediction

Table 2: Top-10 hub genes by Maximal Clique Centrality (MCC) score, as analyzed by CytoHubba.

Rank	Gene symbol	MCC score
1	HSP90AA1	132
2	PARP1	102
3	*CCND1*	98
4	HDAC1	67
5	HSP90AB1	62
6	VEGFA	53
7	CASP9	28
8	AURKB	26
9	HDAC6	24
10	SIRT2	18

HSP90AA1 expression levels. Infiltration levels of macrophages were positively correlated with *CCND1*, *SIRT2*, *CASP9*, and *HSP90AA1* expression levels, whereas they were negatively correlated with *AURKB* expression levels. Neutrophil infiltration levels were positively correlated with *SIRT2*, *AURKB*, *VEGFA*, *HDAC1*, *CASP9*, *HSP90AA1*, and *HSP90AB1*. Dendritic cell infiltration levels were negatively correlated with *CCND1* expression levels and positively correlated with *SIRT2*, *AURKB*, and *HDAC1* expression levels. Other non-mentioned data are not statistically significant.

3.6. Validation of the mRNA Expression Level and the Protein Expression Level of PTTH. The expression levels of *CCND1*, *AURKB*, *HDAC1*, *VEGFA*, *HSP90AA1*, and *HSP90AB1* were increased in the BC tissue, and even higher in mBC (Figure 4(a)). *CASP9* expression levels were not significantly different between normal, tumor, and metastatic breast cancer tissues. Interestingly, *SIRT2* expression was decreased in breast cancer tissues, but increased in metastatic tissues compared to normal tissues. These results were supported by immunohistochemical data from HPA, that showed that CCND1, AURKB, and HDAC1 were overexpressed in the nucleus, while SIRT2, VEGFA, HSP90AA1, and HSP90AB1 were overexpressed in the cytoplasmic/membranous region (Figure 4(b)). Finally, CASP9 was not differentially expressed between the normal tissue and the tumor tissue.

3.7. Molecular Docking. Molecular docking analysis revealed that AURKB and RAC-1 could bind to their respective native ligands and to HNK (Figure 5). The affinity of the interaction between these proteins and HNK was similar to that of their natural ligands. The interaction between AURKB and its native ligand ADP was stronger than that between *AURKB* and HNK according to the docking score (–12.89 and–8.68, respectively, Table 4). Furthermore, ADP interacted with several amino acids of AURKB, such as

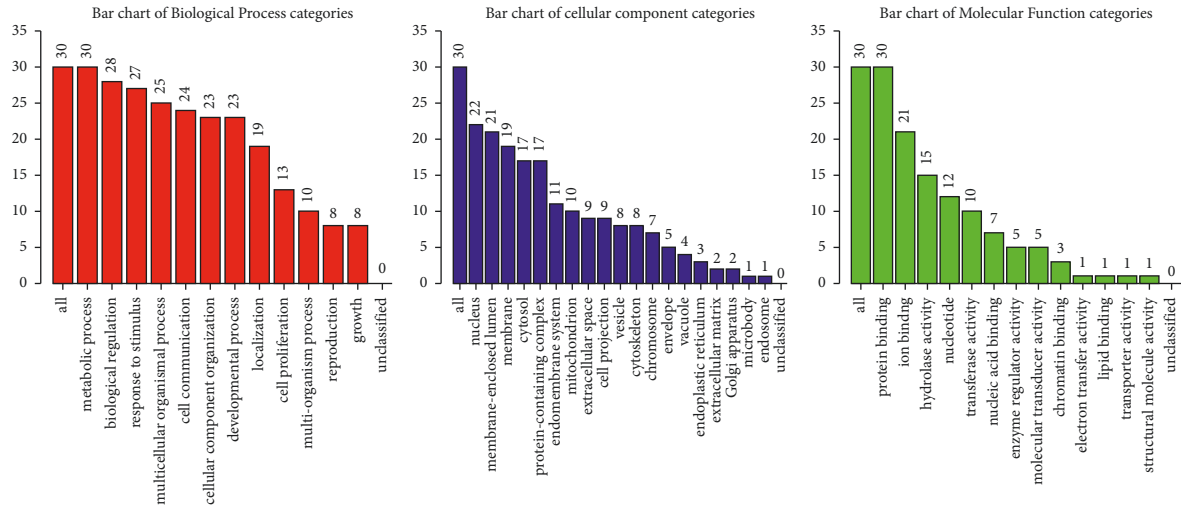

(a)

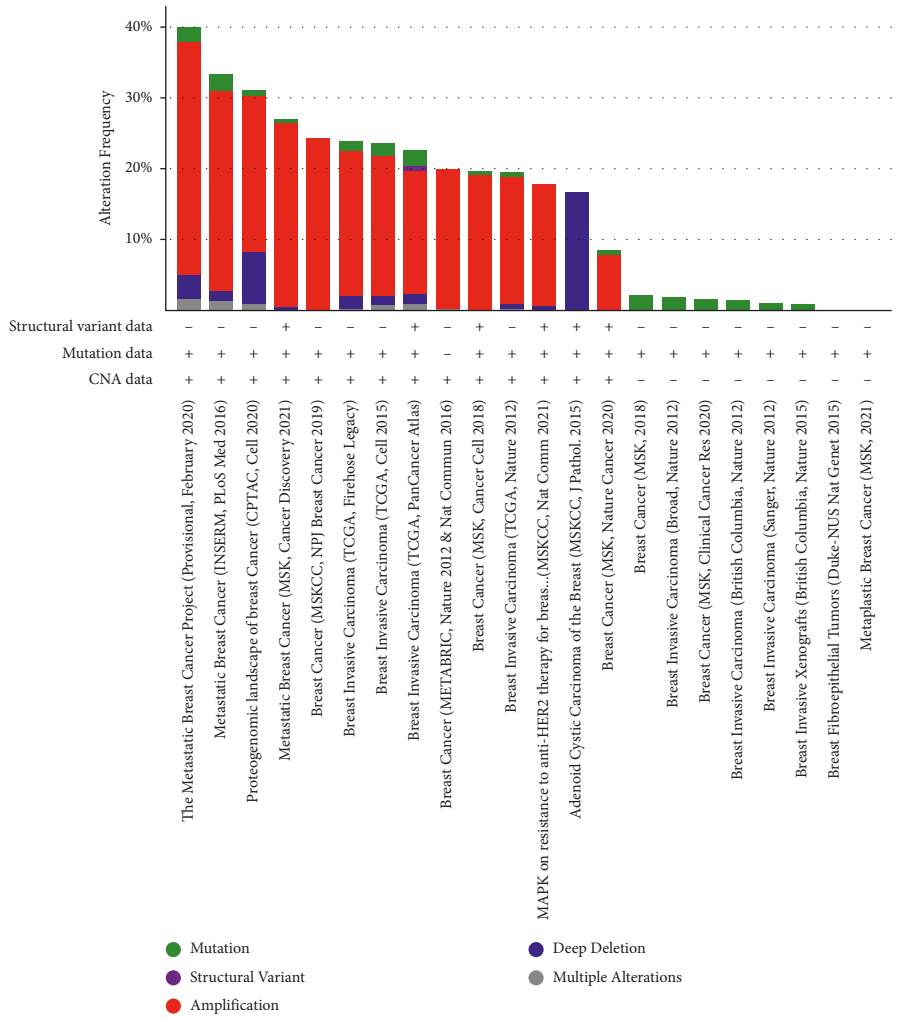

(b)

Figure 2: Continued.

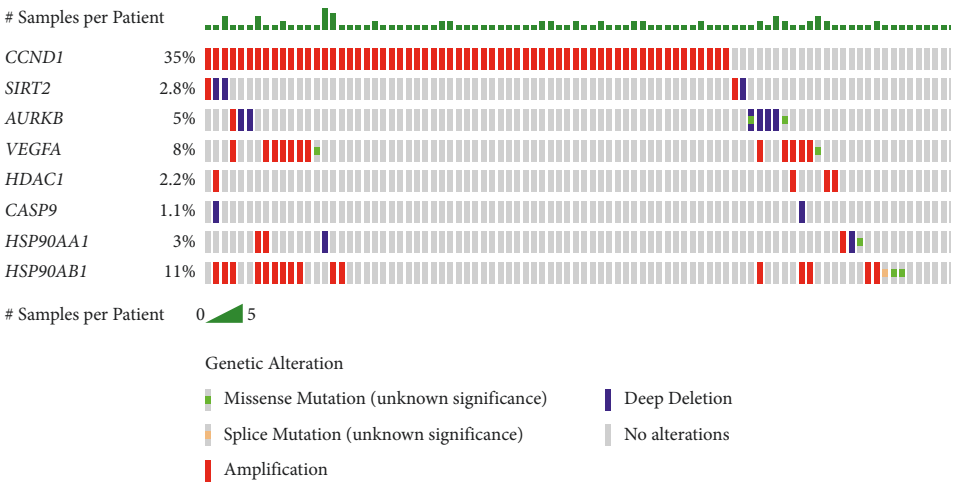

(c)

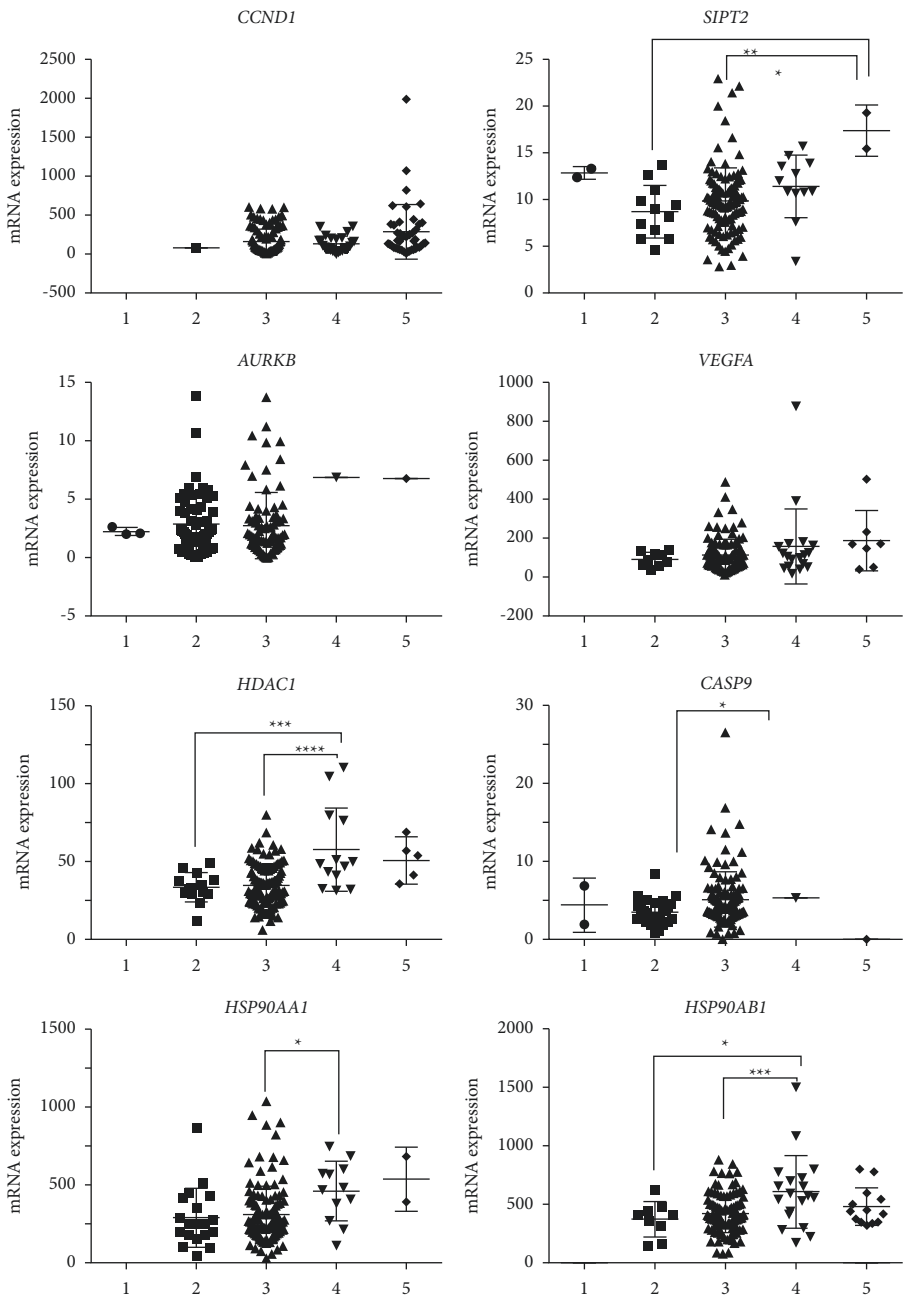

(d)

Figure 2: Continued.

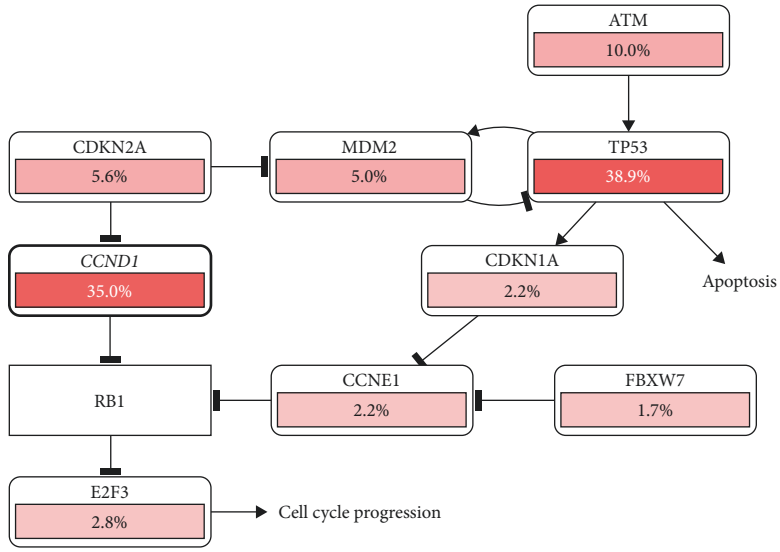

(e)

Figure 2: (a) Gene ontology (GO) analysis of potential therapeutic targets of honokiol (PTTH) results using WebGestalt. (b) Overview of genetic alterations in *CCND1, SIRT2, AURKB, VEGFA, HDAC1, CASP9, HSP90AA1*, and *HSP90AB1* based in samples from several breast cancer studies. (c) Oncoprint analysis of *CCND1, SIRT2, AURKB, VEGFA, HDAC1, CASP9, HSP90AA1*, and HSP90AB1 on The Metastatic Breast Cancer Project (Provisional, February 2020) dataset. (d) mRNA expression levels of *CCND1, SIRT2, AURKB, VEGFA, HDAC1, CASP9, HSP90AA1*, and *HSP90AB1* on the Metastatic Breast Cancer Project (Provisional, February 2020) as analyzed using cBioportal. 1: deep deletion, 2: shallow deletion, 3: diploid; 4: gain; 5: amplification. Statistical analyses were done by one-way ANOVA using Tukey's multiple comparison test. The symbol *or**or***or**** symbolizes $P < 0.05$ or $P < 0.01$ or $P < 0.001$ or $P < 0.001$, respectively. (e) Pathways related to genetic alterations predicted by cBioportal. The results showed that genetic alterations of the PTTH disrupted the pathways regulating the cell cycle.

Table 3: Mutual exclusivity analysis' results of the potential therapeutic targets of honokiol (PTTH).

A	B	Log2 odds ratio	*P* value	Tendency
HSP90AB1	*VEGFA*	>3	<0.001	Co-occurrence

Gly108, Gly110, Lys111, and Thr112, while HNK interacted with only one amino acid (Pro27). Likewise, the binding interaction between Rac-1 and its native ligand (phosphoaminophosphonic acid-guanylate ester/GNP; docking score −21.38) was stronger than that between Rac-1 and HNK (docking score −18.17). This was a result of the number of amino acids that the compounds interacted with and the distance between the interacting amino acids and the compound. For instance, the distance between Thr17 and GNP was much closer (1.82 Å) than that with HNK (3.35). However, despite the lower affinity of the interaction, HNK could potentially compete with the native ligands to inhibit the function of these proteins.

4. Discussion

This study identified eight PTTHs, including *CCND1*, *SIRT2*, *AURKB*, *VEGFA*, *HDAC1*, *CASP9*, *HSP90AA1*, and *HSP90AB1*. The expression levels of these genes were strongly associated with immune infiltration levels. The tumor microenvironment influences angiogenesis and the immune response, and has long been recognized as a primary determinant of long-term tumor progression [39–41]. In addition, it can greatly impact the effectiveness of immunotherapy, highlighting the need of its further understanding [42].

Cyclin D1, encoded by *CCND1*, is considered an oncogene that promotes cell proliferation, growth, angiogenesis, and resistance to chemotherapy and radiotherapy [43, 44]. In this study, we revealed that *CCND1* expression was positively correlated with BRCA purity and macrophage infiltration levels, and negatively correlated with B cell and dendritic cell infiltration levels. Many studies have shown that tumor-associated macrophages play an important role in the proliferation, invasion, angiogenesis, and metastasis of human breast carcinoma, and that increased macrophage tumor infiltration confers metastatic potential and is associated with poor prognosis in breast cancer [42]. Our findings are in line with those of Pestell et al., who demonstrated that cyclin D1 expression was increased in human cancer stroma, and promoted tumor inflammation, angiogenesis, and stem cell expansion in advanced breast cancer [41]. Interestingly, a previous study reported that HNK could inhibit cyclin D1 expression [14].

SIRT2, an NAD-dependent histone deacetylase, has been suggested to be a promising therapeutic target in cancer

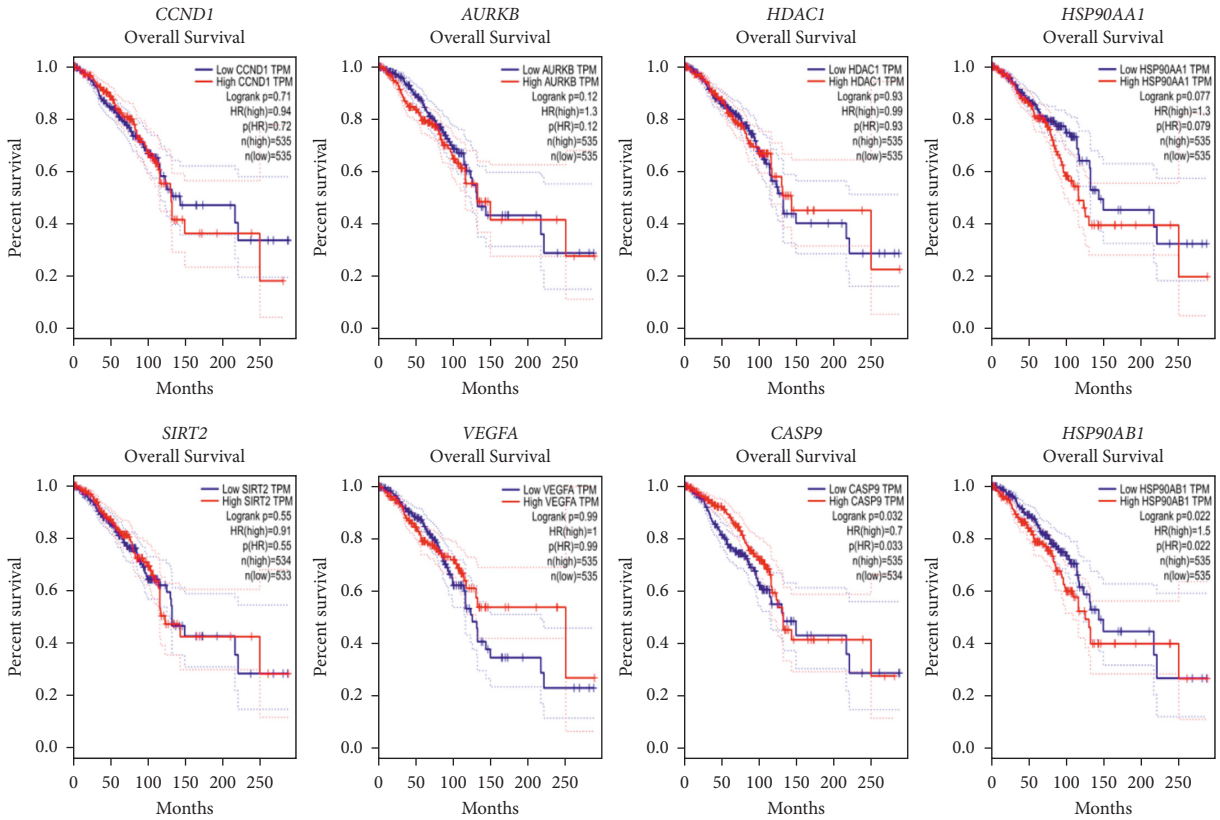

(a)

Figure 3: Continued.

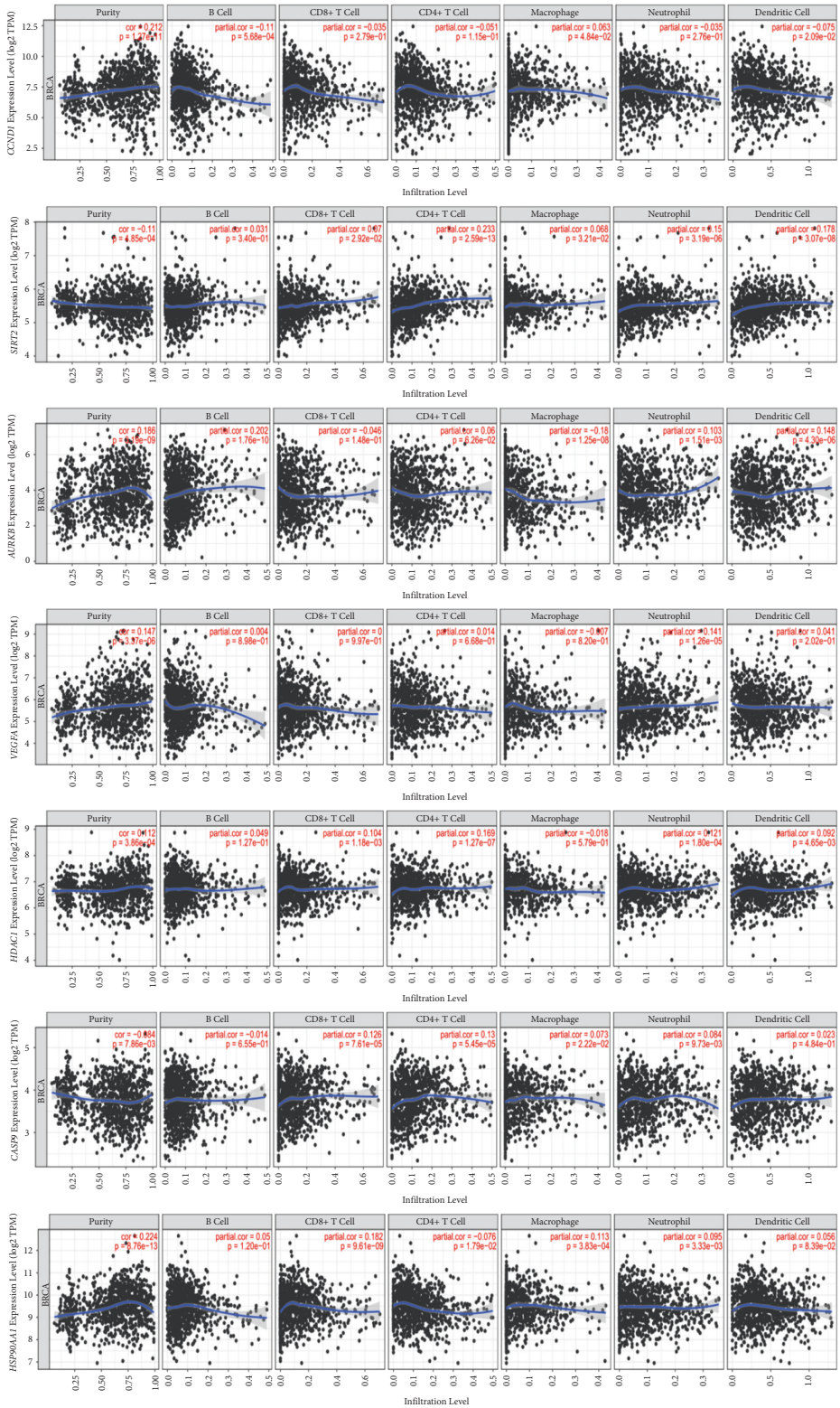

(b)

Figure 3: Continued.

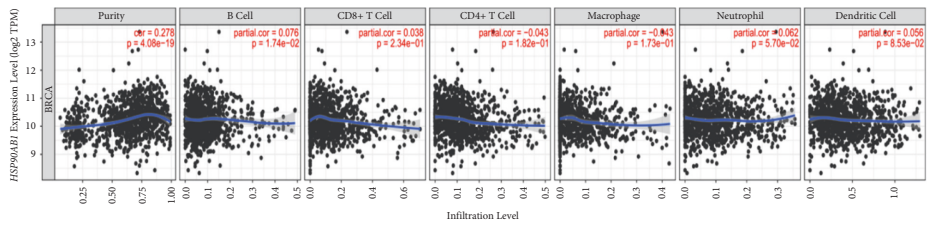

(c)

Figure 3: (a) Association between the expression levels of *CCND1, SIRT2, AURKB, VEGFA, HDAC1, CASP9, HSP90AA1*, and *HSP90AB1* and the overall survival in the breast cancer samples from The Cancer Genome Atlas. (b) Correlation analysis between the expression levels of *CCND1, SIRT2, AURKB, VEGFA, HDAC1, CASP9, HSP90AA1*, and *HSP90AB1* and the infiltration levels of B cells, CD8+ T cells, CD4+ T cells, macrophages, neutrophils, and dendritic cells.

treatment [47]. *SIRT2* is thought to affect carcinogenesis in a context-dependent manner, affecting epigenetic pathways implicated in cancer initiation, development, and progression [48–50]. *SIRT2* expression level was negatively correlated with BRCA purity, but positively correlated with CD8+ T cell, CD4+ T cell, macrophages, neutrophils, and dendritic cells' infiltration levels. These results confirm those of previous studies, in which *SIRT2* expression level and CD8+ T cell infiltration level were positively correlated in breast cancer patients [51]. In addition, systemic SIRT2 has been suggested to promote tumor development by suppressing NK cells [42]. Interestingly, *SIRT2* expression was significantly lower in breast cancer than in normal breast tissue, suggesting that *SIRT2* may act as a tumor suppressor during the initiation of tumorigenesis. Moreover, a previous study reported that high *SIRT2* expression in advanced tumor tissues is associated with poor prognosis, suggesting that *SIRT2* may function as an oncogene [50].

VEGFA is a cytokine that promotes vascular development and the formation of new blood vessels from preexisting vascular networks during embryogenesis [52–54]. In addition, VEGFA can also be released by cancer and stromal cells [55]. In several murine and human cancer models, it has been demonstrated that VEGFA stimulates the tumor-initiating epithelial–mesenchymal transition and metastasis, and that *VEGFA* expression levels are positively correlated with BRAC purity and neutrophil infiltration levels [56–63]. In line with these results, another study reported that patients with mBC had higher levels of circulating VEGFA than patients without metastases [64]. VEGF can stimulate neutrophil migration through the activation of VEGFR1, [65] and can prevent dendritic cells from maturing, resulting in cytotoxic T cells' inactivation [66]. Tregs, tumor-associated macrophages, and myeloid-derived suppressor cells are all highly induced by VEGF, resulting in an immunosuppressive TME [67]. Furthermore, VEGF increases the expression of PD-1 on CD8+ CTLs and Tregs in a VEGFR2-dependent manner, [64] as well as the expression of Fas ligand, interleukin (IL)-10, and prostaglandin E3, leading to cytotoxic T cells' depletion [65]. Hence, VEGF-A can be used as a biomarker for immune-targeting therapy in breast cancer patients [66].

Histone deacetylase 1 (HDAC1) is overexpressed in breast cancer cells and human breast cancer tissues and can trigger the proliferation and migration of these cells via activation of Snail/IL-8 signals [41]. *HDAC1* suppression has been reported to reduce the invasion of breast cancer cells by inhibiting matrix metalloproteinase-9, [67] and to reduce PD-L1 and HLA-DR expression and Treg frequency in triple negative breast cancer [68]. In our study, there was a positive correlation between *HDAC1* expression levels and tumor purity, and CD8+ T cells', CD4+ T cells', neutrophils', and dendritic cells' infilitration levels.

HSP90α, encoded by *HSP90AA1*, is the stress-inducible isoform of HSP90. Previous studies have shown that high expression levels of HSP90 (HSP90α and HSP90β) increase the likelihood of recurrence and distant metastases in triple negative and ER+/HER2-breast cancer, and are associated with higher mortality [69]. Overexpression of HSP90 in human breast cancer cells has been linked to enhanced cell proliferation [42] and metastasis, [70] as well as to short OS and aggressive clinicopathological characteristics, such as high clinical stage, large tumors, and lymph node involvement [71]. Lin et al. reported that elevated *HSP90AB1* expression was linked to a better overall survival of ER- and Basal-like breast cancer patients [55]. However, we found that high *HSP90AB1* expression was associated with poor prognosis in BRCA patients. Additionally, the expression of *HSP90AA1* and *HSP90AB1* was positively correlated with tumor purity; and the expression of *HSP90AA1* was positively related to CD8+ T cells, macrophages, and neutrophils, but negatively correlated with CD4+ T cells. Further studies for exploring the infiltration of CD8+, macrophages, neutrophils, CD4+, and the effects of HNK on *HSP90AA1* and *HSP90AB1* are warranted.

CASP9 encodes caspase-9, an initiator of the intrinsic apoptosis pathway [79]. When the apoptosome, a multimolecular complex comprising cytochrome c and the apoptotic peptidase activating factor 1 (Apaf-1), is formed, it cleaves pro-caspase-9, forming caspase-9, triggering the caspase activation cascade by activating executor caspases, including caspase 3 and caspase 7 to cleave other cellular targets [80].

The aurora kinase family includes Aurora kinase B (AURKB), a mitotic serine/threonine protein kinase, and aurora kinase A (AURKA), which is a member of the Chromosomal Passenger Complex (CPC). The CPC plays a role in cell cycle progression and is a prognostic marker of

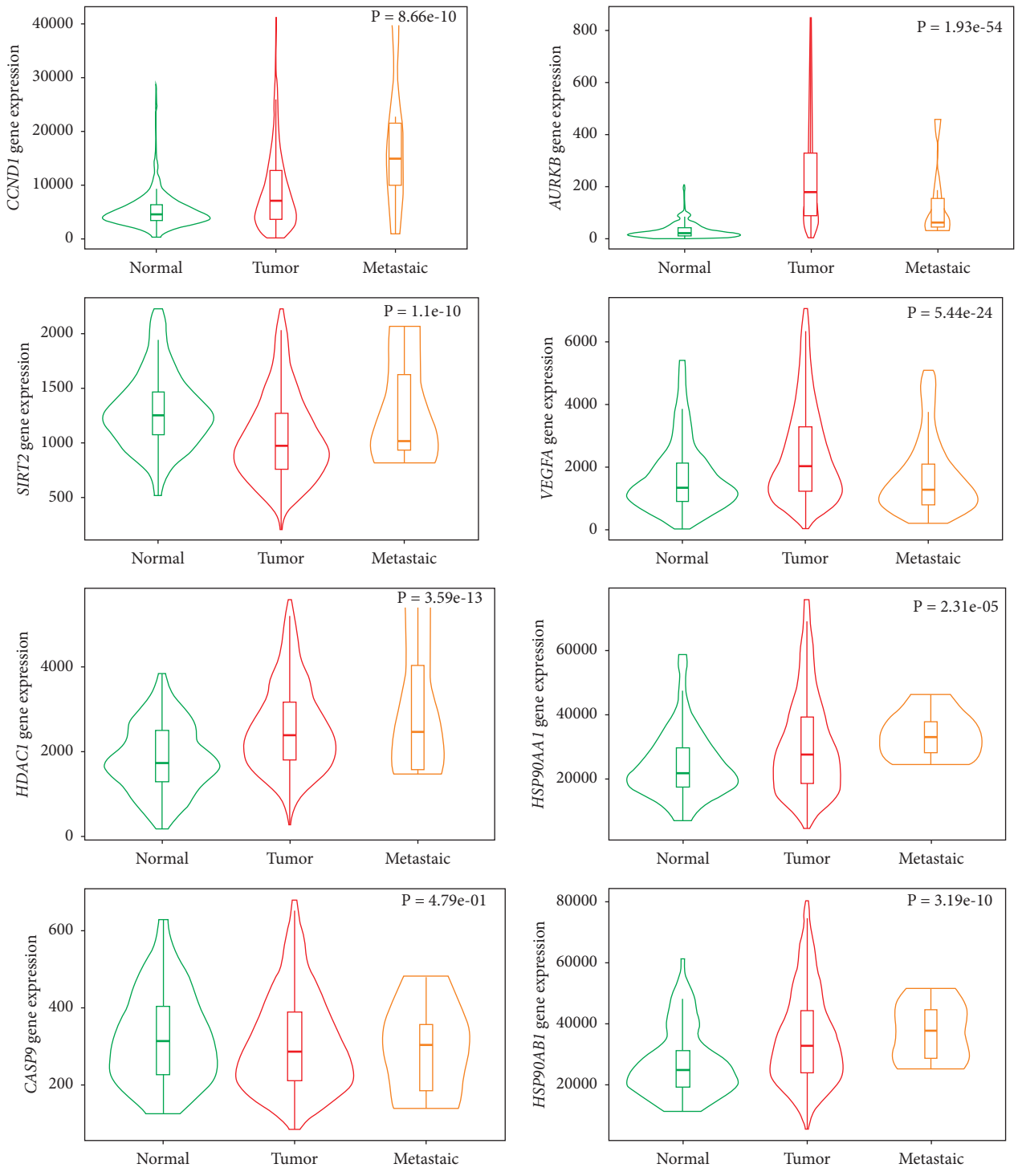

(a)

Figure 4: Continued.

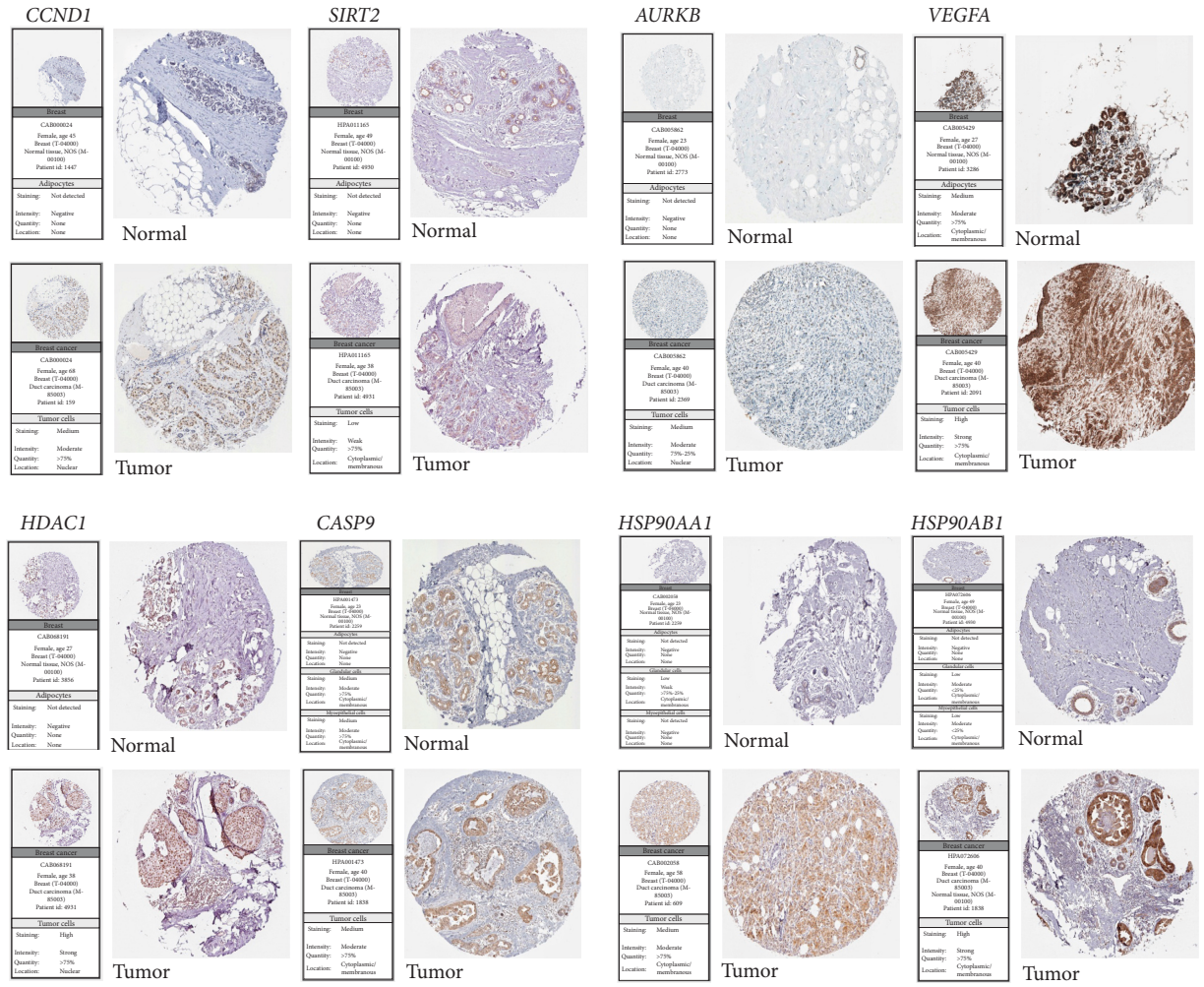

(b)

Figure 4: mRNA and the protein expression levels of *CCND1*, *SIRT2*, *AURKB*, *VEGFA*, *HDAC1*, *CASP9*, *HSP90AA1*, and *HSP90AB1*. (a) mRNA expression levels in the Cancer Genome Atlas (TCGA). (b) Protein expression levels in normal and tumor breast tissues retrieved from the Human Protein Atlas (HPA).

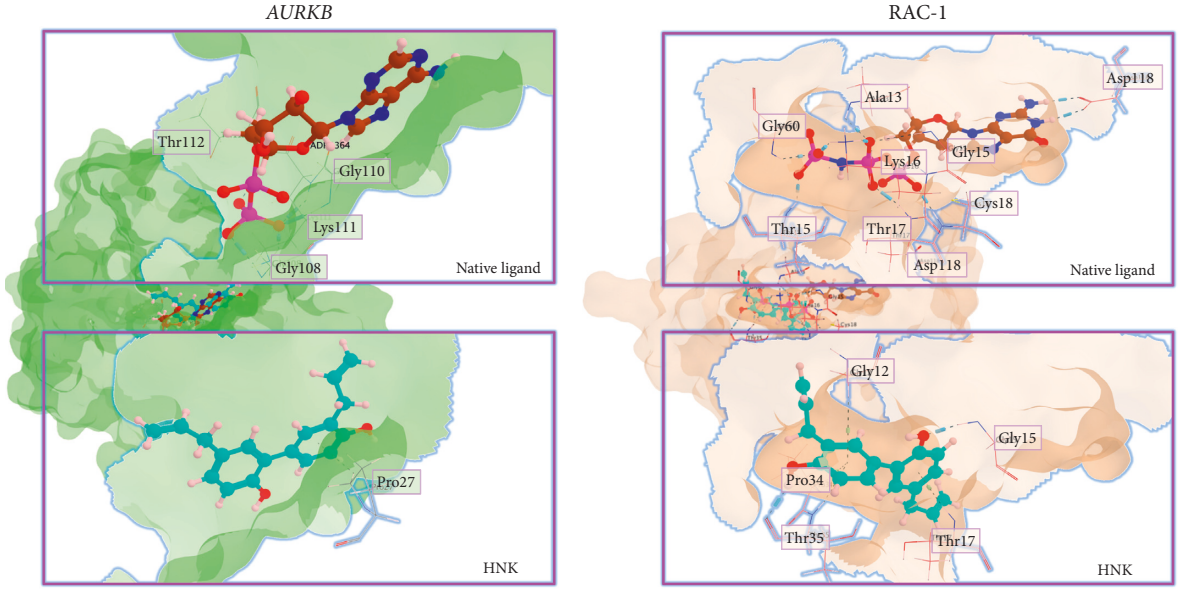

Figure 5: Visualization of molecular docking of honokiol (HNK) toward AURKB and RAC-1.

Table 4: Molecular docking results of honokiol (HNK) toward AURKB and RAC-1.

Protein, PDB ID	Native ligand						Honokiol					
	S	RMSD (Å)	LA	AA	BT	D	S	RMSD (Å)	LA	AA	BT	D
AURKB, PDB ID : 3ZCW	**−12.89**	1.39	O	Gly108	ScD	1.95	−8.68	1.10	C	Pro27	ArH	2.75
			O	Gly110	ScD	1.91						
			O	Lys111	ScD	2.11						
			O	Thr112	ScD	2.24						
			O	Ala13	ScD	2.20						
			O	**Gly15**	ScD	2.49						
RAC-1, PDB ID : 3TH5	**−21.38**	0.48	O	Lys16	ScD	1.73	−18.17	1.86	C	Gly12	ArH	4.01
			O	Lys16	ScD	1.95			O	**Gly15**	ScD	1.83
			O	**Thr17**	ScD	1.90			C	**Thr17**	ArH	3.35
			O	Cys18	ScD	1.79			C	Pro34	ArH	3.96
			O	**Thr35**	ScD	1.82			O	**Thr35**	ScA	2.14
			O	Gly60	ScD	2.37			C	**Thr35**	ArH	2.70
			H	Asp118	ScD	2.09						
			H	Asp118	ScD	2.13						

S: docking score, RMSD: root mean square deviation, LA: ligand atom, AA: amino acid, BT: binding type, D: distance, ScD: sidechain donor, ScA: sidechain acceptor, ArH: arene H, and BbD: backbone donor.

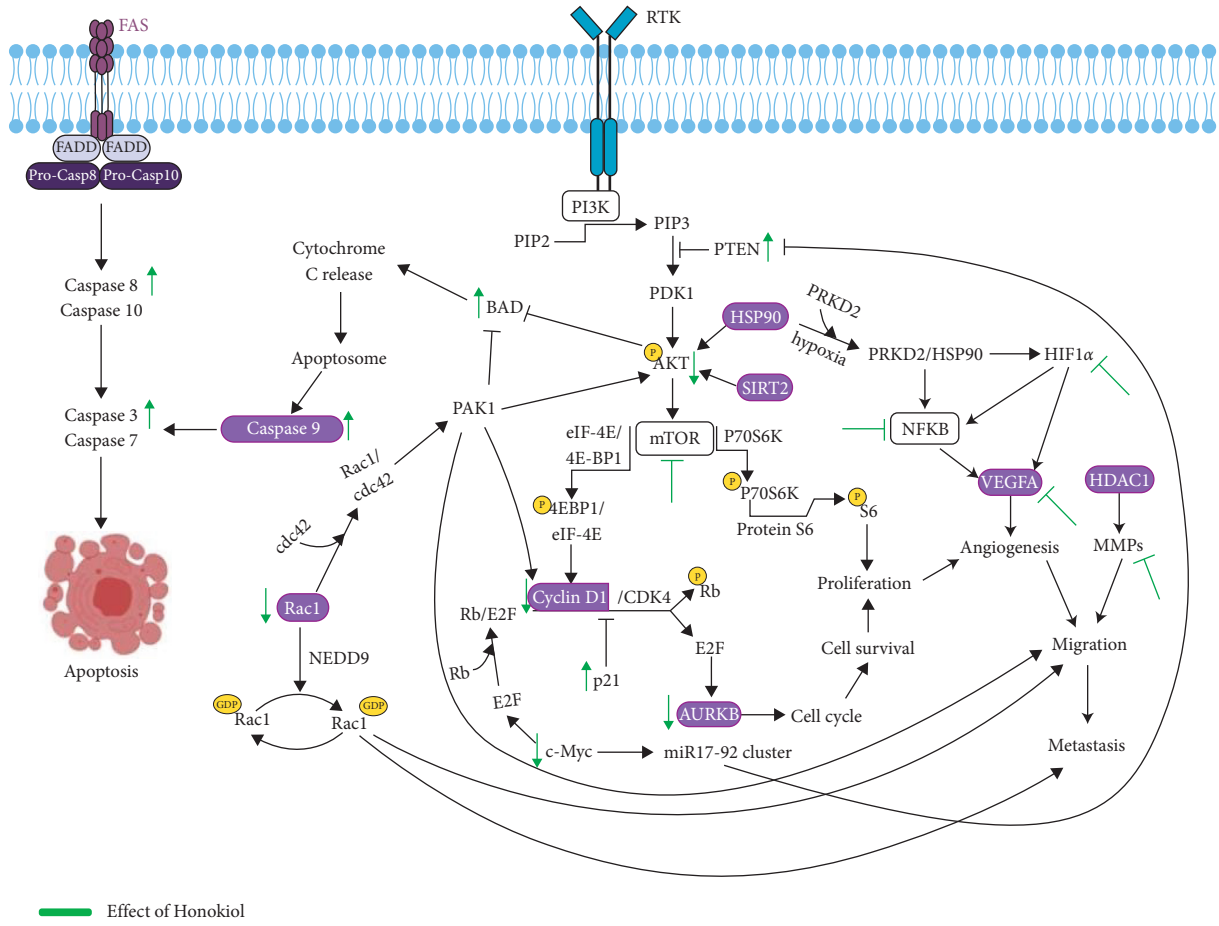

Figure 6: Proposed mechanism of honokiol (HNK) in mBCSCs (created with https://BioRender.com).

breast cancer arising from *BRCA2* mutation [81]. Deregulation of AURKB is observed in several tumors, and its overexpression is frequently linked to tumor cell invasion, metastasis, and drug resistance [82]. Hence, AURKB has emerged as an attractive drug target for the development of small-molecule inhibitors [83].

RAC1 and AURKB were selected for in-depth molecular docking analysis because they were connected to the PTTH-

mBCSCs-cell cycle axis. The Rho-GTPase family, including Rho, Rac1, and Cdc42, regulates the cytoskeleton [84] and thus modulates cell motility, migration, and invasion [85]. Rac-1/Cdc42 activation can induce cell growth by activating the PAK1/cyclin D1 pathway, or cell death by activating the PAK1/Akt/BAD pathway [86]. Rho has been suggested to be a potential therapeutic target, since Rho and *VEGFA* crosstalk leads to cancer progression and metastasis [87].

This study revealed the potential targets and molecular mechanisms of HNK on the cell cycle of mBCSCs (Figure 6). It is known that HNK exerts anticancer effects by suppressing angiogenesis, migration, invasion, and proliferation in a variety of cancer cell lines and tumor models [12]. HNK inhibits the cell cycle via the PI3K/Akt/mTOR pathway by upregulating PTEN and P21, and suppressing p-Akt, cyclin D/CDK4, c-Myc, Rac1, and *AURKB* [13, 14, 22, 71]. Angiogenesis is inhibited through the HIF1/NFkB pathway, which is activated under hypoxic conditions and blocks the release of VEGF. Immune infiltration analysis showed that HNK is correlated with *VEGFA* inhibition, suggesting HNK can effectively block VEGFR2. HNK was also found to reduce HIF-induced VEGFR/VEGF activation and inhibit matrix metalloproteinases activity and cell migration [88]. In addition, HNK can induce apoptosis through the upregulation of BAD, caspase-9, caspase-3, and caspase-8 [89]. In the tumor microenvironment, oncogenic drivers such as β-catenin, STAT3, PI3K/PTEN/AKT/mTOR, p53, NF-kB, and RAS/RAF/MAPK are activated to suppress the production of chemokines, reduce the recruitment of dendritic cells, macrophages, T cells, and NK cells to tumor sites, and to suppress the immune system of these immunocytes [90]. Furthermore, tumor-intrinsic signaling can cause tumor cells to express PD-L1, resulting in T cell dysfunction in the tumor microenvironment. This study highlights the potential of HNK as an immunotherapeutic agent for mBCSCs by modulating the tumor immune environment. However, the results of this study were obtained through bioinformatics studies; therefore, further in vitro, in vivo, and clinical trials are needed to validate the findings.

5. Conclusions

This study identified eight PTTHs consisting of *CCND1*, *SIRT2*, *AURKB*, *VEGFA*, *HDAC1*, *CASP9*, *HSP90AA1*, and *HSP90AB1*, which can inhibit the mBCSC-cell cycle axis. In addition, PTTHs may regulate the PI3K/Akt/mTOR and HIF1/NFkB pathways. This study is speeding up the development of HNK as anti-mBCSCs by targeting certain genes. However, this study have several limitations; for example, the targets of HNK are predicted from database. Other additional machine learning algorithm will provide more validated candidates of HNK targets. Another limitation of this study is that we used a bioinformatics approach; therefore, more needs to be explored further for validation and clarification in laboratory experiments.

Data Availability

The data generated or analyzed during this study are included within the article and its supplementary files.

Conflicts of Interest

The authors declare that they have no conflicts of interest.

Acknowledgments

The authors acknowledge Mrs. Ririn Widarti for her assistance with administrative support. This research was funded by the Directorate of Research, Universitas Gadjah Mada, through the Rekognisi Tugas Akhir program (SK Rektor UGM No. 1185/UN1.P.III/SK/HUKOR/2021).

Supplementary Materials

Supplementary Table 1. Differentially expressed genes (DEGs) in metastatic breast cancer stem cells (mBCSCs) from the GSE 151191 dataset. *Supplementary Table 2*. Honokiol (HNK)-mediated proteins (HMPs), as retrieved from Swiss target prediction, STITCH, canSAR Black, and SEA. *Supplementary Table 3*. KEGG pathway enrichment analysis of OGs from both HMP and DEGs. *Supplementary Figure 1*. Flowchart for the screening of datasets. (*Supplementary Materials*)

References

[1] WHO, "Cancer today. estimated number of incident cases Indonesia, females, all ages," 2020, https://gco.iarc.fr/today/home.

[2] K. D. Miller, L. Nogueira, A. B. Mariotto et al., "Cancer treatment and survivorship statistics, 2019," *CA: A Cancer Journal for Clinicians*, vol. 69, no. 5, pp. 363–385, 2019.

[3] M. A. Elbaiomy, T. Akl, N. Atwan, A. A. Elsayed, M. Elzaafarany, and S. Shamaa, "Clinical impact of breast cancer stem cells in metastatic breast cancer patients," *Journal of Oncology*, vol. 2020, Article ID 2561726, 8 pages, 2020.

[4] J. Zhao, "Cancer stem cells and chemoresistance: the smartest survives the raid," *Pharmacology & Therapeutics*, vol. 160, pp. 145–158, 2016.

[5] D. Raman, A. K. Tiwari, V. Tiriveedhi, and J. A. Rhoades, "Editorial: the role of breast cancer stem cells in clinical outcomes," *Frontiers in Oncology*, vol. 10, p. 299, 2020.

[6] A. A. Ross, "Minimal residual disease in solid tumor malignancies: a review," *Journal of Hematotherapy*, vol. 7, no. 1, pp. 9–18, 1998.

[7] M. De Angelis, F. Francescangeli, and A. Zeuner, "Breast cancer stem cells as drivers of tumor chemoresistance, dormancy and relapse: new challenges and therapeutic opportunities," *Cancers*, vol. 11, no. 10, p. 1569, 2019.

[8] M. Santisteban, J. M. Reiman, M. K. Asiedu et al., "Immune-induced epithelial to mesenchymal transition in vivo generates breast cancer stem cells," *Cancer Research*, vol. 69, no. 7, pp. 2887–2895, 2009.

[9] P. M. Aponte and A. Caicedo, "Stemness in cancer: stem cells, cancer stem cells, and their microenvironment," *Stem Cells International*, vol. 2017, Article ID 5619472, 17 pages, 2017.

[10] J. M. Pitt, A. Marabelle, A. Eggermont, J.-C. Soria, G. Kroemer, and L. Zitvogel, "Targeting the tumor microenvironment: removing obstruction to anticancer immune responses and immunotherapy," *Annals of Oncology*, vol. 27, no. 8, pp. 1482–1492, 2016.

[11] Y. C. Lo, T. Che-Ming, C. Chieh-Fu, C. Chien-Chih, and H. Chuang-Ye, "Magnolol and honokiol isolated from Magnolia officinalis protect rat heart mitochondria against lipid peroxidation," *Biochemical Pharmacology*, vol. 47, no. 3, pp. 549–553, 1994.

[12] S. Arora, S. Singh, G. A. Piazza, C. M. Contreras, J. Panyam, and A. P. Singh, "Honokiol: a novel natural agent for cancer prevention and therapy," *Current Molecular Medicine*, vol. 12, no. 10, pp. 1244–1252, 2012.

[13] I. Wolf, J. O'Kelly, N. Wakimoto et al., "Honokiol, a natural biphenyl, inhibits in vitro and in vivo growth of breast cancer through induction of apoptosis and cell cycle arrest," *International Journal of Oncology*, vol. 30, no. 6, pp. 1529–1537, 2007.

[14] E.-J. Park, H.-Y. Min, H.-J. Chung et al., "Down-regulation of c-Src/EGFR-mediated signaling activation is involved in the honokiol-induced cell cycle arrest and apoptosis in MDA-MB-231 human breast cancer cells," *Cancer Letters*, vol. 277, no. 2, pp. 133–140, 2009.

[15] J. Lee, J. Sul, J. Park, M. Lee, E. Cha, and Y. Ko, "Honokiol induces apoptosis and suppresses migration and invasion of ovarian carcinoma cells via AMPK/mTOR signaling pathway," *International Journal of Molecular Medicine*, vol. 43, no. 5, pp. 1969–1978, 2019.

[16] J. Wen, X. Wang, H. Pei et al., "Anti-psoriatic effects of Honokiol through the inhibition of NF-κB and VEGFR-2 in animal model of K14-VEGF transgenic mouse," *Journal of Pharmacological Sciences*, vol. 128, no. 3, pp. 116–124, 2015.

[17] S. Sengupta, A. Nagalingam, N. Muniraj et al., "Activation of tumor suppressor LKB1 by honokiol abrogates cancer stem-like phenotype in breast cancer via inhibition of oncogenic Stat3," *Oncogene*, vol. 36, no. 41, pp. 5709–5721, 2017.

[18] D. B. Avtanski, A. Nagalingam, P. Kuppusamy et al., "Honokiol abrogates leptin-induced tumor progression by inhibiting Wnt1-MTA1-β-catenin signaling axis in a microRNA-34a dependent manner," *Oncotarget*, vol. 6, no. 18, pp. 16396–16410, 2015.

[19] D. B. Avtanski, A. Nagalingam, M. Y. Bonner, J. L. Arbiser, N. K. Saxena, and D. Sharma, "Honokiol activates LKB1-miR-34a axis and antagonizes the oncogenic actions of leptin in breast cancer," *Oncotarget*, vol. 6, no. 30, pp. 29947–29962, 2015.

[20] N. Muniraj, S. Siddharth, M. Shriver et al., "Induction of STK11-dependent cytoprotective autophagy in breast cancer cells upon honokiol treatment," *Cell Death Discovery*, vol. 6, no. 1, pp. 81–15, 2020.

[21] W. Tian, Y. Deng, L. Li, H. He, J. Sun, and D. Xu, "Honokiol synergizes chemotherapy drugs in multidrug resistant breast cancer cells via enhanced apoptosis and additional programmed necrotic death," *International Journal of Oncology*, vol. 42, no. 2, pp. 721–732, 2013.

[22] C. Crane, A. Panner, R. O. Pieper, J. Arbiser, and A. T. Parsa, "Honokiol-mediated inhibition of PI3K/mTOR pathway," *Journal of Immunotherapy*, vol. 32, no. 6, pp. 585–592, 2009.

[23] M. Kuhn, C. von Mering, M. Campillos, L. J. Jensen, and P. Bork, "STITCH: interaction networks of chemicals and proteins," *Nucleic Acids Research*, vol. 36, pp. D684–D688, 2007.

[24] D. Gfeller, A. Grosdidier, M. Wirth, A. Daina, O. Michielin, and V. Zoete, "SwissTargetPrediction: a web server for target prediction of bioactive small molecules," *Nucleic Acids Research*, vol. 42, no. W1, pp. W32–W38, 2014.

[25] M. D. Halling-Brown, K. C. Bulusu, M. Patel, J. E. Tym, and B. Al-Lazikani, "CanSAR: an integrated cancer public translational research and drug discovery resource," *Nucleic Acids Research*, vol. 40, no. D1, pp. D947–D956, 2012.

[26] M. J. Keiser, V. Setola, J. J. Irwin et al., "Predicting new molecular targets for known drugs," *Nature*, vol. 462, no. 7270, pp. 175–181, 2009.

[27] H. Heberle, G. V. Meirelles, F. R. da Silva, G. P. Telles, and R. Minghim, "InteractiVenn: a web-based tool for the analysis of sets through Venn diagrams," *BMC Bioinformatics*, vol. 16, no. 1, p. 169, 2015.

[28] D. Szklarczyk, A. Franceschini, S. Wyder et al., "STRING v10: protein-protein interaction networks, integrated over the tree of life," *Nucleic Acids Research*, vol. 43, no. D1, pp. D447–D452, 2015.

[29] P. Shannon, A. Markiel, O. Ozier et al., "Cytoscape: a software environment for integrated models of biomolecular interaction networks," *Genome Research*, vol. 13, no. 11, pp. 2498–2504, 2003.

[30] C.-H. Chin, S.-H. Chen, H.-H. Wu, C.-W. Ho, M.-T. Ko, and C.-Y. Lin, "CytoHubba: identifying hub objects and sub-networks from complex interactome," *BMC Systems Biology*, vol. 8, no. S4, p. S11, 2014.

[31] W. da Huang W, B. T. Sherman, and R. A. Lempicki, "Bioinformatics enrichment tools: paths toward the comprehensive functional analysis of large gene lists," *Nucleic Acids Research*, vol. 37, no. 1, pp. 1–13, 2009.

[32] W. Wang, B. T. Vasaikar, R. A. Shi, R. A. Greer, and R. A. Zhang, "WebGestalt 2017: a more comprehensive, powerful, flexible and interactive gene set enrichment analysis toolkit," *Nucleic Acids Research*, vol. 45, no. 1, pp. W130–W137, 2017.

[33] E. Cerami, J. Gao, U. Dogrusoz et al., "The cBio cancer genomics portal: an open platform for exploring multidimensional cancer genomics data: figure 1," *Cancer Discovery*, vol. 2, no. 5, pp. 401–404, 2012.

[34] Z. Tang, C. Li, B. Kang, G. Gao, C. Li, and Z. Zhang, "GEPIA: a web server for cancer and normal gene expression profiling and interactive analyses," *Nucleic Acids Research*, vol. 45, no. W1, pp. W98–W102, 2017.

[35] T. Li, J. Fu, Z. Zeng et al., "TIMER2.0 for analysis of tumor-infiltrating immune cells," *Nucleic Acids Research*, vol. 48, no. W1, pp. W509–W514, 2020.

[36] Á Bartha and B. Győrffy, "TNMplot.com: a web tool for the comparison of gene expression in normal, tumor and metastatic tissues," *International Journal of Molecular Sciences*, vol. 22, no. 5, p. 2622, 2021.

[37] A. N. Tran, A. M. Dussaq, T. Kennell, C. D. Willey, and A. B. Hjelmeland, "HPAanalyze: an R package that facilitates the retrieval and analysis of the Human Protein Atlas data," *BMC Bioinformatics*, vol. 20, no. 1, p. 463, 2019.

[38] B. Zhao, A. Erwin, and B. Xue, "How many differentially expressed genes: a perspective from the comparison of genotypic and phenotypic distances," *Genomics*, vol. 110, no. 1, pp. 67–73, 2018.

[39] D. G. DeNardo, J. B. Barreto, P. Andreu et al., "$CD4^+$ T cells regulate pulmonary metastasis of mammary carcinomas by enhancing protumor properties of macrophages," *Cancer Cell*, vol. 16, no. 2, pp. 91–102, 2009.

[40] M. Binnewies, E. W. Roberts, K. Kersten et al., "Understanding the tumor immune microenvironment (TIME) for effective therapy," *Nature Medicine*, vol. 24, no. 5, pp. 541–550, 2018.

[41] M. F. Santolla and M. Maggiolini, "The FGF/FGFR system in breast cancer: oncogenic features and therapeutic perspectives," *Cancers*, vol. 12, no. 10, p. 3029, 2020.

[42] M. Zhang, S. Acklin, J. Gillenwater et al., "SIRT2 promotes murine melanoma progression through natural killer cell inhibition," *Scientific Reports*, vol. 11, no. 1, Article ID 12988, 2021.

[43] M. Malumbres and M. Barbacid, "To cycle or not to cycle: a critical decision in cancer," *Nature Reviews Cancer*, vol. 1, no. 3, pp. 222–231, 2001.

[44] E. A. Musgrove, C. E. Caldon, J. Barraclough, A. Stone, and R. L. Sutherland, "Cyclin D as a therapeutic target in cancer," *Nature Reviews Cancer*, vol. 11, no. 8, pp. 558–572, 2011.

[45] F. I. Montalto and F. De Amicis, "Cyclin D1 in cancer: a molecular connection for cell cycle control, adhesion and invasion in tumor and stroma," *Cells*, vol. 9, no. 12, p. 2648, 2020.

[46] T. G. Pestell, X. Jiao, M. Kumar et al., "Stromal cyclin D1 promotes heterotypic immune signaling and breast cancer growth," *Oncotarget*, vol. 8, no. 47, pp. 81754–81775, 2017.

[47] I. Karwaciak, A. Sałkowska, K. Karaś et al., "SIRT2 contributes to the resistance of melanoma cells to the multikinase inhibitor dasatinib," *Cancers*, vol. 11, no. 5, p. 673, 2019.

[48] V. Carafa, L. Altucci, and A. Nebbioso, "Dual tumor suppressor and tumor promoter action of sirtuins in determining malignant phenotype," *Frontiers in Pharmacology*, vol. 10, p. 38, 2019.

[49] L. Bosch-Presegue and A. Vaquero, "The dual role of sirtuins in cancer," *Genes & Cancer*, vol. 2, no. 6, pp. 648–662, 2011.

[50] L. Zhang, S. Kim, and X. Ren, "The clinical significance of *SIRT2* in malignancies: a tumor suppressor or an oncogene?" *Frontiers in Oncology*, vol. 10, p. 1721, 2020.

[51] C. Jiang, J. Liu, M. Guo et al., "The NAD-dependent deacetylase *SIRT2* regulates T cell differentiation involved in tumor immune response," *International Journal of Biological Sciences*, vol. 16, no. 15, pp. 3075–3084, 2020.

[52] A.-K. Olsson, A. Dimberg, J. Kreuger, and L. Claesson-Welsh, "VEGF receptor signalling ? in control of vascular function," *Nature Reviews Molecular Cell Biology*, vol. 7, no. 5, pp. 359–371, 2006.

[53] D. W. Leung, G. Cachianes, W.-J. Kuang, D. V. Goeddel, and N. Ferrara, "Vascular endothelial growth factor is a secreted angiogenic mitogen," *Science*, vol. 246, no. 4935, pp. 1306–1309, 1989.

[54] E. Tischer, D. Gospodarowicz, R. Mitchell et al., "Vascular endothelial growth factor: a new member of the platelet-derived growth factor gene family," *Biochemical and Biophysical Research Communications*, vol. 165, no. 3, pp. 1198–1206, 1989.

[55] D. J. Hicklin and L. M. Ellis, "Role of the vascular endothelial growth factor pathway in tumor growth and angiogenesis," *Journal of Clinical Oncology*, vol. 23, no. 5, pp. 1011–1027, 2005.

[56] B. Beck, G. Driessens, S. Goossens et al., "A vascular niche and a VEGF-Nrp1 loop regulate the initiation and stemness of skin tumours," *Nature*, vol. 478, no. 7369, pp. 399–403, 2011.

[57] D. Zhao, C. Pan, J. Sun et al., "VEGF drives cancer-initiating stem cells through VEGFR-2/Stat3 signaling to upregulate Myc and Sox2," *Oncogene*, vol. 34, no. 24, pp. 3107–3119, 2015.

[58] H. L. Goel, B. Pursell, C. Chang et al., "GLI1 regulates a novel neuropilin-2/$\alpha 6\beta 1$ integrin based autocrine pathway that contributes to breast cancer initiation," *EMBO Molecular Medicine*, vol. 5, no. 4, pp. 488–508, 2013.

[59] S. Bao, Q. Wu, S. Sathornsumetee et al., "Stem cell-like glioma cells promote tumor angiogenesis through vascular endothelial growth factor," *Cancer Research*, vol. 66, no. 16, pp. 7843–7848, 2006.

[60] P. Hamerlik, J. D. Lathia, R. Rasmussen et al., "Autocrine VEGF-VEGFR2-neuropilin-1 signaling promotes glioma stem-like cell viability and tumor growth," *Journal of Experimental Medicine*, vol. 209, no. 3, pp. 507–520, 2012.

[61] R. E. Bachelder, M. A. Wendt, and A. M. Mercurio, "Vascular endothelial growth factor promotes breast carcinoma invasion in an autocrine manner by regulating the chemokine receptor CXCR4," *Cancer Research*, vol. 62, no. 24, pp. 7203–7206, 2002.

[62] O. Gonzalez-Moreno, J. Lecanda, J. E. Green et al., "VEGF elicits epithelial-mesenchymal transition (EMT) in prostate intraepithelial neoplasia (PIN)-like cells via an autocrine loop," *Experimental Cell Research*, vol. 316, no. 4, pp. 554–567, 2010.

[63] L. S. Kim, S. Huang, W. Lu, D. Chelouche Lev, and J. E. Price, "Vascular endothelial growth factor expression promotes the growth of breast cancer brain metastases in nude mice," *Clinical & Experimental Metastasis*, vol. 21, no. 2, pp. 107–118, 2004.

[64] J. Adams, P. J. Carder, S. Downey et al., "Vascular endothelial growth factor (VEGF) in breast cancer: comparison of plasma, serum, and tissue VEGF and microvessel density and effects of tamoxifen," *Cancer Research*, vol. 60, no. 11, pp. 2898–2905, 2000.

[65] C. L. Roland, K. D. Lynn, J. E. Toombs, S. P. Dineen, D. G. Udugamasooriya, and R. A. Brekken, "Cytokine levels correlate with immune cell infiltration after anti-VEGF therapy in preclinical mouse models of breast cancer," *PLoS One*, vol. 4, no. 11, Article ID e7669, 2009.

[66] D. I. Gabrilovich, H. L. Chen, K. R. Girgis et al., "Production of vascular endothelial growth factor by human tumors inhibits the functional maturation of dendritic cells," *Nature Medicine*, vol. 2, no. 10, pp. 1096–1103, 1996.

[67] D. Lindau, P. Gielen, M. Kroesen, P. Wesseling, and G. J. Adema, "The immunosuppressive tumour network: myeloid-derived suppressor cells, regulatory T cells and natural killer T cells," *Immunology*, vol. 138, no. 2, pp. 105–115, 2013.

[68] T. Voron, O. Colussi, E. Marcheteau et al., "VEGF-A modulates expression of inhibitory checkpoints on CD8+ T cells in tumors," *Journal of Experimental Medicine*, vol. 212, no. 2, pp. 139–148, 2015.

[69] G. T. Motz, S. P. Santoro, L.-P. Wang et al., "Tumor endothelium fasL establishes a selective immune barrier promoting tolerance in tumors," *Nature Medicine*, vol. 20, no. 6, pp. 607–615, 2014.

[70] T. Fujii, T. Hirakata, S. Kurozumi et al., "VEGF-A is associated with the degree of TILs and PD-L1 expression in primary breast cancer," *In Vivo*, vol. 34, no. 5, pp. 2641–2646, 2020.

[71] Z. Tang, S. Ding, H. Huang et al., "*HDAC1* triggers the proliferation and migration of breast cancer cells via upregulation of interleukin-8," *Biological Chemistry*, vol. 398, no. 12, pp. 1347–1356, 2017.

[72] S. Y. Park, J. A. Jun, K. J. Jeong et al., "Histone deacetylases 1, 6 and 8 are critical for invasion in breast cancer," *Oncology Reports*, vol. 25, no. 6, pp. 1677–1681, 2011.

[73] M. Terranova-Barberio, S. Thomas, N. Ali et al., "HDAC inhibition potentiates immunotherapy in triple negative breast cancer," *Oncotarget*, vol. 8, no. 69, pp. 114156–114172, 2017.

[74] Q. Cheng, J. T. Chang, J. Geradts et al., "Amplification and high-level expression of heat shock protein 90 marks aggressive phenotypes of human epidermal growth factor receptor 2 negative breast cancer," *Breast Cancer Research*, vol. 14, no. 2, pp. R62–R15, 2012.

[75] M. Yano, Z. Naito, M. Yokoyama et al., "Expression of hsp90 and cyclin D1 in human breast cancer," *Cancer Letters*, vol. 137, no. 1, pp. 45–51, 1999.

[76] H. Liu, Z. Zhang, Y. Huang et al., "Plasma *HSP90AA1* predicts the risk of breast cancer onset and distant metastasis," *Frontiers in Cell and Developmental Biology*, vol. 9, Article ID 639596, 2021.

[77] M. Klimczak, P. Biecek, A. Zylicz, and M. Zylicz, "Heat shock proteins create a signature to predict the clinical outcome in breast cancer," *Scientific Reports*, vol. 9, no. 1, p. 7507, 2019.

[78] T. Lin, Y. Qiu, W. Peng, and L. Peng, "Heat shock protein 90 family isoforms as prognostic biomarkers and their correlations with immune infiltration in breast cancer," *BioMed Research International*, vol. 2020, Article ID 2148253, 15 pages, 2020.

[79] H. Liu, C. Zang, A. Emde et al., "Anti-tumor effect of honokiol alone and in combination with other anti-cancer agents in breast cancer," *European Journal of Pharmacology*, vol. 591, no. 1-3, pp. 43–51, 2008.

[80] D. B. Avtanski, A. Nagalingam, M. Y. Bonner, J. L. Arbiser, N. K. Saxena, and D. Sharma, "Honokiol inhibits epithelial-mesenchymal transition in breast cancer cells by targeting signal transducer and activator of transcription 3/Zeb1/E-cadherin axis," *Molecular Oncology*, vol. 8, no. 3, pp. 565–580, 2014.

[81] A. Tang, K. Gao, L. Chu, R. Zhang, J. Yang, and J. Zheng, "Aurora kinases: novel therapy targets in cancers," *Oncotarget*, vol. 8, no. 14, pp. 23937–23954, 2017.

[82] J. Bertran-Alamillo, V. Cattan, M. Schoumacher et al., "AURKB as a target in non-small cell lung cancer with acquired resistance to anti-EGFR therapy," *Nature Communications*, vol. 10, no. 1, pp. 1812–1814, 2019.

[83] A. Ahmed, A. Shamsi, T. Mohammad, G. M. Hasan, A. Islam, and M. I. Hassan, "Aurora B kinase: a potential drug target for cancer therapy," *Journal of Cancer Research and Clinical Oncology*, vol. 147, no. 8, pp. 2187–2198, 2021.

[84] A. J. Ridley, H. F. Paterson, C. L. Johnston, D. Diekmann, and A. Hall, "The small GTP-binding protein rac regulates growth factor-induced membrane ruffling," *Cell*, vol. 70, no. 3, pp. 401–410, 1992.

[85] C. T. Mierke, S. Puder, C. Aermes, T. Fischer, and T. Kunschmann, "Effect of PAK inhibition on cell mechanics depends on Rac1," *Frontiers in Cell and Developmental Biology*, vol. 8, p. 13, 2020.

[86] K. Zins, T. Lucas, P. Reichl, D. Abraham, and S. Aharinejad, "A rac1/cdc42 GTPase-specific small molecule inhibitor suppresses growth of primary human prostate cancer xenografts and prolongs survival in mice," *PLoS One*, vol. 8, no. 9, Article ID e74924, 2013.

[87] N. El Baba, M. Farran, E. A. Khalil, L. Jaafar, I. Fakhoury, and M. El-Sibai, "The role of Rho GTPases in VEGF signaling in cancer cells," *Analytical Cellular Pathology*, vol. 2020, Article ID 2097214, 11 pages, 2020.

[88] C. P. Ong, W. L. Lee, Y. Q. Tang, and W. H. Yap, "Honokiol: a review of its anticancer potential and mechanisms," *Cancers*, vol. 12, no. 1, p. 48, 2019.

[89] H. Xu, W. Tang, G. Du, and N. Kokudo, "Targeting apoptosis pathways in cancer with magnolol and honokiol, bioactive constituents of the bark of Magnolia officinalis," *Drug Discoveries & Therapeutics*, vol. 5, no. 5, pp. 202–210, 2011.

[90] K. Stankov, S. Popovic, and M. Mikov, "C-KIT signaling in cancer treatment," *Current Pharmaceutical Design*, vol. 20, no. 17, pp. 2849–2880, 2014.

Hindawi
Evidence-Based Complementary and Alternative Medicine
Volume 2022, Article ID 9220443, 9 pages
https://doi.org/10.1155/2022/9220443

Research Article

Traditional Chinese Medicine Recognition Based on Target Detection

Bijun Lv,[1] Liyao Wu,[2] Tianran Huangfu,[2] Jiaru He,[2] Wenying Chen ,[2] and Lu Tan [2]

[1]*Department of Pharmacy, Yunfu Hospital of Traditional Chinese Medicine, Yunfu 527399, Guangdong, China*
[2]*Department of Pharmacy, The Third Affiliated Hospital of Southern Medical University, Guangzhou 510000, Guangdong, China*

Correspondence should be addressed to Wenying Chen; chenwenying2016@163.com and Lu Tan; tanlugmu@163.com

Received 22 December 2021; Revised 10 May 2022; Accepted 10 June 2022; Published 8 July 2022

Academic Editor: Daniel Kam Wah Mok

Traditional Chinese medicine (TCM) is widely used in China, but the large variety can easily lead to difficulties in visual identification. This study aims to evaluate the availability of target detection models to identify TCMs. We have collected images of 100 common TCMs in pharmacies, and use three current mainstream target detection models: Faster RCNN, SSD, and YOLO v5 to train the TCM dataset. By comparing the metrics of the three models, the results show that the YOLO v5 model has obvious advantages in the recognition of a variety of TCM, the mean average accuracy of the YOLO v5 is 94.33% and the FPS has reached 75, this model has a smaller number of parameters and solves the problem of detection and occlusion for small targets. Our experiments prove that the target detection technology has broad application prospects in the detection of TCM.

1. Introduction

Traditional Chinese medicine (TCM) refers to prescription drugs that can be directly used in traditional Chinese medicine clinics or the production of preparations after processing Chinese herbs. It has a long history and is widely used in China. However, one of the dilemmas we face now is that there are too many varieties of TCMs in clinical use, even the same kind of TCMs may look different in appearance due to different production regions or processing and preparation techniques [1]. Some different types of TCM have small differences in appearance, making it hard to distinguish them from each other. At present, the dispensing of TCM is still largely dependent on the pharmacist manually [2], so misidentification of TCM is still unavoidable, even experienced pharmacists have difficulty in ensuring that no identification errors occur in their heavy workload. Medication errors caused by misidentification of TCM can affect the health of patients. As China's population continues to grow and age at an accelerating rate, it has brought about an increasing demand for TCM, while the traditional model of TCM personnel has a long cycle, and development is lagging behind the advancement of modern medical technology. Although the development of TCM is now strongly supported by the Chinese government, there is still a shortage of professionals in TCM. The continuous development of deep learning in recent years seems to bring opportunities for the development of TCM, with research in TCM diagnostic models [3,4], TCM toxicity component prediction [5], and TCM theory research [6], which also provides new methodologies for TCM modernization.

In this article, we use the mainstream target detection algorithms represented by Faster RCNN, SSD, and YOLO v5 to train and test by constructing a TCM dataset in VOC format. Experiments show the potential of target detection technology to assist pharmacists with dispensing and verification. The main contributions of this study are the following:

(i) There are few attempts to introduce deep learning into TCM recognition, and this study explores the introduction of target detection into TCM recognition, which is a crossover study in the field of deep learning and TCM.

(ii) There are few publicly available TCM image datasets, we have taken a large number of TCM images and completed manual labeling, and we will open up the datasets we have collected and labeled for evaluation testing in subsequent studies.

(iii) This study compares different target detection algorithms applied to TCM recognition and analyzes the advantages and disadvantages of each, and the results show that YOLO v5 performs better than Faster RCNN and SSD. It provides a reference for subsequent studies.

2. Related Work

2.1. Literature Review. Previous studies of medicinal plants identification mainly focused on image classification by artificially set features. Herdiyeni [7], Mareta [8], and Song [9] classified medicinal plants images by extracting the variability in superficial features such as color, shape, or texture of medicinal plants by different classifiers. This kind of method could achieve satisfactory results, but as we mentioned above there are many types of TCM, so the manual setting of features is limited by the experience of the designer, the environment, and the location of the object, which leads to the lack of robustness of the features. In addition, the use of the manually setting features leads to a large computational effort of the model, and these deficiencies reduce the application scenarios and scope of the method Due to the continuous development of deep learning, Convolutional neural networks (CNN) have achieved outstanding results in computer vision classification and have been applied in many disciplines. CNN is characterized by the addition of convolutional layers and pooling layers; the new network structure can be formed based on different combinations and architectures of the convolutional layers and the pooling layers. In recent years, researchers have successively proposed a series of excellent deep learning models based on CNN, such as AlexNet (2012), VGGNet (2014), ResNet (2015), Inception (2015), DenseNet (2017), and so on, which have all performed well in various visual recognition competitions. For the first time, the AlexNet model [10] uses CNN for visual tasks in complex situations, replacing the Sigmoid function with the ReLu activation function, and preventing overfitting problems through dropout and image enhancement methods. VGGNet [11] and GoogleNet [12] improve the recognition accuracy of the model by continuously deepening the network structure, GoogleNet introduces the Inception module to reduce the number of parameters and increase the width of the model. By adding the residual module, ResNet [13] solves the problem that the error rate of the model does not decrease but increases when the number of network layers is greatly deepened and achieves a higher accuracy rate. DenseNet [14] is based on ResNet to connect all the layers with the dense connection, which reduces the number of parameters and makes the network more efficient. At present, some scholars have used CNN for the classification and recognition of Chinese medicine-related images. Huang et al. [15] proposed a network model that can be used to identify Chinese Herbal Medicine Leaves by improving the AlexNet model. Sun, et al. [16] used the VGG16 model to classify 95 Chinese herbal medicines with an average accuracy of 71%. The DenseNet-based recognition model proposed by Xing, et al. [17] could classify images of 80 Chinese herbal medicines with a maximum recognition rate of 97.3%. Liu, et al. [18] used GoogLeNet to classify images of 50 Chinese herbal medicine plants under complex background conditions, the accuracy of TOP-1 was 62.8%. In addition, a few studies used multiple models to compare results, Marwaha, et al. [19] used VGG16, MobileNet, Xception, and Inceptionv3 to classify the microscopic images of the two herbal plant powders with the highest accuracy of 96.4%. Azeez, et al. [20] compared the models of Inceptionv3, Resenet, MobileNet, and Inception-Resenet v2 to classify and identify 5 kinds of herbal plants, with an average accuracy rate of up to 95.5%. Tan, et al. [21] used different CNNs, including VGG, ResNet, Inceptionv4, and DenseNet to identify different types of Zanthoxyli Pericarpium. By comparing them with support vector machines and K-means clustering algorithms, the highest recognition accuracy of the CNN model is 99.35%, which is significantly higher than that of traditional detection and classification methods. Hu et al. [22] proposed to apply multitask learning to recognize Chinese herbal pieces pictures, and this study combined deep learning model and traditional features to improve model accuracy, and also achieved excellent results. Multitask learning enabled the model to have the ability to handle multiple tasks simultaneously, but for TCM recognition there seems to be no need to apply multitask learning, and as mentioned earlier, the manual design of features is laborious and relies on the designer's experience.

From the research mentioned above, it can be seen that deep learning has shown excellent performance in the visual task of TCM detection, the current related research mainly focuses on the classification of TCM, that is, determining the category of the object based on the information in the image. Generally speaking, there are still many challenges and limitations in applying deep learning methods to the field of TCM image processing. For example, in the actual scene of TCM pharmacies, TCMs are often used in combination, which means that multiple TCMs are likely to be present at the same time. When the type and number of recognition targets are uncertain, if we want to know the specific location of the targets, the classification model alone is not enough to deal with the actual problem. Target detection requires identifying targets in an image and determining their location and class. Therefore, target detection is more practical than target classification in work, which provides a basis for the development of automated equipment to assist pharmacists.

Girshick et al. designed the RCNN based on CNN [23], which made a great improvement in the target detection efficiency of the model, and this technique has been developed rapidly on this basis. In recent years, many target detection models such as Faster RCNN, SSD, and YOLO have appeared in the field of target detection, and they have been widely used in many detection problems [24]. The current target detection algorithms are usually divided into

two categories, a two-stage-detector represented by Faster RCNN and a one-stage-detector represented by SSD and YOLO. The advantages between the two are different: the two-stage-detector can achieve higher accuracy, but the generation of target candidate regions will slow down the speed; While the one-stage-detector can maintain a certain accuracy while not needing to generate target candidate regions first, the detection network can directly predict the object category and position, which has obvious advantages in detection speed. In previous studies, the application of a two-stage model or one-stage model transfer learning to the scope of TCM has mainly focused on TCM diagnosis [25,26], and there is no research on its application to image processing of TCM for the time being.

The accuracy of the model is an important metric to determine whether the model can assist the pharmacist's work. Secondly, in a busy hospital scene, whether the model can complete real-time detection is not negligible. The calculation of the deep learning network model takes a lot of time to get the prediction results, and the role of the model in the daily work of the pharmacist is limited. Accurate identification of TCMs and rapid determination of their location are key technologies of the model. But we have not found any relevant research yet, so how to apply target detection technology to the work of pharmacists has research significance and potential application value.

2.2. Target Detection Algorithm. Faster RCNN [27] uses a region proposal network (RPN) instead of selective search, which saves the time required for detection and realizes target detection. The detection process is mainly after the image is feature extracted through the CNN, the RPN generates candidate regions of different sizes at each position of the extracted feature map, and finally, the Region Proposal is filtered by the Softmax function. The region of interest pooling is used to integrate the feature map of the CNN and the Region Proposal generated by the RPN, and then the classification is performed to confirm whether it is the detection target, and the position of the target is obtained through regression.

Liu et al. [28] proposed the Single Shot MulitBox Detector (SSD) target detection algorithm in 2016. SSD draws on the anchor mechanism of Faster RCNN and the end-to-end one-stage structure in which target classification and position regression are directly performed in convolution in the YOLO algorithm. The backbone network of the SSD algorithm is based on VGG16. The fully connected layers FC6 and FC7 are replaced with Conv6 and Conv7, the dropout layer and FC8 layer are removed, and adds some new convolutional layers for the extraction and prediction of multiscale feature maps. The advantage of multiscale is that feature maps of different sizes have different emphases on predicting objects. Large-scale feature maps generally contain more detailed information and focus on predicting small objects. Small-scale feature maps contain more global information and focus on predicting large objects.

Redmon et al. [29] proposed a regression-based target detection algorithm YOLO (You only look once) in 2016. YOLO provides a new idea for target detection, that is, using a simple structure of the convolutional network to directly complete the feature extraction, classification, and regression of target detection. YOLO divides the entire image into several grid cells, uses the center of each grid as the center of the bounding box to directly predict, and then eliminates bounding boxes with low probability through a threshold. This method significantly reduces the number of repeated calculations. Compared with the RCNN series of algorithms, YOLO has better overall performance. It realizes the end-to-end target detection process using a CNN, and the detection speed is faster. The YOLO series has been updated many times [30], and now it has launched the YOLO v5 version, which is an improved target detection network based on YOLO v4 [31] by Ultralytics LLC in 2020. The author's experimental results show that YOLO v5 [32] can greatly increase the speed of model calculations with almost no loss of accuracy, and provides an ONNX framework to convert between different models, which can be deployed to embedded and mobile phones. The main structure of YOLO v5 is similar to YOLO v4. As can be seen from Figure 1(a), YOLO v5 incorporates the Focus structure in the first layer of the backbone network. Suppose the input image size is $4 \times 4 \times 3$, after slicing operation and channel concating operation, it becomes a $2 \times 2 \times 12$ image, and then sends the $2 \times 2 \times 12$ feature maps to convlutional layer to get the output. The Focus structure is added to transform the high-resolution image information from the spatial dimension to the channel dimension, which maximizes the preservation of the input information and reduces the input size, which is beneficial to improving the speed of training networks and inference.

YOLO v5 references the Cross Stage Partial Network (CSPNet) in the backbone and neck sections, as shown in Figure 1(d) and 1(e), YOLO v5 uses two different CSP structures. The CSP structure with residual components is used in the backbone network for feature extraction, while the CSP structure in Neck uses convolutional operations instead of residual components. The CSP structure aims to divide the feature map into two parts, one part continues the convolution operation to obtain deeper feature information, and the other part is concated with the feature map after the convolution operation. The advantages of this design include: reducing computation, improving inference speed, reducing memory cost, and ensuring accuracy.

Spatial pyramid pooling (SPP) layer is added at the end of the backbone network due to the inconsistent size of the input images, which would increase the computation and consume a lot of training and inference time if reshape operation is performed on each image. The SPP layer, as shown in Figure 1(f), goes through different sizes of pooling layers to get the pooled output. The pooling kernel size and step size change adaptively according to the different image sizes during the maximum pooling, and the output of $1 + 4 + 16$ dimensions is obtained after the SPP layer for any size of the feature map so that the size of the feature map input to the backbone network is no longer limited. In addition, the SPP layer plays an essential role in separating contextual features.

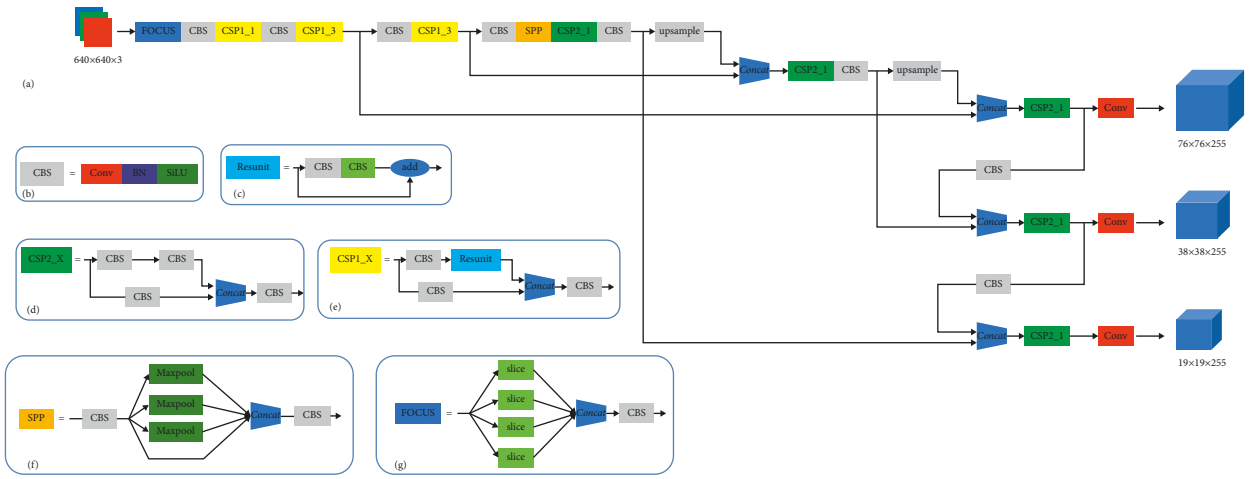

Figure 1: YOLO v5 network structure diagram.

In the Neck part of the network, YOLO v5 uses Feature Pyramid Network (FPN) and Path Aggregation Network (PANet). FPN is one of the more popular feature fusion methods that can be predicted separately on multiscale feature maps. The FPN algorithm is divided into two paths, one is bottom-top and the other is top-down, using a horizontal connection. Although the FPN structure adds less computation, this structure effectively fuses low-resolution, high-semantic feature maps with high-resolution, high-geometric feature maps. This enables the fused feature maps to have both high-level semantic features and low-level texture contour features, making full use of the features of different layers.

YOLO v5 takes reference from PANet and adds a bottom-top feature pyramid structure after the up-sampling of FPN for feature fusion. Different from PANet which uses the shortcut connection when fusing two feature maps, YOLO v5 fuses features by concating. After three different concating operations, three feature maps of different sizes are obtained, and then the CSP structure and convolution operations are added separately to make predictions on each of the three final feature maps.

The structure of FPN can extract strong semantic features from top-bottom, while the structure of PAN can extract strong positioning features from bottom-top. This method of fusing the feature maps of different layers of the convolutional neural network is more beneficial to feature extraction.

3. Methods

3.1. TCM Dataset. Since there is no public benchmark TCM dataset yet, we manually collected and labeled 2352 images, then expanded them to 23520 images by data augmentation, including Mirror flip, horizontal flip, rotation, contrast enhancement, affine transformation, mosaic enhancement, and divided the training set, validation set, and test set randomly according to the ratio of 6 : 2: 2.

The dataset covers 100 kinds of TCM images (shown in Figure 2). Considering the practical needs of the work, the dataset also includes some partially occluded, overlapping, multitarget and low-resolution images of TCM to fit the practical application scenarios to increase the robustness and generalization ability of the model. Unify the format of the dataset to the POSCAL VOC2007 format applicable to the three algorithms of Faster RCNN, SSD, and YOLO v5. We use the labelimg tool to mark the images, including the category and bounding box position information of the target to be recognized.

3.2. Models Training. The experimental platform configuration of this article is computer operating system: Windows10, GPU: GeForce GTX 2080Ti, CPU: Intel(R) Core(TM) i7-10700, memory: Kingston 16G*2 DDR4 3200Mhz. For the anchor selection, the anchor size of our dataset is obtained by k-means clustering instead of using the default anchor of the coco dataset. This approach allows the network to converge faster and learn the features of the images in our dataset better. The parameters that the network can learn to update include convolutional kernel parameters and bias parameters, but not Hyperparameter. Hyperparameters are manually set parameters that need to be specified before training and testing the network. Based on the experience of a large number of previous experiments, we analyzed and compared the optimal values of loss convergence, precision, and recall of the experimental results, and finally decided on the choice of hyperparameters. The initial learning rate of the weights is set to 0.001, and each batch contains 64 pictures. Momentum is set to 0.9, and the weight decay coefficient is set to 0.0001. The depth_multiple and width_multiple of the YOLO v5 model choose the default parameters, both of which are 1. The methods to avoid model overfitting in the experiments are as follows: 1) We randomly divide the dataset into training set, testing set, and validation set in the ratio of 6 : 2 : 2. In the process of training the model, the current constructed model is tested in each epoch using validation set to get the loss and accuracy. Comparing the accuracy of the validation set with the training set, If it performs well on the training set, but the

Figure 2: Example images of TCM.

performance on the validation set is bad, which indicates that the model is overfitting and we will stop training and analyze the cause, adjust the parameters and data, retrain the model. The experimental results show that our trained model performs well on the test set without overfitting. 2) When training the model iteratively, we set up an early stop mechanism to measure the performance of each iteration. When the validation loss starts to increase, the training of the model is stopped to prevent overfitting. 3) We increase the number of training samples through data augmentation, including horizontal flip, affine transformation, Mosaic data augment, etc. Using dropout to increase regularization in training the model can also prevent overfitting.

3.3. Evaluation Metrics. There are some important algorithm evaluation metrics in target detection including precision, recall, mean average accuracy (mAP). It is defined as follows:

$$\text{Precision} = \frac{T_P}{F_P + T_P}, \tag{1}$$

$$\text{Recall} = \frac{T_p}{F_p + F_N}, \tag{2}$$

$$AP = \int_0^1 p(r)dr, \tag{3}$$

$$mAP = \frac{1}{n}\sum_{i=1}^{n} APi. \tag{4}$$

In the formula, True Positive (T_P) is judged as a positive sample and it is a positive sample in fact; False Positive (F_P) is judged as a positive sample and it is a negative sample in fact; False Negative (F_N) is judged as a negative sample and it is a positive sample. Average accuracy (AP) is the average accuracy for a certain category, mAP is the mean average accuracy of all categories.

4. Results and Discussion

4.1. Results for Different Epochs. The experiment recorded the values of Precision, Recall, and mAP of the three models at different Epochs. It can be seen in Figure 3 that, with the increase of Epochs, the metrics of the three models are also increasing, which means that the detection effect of the network model is better. After 45 Epochs, YOLO v5 performed better than Faster RCNN and SSD for the same Epochs.

4.2. The Results of Evaluation Metric. The comparison results of the three models on the TCM test set are shown in Table 1. Compared with Faster RCNN and SSD, the precision of the YOLO v5 model has increased by 11.15% and 17.86%, the recall has increased by 8.40% and 15.53%, and the mAP has increased by 8.77% and 13.01%, respectively. The results of these metrics showed that the YOLO v5 model outperformed both the Faster RCNN and SSD on the same TCM dataset. Our experimental results are similar to those of other studies that have applied target detection to medical images. For example, Zhao et al. [33] proposed the use of YOLO v5 and SSD for the real-time detection of blood cells. The authors trained and validated two target detection networks using a blood cell dataset that included red blood cells, white blood cells, and platelets. The experimental results showed that the mAP of YOLO v5 was 0.96, while the mAP of SSD was only 0.62. In terms of detection speed, the detection frame rate of YOLO v5 can reach 62 FPS, which is almost 100 times that of SSD. This demonstrated that YOLO v5 was more accurate in identifying blood cells and could detect them in real-time, making it more suitable for clinical

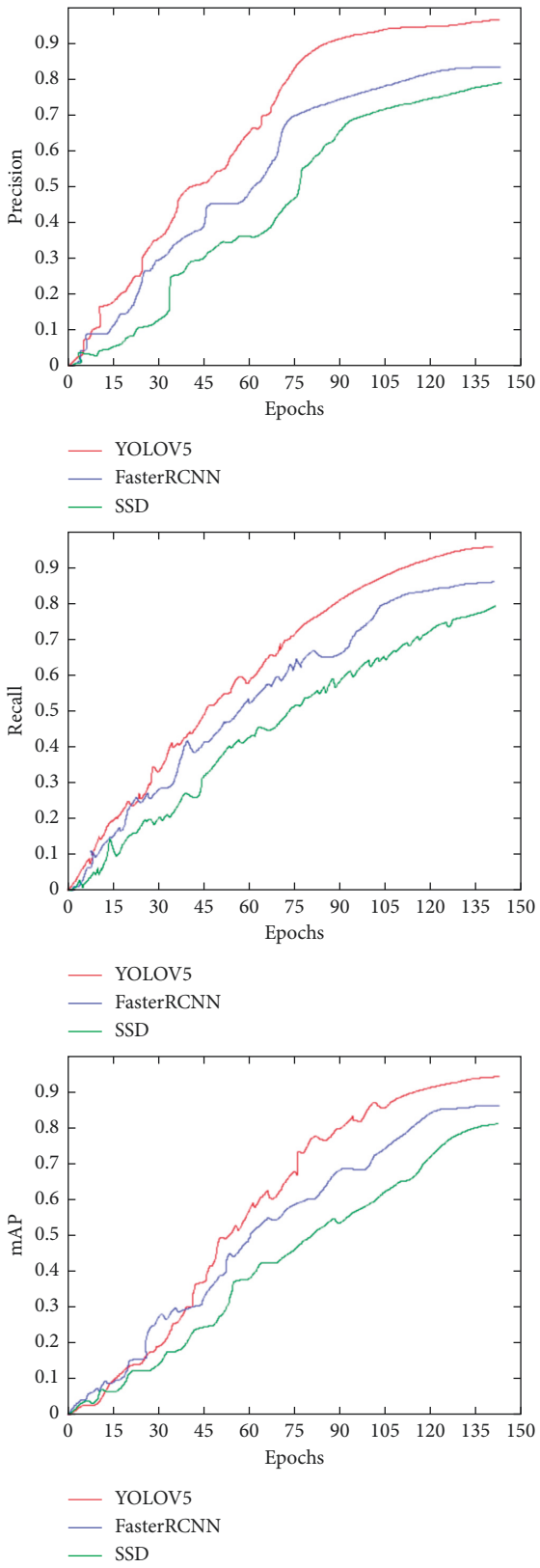

Figure 3: Relationship of epochs with mAP, precision, and recall.

applications than SSD. Qu et al. [34] applied YOLO v5 and Faster RCNN to the CT image detection of COVID-19 and conducted a comparative experiment using the same dataset.

Table 1: Evaluation of deep learning models.

Algorithm	Precision/%	Recall/%	mAP/%
Faster RCNN	85.12	86.71	85.56
SSD	78.41	79.58	81.32
YOLO v5	96.27	95.11	94.33

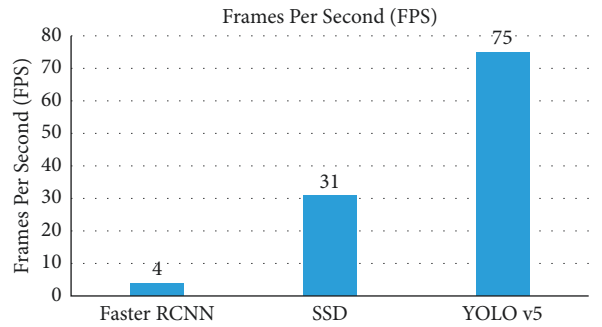

Figure 4: FPS of deep learning models.

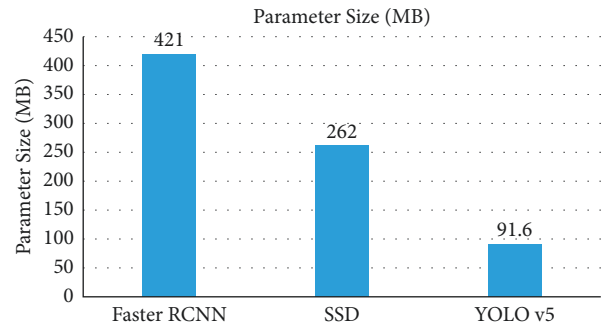

Figure 5: Parameter size of deep learning models.

The results showed that the mAP of YOLO v5 reached 0.623, while that of Faster RCNN was only 0.466. YOLO v5 showed significant advantages in identifying and localizing COVID-19 abnormalities on chest radiographs, providing greater practical value in clinical practice.

4.3. Real-Time Comparison of Models. The common metric for evaluating the detection speed of the model is Frames Per Second (FPS). The FPS of the three models under the same experimental setting is shown in Figure 4. YOLO v5 can detect 75 images per second, and the detection speed is more than 58% higher than that of SSD. And two-stage detector Faster RCNN of the FPS is only 4, significantly behind in comparison with the other two models, it is difficult to achieve real-time recognition, which limits its potential applications. The FPS of the YOLO v5 and SSD models in this experiment has reached the effect of real-time detection, which proves that the one-stage algorithm has more advantageous than the two-stage in terms of detection speed. The SSD algorithm outputs candidate regions for each convolutional layer during the operation, resulting in more candidate regions generated than YOLO v5, so the detection speed is slow.

4.4. Parameter Size Comparison. The model can be deployed through the front-end to avoid network latency in data

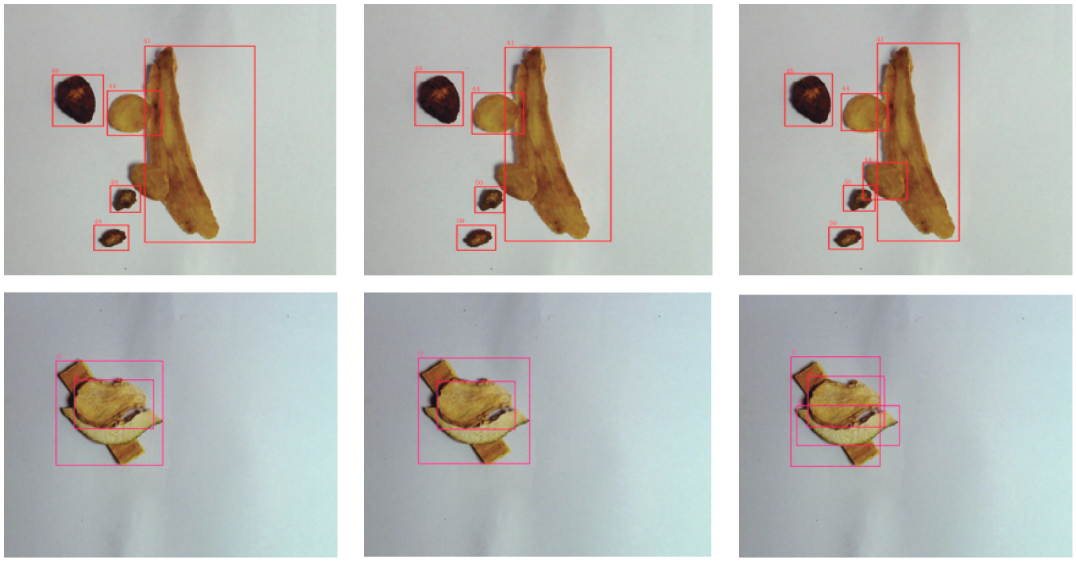

(a) (b) (c)

Figure 6: The detection results of test images. (a) the detection result of the image in the Faster RCNN; (b) the detection result of the image in the SSD; (c) the detection result of the image in the YOLO v5.

propagation, but running the model requires loading weights, and a large number of parameters will occupy the running memory of the device resulting in slower operation, and the size of the model parameters affects the deployment cost of the device. Although the model size can be reduced by model compression, this method tends to reduce the accuracy of the model, so it is more appropriate to choose a model with a smaller number of parameters while ensuring accuracy and real-time performance. The parameter sizes of the three network models are shown in Figure 5, the parameters of YOLO v5 are significantly smaller compared to the other two models. The CSP module of YOLO v5 can optimize repeated gradient information through the use of split and merge strategies across stages, and effectively reduce model parameters. Therefore, the deployment cost of YOLO v5 is lower, and it is easy to quickly deploy and upgrade online.

4.5. Results of Actual Sample Tests. In order to visualize the recognition effect of Faster RCNN, SSD and YOLO v5 on TCM mentioned in this paper, we randomly selected samples from the test dataset in the three algorithms for comparison. As shown in Figure 6, the YOLO v5 network can detect the missed targets of Faster RCNN and SSD, which is more advantageous in dealing with the problems of small target detection and target occlusion, and can complete the detection task well in practical scenarios. This may be related to Mosaic Augmentation, which allows random scaling, distribution, and stitching of images to produce more data and improve the accuracy of the YOLO model for small target detection.

5. Conclusion and Future Work

In this article, we briefly introduce the development of CNNs and target detection algorithms, focusing on the comparison of three current mainstream target detection methods, namely Faster RCNN, SSD, and YOLO v5, and then train and test the three models using TCM datasets. It is concluded that the recently released YOLO v5 model has significant advantages over faster RCNN and SSD in terms of mAP, FPS, parameter size, and actual detection effect of target detection for TCM.

Overall, the deep learning-based target detection algorithm provides a new way of thinking and approach for TCM detection, not only to identify specific targets in images, but also to determine where the targets are located, with the advantages of accuracy, speed, and ease of deployment. The target detection model can effectively reduce labor input and reduce the work intensity of pharmacists by performing operations related to detection of TCM in specific scenarios, and the application prospect is wide. Through the analysis of the experimental results, we found the direction of model performance improvement. In further work, we will try to reduce the time required for model inference through model pruning and lightweight with almost no loss of accuracy, so that the algorithm is suitable for TCM detection in real scenes. In addition, we will continue to supplement the dataset to ensure the comprehensiveness of the TCM dataset.

Data Availability

The data used to support the findings of this study are available from the corresponding author upon reasonable request.

Conflicts of Interest

The authors declare that they have no conflicts of interest.

References

[1] T. Li, F. Sun, R. Sun, L. Wang, M. Li, and H. Yang, "Chinese herbal medicine classification using convolutional neural network with multiscale images and data augmentation," in *Proceedings of the 2018 International Conference on Security, Pattern Analysis, and Cybernetics (SPAC)*, Jinan, China, 2018.

[2] C. Y. Lin and H. Ping-Jung, "Development of an automatic dispensing system for traditional Chinese herbs," *Journal of Healthcare Engineering*, vol. 2017, Article ID 9013508, 12 pages, 2017.

[3] H. Zhang, W. Ni, J. Li, and J. Zhang, "Artificial intelligence–based traditional Chinese medicine assistive diagnostic system: validation study," *JMIR medical informatics*, vol. 8, no. 6, Article ID e17608, 2020.

[4] X. Wang, J. Liu, C. Wu et al., "Artificial intelligence in tongue diagnosis: using deep convolutional neural network for recognizing unhealthy tongue with tooth-mark," *Computational and Structural Biotechnology Journal*, vol. 18, pp. 973–980, 2020.

[5] Q. Wu, C. Cai, P. Guo et al., "In silico identification and mechanism exploration of hepatotoxic ingredients in traditional Chinese medicine," *Frontiers in Pharmacology*, vol. 10, p. 458, 2019.

[6] Q. Hu, T. Yu, J. Li, Q. Yu, L. Zhu, and Y. Gu, "End-to-End syndrome differentiation of Yin deficiency and Yang deficiency in traditional Chinese medicine," *Computer Methods and Programs in Biomedicine*, vol. 174, pp. 9–15, 2019.

[7] Y. Herdiyeni, A. R. Ginanjar, M. R. L. Anggoro, S. Douady, and E. A. M. Zuhud, "Medleaf: mobile biodiversity informatics tool for mapping and identifying indonesian medicinal plants," in *Proceedings of the 2015 7th International Conference of Soft Computing and Pattern Recognition (SoCPaR)*, Fukuoka, Japan, 2015.

[8] A. Mareta, I. Soesanti, and O. Wahyunggoro, "Herbal leaf classification using images in natural background," in *Proceedings of 2018 International Conference on Information and Communications Technology (ICOIACT)*, pp. 612–616, Yogyakarta, Indonesia, 2018.

[9] Y. S., Y. Li Li et al., "Automatic target segmentation based on texture for microscopic images of chinese herbal powders," in *Proceedins of the 2013 25th Chinese Control and Decision Conference (CCDC)*, Guiyang, China, 2013.

[10] A. Krizhevsky, I. Sutskever, and G. E. Hinton, "Imagenet classification with deep convolutional neural networks," *Advances in Neural Information Processing Systems*, vol. 25, pp. 1097–1105, 2012.

[11] K. Simonyan and A. Zisserman, "Very deep convolutional networks for large-scale image recognition," 2014, https://arxiv.org/abs/1409.1556.

[12] K. He, X. Zhang, S. Ren, and J. Sun, "Deep residual learning for image recognition," 2016, https://arxiv.org/abs/1512.03385.

[13] C. Szegedy, W. Liu, Y. Jia et al., "Going deeper with convolutions," 2015, https://arxiv.org/abs/1409.4842.

[14] G. Huang, Z. Liu, L. Van Der Maaten, and K. Q. Weinberger, "Densely connected convolutional networks," 2017, https://arxiv.org/abs/1608.06993.

[15] F. Huang, L. Yu, T. Shen, and L. Jin, "Chinese herbal medicine leaves classification based on improved AlexNet convolutional neural network," in *Proceedings of the 2019 IEEE 4th Advanced Information Technology, Electronic and Automation Control Conference (IAEAC)*, Chengdu, China, 2019.

[16] X. Sun and H. Qian, "Chinese herbal medicine image recognition and retrieval by convolutional neural network," *PLoS One*, vol. 11, no. 6, Article ID e0156327, 2016.

[17] C. Xing, Y. Huo, X. Huang, C. Lu, Y. Liang, and A. Wang, "Research on image recognition technology of traditional chinese medicine based on deep transfer learning," in *Proceedings of the 2020 International Conference on Artificial Intelligence and Electromechanical Automation (AIEA)*, IEEE, Tianjin, China, 2020.

[18] S. Liu, W. Chen, and X. Dong, "Automatic classification of chinese herbal based on deep learning method," in *Proceedings of the 2018 14th International Conference on Natural Computation, Fuzzy Systems and Knowledge Discovery (ICNC-FSKD)*, Huangshan, Anhui, China, 2018.

[19] R. Marwaha and B. Fataniya, "Classification of indian herbal plants based on powder microscopic images using transfer learning," in *Proceedings of the 2018 Fifth International Conference on Parallel, Distributed and Grid Computing (PDGC)*, Solan, India, 2018.

[20] Y. R. Azeez and C. Rajapakse, "An application of transfer learning techniques in identifying herbal plants in sri lanka," in *Proceedings of the 2019 International Research Conference on Smart Computing and Systems Engineering (SCSE)*, Colombo, Sri Lanka, 2019.

[21] C. Tan, C. Wu, Y. Huang, C. Wu, and H. Chen, "Identification of different species of Zanthoxyli Pericarpium based on convolution neural network," *PLoS One*, vol. 15, no. 4, Article ID e0230287, 2020.

[22] J.-L. Hu, Y.-K. Wang, Z.-Y. Che et al., "Image recognition of Chinese herbal pieces based on multi-task learning model," in *Proceedings of the 2020 IEEE International Conference on Bioinformatics and Biomedicine (BIBM)*, Seoul, Korea, 2020.

[23] R. Girshick, J. Donahue, T. Darrell, and J. Malik, "Rich feature hierarchies for accurate object detection and semantic segmentation," 2014, https://arxiv.org/abs/1311.2524.

[24] J. Kim, J. Y. Sung, and S. Park, "Comparison of Faster-RCNN, YOLO, and SSD for Real-Time Vehicle Type recognition," in *Proceedings the 2020 IEEE International Conference on Consumer Electronics-Asia (ICCE-Asia)*, Seoul, Korea, 2020.

[25] Z. Liu, H. He, S. Yan, Y. Wang, T. Yang, and G. Z. Li, "End-to-End models to imitate traditional Chinese medicine syndrome differentiation in lung cancer diagnosis: model development and validation," *JMIR Med Inform*, vol. 8, no. 6, Article ID e17821, 2020.

[26] Z. An, E. Nonaka, R. Wu, M. Nakata, and Q.-W. Ge, "Automatic diagnosis of tongue using mask-RCNN," in *Proceedings of the 2021 36th international technical conference on circuits/systems, Computers and Communications (ITC-CSCC)*, Jeju, Korea, 2021.

[27] S. Ren, K. He, R. Girshick, and J. Sun, "Faster R-CNN: towards real-time object detection with region proposal networks," *IEEE Transactions on Pattern Analysis and Machine Intelligence*, vol. 39, no. 6, pp. 1137–1149, 2017.

[28] W. Liu, D. Anguelov, D. Erhan et al., "Ssd: Single Shot Multibox detector," 2016, https://arxiv.org/abs/1512.02325.

[29] J. Redmon, S. Divvala, R. Girshick, and A. Farhadi, "You only look once: unified, real-time object detection," 2016, https://arxiv.org/abs/1506.02640.

[30] J. Fang, Q. Liu, and J. Li, "A deployment scheme of YOLOv5 with inference optimizations based on the triton inference server," in *Proceedings of the 2021 IEEE 6th international conference on cloud computing and big data analytics (ICCCBDA)*, Chengdu, China, 2021.

[31] G. Jocher, A. Stoken, and J. Borovec, "Ultralytics/yolov5: V4. 0-Nn. Silu () Activations Weights & Biases Logging Pytorch Hub Integration," 2021, https://zenodo.org/record/4418161#. YrWz6v1BzIU.
[32] A. Bochkovskiy, C. Y. Wang, and H. Y. M. Liao, "Yolov4: Optimal Speed and Accuracy of Object detection," 2020, https://arxiv.org/abs/2004.10934.
[33] J. Zhao, Y. Cheng, and X. Ma, "A real time intelligent detection and counting method of cells based on YOLOv5," in *Proceedings of the 2022 IEEE International Conference on Electrical Engineering, Big Data and Algorithms (EEBDA)*, Changchun, China, 2022.
[34] R. Qu, Y. Yang, and Y. Wang, *COVID-19 Detection Using CT Image Based on YOLOv5 Network*, 2021, https://arxiv.org/abs/2201.09972.

Hindawi
Evidence-Based Complementary and Alternative Medicine
Volume 2022, Article ID 7252213, 7 pages
https://doi.org/10.1155/2022/7252213

Research Article

Combined Acupoints for the Treatment of Patients with Obesity: An Association Rule Analysis

Ping-Hsun Lu,[1,2] **Yu-Yang Chen**,[3] **Fu-Ming Tsai**,[4] **Yuan-Ling Liao**,[1] **Hui-Fen Huang**,[1,2] **Wei-Hsuan Yu**,[3] **and Chan-Yen Kuo**[4]

[1]*Department of Chinese Medicine, Taipei Tzu Chi Hospital, Buddhist Tzu Chi Medical Foundation, New Taipei City, Taiwan*
[2]*School of Post-Baccalaureate Chinese Medicine, Tzu Chi University, Hualien, Taiwan*
[3]*Department of Mathematics National Central University, Taoyuan, Taiwan*
[4]*Department of Research, Taipei Tzu Chi Hospital, Buddhist Tzu Chi Medical Foundation, New Taipei City, Taiwan*

Correspondence should be addressed to Hui-Fen Huang; huanghf37@mail.tcu.edu.tw, Wei-Hsuan Yu; whyu@math.ncu.edu.tw, and Chan-Yen Kuo; cykuo863135@gmail.com

Received 9 August 2021; Revised 28 January 2022; Accepted 15 February 2022; Published 17 March 2022

Academic Editor: Talha Bin Emran

Obesity is a prevalent metabolic disease that increases the risk of other diseases, such as hypertension, diabetes, hyperlipidemia, cardiovascular disease, and certain cancers. A meta-analysis of 11 randomized sham-controlled trials indicates that acupuncture had adjuvant benefits in improving simple obesity, and previous studies have reported that acupoint combinations were more useful than single-acupoint therapy. The Apriori algorithm, a data mining-based analysis that finds potential correlations in datasets, is broadly applied in medicine and business. This study, based on the Apriori algorithm-based association rule analysis, found the association rules of acupoints among 11 randomized controlled trials (RCTs). There were 23 acupoints extracted from 11 RCTs. We used Python to calculate the association between acupoints and disease. We found the top 10 frequency acupoints were Extra12, TF4, LI4, LI11, ST25, ST36, ST44, CO4, CO18, and CO1. We investigated the 1118 association rule and found that $\{LI4, ST36\} \geq \{ST44\}$, $\{LI4, ST44\} \geq \{ST36\}$, and $\{ST36, ST44\} \geq \{LI4\}$ were the most associated rules in the data. Acupoints, including LI4, ST36, and ST44, are the core acupoint combinations in the treatment of simple obesity.

1. Introduction

Obesity is a disease involving an excessive amount of body fat that increases the risk of conditions, such as cardiovascular diseases, diabetes mellitus, elevated blood pressure, and certain cancers. It is estimated that by the year 2030, there will be 2.16 billion individuals who are overweight and 1.12 billion individuals with obesity globally [1, 2]. Moreover, the obesity and overweight epidemics are not only limited to developed countries but are also increasing among people in developing countries. Obesity is often defined by body mass index (BMI) values. According to the WHO definition, a BMI of over 25 kg/m^2 indicates an overweight state, while one over 30 kg/m^2 is considered obese [3]. Simple obesity refers to obesity caused by no obvious etiology of genetic, endocrine, and metabolic diseases, and it is classified as nonpathological obesity [4, 5]. Simple obesity is related to diet habits, lack of exercise, and characteristics of adipose tissue [6–8]. Weight can be managed through dietary changes and lifestyle modifications, such as regular exercise and regular sleeping hours; however, the results may be unsatisfactory [9]. Pharmaceutical treatments, such as fenfluramine and sibutramine, are effective but may be limited due to safety issues [10, 11].

As an alternative intervention, acupuncture is relatively safe and convenient and has been used in clinical practice for obesity therapy [12]. Its possible mechanisms include endocrine system regulation, digestion promotion, oxidative stress reduction, and metabolism modulation [13]. A recent meta-analysis demonstrated that acupuncture therapy is effective for the reduction of BMI, body fat mass (BFM), hip circumference (HC), and waist circumference (WC) [12].

When treating diseases, the Yellow Emperor's Internal Classic and the ancient meridian theory guide the selection and combination of acupoints, which are key for successful acupuncture treatment [14, 15]. However, there is no clear consensus regarding the standard acupoint combinations for simple obesity treatment.

Data mining techniques have recently been used in Chinese medicine and acupuncture. Based on these methods, previous studies provide benchmarks for selecting and combining herbs in the herbal bath for treating uremic pruritus [16], acupoints for treating diabetic gastroparesis [17], chronic obstructive pulmonary disease [18], and Alzheimer's disease [19]. Acupuncture therapy is based on selecting and combining numerous acupoints simultaneously in clinical practice. The Apriori algorithm-based association rule is a promising and useful strategy with which to explore the underlying rules. Nevertheless, there is no consensus on the standard acupoint combinations for obesity treatment. Apriori determines each data's association, identifies the frequency of every item in the database, and finds the association with other objects. This clarifies which items are the most relative [20].

While data mining has been used to explore acupoint combinations for treating obesity, the data they analyzed came from low-level evidence sources, not randomized controlled trials (RCTs), and some were studies of secondary obesity [21, 22]. We explored the promising core acupoint combinations used to treat simple obesity using Apriori association rule analysis via a meta-analysis of 11 RCTs [12].

2. Materials and Methods

2.1. Data Sources and Selection Criteria. This study was based on a previous meta-analysis of 11 RCTs on acupuncture treatment for obesity. The data on acupoints used for obesity were extracted from 11 RCTs [12]. All enrolled studies were required to meet the following criteria: (1) the patients met the diagnostic criteria for being overweight (23.0 kg/m^2) for ages >18 set by the Asia-Pacific adult BMI; and (2) standard electro or auricular acupuncture was applied to the experimental group, and sham acupuncture was applied to the control group. The exclusion criteria were as follows: (1) secondary obesity; (2) using other forms of acupuncture; and (3) use of complementary or alternative therapies whose efficacy has not been determined yet in the control group.

2.2. Risk of Bias Assessment. We applied the modified Jadad scale to assess the methodological quality of all included studies [23]. This tool contained four domains, including randomization, randomization hidden, and blinding, which were assigned zero to two points, respectively. Withdrawals and dropouts were assigned scores of zero to one. The scores of each domain were combined to evaluate the overall quality of each RCT. A high-quality RCT should get three or more points. The detailed quality scoring was described in a previous study [12]. The Cochrane risk of bias (RoB) 2.0 tool was used to evaluate the risk of bias summary figure for the 11 RCTs [24].

2.3. Data Analysis. We used Python (version 3.7, Python Software Foundation, Python Language Reference, London, UK) to conduct an Apriori algorithm and plot charts [25]. Table 1 shows the summaries of the selected studies from which we extracted and analyzed the acupoint frequencies. In this study, the Apriori algorithm-based association rule analysis and plotting were processed using Python. Using Apriori, we can find hidden relationships in the data. $\{A\} \geq \{B\}$ is defined as the association rule with B when A occurs. We used conditional probability to calculate each acupoint's support, which mathematically is the number of events occurring over the total number. We disregarded acupoints with support of less than 30%.

$$\text{Support}(A) = P(A) = \frac{\text{frequency of } A}{\text{total number of point } s}. \quad (1)$$

Next, we considered the data confidence and lift. The explicit formulas for confidence and lift are as follows:

$$\text{confidence } (A \longrightarrow B) = P(B|A) = P(A \cap B)/P(A)$$

$$\text{lift } (A \longrightarrow B) = \text{confidence } (A \longrightarrow B)/P(B) = P(A \cap B)/(P(A) * P(B))$$

The confidence is A's probability when B occurs. Lift means that A and B have a relative association. That is, if A and B are independent, lift $(A \longrightarrow B) = 1$, since $P(A \cap B) = (P(A) * P(B))$. If lift $(A \longrightarrow B) = 0$, A and B are mutually exclusive events. If the lift is higher than 2, the two objects are highly correlated. We chose acupoints with confidence values higher than 80%, as values lower than this would involve too much data to study, and anything higher involve too little data. We recursively took it to layer three and drew it as a chart.

3. Results

3.1. Study Characteristics and RoB Assessment. The acupuncture treatment for simple obesity used an average of six acupoints, and the mean period of therapy was 35 days. In this meta-analysis, acupuncture therapy showed statistically significant changes in BMI, BFM, WC, and HC compared to the sham acupuncture group; however, there was no statistically significant difference between the two groups in terms of body weight (BW).

Table 1 summarizes the methodological quality of the retrieved RCTs. Supplementary Table 1 presents the detailed modified Jadad scale scoring assessment [12]. The overall quality of the 11 RCTs was high, with an average Jada score of 5.27. All studies provided a detailed description of their randomized and randomization-hidden protocols and used single-blind designs combined with sham acupuncture treatments. Only three studies elucidated the reasons for patient withdrawals and exits. The RoB summary figure of the included RCTs is provided in Supplementary Figure 1.

3.2. Distribution of the Acupoints. We identified 23 acupoints from the 11 RCTs retrieved from the meta-analysis. Figure 1 shows the frequency distribution of the acupoints. The top 10 most frequently selected acupoints for simple

Table 1: Summary of selected studies.

Study (year)	Study design	Inclusion criteria (kg/m^2)	Acupoints	Jadad score
Tuğrul Cabioğlu and Ergene (2005) [41]	RCT	BMI > 30	Extra12, TF4, LI 4, LI11, ST25, ST36, ST44	5
Cabioğlu and Ergene (2006) [42]	RCT	BMI > 30	Extra12, TF4, LI 4, LI11, ST25, ST36, ST44	5
Cabioğlu et al. (2008) [43]	RCT	BMI > 30	Extra12, TF4, LI 4, LI11, ST25, ST36, ST44	5
Hsu et al. (2009) [44]	RCT	BMI > 27	TF4, CO4, Extra12, CO18	6
Abdi et al. (2012) [45]	RCT	BMI > 30	TF4, CO4, Extra12, CO1, HX1, CO17	5
Güçel et al. (2012) [46]	RCT	BMI > 30	LI4, HT7, ST36, ST44, SP6	6
Lien et al. (2012) [47]	RCT	BMI > 27	TF4, CO4, Extra12, CO18	6
Darbandi et al. (2013) [48]	RCT	BMI > 25	ST25, GB28, RN12, RN9, RN4, SP6	5
Yeo et al. (2014) [49]	RCT	BMI > 23	TF4, CO4, CO13, Extra12, CO18	5
Darbandi et al. (2014) [50]	RCT	BMI > 30–40	ST25, GB28, REN12, REN9, REN4, SP6, TF4, CO4, Extra12, CO1, HX1, CO17	5
Fogarty et al. (2015) [51]	RCT	BMI > 25	LI4, LI11, ST36, ST44, LR3	5

RCT = randomized controlled trial; BMI = body mass index.

obesity treatment were Extra12, TF4, LI4, ST25, ST36, ST44, CO4, LI11, SP6, and CO18.

3.3. Apriori Algorithm-Based Association Rule Analysis for Item Sets of Acupoint Combinations. We investigated 1,118 association rules based on the acupoints data (Table 1) and deleted those with confidence values lower than 80%. The number 1,118 was calculated by the sum of choosing 2 and 3 out of the 23 identified acupoints and deleting the combinations not in the table. The association rules are shown in Figure 2. The chart shows the acupoints with greater than 80% support. Acupoints Extra12 and TF4 appeared most frequently in the data. We used this to determine the confidence and lift. The top 10 association rules for the selected acupoints are listed in Table 2. We plotted this in a three-dimensional chart (Figure 2).

We can see the scatter in space. For the grouped item sets, we used graph-based visualization according to color or size. The features were visually presented based on a grouped matrix of 10 association rules (Figure 3). In Section 2.3, we demonstrate that a higher lift indicates a stronger association. If the support and lift values are larger, the circle size will be bigger and red. Otherwise, it will be smaller and lighter. In Table 2 we see that {LI4, ST36}, {LI4, ST44}, and {ST36, ST44} have high support and lift. This association rules were consistent for {LI4, ST36} ≥ {ST44}, {LI4, ST44} ≥ {ST36}, and {ST36, ST44} ≥ { LI4}.

4. Discussion

Our results indicated that LI4, ST36, and ST44; LI4, ST44, and ST36; and ST36, ST44, and LI4 were the core acupoint combinations for treating patients with obesity (Figure 4). Notably, a meta-analysis of acupuncture therapy for simple obesity revealed that the acupoint combination played a significant role in reducing BMI, BFN, WC, and HC. The utility of evidence-based strategies for selecting acupoints for further treatment can be ascertained by their efficacy. This is the first report on potential core acupoint combinations for simple obesity therapy based on RCTs.

Although a few similar studies to the one presented here exist, the data sources of acupuncture for simple obesity that were used had lower levels of evidence, including non-RCTs, case reports, and case series [22, 26, 27]. There are differences in the combinations of acupoints that were reported by clinical trials with different levels of evidence for simple obesity. The core acupoint combination we reported here is different from other studies. For example, the core acupoint combination summarized by Jiang et al. was RN12 and ST36 [27], while when Deng et al. used acupoint catgut embedding, their acupoint combination was reported as RN12 and ST25 [22]. Our study focused on acupuncture for simple obesity, which is different from other studies that have studied acupuncture for secondary obesity, such as diabetes mellitus or hyperlipidemia complicated with obesity [21, 28]. The core acupoint combination summarized here for the treatment of nonsimple obesity and simple obesity is different from those reported in other studies. For instance, the core acupoint combination reported by Sun et al. for treating type 2 diabetes mellitus complicated with obesity was RN12, SP6, and SP9 [21]. In contrast, Wang et al.'s core acupoint combination for hyperlipidemia complicated with obesity was SP3, ST36, and ST40 [28]. Although our core acupoint combination is different from other studies, ST36 is an acupoint that was identified both by us and by Jiang and Wang [27, 28].

Core acupoint combinations are useful for patients with simple obesity. There are some possible mechanisms as to how acupuncture helps with obesity, including regulating lipid metabolism, modulating inflammatory responses, suppressing appetite, and promoting white adipose tissue (WAT) browning [13]. A C57/B6 mouse model study demonstrated that EA at ST36 could reduce BW by decreasing WAT weight and increasing TRPV1 levels, which regulate lipids [29]. Current studies have confirmed that obesity is related to inflammation and that levels of the proinflammatory cytokines IL-6 and TNF-α increase in individuals with obesity [30, 31]. In obese rat models, electroacupuncture at CV12/CV4 can significantly reduce adiponectin and increase serum leptin [32]. It can also

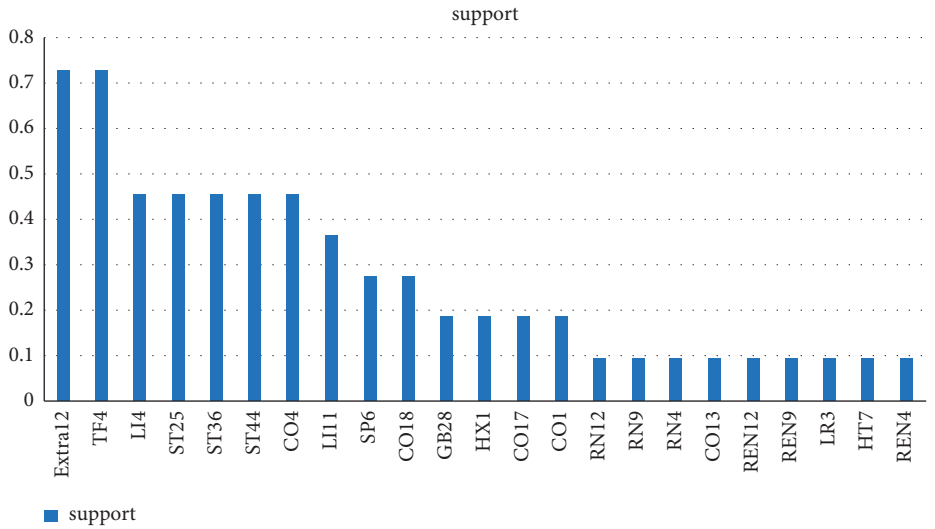

Figure 1: Frequency distribution of acupoints used in the 11 RCTs included in the meta-analysis.

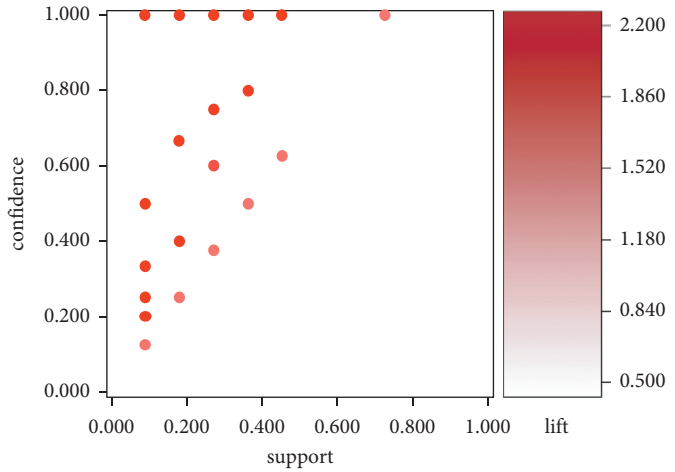

Figure 2: Scatter plot for the 1118 association rules obtained in the 11 RCTs included in the meta-analysis.

Table 2: Apriori algorithm-based association rules for acupoints used for obesity treatment.

No.	Association rules	Support	Confidence	Expected confidence	Lift
1	{Extra12} ≥ {TF4}	0.727272	1.000000	0.727272	1.37500
2	{TF4} ≥ {Extra12}	0.727272	1.000000	0.727272	1.37500
3	{CO4} ≥ {Extra12}	0.454545	1.000000	0.727272	1.37500
4	{CO4} ≥ {TF4}	0.454545	1.000000	0.727272	1.37500
5	{LI4} ≥ {ST36}	0.454545	1.000000	0.454545	2.20000
6	{ST36} ≥ {LI4}	0.454545	1.000000	0.454545	2.20000
7	{LI4} ≥ {ST44}	0.454545	1.000000	0.454545	2.20000
8	{ST44} ≥ {LI4}	0.454545	1.000000	0.454545	2.20000
9	{ST36} ≥ {ST44}	0.454545	1.000000	0.454545	2.20000
10	{ST44} ≥ {ST36}	0.454545	1.000000	0.454545	2.20000
11	{ST25} ≥ {Extra12}	0.363636	0.800000	0.909090	1.10000
12	{ST25} ≥ {TF4}	0.363636	0.800000	0.909090	1.10000
13	{LI4} ≥ {LI11}	0.363636	0.800000	0.454545	2.20000
14	{LI11} ≥ {LI4}	0.363636	1.000000	0.454545	2.20000
15	{LI11} ≥ {ST36}	0.363636	1.000000	0.454545	2.20000
16	{ST36} ≥ {LI11}	0.363636	0.800000	0.454545	2.20000
17	{LI11} ≥ {ST44}	0.363636	1.000000	0.454545	2.20000
18	{ST44} ≥ {ST11}	0.363636	0.800000	0.454545	2.20000

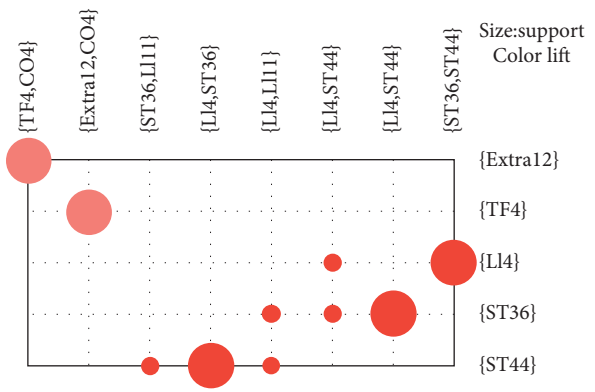

Figure 3: Grouping matrix for the 10 association rules obtained in the 11 RCTs included in the meta-analysis.

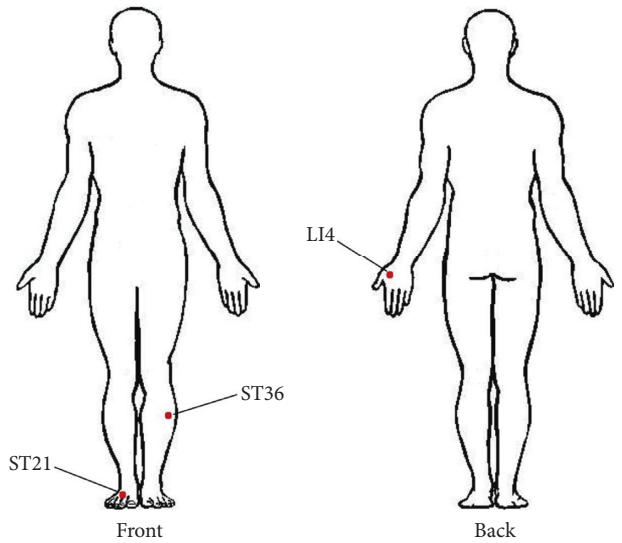

Figure 4: Location of core acupoints in the treatment of patients with obesity.

increase the levels of the anti-inflammatory factor IL-10 and reduce levels of the proinflammatory factor TNF-α [33]. Liu et al. reported that EA at ST36 and ST44 could enhance the excitability of the ventromedial hypothalamic nucleus (VMH) to reduce food intake in obese rats [34]. In addition, in an obese rat model, Qiang et al. found that acupuncture on ST44 and ST36 could decrease adipocyte size and prompt lipolysis in WAT by inducing the expression of uncoupling protein-1 (UCP-1) to promote WAT browning [35].

In clinical disease treatment, acupuncture often uses multiple acupoints at the same time. The therapeutic effect of an acupoint combination is usually better than that of a single acupoint [17, 18]. Animal experiments have shown the same results [36]. Zhang et al. conducted an RCT with hypertension patients; in their study, resting-state fMRI scans indicated that the acupoint combination group using LR3 and KI3 promoted brain activation over a greater area than when using a single acupoint (LR3 or KI3) group [37].

Table 3: Potential efficacy of the core acupoints for obesity treatment.

Acupoint	Chinese name	English name	Primary meridians	Efficacy
LI4 [39]	Ho-Ku	Connecting valleys	Large intestine	To increase the levels of serum insulin and C peptide
ST36 [35, 39, 40]	Tsu-San-Li	Walking three miles	Stomach	To increase the levels of serum insulin and C peptide; to remodel WAT to BAT
ST44 [35, 39, 40]	Nei-T'ing	Inner court	Stomach	To increase the levels of serum insulin and C peptide; to remodel WAT to BAT

WAT: white adipose tissue; BAT: brown adipose tissue.

A crossover test using BL21 and CV12 to treat healthy subjects under a water load condition showed lower electrogastrogram (EGG) amplitudes and more new brain region activation than when using a single acupoint (BL21 or CV12) group [38]. Consequently, some evidence suggests that the synergistic pharmacological effect of acupuncture on multiple acupoint combinations is better than that of a single acupoint. The core acupoint combinations found in our article can improve simple obesity by increasing the levels of serum insulin and C peptide and by remodeling WAT to brown adipose tissue (BAT), which has been supported by many modern pharmacological studies [35, 39, 40] (Table 3).

4.1. Limitations. There are a few limitations to our study. First, publication bias may occur because there were only 11 trials published in English. None of the studies were from mainland China due to the inclusion criteria. Second, this meta-analysis only included 11 RCTs and a total of 643 patients. Third, the mean therapy duration was 35 days, and only one of the RCTs included had a careful follow-up. Finally, the mechanisms involved in acupoint combinations for treating simple obesity are unclear. Thus, further large-scale, high-quality RCTs are required for a more thorough assessment.

5. Conclusions

The acupoint combination of LI4, ST36, and ST44 is the core acupoint combination for simple obesity treatment that could significantly improve BMI, BFN, WC, and HC, as supported by modern pharmacological evidence. However, further rigorous clinical trials are warranted.

Data Availability

The original data used to support the study findings are included within the article.

Conflicts of Interest

The authors have no conflicts of interest.

Acknowledgments

We thank all our colleagues at National Central University and Taipei Tzu Chi Hospital for helping with this study. We greatly appreciate technical support from the Core Laboratory of the Taipei Tzu Chi Hospital and the Buddhist Tzu Chi Medical Foundation. This study was supported by grants from the Buddhist Tzu Chi Medical Foundation, Taiwan (TCMF-CM1-111-03 and TCMF-P 111-16) and Taipei Tzu Chi Hospital (TCRD-TPE-111-45).

Supplementary Materials

Supplementary Table 1: quality scores of the included RCTs. Supplementary Figure 1: risk of bias of the included RCTs. (*Supplementary Materials*)

References

[1] C. S. Tam, V. Lecoultre, and E. Ravussin, "Brown adipose tissue," *Circulation*, vol. 125, no. 22, pp. 2782–2791, 2012.

[2] Y. C. Chooi, C. Ding, and F. Magkos, "The epidemiology of obesity," *Metabolism*, vol. 92, pp. 6–10, 2019.

[3] WHO, *Obesity: Preventing and Managing the Global Epidemic*, WHO, Geneva, Switzerland, 2000.

[4] A. G. Tsai and T. A. Wadden, "Obesity," *Annals of Internal Medicine*, vol. 159, no. 5, 2013.

[5] R. J. F. Loos, "Genetic determinants of common obesity and their value in prediction," *Best Practice & Research Clinical Endocrinology & Metabolism*, vol. 26, no. 2, pp. 211–226, 2012.

[6] M. Vanderschueren-Lodeweyckx, "The effect of simple obesity on growth and growth hormone," *Hormone Research*, vol. 40, no. 1–3, pp. 23–30, 1993.

[7] J. M. Guo, H. C. Lin, and P. Ou, "[Prevalence of simple obesity and its high-risk factors in preschool children in Fuzhou, China]," *Zhong Guo Dang Dai Er Ke Za Zhi*, vol. 20, no. 11, pp. 943–1038, 2018.

[8] C. Mattsson and T. Olsson, "Estrogens and glucocorticoid hormones in adipose tissue metabolism," *Current Medicinal Chemistry*, vol. 14, no. 27, pp. 2918–2924, 2007.

[9] M. L. Vetter, L. F. Faulconbridge, V. L. Webb, and T. A. Wadden, "Behavioral and pharmacologic therapies for obesity," *Nature Reviews Endocrinology*, vol. 6, no. 10, pp. 578–588, 2010.

[10] A. Ballinger, "Orlistat in the treatment of obesity," *Expert Opinion on Pharmacotherapy*, vol. 1, no. 4, pp. 841–847, 2000.

[11] G. D. Curfman, S. Morrissey, and J. M. Drazen, "Sibutramine—another flawed diet pill," *The New England Journal of Medicine*, vol. 363, no. 10, 2010.

[12] R.-Q. Zhang, J. Tan, F.-Y. Li, Y.-H. Ma, L.-X. Han, and X.-L. Yang, "Acupuncture for the treatment of obesity in adults: a systematic review and meta-analysis," *Postgraduate Medical Journal*, vol. 93, no. 1106, pp. 743–751, 2017.

[13] L. H. Wang, W. Huang, D. Wei et al., "Mechanisms of acupuncture therapy for simple obesity: an evidence-based review of clinical and animal studies on simple obesity," *Evidence-Based Complementary and Alternative Medicine: eCAM*, vol. 2019, Article ID 5796381, 12 pages, 2019.

[14] W.-B. Zhang, Y.-P. Wang, and H.-Y. Li, "Analysis on correlation between meridians and viscera in book the yellow emperor's internal classic," *Zhen Ci Yan Jiu = Acupuncture Research*, vol. 43, no. 7, pp. 424–429, 2018.

[15] W. Zhou and P. Benharash, "Effects and mechanisms of acupuncture based on the principle of meridians," *Journal of Acupuncture and Meridian Studies*, vol. 7, no. 4, pp. 190–193, 2014.

[16] P. H. Lu, J. L. Keng, K. L. Kuo, Y. F. Wang, Y. C. Tai, and C. Y. Kuo, "An Apriori algorithm-based association rule analysis to identify herb combinations for treating uremic pruritus using Chinese herbal bath therapy," *Evidence-Based Complementary and Alternative Medicine: eCAM*, vol. 2020, Article ID 8854772, 9 pages, 2020.

[17] P. H. Lu, J. L. Keng, F. M. Tsai, P. H. Lu, and C. Y. Kuo, "An Apriori algorithm-based association rule analysis to identify acupoint combinations for treating diabetic gastroparesis," *Evidence-Based Complementary and Alternative Medicine: eCAM*, vol. 2021, Article ID 6649331, 9 pages, 2021.

[18] P. C. Hsieh, C. F. Cheng, C. W. Wu et al., "Combination of acupoints in treating patients with chronic obstructive pulmonary disease: an Apriori algorithm-based association rule analysis," *Evidence-Based Complementary and Alternative Medicine*, vol. 2020, Article ID 8165296, 7 pages, 2020.

[19] Y. Chaochao, W. Li, K. Lihong et al., "Acupoint combinations used for treatment of Alzheimer's disease: a data mining analysis," *Journal of Traditional Chinese Medicine*, vol. 38, no. 6, pp. 943–952, 2018.

[20] R. J. Bayardo and R. Agrawal, "Mining the most interesting rules," in *Proceedings of the Fifth ACM SIGKDD International Conference on Knowledge Discovery and Data Mining*, pp. 145–154, Association for Computing Machinery, San Diego, CA, USA, 1999.

[21] S.-Y. Sun, R.-Z. Huang, and W.-W. Zheng, "Research on the rules of acupoints selection in treating type 2 diabetes mellitus complicated with obesity based on data mining," *Chinese Medicine Modern Distance Education of China*, vol. 19, no. 24, pp. 37–39, 2021.

[22] X.-M. Deng, "Study on acupoint selection and compatibility rule of acupuncture for abdominal obesity based on data mining," Master's Thesis, Guangxi University of Chinese Medicine, Guangxi, China, 2021.

[23] A. R. Jadad, R. A. Moore, D. Carroll et al., "Assessing the quality of reports of randomized clinical trials: is blinding necessary?" *Controlled Clinical Trials*, vol. 17, no. 1, pp. 1–12, 1996.

[24] J. P. Higgins, J. A. Sterne, J. Savovic et al., "A revised tool for assessing risk of bias in randomized trials," *Cochrane Database of Systematic Reviews*, vol. 10, no. Suppl 1, pp. 29–31, 2016.

[25] R. Gv and F. L. Drake, *The Python Language Reference Manual*, Network Theory Ltd., Godalming, UK, 2011.

[26] L. Chen, Y.-X. Huang, Q.-F. Wu et al., "Study on acupoint selection and compatibility rule of catgut implantation at acupoint for simple obesity based on data mining," *Journal of Clinical Acupuncture and Moxibustion*, vol. 33, no. 2, pp. 61–65, 2019.

[27] D.-S. Jiang, "Study on acupoint selection and compatibility spectrum of acupuncture and moxibustion for simple obesity based on data mining," Master's Thesis, Changchun University of Chinese Medicine, Jilin, China, 2019.

[28] L.-H. Wang and Z.-Y. Zhou, "Study on acupoint selection and compatibility rule of acupuncture for obesity with hyperlipidemia based on data mining," *Hubei Journal of Traditional Chinese Medicine*, vol. 41, no. 2, pp. 62–64, 2019.

[29] M. Choowanthanapakorn, K.-W. Lu, J. Yang, C.-L. Hsieh, and Y.-W. Lin, "Targeting TRPV1 for body weight control using TRPV1−/−mice and electroacupuncture," *Scientific Reports*, vol. 5, no. 1, pp. 1–9, 2015.

[30] R. Medzhitov, "Origin and physiological roles of inflammation," *Nature*, vol. 454, no. 7203, pp. 428–435, 2008.

[31] A. S. Greenberg and M. S. Obin, "Obesity and the role of adipose tissue in inflammation and metabolism," *The American Journal of Clinical Nutrition*, vol. 83, no. 2, pp. 461S–465S, 2006.

[32] J. J. T. Liaw and P. V. Peplow, "Effects of electroacupuncture on pro-/anti-inflammatory adipokines in serum and adipose tissue in lean and diet-induced obese rats," *Journal of Acupuncture and Meridian Studies*, vol. 9, no. 2, pp. 65–72, 2016.

[33] J. J. T. Liaw and P. V. Peplow, "Differential effect of electroacupuncture on inflammatory adipokines in two rat models of obesity," *Journal of Acupuncture and Meridian Studies*, vol. 9, no. 4, pp. 183–190, 2016.

[34] Z. Liu, F. Sun, J. Su et al., "Study on action of acupuncture on ventromedial nucleus of hypothalamus in obese rats," *Journal of Traditional Chinese Medicine*, vol. 21, no. 3, pp. 220–224, 2001.

[35] L. Qiang, L. Wang, N. Kon et al., "Brown remodeling of white adipose tissue by SirT1-dependent deacetylation of pparγ," *Cell*, vol. 150, no. 3, pp. 620–632, 2012.

[36] Y. Q. Li, B. Yu, T. Li, Z. J. Zhao, M. J. Yang, and F. C. Wang, "Effect of acupuncture at single acupoint and combined acupoints on antral interstitial cells of cajal in diabetic gastroparesis model rats," *World Chinese Medicine*, vol. 11, no. 2, pp. 214–218, 2016.

[37] J. Zhang, X. Cai, Y. Wang et al., "Different brain activation after acupuncture at combined acupoints and single acupoint in hypertension patients: an rs-fMRI study based on ReHo analysis," *Evidence-Based Complementary and Alternative Medicine: eCAM*, vol. 2019, Article ID 5262896, 10 pages, 2019.

[38] R. Cai, Y. Guan, H. Wu et al., "[Effects on the regional homogeneity of resting-state brain function in the healthy subjects of gastric distention treated with acupuncture at the front-mu and back-shu points of the stomach, Weishu (BL 21) and Zhongwan (CV 12)]," *Zhongguo Zhen Jiu*, vol. 38, no. 4, pp. 379–386, 2018.

[39] M. T. Cabioğlu and N. Ergene, "Changes in levels of serum insulin, C-Peptide and glucose after electroacupuncture and diet therapy in obese women," *The American Journal of Chinese Medicine*, vol. 34, no. 3, pp. 367–376, 2006.

[40] W. Shen, Y. Wang, S. F. Lu et al., "Acupuncture promotes white adipose tissue browning by inducing UCP1 expression on DIO mice," *BMC Complementary and Alternative Medicine*, vol. 14, no. 1, pp. 501–508, 2014.

[41] M. Tuğrul Cabıoğlu and N. Ergene, "Electroacupuncture therapy for weight loss reduces serum total cholesterol, triglycerides, and LDL cholesterol levels in obese women," *The American Journal of Chinese Medicine*, vol. 33, no. 4, pp. 525–533, 2005.

[42] M. T. Cabıoğlu and N. Ergene, "Changes in levels of serum insulin, C-peptide and glucose after electroacupuncture and diet therapy in obese women," *The American Journal of Chinese Medicine*, vol. 34, no. 3, pp. 367–376, 2006.

[43] M. T. Cabioglu, N. Gündoğan, and N. Ergene, "The efficacy of electroacupuncture therapy for weight loss changes plasma lipoprotein A, apolipoprotein A and apolipoprotein B levels in obese women," *The American Journal of Chinese Medicine*, vol. 36, no. 6, pp. 1029–1039, 2008.

[44] C.-H. Hsu, C.-J. Wang, K.-C. Hwang, T.-Y. Lee, P. Chou, and H.-H. Chang, "The effect of auricular acupuncture in obese women: a randomized controlled trial," *Journal of Women's Health*, vol. 18, no. 6, pp. 813–818, 2009.

[45] H. Abdi, P. Abbasi-Parizad, B. Zhao et al., "Effects of auricular acupuncture on anthropometric, lipid profile, inflammatory, and immunologic markers: a randomized controlled trial study," *Journal of Alternative & Complementary Medicine*, vol. 18, no. 7, pp. 668–677, 2012.

[46] F. Güçel, B. Bahar, C. Demirtas, S. Mit, and C. Cevik, "Influence of acupuncture on leptin, ghrelin, insulin and cholecystokinin in obese women: a randomised, sham-controlled preliminary trial," *Acupuncture in Medicine: Journal of the British Medical Acupuncture Society*, vol. 30, no. 3, pp. 203–207, 2012.

[47] C.-Y. Lien, L.-L. Liao, P. Chou, and C.-H. Hsu, "Effects of auricular stimulation on obese women: a randomized, controlled clinical trial," *European Journal of Integrative Medicine*, vol. 4, no. 1, pp. e45–e53, 2012.

[48] S. Darbandi, M. Darbandi, P. Mokarram et al., "Effects of body electroacupuncture on plasma leptin concentrations in obese and overweight people in Iran: a randomized controlled trial," *Alternative Therapies in Health and Medicine*, vol. 19, no. 2, pp. 24–31, 2013.

[49] S. Yeo, K. S. Kim, and S. Lim, "Randomised clinical trial of five ear acupuncture points for the treatment of overweight people," *Acupuncture in Medicine*, vol. 32, no. 2, pp. 132–138, 2014.

[50] M. Darbandi, S. Darbandi, A. A. Owji et al., "Auricular or body acupuncture: which one is more effective in reducing abdominal fat mass in Iranian men with obesity: a randomized clinical trial," *Journal of Diabetes and Metabolic Disorders*, vol. 13, no. 1, p. 92, 2014.

[51] S. Fogarty, L. Stojanovska, D. Harris, C. Zaslawski, M. L. Mathai, and A. J. McAinch, "A randomised cross-over pilot study investigating the use of acupuncture to promote weight loss and mental health in overweight and obese individuals participating in a weight loss program," *Eating and Weight Disorders—Studies on Anorexia, Bulimia and Obesity*, vol. 20, no. 3, pp. 379–387, 2015.

Hindawi
Evidence-Based Complementary and Alternative Medicine
Volume 2022, Article ID 2454678, 11 pages
https://doi.org/10.1155/2022/2454678

Research Article

A Study of Logistic Regression for Fatigue Classification Based on Data of Tongue and Pulse

Yu Lin Shi,[1] **Tao Jiang**,[1] **Xiao Juan Hu**,[2] **Ji Cui**,[1] **Long Tao Cui**,[1] **Li Ping Tu**,[1] **Xing Hua Yao**,[1] **Jing Bin Huang**,[1] **and Jia Tuo Xu**[1]

[1]*Department of Basic Medical College, Shanghai University of Traditional Chinese Medicine, 1200 Cailun Road, Pudong, Shanghai, China*
[2]*Shanghai Collaborative Innovation Center of Health Service in Traditional Chinese Medicine, Shanghai University of Traditional Chinese Medicine, 1200 Cailun Road, Pudong, Shanghai, China*

Correspondence should be addressed to Jing Bin Huang; jmy61@163.com and Jia Tuo Xu; xjt@fudan.edu.cn

Received 3 September 2021; Accepted 5 January 2022; Published 5 March 2022

Academic Editor: Haifa Qiao

Background and Objective. Fatigue is a subjective symptom which is hard to quantify, it is prevalent in the subhealth and disease population, and there is still no accurate and stable method to distinguish disease fatigue from subhealth fatigue. Tongue diagnosis and pulse diagnosis are the reflection of the overall state of the body, and the modern research of tongue diagnosis and pulse diagnosis has made great progress. This study aims to explore the distribution rules of tongue and pulse data in a disease fatigue and subhealth fatigue population and evaluate the contribution rate of tongue and pulse data to fatigue diagnosis through modeling. *Methods*. The Tongue and Face Diagnosis Analysis-1 instrument and Pulse Diagnosis Analysis-1 instrument were used to collect the tongue image and sphygmogram of the subhealth fatigue population ($n = 252$) and disease fatigue population ($n = 1160$), and we mainly analyzed the tongue and pulse characteristics and constructed the classification model by using the logistic regression method. *Results*. The results showed that subhealth fatigue people and disease fatigue people had different characteristics of tongue and pulse, and the logistic regression model based on tongue and pulse data had a good classification effect. The accuracies of models of healthy controls and subhealth fatigue, subhealth fatigue and disease fatigue, and healthy controls and disease fatigue were 68.29%, 81.18%, and 84.73%, and the AUC was 0.698, 0.882, and 0.924, respectively. *Conclusion*. This study provided a new noninvasive method for the fatigue diagnosis from the perspective of objective tongue and pulse data, and the modern tongue diagnosis and pulse diagnosis have good application prospects.

1. Introduction

Fatigue refers to physical tiredness with lack of energy or mental exhaustion with lack of concentration. It can be divided into physical fatigue and mental fatigue [1]. Fatigue is the first cause of subhealth and is one of the most common symptoms in primary care, and it is experienced by many patients with chronic hepatitis [2, 3], depression [4], and various types of cancers [5]. Subhealth and a wide variety of diseases are associated with different degrees of fatigue with a negative effect on people's life. With the improvement of general medical care and living standard, fatigue is more and more known by people; however, due to the lack of objective diagnostic evidence, there is still no reliable and stable evaluation method to distinguish disease fatigue and subhealth fatigue.

A large number of clinical practices and studies have shown that tongue and pulse can reflect the overall state of body [6]. Tongue and pulse of fatigue people have their own characteristics. Studies have shown that the tongue of patients with brain fatigue is usually dull, slow in movements, weak, or difficult to stretch [7]. In the physical examination population, the tongue of fatigue population has certain specificity in tongue body color, tongue coating color, and tongue shape. Fatigue is closely related to the tooth mark tongue, and the degree of fatigue is positively related to the

tooth mark area [8]. The tongue of patients with fatigue syndrome has obvious characteristics of stasis, mainly purple tongue, petechiae or ecchymosis tongue, sublingual varices, and white thick tongue coating [9]. In patients with chronic fatigue syndrome in Hong Kong, the tongue body is usually light fat and dull, tongue coating is thin white, or thin greasy, and the pulse is usually deep and thin [10].

Intelligent diagnosis of TCM is a new research field in recent years, and it meets the trend that TCM diagnosis methods are developing gradually towards intelligence and potential application in clinical practice [11, 12]. In recent research of tongue diagnosis and pulse diagnosis, new diagnosis systems are adopted to collect and analyze clinical data related to disease, and machine learning methods such as Artificial Neural Network [13, 14], Support Vector Machine(SVM) [15, 16], and KNN [17] are used to establish the corresponding diagnosis model, which can effectively assist doctor on the diagnosis of disease. In recent years, there have been more and more objectified and standardized studies on fatigue based on tongue diagnosis and pulse diagnosis [18–20].

Based on the modern research of tongue diagnosis and pulse diagnosis, this study aims to explore the distribution rules of tongue and pulse data in disease fatigue and subhealth fatigue and evaluate the contribution rate to fatigue diagnosis through modeling, so as to provide a new reference for convenient and noninvasive methods of fatigue diagnosis, and if an objective evaluation method based on tongue and pulse data can be established, it will play an important role in the clinical diagnosis of fatigue.

2. Methods

2.1. Study Design. A total of 7,025 subjects were collected from January 2015 to December 2018 in the medical examination center of Shuguang Hospital Affiliated to Shanghai University of Traditional Chinese Medicine, collecting their Western medicine physical examination index and tongue and pulse data of TCM. The 7,025 subjects were divided into healthy controls ($n = 799$), a subhealth fatigue group ($n = 361$), and a disease fatigue group ($n = 1529$). After excluding the outliers with extreme values in tongue or pulse data, there were 551, 252, and 1,160 subjects in healthy controls, the subhealth fatigue group, and the disease fatigue group, respectively. The overall flow diagram of the study is shown as Figure 1.

2.2. Diagnostic Criteria. Health and subhealth of each individual were determined using the Health Status Assessment Questionnaire H20 Scale [21] and the Information Record Form of Four Diagnosis of TCM [22] (Copyright No. 2016Z11L025702) which were designed by the Sub-Health Research Group. Excluding the disease population, the population with a score between 60 and 79 on the H20 scale was the subhealth population, and the population with a score between 80 and 100 on the H20 scale was healthy controls. The diagnostic criteria of disease are shown in Table 1.

Disease was diagnosed by four well-trained clinicians according to the abovementioned diagnostic criteria of Western medicine. The Information Record Scale of Four Diagnosis of TCM and H20 scale were used to select fatigue population, and people with "fatigue" symptom in the two scales were judged as the fatigue population.

2.3. Tongue Diagnosis and Pulse Diagnosis Instruments. The TFDA-1 tongue and face diagnosis instrument (Patent no. 2018SR033451) [27] and PDA-1 pulse diagnosis instrument (Patent no. ZL201620157027.6) [28] are shown in Figures 2 and 3; they were used for data collection. The tongue was imaged by using a video camera (Nikon 1 J5) with a fixed-focal lens which has 12 megapixels, and the picture resolution is $5568 * 3712$. The color rendering index of light source was 96, and color temperature was around 5,000–6,500 K. The indices of the tongue image were from color spaces of RGB, HSI, Lab, and YCrCb. The prefix TB represented the tongue body index, and TC represented the tongue coating index. The PDA-1 pulse diagnosis instrument uses a pressure sensor (model: HK-2000H). Each of the indices of the tongue and pulse has its meaning [11, 13]. In our research, the normal range of L value was 0–255, and in order to better observe the continuity of the trend of data changes and find the data rules and real differences, we rotated the axis of H value by 180 degrees according to the law.

2.4. Data Analysis. SPSS 25.0 was used for statistical analysis. The normal distribution measurement data were expressed as " Mean ± SD". Nonnormal distribution data were expressed as quartiles expressed as " Median (P25, P75)." Analysis of Variance (ANOVA) was performed for normality and homogeneity data among groups, the Kruskal–Wallis H test was performed for nonnormal distribution data, and GraphPad Prism Version 8.0 was used for the violin plot. Test level was $\alpha = 0.05$, and a P value <0.05 (2 tailed) was considered statistically significant.

2.5. Modeling. Logistic regression analysis was performed for factors with statistical significance by ANOVA or the Rank Sum Test. Logistic regression is often used in data mining, automatic disease diagnosis, economic prediction, and others, and the accuracy of decision can be improved by adjusting the parameters of the regression model [29, 30]. The evaluation indices of the model were accuracy, sensitivity, and specificity, as well as ROC curves. They were defined as follows:

$$\begin{aligned} \text{Accuracy} &= \frac{\text{TP} + \text{TN}}{\text{TP} + \text{TN} + \text{FP} + \text{FN}} \times 100\%, \\ \text{Sensitivity} &= \frac{\text{TP}}{\text{TP} + \text{FN}} \times 100\%, \\ \text{Specificity} &= \frac{\text{TN}}{\text{TN} + \text{FP}} \times 100\%. \end{aligned} \tag{1}$$

In the abovementioned formulas, TP represents the true positive rate, TN represents the true negative rate, FP

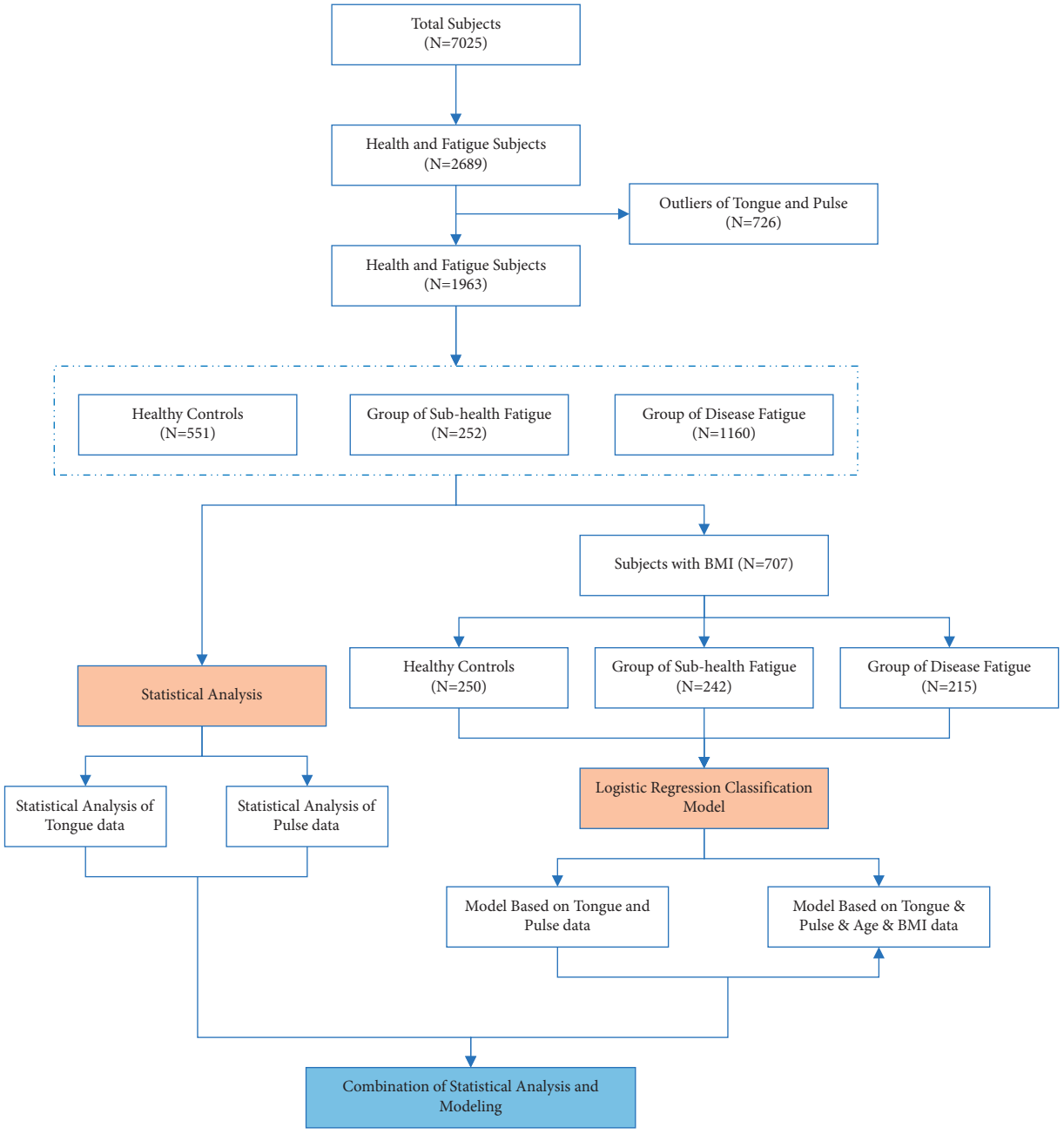

Figure 1: Overall flow diagram.

represents the false positive rate, and FN represents the false negative rate.

3. Results

3.1. The Baseline Characteristics of Studied Participants. The main diseases in the disease fatigue group were hypertension, diabetes, hyperlipidemia, and fatty liver, and their distribution is shown in Figure 4. The numbers and percentage in Figure 4 represent the number of patients and the ratio of the number of patients with the disease to the total number of patients, and the overlapping part represents the number and percentage of patients suffering from multiple diseases at the same time. Table 2 shows the general result of the healthy controls, the group of subhealth fatigue, and the group of disease fatigue.

The statistical result showed that compared with the healthy controls, there were significant differences in age and BMI between the group of disease fatigue and the subhealth fatigue ($P < 0.01$).

3.2. Statistical Analysis of Tongue Indices. Table 3 shows the statistical analysis result of distribution of the characteristic parameters of the tongue body and tongue coating among the healthy controls, the group of subhealth fatigue, and the group of disease fatigue.

Table 1: Diagnostic criteria of disease.

Disease	Diagnostic criteria
Diabetes [23]	Fasting blood glucose ≥7.0 mmol/L and/or blood glucose at any point ≥7.8 mmol/L and/or blood glucose at two hours after meal ≥11.1 mmol/L
Hypertension [24]	Systolic blood pressure≥140 mmHg and/or diastolic blood pressure ≥90 mmHg
Hyperlipidemia [25]	TC ≥ 6.2 mmol/L and/or LDL-C ≥ 4.1 mmol/L and/or HDL-C ≥ 4.9 mmol/L and/or TG ≥ 2.3 mmol/L and/or non-HDL-C ≥ 1.55 mmol/L
Fatty liver disease [26]	Ultrasound examination

(a) (b)

Figure 2: TFDA-1 tongue and face diagnosis instrument. (a) Front view. (b) Profile view.

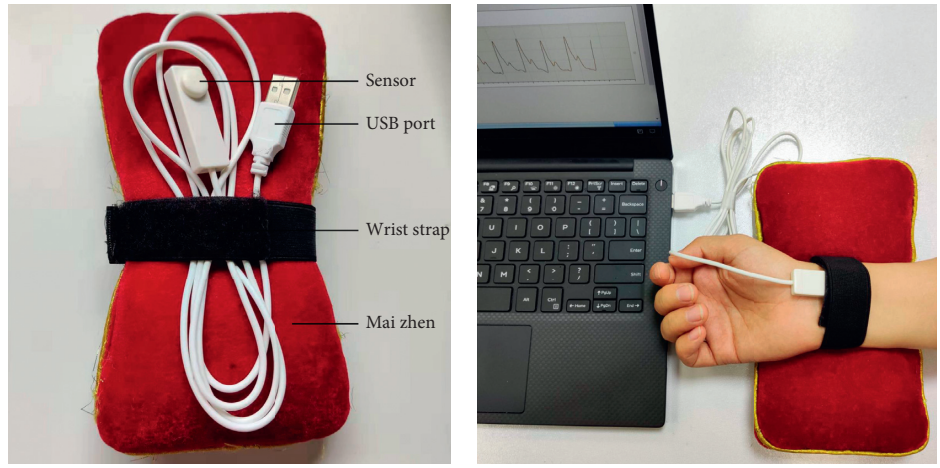

(a) (b)

Figure 3: PDA-1 pulse diagnosis instrument and the corresponding collection picture. (a) PDA-1 pulse diagnosis instrument. (b) Real picture of pulse acquisition.

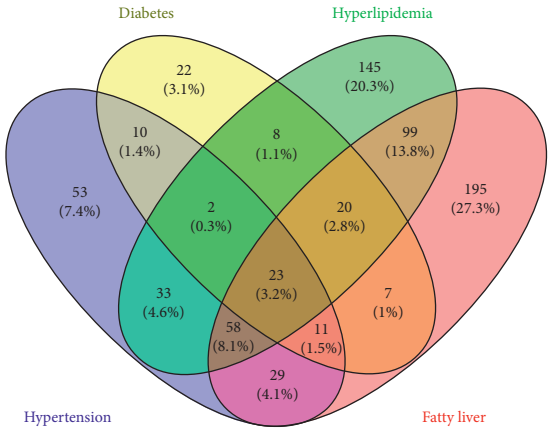

Figure 4: Distribution of main diseases in the group of disease fatigue.

In order to observe the distribution trend of data more clearly, the violin plots of selected parameters of tongue body and tongue coating with statistical significance were drawn as shown in Figure 5.

The main results of tongue indices were as follows: (1) Comparing among the three groups, the changes of TB indices in the group of subhealth fatigue and disease fatigue were more significant than those in the TC indices. (2) Index difference was more significant between the group of disease fatigue and subhealth fatigue. (3) Several indices (TB-B, TB-R, TB-G, TC-B, TB-I, TB-Y, TB-L, TB-Cb, and TB-Cr) in the healthy controls were between the two fatigue groups. It reflected that the two groups of fatigue people had different tendencies in the changing nature of the tongue.

3.3. Statistical Analysis of Pulse Indices. Table 4 shows the statistical analysis result of the distribution of pulse characteristic parameters in healthy controls, the group of subhealth fatigue, and the group of disease fatigue.

Figure 6 shows the violin plots of selected parameters of pulse characteristic with statistical significance.

The main result of pulse feature parameters showed that t_1, t_2, t_3, t_4, h_1, h_4, h_5, w_1, w_2, w_1/t, w_2/t, h_1/t_1, h_3/h_1, As, and Ad had significant statistical differences between the group of disease fatigue and healthy controls ($P < 0.05, P < 0.01$), t_4 had significantly statistical differences between the group of subhealth fatigue and the healthy controls ($P < 0.05$), and t_1, h_1, h_4, h_5, h_1/t_1, Ad, w_1, w_2, w_1/t, and w_2/t had significantly statistical differences between the group of subhealth fatigue and the disease fatigue ($P < 0.05, P < 0.01$). The main characteristic of result was that the group of subhealth fatigue and disease fatigue showed a gradual increasing tendency in each parameter compared with the healthy controls, and it reflected that the two groups of fatigue people had a consistent tendency in the changing nature of pulse. In addition, the changes of pulse feature in the group of disease fatigue were more significant than those in the group of subhealth fatigue.

3.4. Modeling Results. Logistic regression was used to establish a classification model based on tongue and pulse data of the three groups. The classification result is shown in Table 5.

The ROC curves are shown in Figure 7.

In addition, the classification model was reconstructed after adding BMI and age into tongue and pulse data. Table 6 shows the classification result of the reconstructed model.

The ROC curves are shown in Figure 8.

The research result showed that tongue and pulse data had a good classification effect on healthy controls and disease fatigue, followed by healthy controls and subhealth fatigue. After adding BMI and age, both of the model accuracy and ROC curves were improved. BMI and age are convenient and noninvasive data, which suggested that we could combine BMI and age with tongue and pulse data to improve the diagnostic accuracy of fatigue.

4. Discussion

In this study, the distribution trends of the objective tongue data were different between the subhealth fatigue population and the disease fatigue population. The study showed that TB-B, TB-R, TB-G, TC-B, TB-I, TB-Y, TB-L, TB-Cb, TB-Cr, TB-a, and TC-a were in an ascending order in the group of subhealth fatigue, healthy controls, and the group of disease fatigue, which indicated that disease fatigue people in general had more purple or red-purple tongue body and more white-greasy tongue coating. The tongue parameters of the subhealth fatigue population were lower than those of the healthy controls, while those of disease fatigue were higher than those of the healthy controls. Certain differences were found in tongue parameters of fatigue groups compared with the healthy controls; that is, subjects in the group of disease fatigue had darker tongue body and tongue coating and more yellow or brown tongue coating, which was more associated with excess syndrome, and the subjects in the group of subhealth fatigue had a pale red tongue body with white coating, which was more associated with the deficiency syndrome. The finding was consistent with the TCM theory that subhealth was manifested as decreased vitality, function, and adaptability, and disease was mostly due to the hyperactivity of evil spirits or dysfunction of the dysfunctional organs caused by phlegm [31], dampness [32], and blood stasis [33] and other pathological products. The result could help to distinguish subhealth fatigue and disease fatigue.

In our study, the pulse analysis result of the three groups showed that fatigue state can directly affect the changes of sphygmogram parameters, and the change had a consistent trend; so to say, the indices of disease fatigue were more abnormal and the differences were more significant compared to healthy controls, while between the group of subhealth fatigue and health controls, only w_2/t had a statistical difference, and several indices had a significant difference between the group of subhealth fatigue and disease fatigue. As to the distribution trend of pulse indices, the group of subhealth fatigue was located between healthy controls and the group of disease fatigue. Studies have shown that pulse can directly reflect various cardiovascular functional states [34, 35], and the results

Table 2: General result (mean (SD) and median (P25, P75)).

Group		N	Male N (%)	Female N (%)	Age (Mean ± SD, year)	BMI (Kg/m^2)
Healthy controls		551	394 (71.5)	157 (28.5)	29.00 (25.00,35.00)	22.31 (20.55,24.51)
Subhealth fatigue		252	149 (59.1)	103 (40.9)	32.00 (28.00,37.00)*	22.39 (20.28,24.68)
Disease fatigue	Hypertension	219	160 (73.1)	59 (26.9)	46.00 (36.00,57.00)** ##	25.30 (23.40,27.40)** ##
	Diabetes	103	84 (81.6)	19 (18.4)	56.00 (45.00,63.00)** ##	25.20 (23.50,27.70)** ##
	Hyperlipidemia	388	272 (70.1)	116 (29.9)	43.50 (34.00,53.00)** ##	24.90 (22.90,26.90)** ##
	Fatty liver	442	334 (75.6)	108 (24.4)	45.00 (34.00,55.00)** ##	26.20 (24.60,28.10)** ##

Vs. healthy controls, $^{*}P < 0.05$, vs. healthy controls, $**P < 0.01$, vs. subhealth fatigue, $^{\#}P < 0.05$, vs. subhealth fatigue, $^{\#\#}P < 0.01$.

Table 3: Statistical result of the tongue body and tongue coating (mean (SD) and median (P_{25}, P_{75})).

Domain	Color space	Index	Healthy controls ($N = 551$)	Subhealth fatigue ($N = 252$)	Disease fatigue ($N = 1160$)
TB	RGB	TB-R	156.00(143.00,171.00)	153.00(139.00,165.75)	158.00(147.00,169.00)##
		TB-G	99.00(90.00,110.00)	98.00(87.00,110.00)	100.00(92.00,110.75)#
		TB-B	105.00(94.00,118.00)	104.00(93.00,118.00)	108.00(99.00,120.00)** ##
	YCrCb	TB-Y	115.77(107.05,126.27)	115.40(105.14,125.09)	117.46(110.08,126.16)##
		TB-Cr	152.17(149.64,154.65)	151.31(148.37,153.84)**	152.21(148.82,155.17)#
		TB-Cb	121.46(119.99,124.21)	121.32(119.84,126.08)	121.74(120.00,127.46)*
	HSI	TB-H	176.27(169.98,179.15)	176.52(166.25,180.00)	175.16(162.12,178.32)** ##
		TB-S	0.18(0.16,0.20)	0.18(0.15,0.20)	0.18(0.16,0.20)
		TB-I	119.00(108.00,132.00)	118.50(106.00,130.00)	121.00(113.00,132.00)* ##
	Lab	TB-L	104.33(100.72,108.58)	104.08(99.70,108.05)	104.94(101.84,108.42)##
		TB-a	20.62(18.42,22.79)	20.49(18.11,22.68)	20.98(18.69,23.13)
		TB-b	4.91(1.64,6.59)	5.01(−0.17,6.87)	4.35(−1.82,6.23)** #
	Texture index	TB-CON	65.33(42.36,92.43)	66.07(40.86,97.57)	60.92(41.26,85.49)
		TB-ENT	1.19(1.09,1.27)	1.19(1.08,1.28)	1.17(1.08,1.26)
		TB-ASM	0.08(0.07,0.10)	0.08(0.07,0.10)	0.08(0.07,0.10)*
		TB-MEAN	0.02(0.02,0.03)	0.02(0.02,0.03)	0.02(0.02,0.03)*
TC	RGB	TC-R	152.00(17.65)	149.56(17.84)	152.44(16.62)
		TC-G	115.00(103.00,126.00)	114.50(103.00,127.00)	114.00(104.00,126.00)
		TC-B	120.00(106.00,134.00)	118.00(105.25,135.00)	121.00(109.00,138.00) *
	YCrCb	TC-Y	124.63(115.36,134.38)	123.65(113.84,134.00)	124.44(116.39,134.07)
		TC-Cr	143.88(141.46,146.59)	143.15(140.51,145.71) *	143.95(140.29,147.04)
		TC-Cb	123.25(121.65,126.17)	123.25(121.64,128.76)	123.76(121.83,129.82)**
	HSI	TC-H	177.27(167.16,181.53)	177.39(156.48,182.40)	175.23(151.57,180.00)** ##
		TC-S	0.12(0.10,0.14)	0.12(0.09,0.14)	0.12(0.10,0.14)
		TC-I	129.00(117.00,140.00)	128.00(115.00,140.00)	129.00(119.00,140.00)
	Lab	TC-L	108.41(104.62,112.06)	108.11(104.12,112.09)	108.28(105.06,112.02)
		TC-a	13.10(2.78)	12.71(2.78)	13.27(2.75)
		TC-b	3.17(0.03,4.86)	3.22(-1.97,4.95)	2.63(−3.34,4.68)*
	Area index	perAll	0.50(0.41,0.67)	0.53(0.41,0.76)	0.49(0.38,0.79)
		perPart	1.11(1.04,1.25)	1.08(1.03,1.22)	1.10(1.02,1.21)
	Texture index	TC-CON	82.23(57.65,115.59)	88.97(58.76,125.73)	82.58(56.88,114.81)
		TC-ENT	1.25(1.16,1.32)	1.27(1.17,1.34)	1.25(1.16,1.33)
		TC-ASM	0.07(0.06,0.08)	0.07(0.06,0.08)	0.07(0.06,0.09)
		TC-MEAN	0.03(0.02,0.03)	0.03(0.02,0.03)	0.03(0.02,0.03)

Vs. healthy controls, $^{*}P < 0.05$, vs. healthy controls, $**P < 0.01$, vs. subhealth fatigue, $^{\#}P < 0.05$, vs. subhealth fatigue group, $^{\#\#}P < 0.01$.

of this study, to a certain extent, indicated that patients with disease fatigue had more severe functional decline and other abnormal changes in cardiovascular functions, such as left ventricular function, peripheral resistance, great artery compliance, wall elasticity, and blood viscosity. Since fatigue in the most serious case can cause sudden cardiac death, it was of great practical value to use a sphygmograph to detect fatigue in order to diagnose cardiovascular disease and help to guide the early intervention.

In this study, our focus was on whether tongue and pulse data or tongue and pulse combined with age and BMI could distinguish different fatigue states well and whether age and BMI affected tongue and pulse, but to what extent

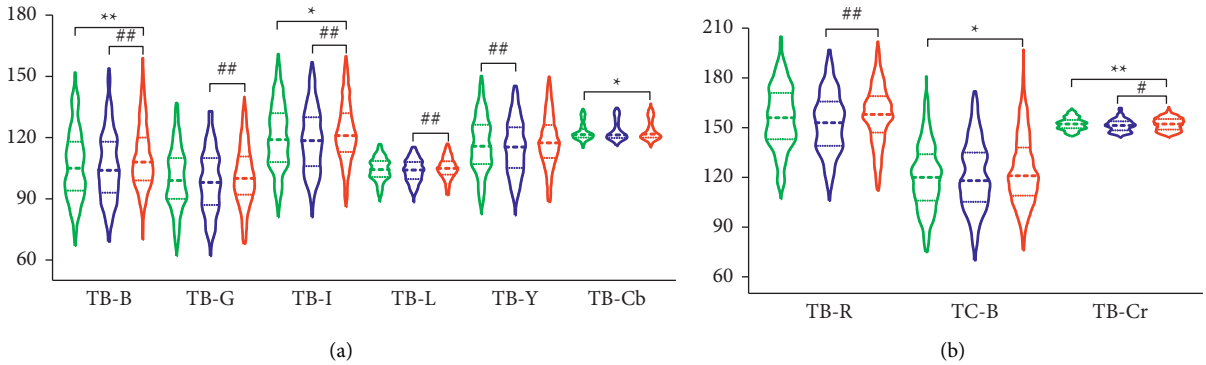

Figure 5: Violin plots of the tongue characteristic parameters of the three groups.

Table 4: Statistical result of pulse characteristic parameters (mean (SD) and median (P_{25}, P_{75})).

Index	Healthy controls ($N = 551$)	Subhealth fatigue ($N = 252$)	Disease fatigue ($N = 1160$)
t_1(s)	0.13(0.12,0.14)	0.13(0.12,0.14)	0.13(0.12,0.14)$**^{\#\#}$
t_2(s)	0.22(0.21,0.24)	0.22(0.21,0.24)	0.23(0.22,0.24)$**^{\#\#}$
t_3(s)	0.26(0.25,0.27)	0.26(0.25,0.27)	0.26(0.25,0.28)$**^{\#}$
t_4(s)	0.34(0.33,0.36)	0.34(0.33,0.36)	0.35(0.34,0.37)$**^{\#\#}$
t_5(s)	0.40(0.39,0.42)	0.41(0.39,0.42)	0.41(0.39,0.42)
h_1(mv)	112.37(91.47,131.98)	110.54(89.53,132.73)	102.70(79.10,129.20)$**^{\#}$
h_2(mv)	76.26(57.64,96.64)	76.52(60.46,95.92)	72.92(53.31,96.65)
h_3(mv)	68.33(53.88,88.51)	69.70(55.68,87.59)	65.87(48.83,86.66)
h_4(mv)	42.20(32.03,51.17)	41.58(32.52,51.59)	38.25(28.18,49.68)$**^{\#}$
h_5(mv)	3.54(1.08,6.80)	3.35(0.66,6.18)	1.76(0.18,4.22)$**^{\#}$
w_1 (s)	0.16(0.13,0.19)	0.17(0.14,0.19)	0.17(0.14,0.20)**
w_2 (s)	0.10(0.09,0.13)	0.11(0.09,0.14)	0.12(0.09,0.15)$**^{\#}$
w_1/t	0.20(0.16,0.22)	0.20(0.18,0.23)	0.21(0.18,0.24)$**^{\#}$
w_2/t	0.13(0.11,0.16)	0.14(0.11,0.17) *	0.15(0.12,0.18)$**^{\#}$
h_1/t_1	874.36(701.84,1041.02)	862.66(693.70,1046.20)	775.13(607.61,972.90)$**^{\#\#}$
h_3/h_1	0.62(0.55,0.73)	0.64(0.56,0.73)	0.66(0.56,0.74)**
h_4/h_1	0.38(0.08)	0.38(0.08)	0.37(0.08)
As(mv·s)	0.20(0.03)	0.21(0.03)	0.21(0.03)$**^{\#}$
Ad(mv·s)	0.11(0.09,0.13)	0.11(0.09,0.13)	0.10(0.08,0.12)$**^{\#\#}$
t(s)	0.82(0.75,0.90)	0.82(0.77,0.90)	0.82(0.75,0.90)

Vs. healthy controls, $*P < 0.05$, vs. healthy controls, $**P < 0.01$, vs. subhealth fatigue, $^{\#}P < 0.05$, vs. subhealth fatigue, $^{\#\#}P < 0.01$.

was not the focus of our study. Age and BMI are the basic information of human health and are closely related to disease. Studies have shown that there was a correlation between age and disease [36]; with the increase in age, the risk of disease gradually increased. BMI is an index of obesity which is closely related to health state, and studies have shown that the BMI combined circumference level can be used to assess the risk of coronary heart disease in diabetic patients [37]. Our actual research results also conform to this law, age and BMI combined with tongue and pulse data had a better effect on the classification of fatigue.

This study provided a noninvasive differential diagnosis method for the data-driven evaluation of different fatigue states based on the data of tongue and pulse, and modern tongue diagnosis and pulse diagnosis have good application prospects. The modern technique of tongue diagnosis and pulse diagnosis is simple and feasible. With the development of the information technology of tongue diagnosis and pulse diagnosis, a small, convenient, and movable tongue diagnosis and pulse diagnosis instrument has provided the possibility of family health monitoring. With the development of more wearable health products and more personal health data collection and use, the integration of tongue diagnosis and pulse diagnosis information with other health information can effectively judge fatigue and other health conditions and make early warning of diseases, and it also can effectively promote the development of Internet smart medical treatment and remote diagnosis and treatment and innovate and develop the intelligent diagnosis and treatment model of TCM. In the future, on the basis of multidisciplinary interaction, natural language interaction or graphical interface, multichannel intelligent human-computer interaction, data mining, and machine learning based on big data to achieve automated analysis, we can effectively improve the accuracy of diagnosis and treatment.

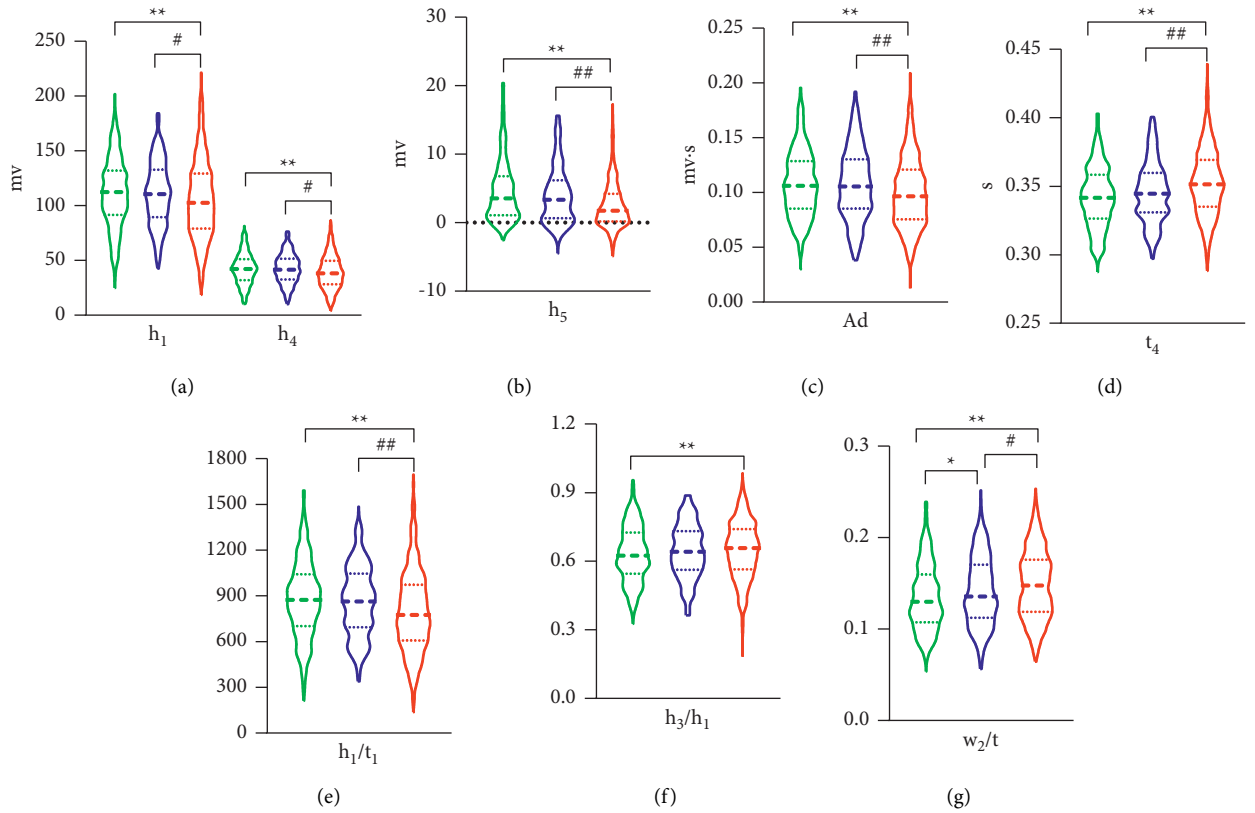

Figure 6: Violin plots of the pulse characteristic parameters of the three groups.

Table 5: Classification result of the model based on tongue and pulse data.

Model	AUC	Accuracy (%)	Sensitivity (%)	Specificity (%)
Healthy controls and subhealth fatigue	0.678	65.70	73.60	57.44
Subhealth and disease fatigue	0.759	67.40	73.55	60.47
Healthy controls and disease fatigue	0.847	76.30	80.40	71.63

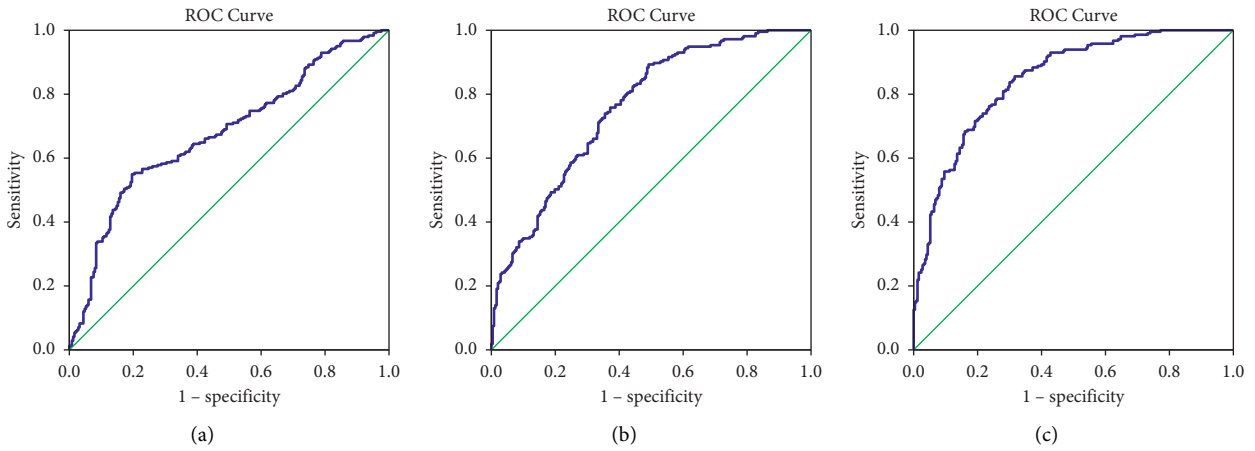

Figure 7: ROC curves of the classification model based on tongue and pulse data. (a) Healthy and subhealth fatigue. (b) Subhealth and disease fatigue. (c) Healthy and disease fatigue.

Table 6: Classification result of the model based on tongue and pulse data and BMI and age.

Model	AUC	Accuracy (%)	Sensitivity (%)	Specificity (%)
Healthy controls and subhealth fatigue	0.698	68.29	80.80	55.37
Subhealth and disease fatigue	0.882	81.18	83.06	79.07
Healthy controls and disease fatigue	0.924	84.73	87.60	81.40

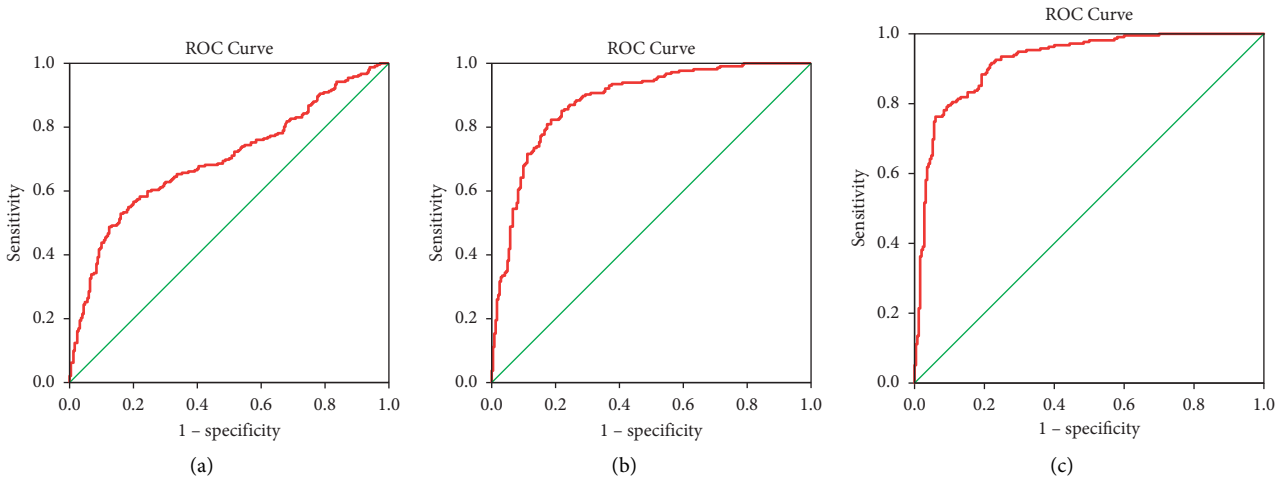

Figure 8: ROC curves of the classification model based on tongue and pulse data and BMI and age. (a) Healthy and subhealth fatigue. (b) Subhealth and disease fatigue. (c) Healthy and disease fatigue.

5. Conclusions

In this study, we successfully analyzed the tongue and pulse data characteristics and distribution trend of the fatigue and healthy population; at the same time, logistic regression modeling can realize the diagnosis of disease fatigue and subhealth fatigue to a certain extent. It provided a noninvasive differential diagnosis method for the data-driven evaluation of different fatigue states based on the data of the tongue and pulse.

Data Availability

The datasets generated and analyzed during the current study are not publicly available due to the confidentiality of the data, which is an important component of the National Key Technology R & D Program of the 13th Five-Year Plan (no. 2017YFC1703301) in China, but are available from the corresponding author on reasonable request.

Ethical Approval

The IRB approved the study protocol of Shuguang Hospital affiliated with Shanghai University of TCM (No. 2018-626-55-01).

Consent

Written informed consent was obtained from all patients.

Disclosure

This manuscript has been presented as a preprint in "Research Square" [38]. It has been withdrawn. The funders were not involved in preparing this manuscript or in the decision to submit it for publication. They had no role in the study's design, collection, analysis, and interpretation of data, or writing the manuscript.

Conflicts of Interest

The authors declare no conflicts of interest.

Authors' Contributions

Yu-lin Shi and Tao Jiang drafted the initial manuscript, Xiao-juan Hu assisted with data statistical analysis, Li-ping Tu contributed to writing and revising process, all other authors assisted in data collection of the tongue and pulse, and Jia-tuo Xu and Jing-bin Huang contributed to the schemes design and guidance. All authors read and approved the final manuscript.

Acknowledgments

This research was funded by the National Key Research and Development Program of China (2017YFC1703301), National Natural Science Foundation of China (81873235, 81973750, and 81904094), and Yulin Shi of the Experiment Center for Teaching and Learning Campus Budget Item, 2021LK029.

References

[1] P. B. Persson and A. Bondke Persson, "Fatigue," *Acta Physiology (Oxford)*, vol. 218, no. 1, pp. 3-4, 2016.

[2] P. Golabi, M. Sayiner, H. Bush, L. H. Gerber, and Z. M. Younossi, "Patient-reported outcomes and fatigue in patients with chronic hepatitis C infection," *Clinics in Liver Disease*, vol. 21, no. 3, pp. 565–578, 2017.

[3] M. G. Swain and D. E. J. Jones, "Fatigue in chronic liver disease: new insights and therapeutic approaches," *Liver International*, vol. 39, no. 1, pp. 6–19, 2019.

[4] K. F. Chung, Y. M. Yu, and W. F. Yeung, "Correlates of residual fatigue in patients with major depressive disorder: the role of psychotropic medication," *Journal of Affective Disorders*, vol. 186, pp. 192–197, 2015.

[5] C. C. Ebede, Y. Jang, and C. P. Escalante, "Cancer-related fatigue in cancer survivorship," *Medical Clinics of North America*, vol. 101, no. 6, pp. 1085–1097, 2017.

[6] U. Thirunavukkarasu, S. Umapathy, P. T. Krishnan, and K. Janardanan, "Human Tongue thermography could be a prognostic tool for prescreening the type II diabetes mellitus," *Evidence Based Complementary Alternative Medicine*, vol. 2020, Article ID 3186208, 16 pages, 2020.

[7] N. M. Li, S. W. Li, S. Liu, C. Y. Wang, and Z. C. Cui, "Clinical study of brain fatigue of tongue picture[J]," *Lishizhen Medicine and Materia Medica Research*, vol. 25, no. 10, pp. 2424–2426, 2014.

[8] T. Ding, L. Feng, L. Rong, L. Danxi, Y. Y. Syria, and T. Ying, "Tongue inspection on fatigue," in *Proceedings of the 10th Annual Academic Conference of TCM Rehabilitation Committee of China Disabled Persons rehabilitation Association*, p. 4, Beijing, China, 2015.

[9] W. Chunyan, "Observation of tongue and pulse representation in 147 cases of fatigue syndrome," in *Proceedings of the first National Conference on Integrated Traditional Chinese and Western Medicine diagnosis*, p. 1, Beihai, Guangxi, China, 2006.

[10] Y. M. Yiu and M. Y. Qiu, "A preliminary epidemiological study and discussion on traditional Chinese medicine pathogenesis of chronic fatigue syndrome in Hong Kong," *Journal of Chinese Integrative Medicine*, vol. 3, no. 5, pp. 359–362, 2005.

[11] Z. Y. Luo, J. Cui, X. J. Hu, L. P. Tu, H. D. Liu, and W. Jiao, "A study of machine-learning classifiers for hypertension based on radial pulse wave," *Biomed Research International*, vol. 2018, Article ID 2964816, 12 pages, 2018.

[12] X. J. Hu, L. Zhang, J. T. Xu, B. C. Liu, J. Y. Wang, and Y. L. Hong, "Pulse wave cycle features analysis of different blood pressure grades in the elderly," *Evidence Based Complement Alternative Medicine*, vol. 2018, Article ID 1976041, 12 pages, 2018.

[13] J. Li, P. Yuan, X. Hu et al., "A tongue features fusion approach to predicting prediabetes and diabetes with machine learning," *Journal of Biomedical Informatics*, vol. 115, Article ID 103693, 2021.

[14] A. C. Y. Tang, J. W. Y. Chung, and T. K. S. Wong, "Digitalizing traditional Chinese medicine pulse diagnosis with artificial neural network," *Telemedicine and E-Health*, vol. 18, no. 6, pp. 446–453, 2012.

[15] J. Zhang, J. Xu, X. Hu, Q. Chen, L. Tu, and J. Huang, "Diagnostic method of diabetes based on support vector machine and tongue images," *Biomed Research International*, vol. 2017, Article ID 7961494, 9 pages, 2017.

[16] M. C. Hu, K. C. Lan, W. C. Fang et al., "Automated tongue diagnosis on the smartphone and its applications," *Computer Methods and Programs in Biomedicine*, vol. 174, pp. 51–64, 2019.

[17] B. Zhang, X. Wang, J. You, and D. Zhang, "Tongue color analysis for medical application," *Evidence Based Complement Alternative Medicine*, vol. 2013, Article ID 264742, 11 pages, 2013.

[18] Y. Y. Kung, T. B. J. Kuo, C. T. Lai, Y. C. Shen, Y. C. Su, and C. C. H. Yang, "Disclosure of suboptimal health status through traditional Chinese medicine-based body constitution and pulse patterns," *Complementary Therapies in Medicine*, vol. 56, Article ID 102607, 2021.

[19] H. Z. Shi, Q. C. Fan, J. Y. Gao et al., "Evaluation of the health status of six volunteers from the mars 500 project using pulse analysis," *Chinese Journal of Integrative Medicine*, vol. 23, no. 8, pp. 574–580, 2017.

[20] L. L. Wang, X. Y. Zhang, and M. Peng, "Objective analysis of complexion and tongue color in patients with chronic fatigue syndrome," *Shandong Medical Journal*, vol. 59, no. 05, pp. 81–83, 2019.

[21] H. H. Zhu, Z. F. Zhang, X. Chen, Z. F. Fei, and J. T. Xu, "Design and evaluation of the simple health assessment questionnaire H2O," in *Proceedings of the Fourth National Symposium on Integrated Chinese and Western Medicine Diagnosis*, p. 4, Hohhot, Inner Mongolia, China, 2010.

[22] J. F. Zhang, J. T. Xu, L. P. Tu, Z. F. Zhang, X. J. Hu, and J. Cui, "Study on the characteristics of sub-health symptoms and TCM syndrome patterns distribution in 1 754 non-disease population," *Chinese Journal of Integrative Medicine*, vol. 37, no. 08, pp. 934–938, 2017.

[23] Chinese Diabetes Society, "Guidelines for the prevention and control of type 2 diabetes in China," *Chinese Journal of Practical Internal Medicine*, Chinese Diabetes Society, Shanghai, China, vol. 38, no. 04, pp. 292–344, 2018.

[24] J. Liu, "Highlights of the 2018 Chinese hypertension guidelines," *Clinical Hypertension*, vol. 26, no. 1, p. 8, 2020.

[25] Y. Chen, Y. B. Chen, and R. T. Tao, "Interpretation of "guideline for prevention and treatment of dyslipidemia in Chinese adults in 2016," *Chinese Journal of Practical Internal Medicine*, vol. 37, no. S1, pp. 38–42, 2017.

[26] Fatty Liver and Alcoholic L:iver Disease Group, Hepatology Society, Chinese Medical Association, "Diagnostic criteria for nonalcoholic fatty liver disease (draft)," *Chinese Journal of Hepatology*, no. 6, p. 325, 2001.

[27] J. B. Huang, J. T. Xu, Z. F. Zhang, L. P. Tu, J. Cui, and X. J. Hu, "Influence of "daily rhythm" factors on tongue image characteristics of healthy people," *China Journal of Traditional Chinese Medicine and Pharmacy*, vol. 33, no. 08, pp. 3462–3465, 2018.

[28] J. Cui, L. P. Tu, J. F. Zhang, X. J. Hu, J. B. Huang, and G. L. Wang, "Research on pulse graph characteristics of 1 720 cases with different health status and age gradient," *Shanghai Journal of Traditional Chinese Medicine*, vol. 52, no. 04, pp. 15–23, 2018.

[29] E. Bucur, A. F. Danet, C. B. Lehr, E. Lehr, and M. Nita-Lazar, "Binary logistic regression-instrument for assessing museum indoor air impact on exhibits," *Journal of the Air & Waste Management Association*, vol. 67, no. 4, pp. 391–401, 2017.

[30] K. Zhang, W. Geng, and S. Zhang, "Network-based logistic regression integration method for biomarker identification," *BMC Systems Biology*, vol. 12, no. S9, p. 135, 2018.

[31] D. Z. Sun, L. Xu, P. K. Wei, L. Liu, and J. He, "Syndrome differentiation in traditional Chinese medicine and

E-cadherin/ICAM-1 gene protein expression in gastric carcinoma," *World Journal of Gastroenterology*, vol. 13, no. 32, pp. 4321–4327, 2007.

[32] N. Zhang, C. Li, Y. Guo, and H. C. Wu, "Study on the intervention effect of qi gong wan prescription on patients with phlegm-dampness syndrome of polycystic ovary syndrome based on intestinal flora," *Evidence Based Complementary Alternative Medicine*, vol. 2020, p. 18, Article ID 6389034, 2020.

[33] J. N. Zhao, Y. Zhang, X. Lan et al., "Efficacy and safety of xinnaoning capsule in treating chronic stable angina (qi stagnation and blood stasis syndrome)," *Medicine*, vol. 98, no. 31, Article ID e16539, 2019.

[34] L. J. Qiao, Z. Qi, L. P. Tu, Y. H. Zhang, L. P. Zhu, and J. T. Xu, "The association of radial artery pulse wave variables with the pulse wave velocity and echocardiographic parameters in hypertension," *Evidence Based Complementary Alternative Medicine*, vol. 2018, Article ID 5291759, 11 pages, 2018.

[35] N. Gomes Ribeiro Moura and A. Sá Ferreira, "Pulse waveform analysis of Chinese pulse images and its association with disability in hypertension," *Journal of Acupuncture and Meridian Studies*, vol. 9, no. 2, pp. 93–98, 2016.

[36] B. Wolff, V. Macioce, V. Vasseur et al., "Ten-year outcomes of anti-vascular endothelial growth factor treatment for neovascular age-related macular disease: a single-centre French study," *Clinical & Experimental Ophthalmology*, vol. 48, no. 5, pp. 636–643, 2020.

[37] T. Komatsu, K. Fujihara, M. H. Yamada, T. Sato, M. Kitazawa, and M. Yamamoto, "449-P: impact of body mass index (BMI) and waist circumference (WC) on coronary artery disease (CAD) in Japanese with and without diabetes mellitus (DM)," *Diabetes*, vol. 69, no. Supplement 1, p. 449, 2020.

[38] Y. L. Shi, T. Jiang, X. J. Hu, J. Cui, L. T. Cui, and L. P. Tu, "A study on fatigue classification by logistic regression method: based on data of tongue and pulse. 2021, research square," https://www.researchsquare.com/article/rs-551999/v1.

Hindawi
Evidence-Based Complementary and Alternative Medicine
Volume 2022, Article ID 5841451, 9 pages
https://doi.org/10.1155/2022/5841451

Research Article

An Algorithm for Automatic Rib Fracture Recognition Combined with nnU-Net and DenseNet

Junzhong Zhang,[1] **Zhiwei Li**,[2] **Shixing Yan**,[3] **Hui Cao**,[2] **Jing Liu**,[2] **and Dejian Wei**[2]

[1]*School of Clinical, Shandong University of Traditional Chinese Medicine, Jinan 250355, China*
[2]*School of Intelligence and Information Engineering, Shandong University of Traditional Chinese Medicine, Jinan 250355, China*
[3]*Shanghai Daosh Medical Technology, Shanghai 201203, China*

Correspondence should be addressed to Dejian Wei; 289608678@qq.com

Received 18 October 2021; Accepted 31 January 2022; Published 25 February 2022

Academic Editor: Zhaohui Liang

Rib fracture is the most common thoracic clinical trauma. Most patients have multiple different types of rib fracture regions, so accurate and rapid identification of all trauma regions is crucial for the treatment of rib fracture patients. In this study, a two-stage rib fracture recognition model based on nnU-Net is proposed. First, a deep learning segmentation model is trained to generate candidate rib fracture regions, and then, a deep learning classification model is trained in the second stage to classify the segmented local fracture regions according to the candidate fracture regions generated in the first stage to determine whether they are fractures or not. The results show that the two-stage deep learning model proposed in this study improves the accuracy of rib fracture recognition and reduces the false-positive and false-negative rates of rib fracture detection, which can better assist doctors in fracture region recognition.

1. Introduction

Rib fracture is a common clinical trauma of the chest, specifically a complete or partial break in the continuity of the rib structure. Rib fractures can be caused by a variety of reasons, such as falls, traffic accidents, and fights. They are more common not only for children and the elderly but also for young and middle-aged people [1]. Most patients with rib fractures have more than one fracture area, so it is important to detect all areas of trauma in a short time for follow-up treatment [2]. Computed tomography (CT) is an important medical aid used to diagnose rib fractures in the chest [3]. However, each patient's chest CT image consists of hundreds of slices [4], which is time-consuming and labor-intensive to manually review. It not only increases the workload of the orthopedic medical staff but also easily leads to visual and psychological fatigue, which will increase the probability of misdiagnosis or even missed diagnosis.

Existing systems for the diagnosis of rib fractures can be broadly classified into two categories [5]. The first category is traditional fracture recognition models, which are used to obtain suspected fracture areas and assist the physician in diagnosis [6]. The second type is fracture recognition models based on deep learning [7]. The following are characteristics that exist in the current rib fracture diagnosis using deep learning: (1) the CT image-based rib fracture dataset has samples with doubtful annotation [8], and different doctors have different annotations for the same case [9]. The doubtful annotation is a great challenge for deep learning models. (2) In general, CT images of fractures are 3D medical images. Deep learning models dealing with 3D data usually have problems such as occupying large memory, slow computation speed, and being prone to overfitting [10]. (3) Deep learning-based fracture region detection models usually suffer from high false-negative and false-positive rates.

To solve the above problems, we propose a rib fracture region recognition model based on the nnU-Net [11] segmentation network and DenseNet [12] classification network, which consists of two stages of training. In the first stage, segmentation of rib fracture regions is completed to

generate candidates of fracture regions. At the second stage, the secondary judgment of candidate fracture regions is completed. DenseNet classification network is mainly performed to remove false-positive fracture regions. The experiments show that the new proposed model improves the accuracy of rib fracture recognition by achieving a 95% recognition rate for rib fractures and reducing the false-positive and false-negative rates for rib fracture detection to 5%. The rib fracture recognition algorithm proposed in this study can well assist physicians in the recognition of all fracture regions.

2. Related Work

In recent years, the rapid development of deep learning has made a great contribution to medical image-assisted diagnosis. Many researchers have applied deep learning techniques to fracture-assisted diagnosis. It has been proven that the use of fracture-assisted diagnosis systems can improve the accuracy of the doctor's recognition of fractures and effectively save time. For example, Tourassi et al. applied deep convolutional networks (ConvNets) to automatically detect posterior spine fractures. They used the multi-atlantoaxial fusion technique to segment spine and its posterior vertebrae in spine CT and predict the probability of fracture at the image edges using ConvNets (three orthogonal patches in axial, coronal, and sagittal planes) in a 2.5D manner [13]. This method is effective in improving the sensitivity of posterior spine fracture identification. Olczak et al. selected five openly available deep learning networks and trained them to determine fracture, lateral body, and examination views for 256,000 wrist, hand, and ankle x-rays. The experimental results showed that all networks achieved over 90% accuracy in identifying lateral body parts and examination views [14]. Lindsey et al. developed a deep convolutional neural network (DCNN) to assist emergency medicine clinicians in reading x-rays of fracture patients, and experimental results showed that the average misinterpretation rate of emergency medicine clinicians was relatively reduced by 47% with the assistance of this system [7]. Raghavendra et al. proposed an automated technique for thoracolumbar fracture detection based on convolutional neural networks (CNNs) [15], which was able to perform thoracolumbar fracture detection without segmenting the vertebral body, and its detection accuracy was able to reach 99.1% [16]. Takaaki et al. experimentally compared the intertrochanteric fracture diagnostic performance of convolutional neural networks and orthopedic surgeons through the radiograph of proximal femoral [17]. The study showed that convolutional neural networks were three percentage points more accurate than orthopedic surgeons in detecting intertrochanteric fractures. Pranata et al. evaluated the performance of the residual network (ResNet) and visual geometry group (VGG) for heel fracture detection and used the classification results of the better-performing ResNet as input to the SURF algorithm for detecting fracture location and type [18], which validated the feasibility of deep learning neural networks for automatic heel fracture detection.

In previous studies, numerous researchers have also applied deep learning to the detection of rib fractures. To effectively detect and segment rib fracture regions, Jin et al. proposed a deep learning model named FracNet [19], which was based on the classical segmentation network-3D UNet, improved by a sampling strategy during training, and did not rely on the extraction of the rib centerline. This method achieved a detection sensitivity of 92.9% and reduced the time required for clinical testing. Weikert et al. evaluated the diagnostic performance of automatic detection of acute and chronic rib fractures using a deep learning algorithm for whole-body trauma CT [20]. The algorithm consisted of a ResNet-based region proposal phase followed by a fast region-based CNN, which had a final sensitivity of 87.4% and a specificity of 91.5% for rib fracture detection. Zhou et al. evaluated the performance of a two-dimensional convolutional neural network (CNN) model to automatically detect and classify rib fractures and was able to output a structured report [21]. After using this rib fracture automatic detection system to aid clinical trials, it was found that the diagnostic accuracy of radiologists increased from 80.3% to 91.1%, sensitivity increased from 62.4% to 86.3%, and significantly reduced the time required for diagnosis. Meng et al. proposed a heterogeneous neural network consisting of a cascaded feature pyramid network and a classification network for rib fracture detection and classification. They compared the effectiveness of CT images with and without a deep learning model for rib fracture detection and classification [22]. The experimental results show that, with the aid of the deep learning model, clinicians can effectively improve the recall rate and classification accuracy of CT images of rib fractures. Castro-Zunti et al. evaluated the performance of InceptionV3 [23], ResNet50 [24], MobileNetV2 [25], and VGG16 [26] models when classifying acute, aged, and nonfractured ribs in axial CT images [27]. The experimental results showed that the model consisting of the first seven blocks of InceptionV3 was more accurate and faster and achieved a 5-fold cross-validated accuracy and macrosensitivity of 96% and 94%, respectively. These preliminary works provide us with feasible methods for studying rib fracture recognition, but most of the studies summarized above were conducted on a two-dimensional basis, losing three-dimensional information. Therefore, we propose an algorithm for automatic rib fracture recognition with nnU-Net and DenseNet in this study.

3. Materials and Methods

3.1. Rib Fracture Dataset. The experimental data were the publicly available RibFrac Dataset from the MICCAI 2020 RibFrac Challenge: Rib Fracture Detection and Classification competition, which was published by Liang Jin et al., the authors of the FracNet network structure. The data can be accessed at https://ribfrac.grand-challenge.org/dataset/. The competition dataset contains a total of 420 samples from the training set, 80 samples from the validation set, and 160 samples from the test set. The data are 3D rib CT images annotated by a number of radiologists with different years of experience in the interpretation of chest CT. An example image of a 3D rib CT data is shown in Figure 1. The lower left view shows the current 3D view, and the remaining three views show the results of slicing the data in the axial, coronal,

and sagittal planes, respectively. The blue crosshairs represent the current slice position, and the red area is the rib fracture region that was manually marked by physicians.

3.2. Dataset Preprocessing. Considering that the test set samples that were not annotated could not be used for calculating prediction accuracy, 160 test set samples were removed from this experiment. Due to the limitation of the experimental equipment and GPU computing power, it was impossible to use the whole training set for training. So, we chose 200 training samples with 1,910 different fracture regions, which can reflect the proportional characteristics of the original dataset, as the training set data. The validation set of the dataset contains no rib fracture images. To reduce the model validation time, this experiment removes no rib fracture images and uses the 3D CT images of 60 rib fractures in the validation set. Table 1 shows the statistics of rib fracture regions.

From Table 1, after integrating the fracture labels, the ratio of the number of fracture regions in the training and validation sets is approximately 8 : 2, which is in line with the common ratio of data in the training and validation sets.

4. Model Description

The structure of our model includes the rib fracture region segmentation and the fracture region false-positive exclusion. The first stage used nnU-Net as the fracture region segmentation model, and the second stage used DenseNet as the fracture classification model. Since the second stage of the fracture region false-positive exclusion experiment was based on the first stage of the fracture region segmentation experiment, the network structure of the two-stage rib fracture automatic recognition model based on deep learning proposed in this study is shown in Figure 2.

4.1. Stage1: Regional Segmentation of Rib Fractures. This stage mainly completes the segmentation of the rib fracture region and generates the fracture region to be candidates. The main steps are as follows: a series of data preprocessing is taken on the 3D CT rib fracture training set. Then, nnU-Net is selected as the segmentation model and the processed training set is fed into this model for segmentation model training. After training, the rib images in the validation set are predicted to be segmented to generate the fracture regions to be candidates, which facilitate further determination of false positives in the segmented regions.

4.1.1. Preprocessing

(a) Category label processing: the fracture region of this competition dataset was labeled using instance segmentation, with the original label containing five values. 0 indicates the background region, 1–4 represents different types of rib fractures, respectively, and −1 denotes that this region is a rib fracture. Since the images are blurred and ambiguous, it makes rib fracture difficult to be diagnosed and no specific category can be given. In practice, all labels 1–4 and −1 are combined into one category to increase the number of images of rib fracture regions, reducing the influence of suspected fracture regions in the sample on the segmentation results and increasing the accuracy of rib fracture segmentation. Therefore, this experiment is binary fracture region segmentation regardless of the category of fracture.

(b) Since there are inconsistencies in the resolution of the 3D CT fracture images in the training set, they need to be adjusted to a uniform resolution, e.g., 1 mm × 1 mm × 1 mm voxel size, which varies with the training set. The result is obtained by calculating the average voxel size of the training set. After determining the voxel size, each sample in the training set is resampled to obtain the new image size with the following equation.

$$\text{size} = \text{spacing} \times \text{voxel}. \tag{1}$$

In equation (1), *size* is the new 3D image size, spacing is the calculated voxel size, and voxel is the 3D pixel value.

(c) By counting the range of HU (Hounsfield unit) values for pixels within the mask of the entire dataset, a range of HU values in the percentage range of [0.5, 99.5] was cropped and then normalized using the z-score method. In particular, each voxel value of each 3D CT sample is normalized to a mean of 0 so that the processed 3D CT data conforms to a standard normal distribution, i.e., with a mean of 0 and a standard deviation of 1. Such processing facilitates model training and model convergence, improving the training speed of the model with the following equation:

$$y = \frac{x - \text{mean}}{\text{std}}. \tag{2}$$

In equation (2), y is the normalized data, mean denotes the mean of the 3D CT sample, and std denotes the variance of the 3D CT sample.

4.1.2. Loss Function. The Dice similarity coefficient is an important indicator for evaluating the degree of overlap between the two samples and the effectiveness of the segmentation, so the segmentation loss function of the model also uses Dice as the loss function. The formula for the Dice loss function is as follows:

$$L_{\text{dice}} = 1 - \frac{2|P \cap T|}{|P| + |T|}, \tag{3}$$

where P and T are the predicted segmentation mask and the true segmentation annotation, respectively.

When using Dice loss, generally positive samples for small targets will produce severe oscillations. Because in the case of only foreground and background, once some of the

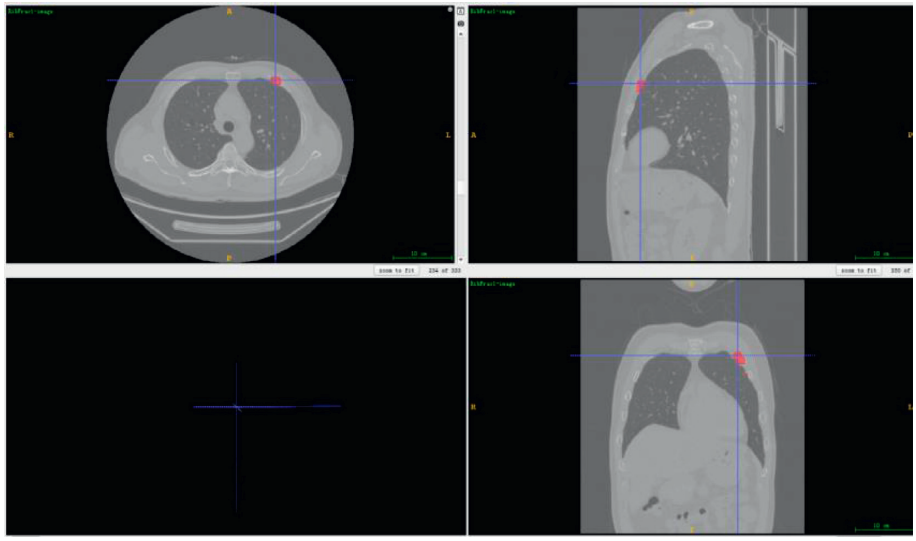

Figure 1: Example of a 3D rib CT image.

Table 1: Regional statistics for rib fractures.

Dataset	Sample size	Number of fracture areas
Training set	200	1910
Validation set	60	435

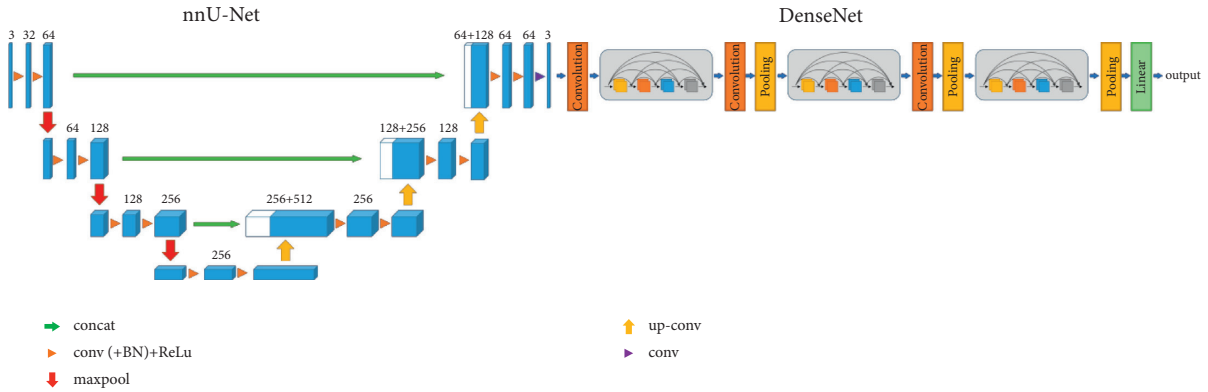

Figure 2: The network structure model proposed in this study. It consists of nnU-Net and DenseNet.

pixels in the small target are incorrectly predicted, it will lead to a drastic change in the loss value and the gradient. The loss function is improved, and the final loss function is shown as follows:

$$L = L_{\text{dice}} + L_{\text{ce}} + L_{\text{contour}}, \tag{4}$$

where L_{ce} denotes the error loss arising from binary cross-entropy. L_{contour} denotes the error loss in the 3D profile of the fracture, which is formulated as follows:

$$L_{\text{contour}} = \int_{\Omega} \left|\nabla H_{\varepsilon}(\phi)\right|, \tag{5}$$

where Ω represents the region to be segmented that belongs to the whole sample, ϕ represents the level set function, the zero-level curve represents the segmentation boundary, and H_{ε} represents the smoothed approximation of the Heaviside function.

4.1.3. Model Architecture. In this phase, the nnU-Net is used as the experimental framework. It is a robust adaptive framework based on 2D Unet [28] and 3D Unet [29] that adapts to any medical image dataset and performs different data preprocessing for different datasets. The framework focuses on the following: preprocessing (resampling and normalization), training (loss, optimizer settings, and data augmentation), inference (patch-based strategies, test-time-augmentation integration, and model integration), and postprocessing (e.g., enhanced single-connected domains), while making substantial modifications to the original Unet structure and not adopting new structures such as residual connectivity, dense connectivity, and attention mechanisms.

The framework has three basic versions of the Unet model: 2D Unet, 3D Unet, and 3D cascade Unet. The first two models are 2D Unet and 3D Unet. The third model is a cascaded Unet structure, where the first stage performs coarse segmentation of downsampled low-resolution images, and the second stage combines the results of the first stage for fine-tuning. 3D Unet is used for both stages. Compared with the original Unet, the Unet model in nnU-Net replaces ReLU with leaky ReLU and replaces Batch Norm with Instance Norm.

4.1.4. Postprocessing. After training the segmentation model, the 3D CT images are predicted by means of patches. There will be overlap regions in the sliding prediction, and they will be predicted several times. In this study, we take the maximum value to fuse the prediction results multiple times, as shown in the following equation:

$$P_s(\text{voxel}) = \max\left(P_{s1}, P_{s2}, \ldots, P_{si}\right), \tag{6}$$

where P_s(voxel) represents the segmentation prediction for each voxel and P_{si} represents the *i-th* segmentation prediction for that voxel.

4.2. Stage2: Fracture Area False-Positive Exclusion. In the first stage of the segmentation network, because of the restricted size of the network structure and the insufficient abundance of random negative samples, the variability of morphological features of these false-positive regions and the morphological features of the fracture are not sufficiently learned. A false-positive exclusion network needs to be designed for targeted learning to reduce the false-positive rate. Therefore, the second stage completes the false-positive exclusion of the fracture area and makes a secondary judgment of the predicted fracture area from the first stage.

The main steps are shown as follows. First, a series of data preprocessing is performed on candidate fracture regions produced by segmentation in the first stage. Subsequently, the processed data are fed into the classification model for training a classification model. Eventually, local fracture regions in the validation set are predicted and category labels of the regions are output, with 0 indicating no fracture and 1 indicating a fracture. In addition, the input data for the second stage were preprocessed in the same way as the first stage, and the 3D DenseNet was used as the fracture classification model for the experiments.

4.2.1. Model Inputs. To make the classification model to pay more attention to the contextual information around the fracture region and improve the accuracy of fracture classification, when preprocessing for clipping local fracture regions, three different sizes of local fracture regions are clipped in turn, e.g., $48 \times 48 \times 48$, $64 \times 64 \times 64$, and $80 \times 80 \times 80$. They can also be adjusted according to the actual fracture region size. After cropping local fracture regions of different sizes, three different sizes of fracture images were used as input to train the classification models for each of the three different input sizes.

4.2.2. Postprocessing of Classified Probability Values. After separately training the classification model for the three different input sizes, the final classification results are performed using a weighted average, as shown in the following equation:

$$P_c = \lambda_{c1} \times P_{c1} + \lambda_{c2} \times P_{c2} + \lambda_{c3} \times P_{c3}, \tag{7}$$

where P_c represents the final classification probability value of a 3D CT image, λ_{c1} denotes the classification accuracy of the classification model on the validation set under the first size, P_{c1} represents the probability value of the classification model on the validation set under the first size, λ_{c2} denotes the classification accuracy under the second size, P_{c2} represents the probability value under the second size, λ_{c3} denotes the classification accuracy under the third size, and P_{c3} represents the probability value under the third size. The given equation is used to calculate whether a fracture is present in the input local 3D CT image.

4.3. Model Evaluation and Parameter Settings

4.3.1. Evaluation Metrics. In this study, the diagnostic model evaluation metrics use Dice similarity coefficient (Dice), intersection over union (IoU), average symmetric surface distance (ASSD), and Hausdorff distance (HD).

Dice is a similarity measure used to calculate the similarity of two samples. The value of Dice is in the range [0–1], 1 for the best segmentation result and 0 for the worst. The formula is as follows:

$$\text{Dice}(P, T) = \frac{2|P \wedge T|}{|P| + |T|}, \tag{8}$$

where P is the predicted segmentation result, and T is the labeled segmentation result. The above equation is also equivalent to the following equation:

$$\text{Dice}(P, T) = \frac{2\text{TP}}{\text{FP} + 2\text{TP} + \text{FN}}. \tag{9}$$

IoU is also used to calculate the similarity of two samples. It equals to the overlap of the two regions divided by the pooled portion of the two regions, with the following formula:

$$\text{IoU} = \frac{\text{TP}}{\text{FP} + \text{TP} + \text{FN}}. \tag{10}$$

ASSD is the average surface distance, which is an evaluation metric in the medical image segmentation competition CHAOS. ASSD is given by the following equation:

$$\mathrm{ASSD}(A,B)=\frac{1}{|S(A)|+|S(B)|}\left(\sum_{a\in S(A)}\min_{b\in S(B)}\|a-b\|+\sum_{b\in S(B)}\min_{a\in S(A)}\|b-a\|\right), \tag{11}$$

where $S(A)$ denotes the surface voxel of set A, $S(B)$ denotes the surface voxel of set B, and a and b denote the voxels in sets A and B, respectively. $\|\cdot\|$ is the distance paradigm between the point sets A and B, which generally is the Euclidean distance.

The Dice is more sensitive to the internal filling of the mask, while the HD is more sensitive to the segmented boundary. HD is a measure describing the degree of similarity between two sets of points. It is also a definition of the distance between two sets of points. In contrast to ASSD, HD is also known as the maximum surface distance. HD between $A=\{a_1,\ldots,a_p\}$ and $B=\{b_1,\ldots,b_p\}$ is defined as

$$H(A,B)=\max\left(\max_{a\in A}\left\{\min_{b\in B}\|a-b\|\right\},\max_{b\in B}\left\{\min_{a\in A}\|b-a\|\right\}\right). \tag{12}$$

4.3.2. Parameter Settings. After data preprocessing, the input data size (patch size column), the training batch size, the number of pooling layers, the resolution of the input image, and the average image size for 2D Unet and 3D Unet are shown in Table 2.

5. Results

5.1. Quantitative Indicator Assessment Results. Among the above metrics, larger is better for both Dice and IoU, and smaller is better for ASSD and HD-95, indicating that the predicted segmentation results are very close to the true segmentation results. HD-95 denotes the value of the Hausdorff distance multiplied by 0.95, with the aim of eliminating the effect of a very small subset of the outliers. The results can be seen from Table 3:

(1) The 2D Unet segmentation model trained with 2D fracture images as input has the worst performance in all indicators, because the 2D image segmentation does not consider the three-dimensional structure of 3D fractures and lacks the contextual information of the Z-axis expression of the fracture region.

(2) Since 3D_lowres Unet has a small image resolution compared to 3D_fullres Unet during training, the input image size after sampling is smaller. It results in a loss of some detailed information in the 3D image, so it is lower than 3D_fullres Unet in all indexes, 0.82 lower in Dice, 1.21 lower in IoU, 9.21 mm higher in ASSD, and 14.9 mm higher in HD-95. Despite the loss of some information, the 3D Unet segmentation model learns contextual and global information about the fracture region. Its result is better than 2D Unet, with 10.93 higher in Dice, 11.06 higher in IoU, 10.39 mm lower in ASSD, and 31.41 mm lower in HD-95.

(3) We use 3D_lowres Unet as a first stage in the 3D cascade Unet and fine-tune it with 3D_fullres Unet, which is better than 3D_lowres Unet in all metrics, with 0.27 higher in Dice and 0.43 higher in IoU. However, it decreases in ASSD and HD-95. Because some detailed information is lost in the first stage, in the second stage, the predictions from the first stage are preprocessed again. The two preprocessing processes make the loss of detail information in the 3D fracture region more severe. Moreover, ASSD and HD-95 indicators belong to the distance category and are extremely sensitive to image resolution, resulting in a slightly worse result for ASSD and HD-95. But Dice and IoU work well.

The result in Table 3 shows that using high-fractional images as input to the segmentation model gives optimal segmentation results. Low-fractional images do not achieve optimal segmentation of the fracture region due to the loss of detail.

5.2. Model Loss Curves. Figure 3 shows the training set loss curve, the validation set loss curve, and the trained Dice value curve for each Unet model. The following results can be shown in Figure 3:

(1) The training loss and validation loss of each Unet model both gradually decrease, indicating that each Unet model slowly converges. The training loss and validation loss of 3D_fullres Unet are the lowest, at around 0.28 and 0.35, respectively.

(2) In terms of the training Dice values, it is similar to the results calculated for the quantitative metrics. It also shows that 3D_fullres Unet and 3D cascade Unet have the highest training Dice values, both around 0.75, and 2D Unet has the lowest Dice values, only around 0.68.

(3) In the training process of the two-stage 3D cascade Unet, training loss can be seen to significantly drop, while the validation loss shows fluctuations. It is because the two-stage 3D Unet loses some detailed information, which makes the model to learn limited features, and the model gradually shows an overfitting situation.

From the above analysis, 3D Unet performs best in rib fracture region segmentation. Its training results are fed into a false-positive exclusion model for the fracture region in the second phase of the experiment. Its effectiveness in validating the identification of rib fracture regions on the validation set achieved a 95% identification rate and only a 5% false-positive rate. This result indicates that this study can better assist physicians in the identification of rib fracture regions.

Table 2: Input parameter settings.

Model	Patch size	Batch size	Pooling layers	Spacing/mm	Median size
2D Unet	512 × 512	12	[7, 7]	1.25 × 0.74 × 0.74	328 × 512 × 512
3D_lowres Unet	96 × 160 × 160	2	[4, 5, 5]	2.58 × 1.53 × 1.53	159 × 248 × 248
3D_fullres Unet	96 × 160 × 160	2	[4, 5, 5]	1.25 × 0.74 × 0.74	328 × 512 × 512

Table 3: Assessment results of different Unet models with rib fracture segmentation.

Unet	Dice	IOU	ASSD/mm	HD-95/mm
2D	51.05	36.54	35.00	124.42
3D-fuller	62.80	48.81	11.40	78.11
3D-lower	61.98	47.60	20.61	93.01
3D-cascade	62.25	48.03	22.13	100.61

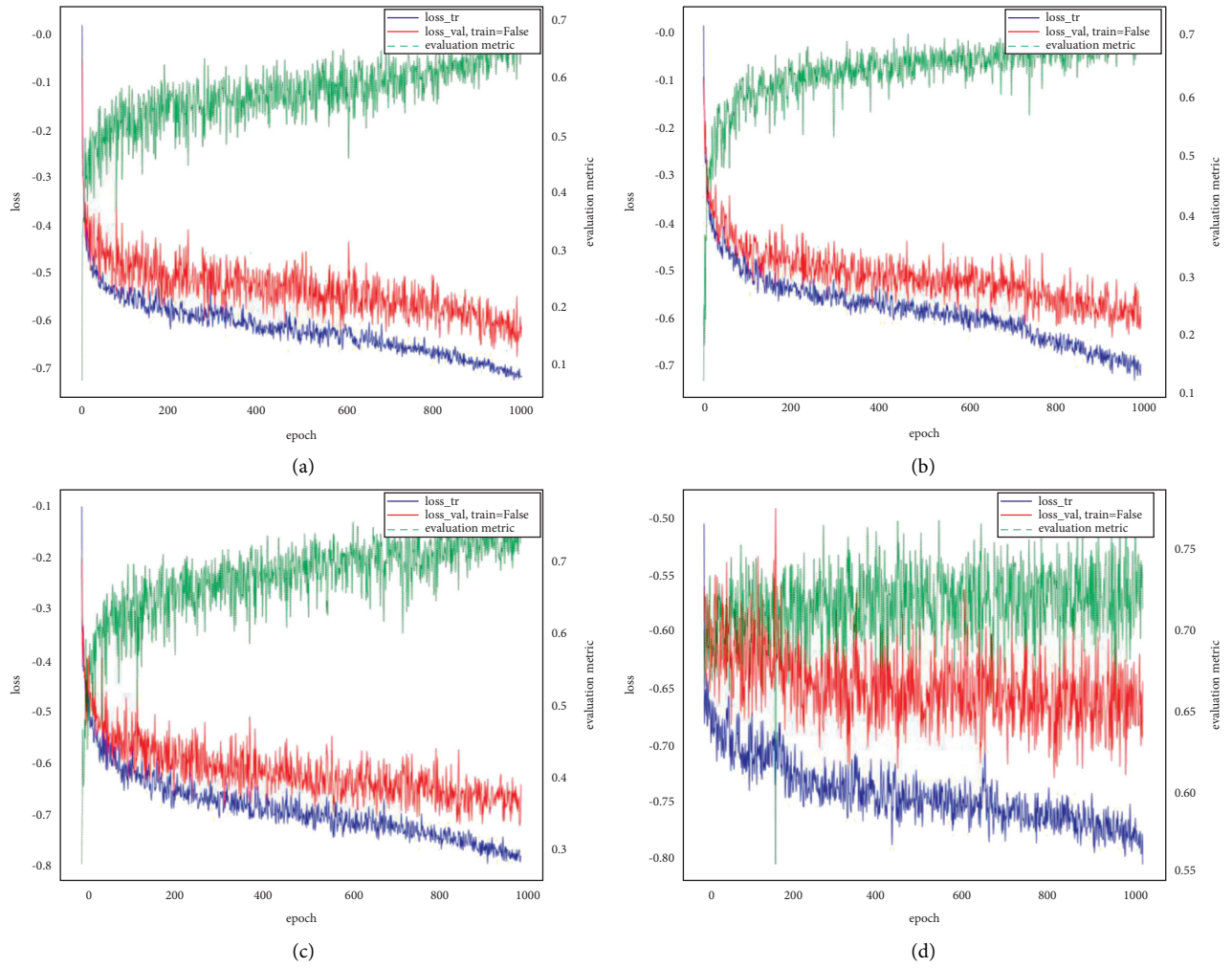

Figure 3: The training set loss curve. (a) Loss curves and Dice value curves for 2D Unet. (b) Loss curves and Dice value curves for 3D_lowres Unet. (c) Loss curves and Dice value curves for 3D_fullres Unet. (d) Loss curves and Dice value curves for 3D cascade Unet.

6. Discussion

We propose a two-stage rib fracture automatic recognition algorithm, which is mainly used to rapidly identify multiple rib fracture lesions in patients with rib fractures, which assists clinicians to diagnose multiple rib fractures from CT scans. As a deep learning-assisted diagnostic system, it was trained on a training set of 1,910 rib fracture regions from 200 patients and tested on a test set of 435 rib fracture regions from 60 patients. It achieved a 5% false-positive rate and 95% recognition rate in the final rib fracture detection and significantly reduced the time required for clinical judgment.

There are two main reasons for these results. First, we used nnU-Net as the network framework for training in the first phase of rib fracture region segmentation. The nnU-Net is proposed as a framework for automatic adaptation to any new dataset. It has a good segmentation result for the RibFrac dataset. Furthermore, we trained each of the three models in the nnU-Net network framework—2D Unet, 3D Unet, and 3D cascade Unet—to select the network model with the best results for subsequent experiments. Second, we conducted an experiment to exclude false-positive fracture regions on the basis of rib fracture region segmentation. We use 3D DenseNet as the classification model. Using the segmented fracture regions as the input to the classification model can narrow the classification range and exclude the false-positive fracture regions in the first stage of segmentation, which effectively improved the accuracy of rib fracture recognition.

From the final identification results, it can be concluded that the two-stage rib fracture automatic recognition algorithm proposed in this study is helpful in assisting physicians in multiple rib fracture recognition and detection, indicating that the artificial intelligence-aided diagnosis system is feasible for multiple rib fracture recognition.

Data Availability

The experimental data were the publicly available RibFrac Dataset from the MICCAI 2020 RibFrac Challenge: Rib Fracture Detection and Classification competition, which was published by Liang Jin et al., the authors of the FracNet network structure. The data can be accessed at https://ribfrac.grand-challenge.org/dataset/.

Conflicts of Interest

The authors declare that there are no conflicts of interest regarding the publication of this paper.

Acknowledgments

This research was sponsored by the National Natural Science Foundation of China (nos. 82074579 and 81973981), the Traditional Chinese Medicine Science and Technology Project of Shandong Province (no. 2020M006), and the Natural Science Foundation of Shandong Province (no. ZR2020MH360).

References

[1] Y. Jinliang and H. Guang, "Strategies, operational techniques and future directions in the treatment of rib fractures," *Journal of Traumatic Surgery*, vol. 18, no. 1, pp. 1–5, 2016.

[2] S. Khung, P. Masset, A. Duhamel et al., "Automated 3D rendering of ribs in 110 polytrauma patients: strengths and limitations," *Academic Radiology*, vol. 24, no. 2, pp. 146–152, 2017.

[3] Y. Jun and T. Guoyu, "Exploring the working principles of CT in medical imaging technology and new applications," *Imaging Research and Medical Applications*, vol. 4, no. 3, pp. 87-88, 2020.

[4] H. Ringl, M. Lazar, M. Töpker et al., "The ribs unfolded - a CT visualization algorithm for fast detection of rib fractures: effect on sensitivity and specificity in trauma patients," *European Radiology*, vol. 25, no. 7, pp. 1865–1874, 2015.

[5] J. He, S. L. Baxter, J. Xu, J. Xu, X. Zhou, and K. Zhang, "The practical implementation of artificial intelligence technologies in medicine," *Nature Medicine*, vol. 25, no. 1, pp. 30–36, 2019.

[6] Y. LeCun, Y. Bengio, and G. Hinton, "Deep learning," *Nature*, vol. 521, no. 7553, pp. 436–444, 2015.

[7] R. Lindsey, A. Daluiski, S. Chopra et al., "Deep neural network improves fracture detection by clinicians," *Proceedings of the National Academy of Sciences*, vol. 115, no. 45, pp. 11591–11596, 2018.

[8] A. Urbaneja, J. De Verbizier, A.-S. Formery et al., "Automatic rib cage unfolding with CT cylindrical projection reformat in polytraumatized patients for rib fracture detection and characterization: feasibility and clinical application," *European Journal of Radiology*, vol. 110, pp. 121–127, 2019.

[9] M. Lenga, T. Klinder, C. Bürger, J. V. Berg, A. Franz, and C. Lorenz, "Deep learning based rib centerline extraction and labeling," in *Proceedings of the International Workshop on Computational Methods and Clinical Applications in Musculoskeletal Imaging*, Granada, Spain, September 2018.

[10] X. Xu, F. Zhou, B. Liu, D. Fu, and X. Bai, "Efficient multiple organ localization in CT image using 3D region proposal network," *IEEE Transactions on Medical Imaging*, vol. 38, 2019.

[11] F. Isensee, P. F. Jaeger, S. A. A. Kohl, J. Petersen, and K. H. Maier-Hein, "nnU-Net: a self-configuring method for deep learning-based biomedical image segmentation," *Nature Methods*, vol. 18, no. 2, pp. 203–211, 2021.

[12] G. Huang, Z. Liu, L. V. D. Maaten, and K. Q. Weinberger, "Densely connected convolutional networks," in *Proceedings of the 2017 IEEE Conference on Computer Vision and Pattern Recognition*, pp. 2261–2269, Honolulu, HI, USA, July 2017.

[13] G. D. Tourassi, S. G. Armato, and H. R. Roth, "Deep convolutional networks for automated detection of posterior-element fractures on spine CT," *Medical Imaging 2016: Computer-Aided Diagnosis*, vol. 9785, Article ID 97850P, 2016.

[14] J. Olczak, N. Fahlberg, A. Maki et al., "Artificial intelligence for analyzing orthopedic trauma radiographs," *Acta Orthopaedica*, vol. 88, no. 6, pp. 581–586, 2017.

[15] X. C. Chen, *Deep Learning Algorithm and Application Research Based on Convolutional Neural Network*, Zhejiang Gongshang University, Zhejiang, China, 2014.

[16] U. Raghavendra, N. S. Bhat, A. Gudigar, and U. R. Acharya, "Automated system for the detection of thoracolumbar fractures using a CNN architecture," *Future Generation Computer Systems*, vol. 85, 2018.

[17] U. Takaaki, T. Yuki, and G. Shinichi, "Detecting intertrochanteric hip fractures with orthopedist-level accuracy using a deep convolutional neural network," *Skeletal Radiology*, vol. 48, 2018.

[18] Y. D. Pranata, K. C. Wang, and J. C. Wang, "Deep learning and SURF for automated classification and detection of calcaneus fractures in CT images," *Computer Methods and Programs in Biomedicine*, vol. 171, 2019.

[19] L. Jin, J. Yang, K. Kuang et al., "Deep-learning-assisted detection and segmentation of rib fractures from CT scans: development and validation of FracNet," *EBioMedicine*, vol. 62, Article ID 103106, 2020.

[20] T. Weikert, L. A. Noordtzij, J. Bremerich et al., "Assessment of a deep learning algorithm for the detection of rib fractures on whole-body trauma computed tomography," *Korean Journal of Radiology*, vol. 21, no. 7, p. 891, 2020.

[21] Q.-Q. Zhou, J. Wang, W. Tang et al., "Automatic detection and classification of rib fractures on thoracic CT using convolutional neural network: accuracy and feasibility," *Korean Journal of Radiology*, vol. 21, no. 7, pp. 869–879, 2020.

[22] X. H. Meng, D. J. Wu, Z. Wang et al., "A fully automated rib fracture detection system on chest CT images and its impact on radiologist performance," *Skeletal Radiology*, vol. 50, no. 9, pp. 1821–1828, 2021.

[23] C. Szegedy, V. Vanhoucke, S. Ioffe, J. Shlens, and Z. Wojna, "Rethinking the inception architecture for computer vision," in *Proceedings of the 2016 IEEE Conference on Computer Vision and Pattern Recognition (CVPR)*, pp. 2818–2826, Las Vegas, NV, USA, June 2016.

[24] K. He, X. Zhang, S. Ren, and J. Sun, "Deep residual learning for image recognition," in *Proceedings of the 2016 IEEE Conference on Computer Vision and Pattern Recognition (CVPR)*, pp. 770–778, Las Vegas, NV, USA, June 2016.

[25] M. Sandler, A. Howard, M. Zhu, A. Zhmoginov, and L. C. Chen, "Mobilenetv2: inverted residuals and linear bottlenecks," in *Proceedings of the 2018 Conference on Computer Vision and Pattern Recognition*, pp. 4510–4520, Salt Lake City, UT, USA, June 2018.

[26] K. Simonyan and A. Zisserman, "Very deep convolutional networks for large-scale image recognition," in *Proceedings of the 3rd International Conference on Learning Representations, ICLR 2015*, San Diego, CA, USA, May 2015.

[27] R. Castro-Zunti, K. J. Chae, Y. Choi, G. Y. Jin, and S.-b. Ko, "Assessing the speed-accuracy trade-offs of popular convolutional neural networks for single-crop rib fracture classification," *Computerized Medical Imaging and Graphics*, vol. 91, Article ID 101937, 2021.

[28] T. Falk, D. Mai, R. Bensch et al., "U-Net: deep learning for cell counting, detection, and morphometry," *Nature Methods*, vol. 16, no. 1, pp. 67–70, 2019.

[29] Ö. Çiçek, A. Abdulkadir, S. S. Lienkamp, T. Brox, and O. Ronneberger, "3D U-net: learning dense volumetric segmentation from sparse annotation," in *Proceedings of the 19th International Conference Medical Image Computing and Computer-Assisted Intervention – MICCAI 2016. MICCAI 2016*, S. Ourselin, L. Joskowicz, M. Sabuncu, G. Unal, and W. Wells, Eds., Athens, Greece, October 2016.

Hindawi
Evidence-Based Complementary and Alternative Medicine
Volume 2022, Article ID 5157870, 10 pages
https://doi.org/10.1155/2022/5157870

Research Article

Assessment of Reporting Quality in Randomized Controlled Trials of Acupuncture for Primary Insomnia with CONSORT Statement and STRICTA Guidelines

Jinsong Yang,[1] **Fanjun Yu**,[1] **Keyi Lin**,[1] **Haotian Qu**,[1] **Yihan He**,[2,3] **Jing Zhao**,[4] **Fen Feng**,[5] **Litao Pan**,[6] **and Yu Kui**[3]

[1]*Guangzhou University of Chinese Medicine, Guangzhou, China*
[2]*Guangdong Provincial Academy of Chinese Medical, Guangzhou, China*
[3]*The Second Clinical Medical College of Guangzhou University of Chinese Medicine, Guangzhou, China*
[4]*Institute of Chinese Medical Science, University of Macau, Macau, China*
[5]*Hospital of Chengdu University of Traditional Chinese Medicine, Chengdu, China*
[6]*The First Affiliated Hospital of Shenzhen University, Shenzhen, China*

Correspondence should be addressed to Litao Pan; ltpan@email.szu.edu.cn and Yu Kui; kuiyutcm@gzucm.edu.cn

Received 31 October 2021; Accepted 26 January 2022; Published 17 February 2022

Academic Editor: Zhaohui Liang

Aim. To assess the reporting quality of randomized controlled trials (RCTs) on acupuncture for primary insomnia (PI). *Methods*. Seven Chinese and English databases were searched for publication reporting RCTs on acupuncture for PI from the inception of the databases to August 6, 2021. The internationally recognized Consolidated Standards of Reporting Trials (CONSORT) statement and the International Standards for Reporting Interventions in Controlled Trials of Acupuncture (STRICTA) guidelines were used to evaluate the reporting quality. The agreement between two researchers was calculated by Cohen's kappa. *Results*. A total of 102 eligible RCTs were assessed. According to the CONSORT statement (2017), the positive reporting rates of items such as "abstract," "background," "participants," and "numbers analyzed" were above 80%. However, the positive reporting rates of items such as "sample size," "randomization implementation," "Outcomes and estimation," "Ancillary analyses," and "Registration" were below 20%. According to STRICTA guidelines, the positive reporting rates of items such as "style of acupuncture," "reasons for acupuncture treatment," "Number of needles inserted," "Needle retention time," "Treatment regimen," and "precise description of the control intervention" were above 80%. However, the positive reporting rates of items such as "setting and context of treatment" and "practitioner background" were below 20%. *Conclusion*. It is essential to advocate the endorsement of the CONSORT statement and STRICTA guidelines to improve the quality of acupuncture RCT reports.

1. Introduction

Primary insomnia (PI) is characterized by difficulty in falling asleep or staying asleep, with the exclusion of insomnia caused by various secondary factors including mental, physical, and neurological disorders, alcohol, or drugs [1]. The overall prevalence of insomnia was 5%–10% worldwide [2], while the incidence rate of insomnia in females is higher than that in males [3]. Severe insomnia affects normal life and work and increases the risk of various diseases [4].

At present, the treatments of insomnia mainly include cognitive behavioral therapy (CBT), drug therapy, physical therapy, and complementary and alternative medicine (CAM) [5]. CBT, the first-line therapy of insomnia, costs a lot and lacks effective training providers, making it difficult to popularize [6]. Although the short-term efficacy of drugs in the treatment of insomnia has been confirmed, it has been reported that there are side effects such as hangover, drug resistance, and drug dependence [5]. The efficacy of physical therapy (such as transcranial magnetic stimulation and

phototherapy) is not certain yet [4, 7]. Acupuncture in CAM has been applied by acupuncture practitioners and accepted by patients and is being increasingly widely used to treat insomnia [8].

The number of RCTs of acupuncture for PI has been increasing gradually in recent years, but their work varies considerably in quality [9]. Accurate and standardized RCT reports not only can reduce the bias of systematic evaluation but also help medical decision-making [10]. With high-quality reports, acupuncture practitioners can easily master effective operating procedures [11].

In the past ten years, there has not been any study on the quality evaluation of RCTs of acupuncture for PI. The CONSORT statement (https://www.consort-statement.org/) is an evidence-based report guide designed to improve research transparency and reduce waste [10]. STRICTA (https://stricta.info/), an independent guide for reporting acupuncture research, has become a formal extended version of the CONSORT report of RCTs [11]. These guidelines ensure transparency and a coherent approach to testing and reporting trials of complex interventions [10]. A range of studies have shown that it can help readers gain information on study design, intervention implementation, data analysis, and so on [12, 13]. Therefore, in this study, the internationally recognized CONSORT statement of nondrug RCTs (2017) and STRICTA were used to evaluate the reporting quality of RCTs of acupuncture for PI so as to lay a foundation for high-quality RCT design of acupuncture treatment for insomnia in the future.

2. Methods

2.1. Document Retrieval Methods. (1) Database for retrieval: China National Knowledge Infrastructure (CNKI), China Science and Technology Journal Database (VIP), Wanfang Database (WF), PubMed, Embase, Web of Science, and Cochrane Library. (2) Publication time: from database creation to August 6, 2021. (3) Search strategy: the following search terms were used in both Chinese and English: (primary insomnia) AND (acupuncture OR acupuncture therapy) AND (randomized controlled trial OR RCT).

2.2. Inclusion Criteria. All the following criteria were met: (1) confirmed diagnosis of PI; (2) RCT of acupuncture to treat PI; and (3) the intervention measures of the experimental group were acupuncture (including hand acupuncture, electroacupuncture, ear acupuncture, abdominal acupuncture, and eye acupuncture) or acupuncture combined with traditional Chinese medicine (TCM) nondrug therapy other than acupuncture (acupressure, moxibustion, ear point treatment, etc.); the control group was treated with Western medicine or sham acupuncture or acupuncture at nonmeridian and nonacupoints.

2.3. Exclusion Criteria. One of the following criteria was met: (1) not in accordance with the inclusion criteria; (2) no confirmed diagnosis of PI in the RCT (such as diagnosis of perimenopausal insomnia); (3) in addition to acupuncture, the intervention measures in the experimental group also included drug treatment; (4) the control group was treated with routine acupuncture; (5) if the content of conference paper and periodical paper or Chinese paper and English paper were similar, the one with higher quality were chosen; (6) if the papers were about the same RCT, the one published later was chosen; (7) the paper was about research protocol; and (8) full-text paper not available.

2.4. Document Screening and Data Extraction. Paper screening, data extraction, and cross-checking were performed by two researchers independently. In case of any disagreement, the two researchers negotiated first. Firstly, the RCT was imported into NoteExpress 3.4 (Guangzhou University of Chinese Medicine library version, released 2021, Beijing, China). After duplicate checking, the title and abstract of the paper were read. After excluding the clearly irrelevant papers, the full text of the paper was read to determine whether the inclusion should be made. The extracted data included the year of publication, author, intervention measures, CONSORT statement (2017), STRICTA standard entries, and relevant information, which were entered into Excel 2016. Disagreements between the two researchers over data selection and extraction were resolved by discussion, with the involvement of a third researcher (Yu Kui).

2.5. Quality Evaluation Method. 25 items from CONSORT (2017) and 6 items from STRICTA were used to evaluate the quality of reports. Two trained researchers with no interest conflicts extracted the data independently and evaluated the report item by item as "reported," "partially reported," or "not reported." Then, their results were cross-checked. In case of disagreement, a third researcher with no interest conflicts should arbitrate. The number of RCTs meeting each item was calculated, and the percentage of items reported was also calculated.

Cohen's κ-statistic was calculated to assess the agreement between two researchers. We judged agreement as poor if $\kappa \leq 0.2$; fair if $0.2 < \kappa \leq 0.4$; moderate if $0.4 < \kappa \leq 0.6$; substantial if $0.6 < \kappa \leq 0.8$; good if $0.8 < \kappa < 1$; and prefect if $\kappa = 1$ [14]. Cohen's κ-statistic and 95% CI of each item were performed by using PASW Statistics for Windows, version 18.0 (SPSS Inc., Released 2009, Chicago, USA).

3. Results

3.1. Document Retrieval Results. According to the above retrieval strategies, a total of 1269 relevant RCTs were detected. Among them, 377 duplicated ones were screened out, and 454 clearly irrelevant ones were excluded by titles and abstracts. After reading the full text, 102 in accordance with the inclusion criteria were included, and 336 were excluded according to the exclusion criteria. Finally, 91 Chinese papers and 11 English papers were included. The process and results of literature screening are shown in Figure 1.

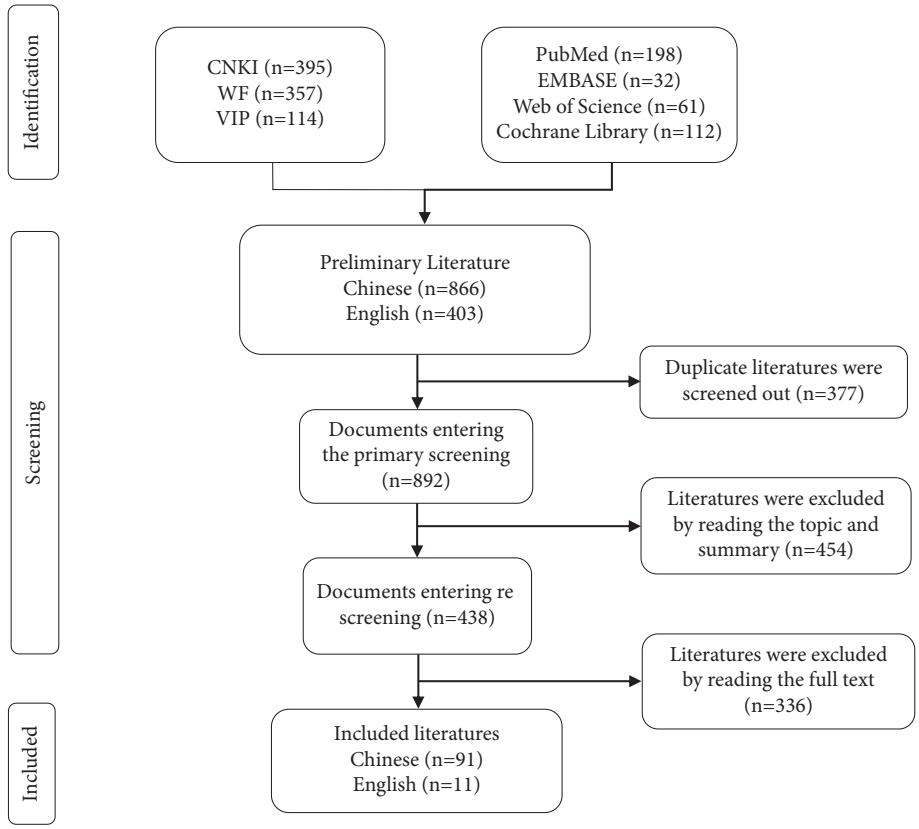

Figure 1: Process and results of literature screening.

3.2. Information of Published Papers per Year. For the 102 RCTs, the publication time was from 2006 to 2021. The number of RCTs published before 2014 was no more than five, and it increased year by year since 2015, indicating that acupuncture for PI is becoming the focused topic. Overall, the total score of CONSORT and STRICTA is on the rise. The average CONSORT and STRICTA total scores and the number of papers published in each year are shown in Figure 2.

3.3. CONSORT Statement (2017). The quality of the included RCTs was assessed by the CONSORT statement (2017), as shown in Table 1. The positive reporting rates of items such as "abstract," "background," "participants," and "numbers analyzed" were above 80%. However, the positive reporting rates of items such as "sample size," "randomization implementation," "Outcomes and estimation," "Ancillary analyses," and "Registration" were below 20%.

3.3.1. Title, Abstract, and Introduction. Of the 102 papers included, 15 (14.7%) can be identified as RCTs by title ($\kappa = 1$); 102 (100%) were structured abstracts including experimental design, methods, results, and conclusions ($\kappa = 1$); 98 (96.1%) described the scientific background and made a reasonable explanation ($0.57 < \kappa < 1.13$); and 102 (100%) were referred to specific purposes or assumptions ($\kappa = 1$).

3.3.2. Trial Methods. Among the 102 papers included, all (100%) described the experimental design and distribution proportion, and none made any changes in experimental methods after the beginning of the experiment ($\kappa = 1$). All (100%) described the eligibility criteria of the participants ($\kappa = 1$), and only 2 (2%) did not mention the place for data collection ($0.04 < \kappa < 1.28$). A vast majority (99%) described the details of interventions for each group ($\kappa = 1$). Among them, 12 (11.8%) described whether and how the interventions were standardized ($0.59 < \kappa < 0.95$), while 5 (4.9%) mentioned whether the measure providers' compliance to the protocol was evaluated or how to enhance their compliance ($0.42 < \kappa < 0.98$), and none (0%) mentioned whether the participants' compliance to the interventions was evaluated or how to enhance that ($\kappa = 1$). 87 (85.3%) completely and accurately explained the primary and secondary outcome indicators ($0.69 < \kappa < 0.99$), and the remaining 15 (14.7%) used only one outcome indicator. One article (1%) changed the outcome indicators and explained the reasons after the start of the trial ($\kappa = 1$). 14 (13.7%) reported how to determine the sample size ($0.73 < \kappa < 1.01$), and 1 (1%) partially reported. 17 articles (16.7%) described the principles of interpretation, analysis, and test suspension if there were corresponding situations ($0.57 < \kappa < 0.89$).

3.3.3. Randomized Methods. 69 (67.6%) described the methods of generating random allocation sequences ($0.77 < \kappa < 0.97$), and 4 (3.9%) mentioned the types of

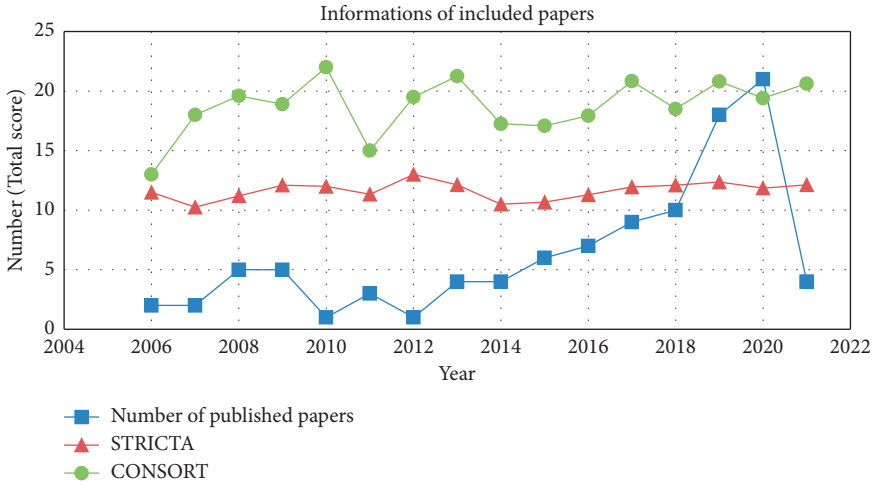

Figure 2: Information of included papers ($n = 102$).

Table 1: Assessment of reporting quality using items from the CONSORT statement ($n = 102$ studies).

Criteria	Item	Description	Number of positive trials	%	Cohen's κ coefficient	95% CI
Title and abstract	1a	Identification as a randomized trial in the title	15	14.71	1.00	1.00
	1b	Structured abstract including trial design, methods, results, and conclusions	102	100	1.00	1.00
		Background and objectives				
Introduction	2a	Scientific background and explanation of rationality	98	96.08	0.85	0.57 to 1.13
	2b	Specific objectives or hypotheses	102	100	1.00	1.00
		Trial design				
Methods	3a	Description of trial design	102	100	0.66	0.04 to 1.28
	3b	Important changes to methods after trial commencement (such as eligibility criteria), with reasons	0	0	1.00	1.00
		Participants				
	4a	Eligibility criteria for participants	102	100	1.00	1.00
	4b	Settings and locations where the data were collected	100	98.04	0.66	0.04 to 1.28
		Interventions				
	5	Interventions for each group with sufficient details to allow replication	101	99.02	1.00	1.00
	5a	Procedure for tailoring the interventions to participants	102	100	1.00	1.00
	5b	Details of whether and how the interventions were standardized	12	11.76	0.77	0.59 to 0.95
	5c	Adherence of researchers to the protocol: whether they adhere to it and how to assess that	5	4.90	0.7	0.42 to 0.98
	5d	Adherence of participants to the intervention: whether they adhere to it and how to assess that	0	0	1.00	1.00
		Outcomes				
	6a	Precisely defined prespecified primary and secondary outcome measures	87	85.29	0.84	0.69 to 0.99
	6b	Any changes to trial outcomes after trial commencement with reasons	1	0.98	1.00	1.00
		Sample size				
	7a	How sample size was determined	14	13.73	0.87	0.73 to 1.01
	7b	Explanation of interim analyses and suspension principles	17	16.67	0.73	0.57 to 0.89
		Sequence generation				

Table 1: Continued.

Criteria	Item	Description	Number of positive trials	%	Cohen's κ coefficient	95% CI
Randomization	8a	Method used to generate the random allocation sequence	69	67.65	0.87	0.77 to 0.97
	8b	Type of randomization with details of any restriction	4	3.92	0.66	0.22 to 1.10
		Allocation concealment mechanism				
	9	Description of the method used to implement the random allocation sequence (such as sequentially numbered containers), assuring concealment until interventions were assigned	34	33.33	0.91	0.82 to 1.00
		Implementation				
	10	Who generated the random allocation sequence, who enrolled participants, and who assigned intervention to participants	10	9.80	0.95	0.86 to 1.04
		Blinding				
	11a	If done, who was blinded and how	23	22.55	0.89	0.79 to 0.99
	11b	If relevant, description of the similarity of interventions	9	8.82	0.8	0.61 to 0.99
	11c	If blinding was not possible, description of attempts to limit bias	7	6.86	0.82	0.58 to 1.06
		Statistical methods				
	12a	Statistical methods used to compare groups for primary and secondary outcomes	100	98.04	0.69	0.43 to 0.95
	12b	Methods for additional analyses, such as subgroup analyses and adjusted analyses	2	1.96	1.00	1.00
		Participant flow				
	13a	For each group, the numbers of participants randomly assigned, received intended treatment, and analyzed for the outcome indicator	102	100	1.00	1.00
Results	13b	For each group, the number of losses and exclusions after randomization with reasons	33	32.35	0.91	0.84 to 0.98
	13c	For each group, report of the delay from randomization to the initiation of the intervention	4	3.92	0.85	0.57 to 1.13
		Recruitment				
	14a	Periods of recruitment and follow-up	55	53.92	0.85	0.75 to 0.95
	14b	Why the trial suspended	0	00	1.00	1.00
		Baseline data				
	15	A table showing baseline demographic and clinical characteristics for each group	62	60.78	1.00	1.00
		Numbers analyzed				
	16	The number of participants in each group included in each analysis and whether they were analyzed according to the original grouping	102	100	1.00	1.00
		Outcomes and estimation				
	17a	The results of primary and secondary outcome indicators, the estimated value of effect size and its accuracy	5	4.90	0.88	0.65 to 1.11
	17b	For dichotomous outcomes, recommendation to provide both absolute and relative effect values	0	0	1.00	1.00
		Ancillary analyses				
	18	Results of any other analyses performed, including subgroup analyses and adjusted analyses, distinguishing prespecified analysis from exploratory one	2	1.96	1.00	1.00
		Harms				
	19	All important harms or unintended effects in each group	45	44.12	0.96	0.91 to 1.01
		Limitations				
Discussion	20	Report of potential source of bias, imprecision, and multiple analyses	47	46.08	0.9	0.82 to 0.98
		Generalizability				

Table 1: Continued.

Criteria	Item	Description	Number of positive trials	%	Cohen's κ coefficient	95% CI
Other information	21	Generalizability (external validity, applicability) of the trial findings	65	63.73	0.88	0.79 to 0.97
		Interpretation				
	22	Interpretation consistent with results, balancing benefits and harms, and considering other relevant evidence	50	49.02	0.89	0.80 to 0.98
		Registration				
	23	Registration number and name of trial registry	12	11.76	1.00	1.00
		Protocol				
	24	Where the full-trial protocol can be accessed, if available	36	35.29	1.00	1.00
		Funding				
	25	Sources of funding and other support (such as supply of drugs) and role of funders	47	46.08	1.00	1.00

random methods and limited details ($0.22 < \kappa < 1.10$). 34 (33.3%) mentioned the mechanism for performing random sequence allocation and described the steps of concealing sequence numbers ($0.82 < \kappa < 1.00$). 10 (9.8%) reported who generated the random allocation sequence, included the participants, and assigned concealment to the participants ($0.86 < \kappa < 1.04$), while 1 (1%) partially mentioned the abovementioned information. 23 (22.5%) mentioned the implementation of the blind method, to whom it was implemented and how the implementation was carried out ($0.79 < \kappa < 0.99$). In 9 (8.8%), intervention measures were found to have similarities in case of relevant situations ($0.61 < \kappa < 0.99$). 7 (6.9%) described the measures to limit bias in case the blind method could not be implemented ($0.58 < \kappa < 1.06$). 100 (98%) reported the statistical methods used to compare the primary and secondary outcome indicators of each group ($0.43 < \kappa < 0.95$), and 2 (2%) described the methods of additional analysis ($\kappa = 1$).

3.3.4. Trial Results. All the 102 RCTs included described the number of cases randomly assigned to each group, received the assigned treatment, and included in the analysis of outcome indicators ($\kappa = 1$). Among them, 33 (32.4%) reported the number of cases dropped out and eliminated from each group and explained the reasons ($0.84 < \kappa < 0.98$); 10 (9.8%) reported the number of cases dropped out and eliminated from each group but without explanation of the reasons; only 4 (3.9%) reported the time from random allocation to the delay of intervention implementation in each group ($0.57 < \kappa < 1.13$).

3.3.5. Intervention Implementation. Among the 102 papers, 55 (53.9%) reported the specific periods of recruitment and follow-up ($0.75 < \kappa < 0.95$); 41 (40.2%) only reported the recruitment period but not the follow-up period; 6 (5.9%) mentioned neither. None reported suspension of the trial ($\kappa = 1$). 62 (60.8%) listed the baseline data, demographic data, and clinical characteristics of participants of each group in one table ($\kappa = 1$), and 37 (36.3%) only described in words. All papers mentioned the number of participants included in each analysis and whether they were analyzed according to the initial grouping ($\kappa = 1$); only 3 (2.9%) explicitly mentioned the use of intention to treat (ITT) analysis. Only 5 (4.9%) mentioned the results of primary and secondary outcome indicators ($0.65 < \kappa < 1.11$) and estimated effect size and relative effect value. 2 (2%) used correction analysis ($\kappa = 1$). 45 (44.1%) reported all serious harmful or unintended effects in each group ($0.91 < \kappa < 1.01$).

3.3.6. Limitations, Generalizability, and Interpretation of Trial. Among the 102 papers included, 47 (46.1%) described the potential sources of the report bias, imprecision,s and multiple analysis ($0.82 < \kappa < 0.98$); 65 (63.7%) described the generalizability of the trial findings ($0.79 < \kappa < 0.97$); 50 (49%), provided the interpretation corresponding to the results, weighed the advantages and disadvantages of the results ($0.80 < \kappa < 0.98$), and considered other relevant evidence, while another 50 (49%) partially included these.

3.3.7. Other Information. Of the 102 papers included, only 12 (11.8%) included the clinical trial registration number and the name of the trial registry ($\kappa = 1$). 36 (35.3%) provided the author's mailbox with possible access to the complete trial protocol ($\kappa = 1$). 47 (46.1%) provided information of the sources of funding and other support ($\kappa = 1$).

3.4. STRICTA Guidelines. STRICTA guidelines were used to assess the quality of included RCT reports, as shown in Table 2. The positive reporting rates of items such as "style of acupuncture," "reasons for acupuncture treatment," "number of needles inserted," "needle retention time," "treatment regimen," and "precise description of the control intervention" were above 80%. However, the positive reporting rates of items such as "setting and context of treatment" and "practitioner background" were below 20%.

3.4.1. Principle of Acupuncture Treatment. Of the 102 RCTs included, all reported the style of acupuncture treatment ($\kappa = 1$); 84 (82.4%) gave the reasons for providing acupuncture ($0.75 < \kappa < 1.62$); and 27 (26.5%) explained the

Table 2: Assessment of reporting quality of needling details from STRICTA ($n = 102$ studies).

Criteria	Item	Description	Number of positive trials	%	Cohen's κ coefficient	95% CI
Acupuncture rationale	1a	Style of acupuncture	102	100	1.00	1.00
	1b	Reasons for acupuncture treatment	84	82.35	0.87	0.75 to 1.62
	1c	Explanation of changes was caused by what treatment	27	26.47	1.00	1.00
Needling details	2a	Number of needles insertions per session	100	98.03	0.66	0.04 to 1.28
	2b	Acupoint names (or location in case of nonchannel points) (unilateral or bilateral)	62	60.78	0.90	0.82 to 0.98
	2c	Depth of insertion	71	69.61	0.98	0.93 to 1.03
	2d	Responses sought (arrival of Qi)	69	67.65	0.91	0.83 to 0.99
	2e	Needle stimulation (e.g., manual or electrical)	94	92.16	0.83	0.64 to 1.02
	2f	Needle retention time	99	97.06	1.00	1.00
	2g	Needle type (diameter, length, and manufacturer or material)	65	63.73	0.92	0.85 to 0.99
Treatment regimen	3a	Number of treatment sessions	102	100	1.00	1.00
	3b	Frequency and duration of treatment sessions	102	100	1.00	1.00
Other components of treatment	4a	Complementary interventions for the acupuncture group (e.g., moxibustion, cupping, exercises, and lifestyle advice)	30	29.41	0.95	0.88 to 1.02
	4b	Setting and context of treatment, including instructions to practitioners and information and explanations to patients	11	10.78	0.79	0.61 to 0.97
Practitioner background	5	Description of practitioners	18	17.65	0.94	0.86 to 1.02
Control interventions	6a	Rationale for the control or comparator in the context of the research question, with sources that justify the choice(s)	33	32.35	0.87	0.77 to 0.97
	6b	Precise description of the control or comparator intervention	101	99.02	1.00	1.00

changes in treatment and selected acupoints according to syndrome differentiation ($\kappa = 1$).

3.4.2. Details of Needling. Among the 102 RCTs included, a vast majority mentioned the number of needles (98.0%, $0.04 < \kappa < 1.28$), needle stimulation method (92.1%, $0.64 < \kappa < 1.02$), needle retention time (97.1%, $\kappa = 1$), the number of treatment sessions, and the frequency and duration of treatment sessions (100%, $\kappa = 1$). 62 (60.8%) reported the name of acupoints ($0.82 < \kappa < 0.98$); 36 (35.3%) did not specify whether the acupuncture treatment was given to acupoints on one side or both sides of the body; 4 (3.9%) used nonchannel points without specifying their locations. 71 (69.6%) reported the depth of needle insertion ($0.93 < \kappa < 1.03$). 69 (67.6%) mentioned seeking responses after needle insertion ($0.83 < \kappa < 0.99$). 65 (63.7%) described the needle type ($0.85 < \kappa < 0.99$), and 24 (23.5%) only mentioned the diameter and length of the needle.

3.4.3. Complementary Intervention. Among the 102 RCTs included, 30 (29.4%) administered complementary interventions to the acupuncture group ($0.88 < \kappa < 1.02$); 11 (10.8%) described information including treatment site, instructions to practitioners, and explanations to patients ($0.61 < \kappa < 0.97$).

3.4.4. Practitioner Background. 18 (17.6%) described the practitioners' background ($0.86 < \kappa < 1.02$). 1 (1%) only mentioned that acupuncture was given by professional acupuncturists, while the rest did not mention this information.

3.4.5. Control Intervention. The vast majority accurately described the control interventions ($\kappa = 1$), and only 33 (32.4%) described the reasons for control interventions ($0.77 < \kappa < 1.97$).

3.5. Agreement between Two Researchers. The two researchers reached substantial (items 3a, 4b, 5b, 5c, 7b, 8b, and 12a), good (items 2a, 6a, 7a, 8a, 9, 10, 11a, 13b, 13c, 14a, 17a, 19, 20, 21, and 22), and prefect (items 1a, 1b, 2b, 3b, 4a, 5, 5a, 5d, 6b, 12b, 13a, 15, 16, 17b, 18, 23, 24, and 25) agreement in all items in Table 1. They also reached substantial (items 2a and 4b), good (items 1b, 2b, 2c, 2d, 2e, 2g, 4a, 5, and 6a), and prefect (items 1a, 1c, 2f, 3a, 3b, and 6b) agreement in all items in Table 2.

4. Discussion

This study found that RCTs in acupuncture for PI were varied in reporting quality, with only a few in strict compliance with the CONSORT statement (2017) and STRICTA guidelines.

4.1. CONSORT Statement (2017). In terms of the CONSORT statement (2017), most RCTs had high reporting rates in the introduction, description of trial design, results, and so on. However, the following shortcomings existed: (1) By title, only 15 out of 102 included papers could be identified as RCT. (2) In terms of intervention measures, few RCTs described whether and how to standardize the intervention measures and evaluate the compliance of experimenters and participants with the trial protocol. (3) In terms of sample size, only 14 papers estimated the sample size. (4) In terms of random methods, only a few papers completely reported the generation of sequence, allocation concealment mechanism, implementation, and blinding, while most papers only mentioned the words "random," "random number table," or "opaque envelope." Acupuncture is special in the way that acupuncture practitioners cannot be blinded, so blinding was hardly mentioned in these RCTs. Given that adequate randomization is an effective measure to ensure the authenticity of the results [15], and research confirms that allocation concealment and blinding are important protective measures to reduce the bias of implementation, measurement, and estimation of effects [16] and to ensure the feasibility and repeatability of the research, researchers should describe the random sequence generation, allocation concealment, implementation, and blinding in detail. (5) In terms of results, nearly half of the RCTs reported the number of cases that were dropped out and eliminated from each group, but a small part of them did not explain the reasons. (6) In terms of the implementation of interventions, nearly half of the RCTs only reported the recruitment period or neither the recruitment nor follow-up period; one-third of the RCTs did not use a table to list the baseline data of each group; only five mentioned the estimated effect size and its precision; more than half of the RCTs did not report whether there were harmful or unintended effects in each group. (7) In terms of discussion, more than half of the RCTs did not consider the potential sources of bias, imprecision, and multiple analyses in RCTs; a small number of RCTs did not mention the generalizability of the trial findings; half of the literature only gave the results and did not weigh the benefits and harms of the results or consider other relevant evidence. (8) In terms of other information, although the International Committee of Medical Journal Editors (ICMJE) requires all clinical trials must be registered to improve transparency and accountability [17], few RCTs had clinical trial registration numbers and names of the trial registry; most RCTs did not provide access to a complete trial protocol; more than half of the RCTs did not mention the sources of funding and other support.

4.2. STRICTA Guidelines. In terms of STRICTA guidelines, the reporting rates of items 1a, 1b, 2a, 2e, 2f, 3a, 3b, and 6b were above 80%, indicating that most RCTs of acupuncture for PI have paid attention to the contents of these items. However, our study has also found the following shortcomings: (1) In terms of acupuncture details, one-third of the RCTs only mentioned the name of acupoints without the description of whether acupuncture was given to one or both sides. A few RCTs did not report the depth of needle insertion. Some RCTs did not report whether it was necessary to look for acupuncture reaction (Qi arrival) after inserting the needle. A small part of the RCTs did not explain the type of needle, while some mentioned the diameter and length of needles without the name of the manufacturer. The lack of acupuncture details not only reduces the credibility of research conclusions and the objectivity of clinical efficacy but also hinders the promotion and international development of acupuncture therapy [18]. (2) In terms of auxiliary interventions, most of the RCTs did not include the information of treatment and control interventions obtained by patients, such as any wording related to the informed consent and information affecting beliefs and expectations of the treatment. (3) More than 80% of the RCTs did not describe acupuncture practitioners, which could affect the generalizability of the trial results. (4) In terms of control intervention, most RCTs did not explain the reason for selecting the intervention for the control group. The selection of interventions for the control group should be combined with the medical ethics and scientificity of the study, and the reasons should be given [19].

Studies have shown that since CONSORT and STRICTA were firstly introduced to China in 1997 and 2003, respectively, the quality of RCTs report of acupuncture intervention published in Chinese journals has improved over time [12]. The number and quality of RCTs of acupuncture treatment for PI have been greatly improved compared with those before 2010 [20]. Compared with the evaluation of similar acupuncture RCT literature [21, 22], there are still imperfections in the design, implementation of trials, and research reports, while the report on acupuncture details is relatively complete.

4.3. Deficiency. This study has its own deficiencies. (1) Only a small number of foreign RCTs in accordance with the inclusion criteria was included, indicating a possible problem of insufficient representation of foreign literature. (2) RCTs were only searched in Chinese and English databases, so RCTs in other languages may be missed.

5. Conclusion

In conclusion, the report quality of RCTs of acupuncture for PI needs to be improved. Therefore, it is warranted to advocate the endorsement of the CONSORT statement and STRICTA guidelines for the improvement in the quality of acupuncture RCT reports. For standardized RCT reports and improved quality of acupuncture clinical research, clinical researchers need to learn the basics of clinical trials systematically, and journal editors need to learn and adopt CONSORT statements and STRICTA guidelines.

Data Availability

The dataset can be accessed from the corresponding author upon reasonable request.

Disclosure

Jinsong Yang and Fanjun Yu are the co-first authors.

Conflicts of Interest

The authors claim no conflicts of interest.

Authors' Contributions

Jinsong Yang and Yu Kui designed this study design. Fanjun Yu and Haotian Qu developed the search strategy and conducted the data analysis. Jinsong Yang and Keyi Lin extracted the searches, independently screened potential studies, and extracted the data from the included studies. Litao Pan rectified the data analysis. Jinsong Yang drafted and presented the manuscript. Yihan He and Yu Kui revised the manuscript. Fen Feng, Litao Pan, and Jing Zhao discussed the results and polished the manuscript. All authors had approved the publication of the final manuscript. Jinsong Yang and Fanjun Yu contributed equally to this study. Litao Pan and Yu Kui corresponded to this study.

Acknowledgments

The authors would like to thank all authors of the included studies. This work was supported by the programs of the National Natural Science Foundation of China (grant no. 81603682) and the project of the Guangdong Provincial Bureau of Traditional Chinese Medicine (grant no. 20131185).

Supplementary Materials

S1: search strategies in this paper. S2: evaluation records (CONSORT and STRICTA) by researchers. S3: the information of included papers. S4: the CONSORT checklist. S5: the STRICTA checklist. S6: the total scores for CONSORT and STRICTA. (*Supplementary Materials*)

References

[1] P. Zhang and Z. X. Zhao, "Interpretation of Guidelines for the diagnosis and treatment of adult insomnia in China," *Chinese Journal of Contemporary Neurology and Neurosurgery*, vol. 13, no. 5, pp. 363–367, 2013.

[2] J. L. Shergis, X. Ni, M. L. Jackson et al., "A systematic review of acupuncture for sleep quality in people with insomnia," *Complementary Therapies in Medicine*, vol. 26, pp. 11–20, 2016.

[3] Y. Li, X. Y. Zhang, F. Bao, and A. J. Sun, "Clinical curative effect research status and analysis of acupuncture treatment for primary insomnia," *Chinese Acupuncture & Moxibustion*, vol. 38, no. 7, pp. 793–797, 2018.

[4] P. Zhang, Y. P. Li, H. J. Wu, and Z. X. Zhao, "Chinese adult insomnia diagnosis and treatment guidelines (2017 edition)," *Chinese Journal of Neurology*, vol. 51, no. 5, pp. 324–335, 2018.

[5] C. M. Morin, Y. Inoue, C. Kushida, D. Poyares, and J. Winkelman, "Endorsement of European guideline for the diagnosis and treatment of insomnia by the World Sleep Society," *Sleep Medicine*, vol. 81, pp. 124–126, 2021.

[6] J. A. Dopheide, "Insomnia overview: epidemiology, pathophysiology, diagnosis and monitoring, and nonpharmacologic therapy," *American Journal of Managed Care*, vol. 26, no. 4, 2020.

[7] X. Zhang, Z. Xia, and T. Yu, "Physiotherapy and research progress of insomnia," *Journal of International Psychiatry*, vol. 48, no. 1, pp. 17–19, 2021.

[8] J. Chen and M. Dai, "Clinical research progress of acupuncture treatment for insomnia," *Medical Recapitulate*, vol. 27, no. 12, pp. 2446–2451, 2021.

[9] J. Zhang, "A meta-analysis of acupuncture versus western medicine in the treatment of primary insomnia," 2021.

[10] I. Boutron, D. G. Altman, D. Moher, K. F. Schulz, and P. Ravaud, "CONSORT statement for randomized trials of nonpharmacologic treatments: a 2017 update and a CONSORT extension for nonpharmacologic trial abstracts," *Annals of Internal Medicine*, vol. 167, no. 1, pp. 40–47, 2017.

[11] M. Hugh, G. A. Douglas, H. Richard et al., "Revised standards for reporting interventions in clinical trials of acupuncture (STRICTA): extending the CONSORT statement," *Chinese Journal of Evidence-Based Medicine*, vol. 10, no. 10, pp. 1228–1239, 2010.

[12] B. Ma, Z. Chen, J. Xu et al., "Do the CONSORT and STRICTA checklists improve the reporting quality of acupuncture and moxibustion randomized controlled trials published in Chinese journals? A systematic review and analysis of trends," *PLoS One*, vol. 11, no. 1, 2016.

[13] L. Turner, L. Shamseer, D. G. Altman, K. F. Schulz, and D. Moher, "Does use of the CONSORT Statement impact the completeness of reporting of randomised controlled trials published in medical journals? A Cochrane review," *Systematic Reviews*, vol. 1, no. 1, pp. 1–7, 2012.

[14] M. L. McHugh, "Interrater reliability: the kappa statistic," *Biochemia Medica*, vol. 22, no. 3, pp. 276–82, 2012.

[15] V. W. Berger and J. D. Bears, "When can a clinical trial be called "randomized"," *Vaccine*, vol. 21, no. 5, pp. 468–472, 2003.

[16] S. Jelena, J. He, A. Dg et al., "Influence of reported study design characteristics on intervention effect estimates from randomised controlled trials: combined analysis of meta-epidemiological studies," *Health Technology Assessment (Winchester, England)*, vol. 16, no. 35, 2012.

[17] C. D. DeAngelis, J. M. Drazen, F. A. Frizelle et al., "Clinical trial registration: a statement from the international committee of medical journal," *Archives of Otolaryngology-Head and Neck Surgery*, vol. 131, no. 6, 2005.

[18] X. Wu and X. G. Liu, "Analysis of the impact of acupuncture manipulation details for the objectivity of acupuncture clinical efficacy—take acupuncture RCT published on the four top medical journals in recent 10 Years for instance," *Journal of Liaoning University of Traditional Chinese Medicine*, vol. 19, no. 1, pp. 117–121, 2017.

[19] X. Y. Hu, Y. Zhong, and Z. H. Wen, "Evaluation of rationality of control measures and effect index selection in randomized controlled trial of acupuncture and moxibustion in the treatment of post-stroke depression," *Journal of Guangzhou University of Traditional Chinese Medicine*, vol. 32, no. 3, pp. 542–546, 2015.

[20] J. Q. Sun and J. Guo, "Literature quality evaluation of acupuncture in the treatment of primary insomnia," *Acupuncture Research*, vol. 35, no. 2, pp. 151–155, 2010.

[21] X. L. Guo, W. Wei, J. Tian, Y. N. Wang, J. Yang, and J. Xu, "Review and analysis on quality of literature reports on randomized controlled trials of acupuncture treatment for polycystic ovary syndrome at home and abroad," *Journal of Chengdu University of Traditional Chinese Medicine*, vol. 44, no. 2, pp. 101–107, 2021.

[22] Q. A. Cao, H. F. Zhang, G. X. Xu et al., "Evaluation on quality of RCT about acupuncture treatment of menopausal depression based on CONSORT-NPTs(2017) and CONSORT-STRICTA," *Liaoning Journal of Traditional Chinese Medicine*, vol. 46, no. 12, pp. 2490–2495, 2019.

Hindawi
Evidence-Based Complementary and Alternative Medicine
Volume 2022, Article ID 3306420, 9 pages
https://doi.org/10.1155/2022/3306420

Research Article

Herbal Medicine Prescriptions for Functional Dyspepsia: A Nationwide Population-Based Study in Korea

Boram Lee,[1] **Eun Kyoung Ahn**,[2] **and Changsop Yang**[1]

[1]*KM Science Research Division, Korea Institute of Oriental Medicine, Daejeon 34054, Republic of Korea*
[2]*KM Data Division, Korea Institute of Oriental Medicine, Daejeon 34054, Republic of Korea*

Correspondence should be addressed to Changsop Yang; yangunja@kiom.re.kr

Received 3 November 2021; Accepted 10 January 2022; Published 29 January 2022

Academic Editor: Zhaohui Liang

Background. Herbal medicine is widely used for the treatment of functional dyspepsia (FD) in East Asian countries. We aimed to analyze the prescription patterns of herbal medicine for patients with FD in Korean medicine clinical settings through the analysis of national health insurance claims data over the past 10 years and to check how herbal medicine has been used for FD within the scope of national health insurance. *Methods*. All prescription data claimed to the Health Insurance Review and Assessment Service with the diagnosis of FD and herbal medicine prescriptions in 2010–2019 were reviewed. We estimated the demographics, clinical characteristics, and annual prescription amount and cost of each herbal medicine. Frequent comorbidities of FD were investigated by analyzing the frequency of the Korean standard classification of diseases codes used together with FD. *Results*. In total, 19,388,248 herbal medicine prescriptions were identified. Herbal medicine prescriptions were mostly claimed by women, the elderly, outpatients at Korean medicine clinics, and national health insurance; the number increased every year. The most frequently prescribed herbal medicine was *Pingwei-san* (*Pyeongwi-san*) (31.12%), followed by *Xiangshapingwei-san* (*Hyangsa-pyeongwi-san*) (23.20%), *Qiongxia-tang* (*Gungha-tang*) (6.31%), and *Banxiaxiexin-tang* (*Banhasasim-tang*) (6.25%). The total cost of herbal medicine prescriptions increased every year, and it was highest for *Xiangshapingwei-san* (*Hyangsapyeongwi-san*) (19.37%), followed by *Banxiaxiexin-tang* (*Banhasasim-tang*) (17.50%) and then *Pingwei-san* (*Pyeongwi-san*) (15.63%). Musculoskeletal and connective tissue diseases including low back pain and myalgia were the commonest comorbidities associated with FD. *Conclusion*. This is the first study to investigate the disease burden and actual prescription pattern of herbal medicine for FD using claim data. Future clinical research and related healthcare policies should be established based on our study.

1. Introduction

Functional dyspepsia (FD) comprises troublesome upper gastrointestinal chronic symptoms, including early satiety, postprandial fullness, and epigastric pain or burning sensation [1]. The pathophysiology of FD has not been clearly elucidated and FD has a worldwide prevalence of 5–11% [2, 3]. Although not directly life-threatening, FD can significantly impair quality of life and work productivity [4, 5]. Therefore, FD is extremely important in terms of socioeconomic and national burdens.

In Western medicine, FD involves the administration of various therapeutic agents, either individually or in combination, to alleviate symptoms, but this has limited effectiveness due to the chronicity and variable severity of FD [6, 7]. Thus, there is increasing interest in complementary and integrative medicine such as herbal medicines, which have multicomponent and multitarget characteristics [8]. In particular, statistical data of the Health Insurance Review and Assessment Service (HIRA) in the Republic of Korea indicate that FD ranked 8th among the causes of outpatient consultations at Korean medical institutions in 2020 [9], which indicates that many patients receive traditional Korean medical treatments—such as herbal medicine—for FD. The HIRA, a public institution established in July 2000 in the Republic of Korea, conducts healthcare cost–benefit reviews and adequacy assessments. All citizens of the Republic of Korea are legally obligated to subscribe to

National Health Insurance (NHI), and all health insurance claims are reviewed by HIRA. For academic research purposes, the HIRA Health and Medical Big Data Center provides deidentified customized medical care claims data that comprises general prescription details (including patient information such as sex, age, and insurance type and medical information such as disease code, medical institution type, and cost), medical treatment details (including examination, treatment, surgery, and in-hospital dispensing details), diagnosis, and outpatient prescription details. These data are crucial for comprehensively understanding the current status of medical treatments and trends in the Republic of Korea's pharmaceutical market. Recent research using healthcare big data, such as health insurance claims data, has increased. The accessibility and utilization of these data are currently high, thus contributing greatly to policymaking and evidence generation in healthcare [10].

Investigating potential herbal medicines for the treatment of FD, conducting clinical research, and establishing relevant healthcare policies require investigating the current treatment patterns and associated economic burden in actual clinical practice. Such research can lead to the acquisition of relevant political support such as the expansion of NHI coverage and investment in the herbal medicine industry. However, to the best of our knowledge, no study has investigated prescription patterns of herbal medicine for the treatment of FD in a real-world clinical setting. Therefore, this study was conducted with the aim of analyzing the prescription patterns of herbal medicine for FD patients in the Republic of Korea through the analysis of health insurance claims data over the past 10 years to identify evidence that can support healthcare decision-making and policy changes.

2. Materials and Methods

2.1. Data Sources and Research Ethics. This study analyzed big data on health and medical care from HIRA that are anonymized, through the extraction, summarization, and processing of NHI data that are collected, retained, and managed by HIRA to prevent subject identification while facilitating academic research. Our application requesting the use of big data analysis through HIRA's Healthcare Big Data Hub (https://opendata.hira.or.kr/home.do) was reviewed and approved by the Public Data Provision Deliberation Committee of HIRA, and data for analysis that were suitable for research purposes were provided through the remote analysis system (Assigned number: HIRA research data (M20201020802)). The study protocol was exempted from ethical review by the institutional review board of the Korea Institute of Oriental Medicine (I-2010/008-005).

2.2. Study Population. We identified all claims data containing a diagnosis of FD (Korean Standard Classification of Disease [KCD] code: K30 in the primary or first secondary diagnosis, determined with reference to the "Korean Medicine Clinical Practice Guideline for FD") [11] and herbal medicine prescriptions from Korean medical institutions from January 2010–December 2019, regardless of the subjects' age, sex, episodic order, and types of Korean medical institution (clinic, hospital, and public health center). In the KCD, K30 means FD, which includes indigestion, epigastric pain syndrome, and postprandial distress syndrome and excludes heartburn (R12) and nervous (F45.3), neurotic (F45.3), psychogenic (F45.3), and not-otherwise-specified (R10.19) dyspepsia. Herbal medicine prescriptions were obtained by screening the data for 56 herbal formulas (mixed extracts) that are currently covered by the NHI in the Republic of Korea (Supplement 1).

2.3. Study Variables. We extracted data on patients' demographics and clinical characteristics including age and sex (per person) and type of medical institution, health insurance, hospital visit (inpatient or outpatient), herbal medicine prescription period, and cost (per prescription). Then, the annual prescription amount and cost of each of the 56 herbal medicines were analyzed. Furthermore, we investigated the frequent comorbidities associated with FD by analyzing the frequency of KCD codes—used together with the K30 code indicating FD—for each prescription.

2.4. Data Preprocessing and Analysis. The HIRA provides a data analysis environment through a virtualization server that is based on a preapproved media access control and network address and can be assessed with the SAS Enterprise Guide (SAS EG) analytical tool. Therefore, basic data preprocessing was conducted using SAS EG. For preanalytical processing, first, data on the subjects and their prescription keys with the K30 diagnosis code were obtained for the primary and the first secondary diagnoses. In the prescription table, herbal medicine prescriptions, prescription duration (in days), and prescription costs (in Korean won (₩KRW)) were extracted for each visit. Diagnostic codes registered for each patient's visit were extracted from the diagnosis history table. Frequent comorbidities were extracted and divided alphabetically according to the first letter among the KCD classification criteria. After refining the data set, clinical characteristics, herbal medicine prescriptions, and frequent comorbidities, their trends stratified by sex, age, and year were analyzed. When calculating the number of herbal medicine prescriptions, in cases with more than two herbal medicine prescriptions per visit, each individual prescription was counted as separate. Data such as sex, age, and type of health insurance were extracted based on the date of the subject's first visit during the observation period. We counted the subjects' clinical characteristics based on the patient. In addition, to extract information on the characteristics of prescriptions and comorbidities at the time of prescribing, we counted the events based on prescriptions per visit.

3. Results

3.1. Selection Process of Target Prescriptions. In total, 123,506,249 prescriptions (medications, procedures, etc.) included K30 in either the primary or first secondary diagnosis in Korean medical institutions. Among them,

19,428,028 prescriptions included herbal medicines. After excluding prescriptions of individual herbs, only the prescriptions that corresponded to the predefined 56 herbal formulas (mixed extracts) were selected for analysis. Finally, 19,388,248 herbal medicine prescriptions from 3,687,700 patients were included in the analysis.

3.2. Demographics and Clinical Characteristics. The study population comprising 3,687,700 FD patients—1,105,503 men (29.98%) and 2,582,197 women (70.02%)—showed a mean age (standard deviation) of 49.17 (22.02) years. Regarding the type of medical institution, Korean medical clinics issued most ($n = 19,152,474$ [98.58%]) of the 19,388,248 herbal medicine prescriptions issued during the study period. Stratification by the type of health insurance showed that the NHI covered most of the herbal medicine prescriptions ($n = 18,539,775$ [95.62%]). In addition, most hospital visits were made by outpatients ($n = 19,341,996$, 99.76%). The mean prescription period and cost were 1.68 days and approximately ₩1,880 KRW, respectively (Table 1).

3.3. Number of Herbal Medicine Prescriptions for FD Stratified by Sex, Age, and Year. A sex-stratified comparison of the number of herbal medicine prescriptions showed that approximately three times more women ($n = 14,414,514$, 74.3%) than men ($n = 4,973,734$, 25.7%) received these prescriptions. Age-stratified analysis showed that the number of herbal medicine prescriptions tended to increase proportionally with age: patients in their 70s accounted for the most prescriptions ($n = 6,745,042$; 34.8%), followed by those in their 60s ($n = 4,430,108$; 22.8%); thus, subjects in their 60s and 70s accounted for more than half of all herbal medicine prescriptions (Figure 1). The total number of herbal medicine prescriptions steadily increased throughout the study period and, in particular, increased 5.5-fold from 2010 ($n = 536,372$) to 2019 ($n = 2,914,167$). A similar trend was observed in the age-stratified analyses; the upward trend was particularly evident in subjects aged 60 or older (Figure 2).

3.4. Number and Cost of Frequently Prescribed Herbal Medicines for FD Based on the Year. According to the number of herbal medicine prescriptions for FD that were submitted in claims to the HIRA over 10 years, *Pingwei-san* (*Pyeongwi-san*) was the most prescribed medication, accounting for 31.12% ($n = 6,033,229$) of all prescriptions. *Xiangshapingwei-san* (*Hyangsapyeongwi-san*) was the second most prescribed agent ($n = 4,497,837$; 23.20%), followed by *Qiongxia-tang* (*Gungha-tang*; $n = 1,222,565$; 6.31%), *Banxiaxiexin-tang* (*Banhasasim-tang*; $n = 1,210,996$; 6.25%), and *Erchen-tang* (*Yijin-tang*; $n = 1,169,238$; 6.03%) (Figure 3). The year-wise comparison showed that *Pingwei-san* (*Pyeongwi-san*) was the most prescribed medicine across all years during the study period except 2010. The total cost of herbal medicine prescriptions was highest for *Xiangshapingwei-san* (*Hyangsapyeongwi-san*) at ₩7,051,079,037 KRW (19.37%), followed by *Banxiaxiexin-tang* (*Banhasasim-tang*; ₩6,370,364,917 KRW, 17.50%), *Pingwei-san* (*Pyeongwi-san*; ₩5,687,566,199 KRW, 15.63%), *Neixiao-san* (*Naeso-san*; 2,335, ₩428,678 KRW, 6.42%), and *Buzhongyiqi-tang* (*Bojungikgi-tang*; ₩1,905,819,409 KRW, 5.24%) (Figure 4). The total cost of 56 herbal medicine prescriptions for the treatment of FD during the 10-year study period was ₩36,399,342,776 KRW (Supplement 2).

3.5. Frequent Comorbidities of FD. This study cohort comprised 21,771,403 comorbidities in total that were associated with the FD code (K30). Among them, M code (Diseases of the Musculoskeletal System and Connective Tissue) accounted for most (57.05%; $n = 12,420,825$) comorbidities, followed by the R code (Symptoms, Signs, and Abnormal Clinical and Laboratory Findings, Not Elsewhere Classified; 11.39%), S code (Injury, Poisoning, and Certain Other Consequences of External Causes; 9.82%), U code (Codes for Special Purposes; 8.07%), G code (Diseases of the Nervous System; 4.49%), J code (Diseases of the Respiratory System; 3.89%), and K code (Diseases of the Digestive System; 1.75%). The commonest comorbidity was lower back pain (M545; $n = 3,225,059$), followed by myalgia (M791; $n = 1,390,267$), muscle strain (M626; $n = 1,118,574$), joint pain (M255; $n = 870,202$), and pain localized to the upper abdomen (R101; $n = 796,848$) (Table 2). When the K30 code was the primary, secondary, or primary and secondary diagnosis, the ranking of comorbidities showed a similar trend. However, when the K30 code was the primary, the U code (Codes for special purposes, encompassing diseases name in Oriental medicine, disease patterns/syndromes in Oriental medicine, and disease patterns/syndromes of Four-Constitution Medicine) comprised the most frequent comorbidity. In particular, the "spleen *qi* deficiency pattern (U680)" and "food-retention disorder (U280)" were frequently reported when the K30 code was the primary or secondary diagnosis (Supplement 3).

4. Discussion

This is the first nationwide population-based study to analyze the herbal medicine prescription patterns for FD using NHI data in the Republic of Korea. A total of 19,388,248 herbal medicine prescriptions were included in the analysis based on a review of claims data for the total study period of 10 years. The results showed that the total amount and cost of herbal medicine prescriptions for FD have been continually increasing every year.

According to the findings of our study, women and older adults frequently used herbal medicines to treat FD. This trend is presumably attributable to the higher global prevalence of FD among women and older adults [3, 12] as well as the higher trust in—and usage of—Korean medicines among these populations [13]. Among those who were older than 60 years, the number of FD patients who were prescribed herbal medicines showed a tendency to increase sharply each year. Older adults have a high preference for herbal medicines [14] and as the rate at which the

Table 1: Clinical characteristics of herbal medicine prescriptions.

Clinical characteristics	*N*	%
Type of medical institution (including 39,780 duplicates)		
Korean medical hospital	269,427	1.39
Korean medical clinic	19,152,474	98.58
Public health center	6,127	0.03
Type of health insurance		
National health insurance	18,539,775	95.62
Medical aid	848,473	4.38
Type of administration		
Inpatient	46,252	0.24
Outpatient	19,341,996	99.76
Prescription period (days)		
	Mean 1.68	SD 1.75
Prescription cost (₩KRW)*		
	Mean 1,880.04	SD 2,911.42

KRW, Korean won; SD, standard deviation. *$1 USD ≒₩1,156.4 KRW (2019).

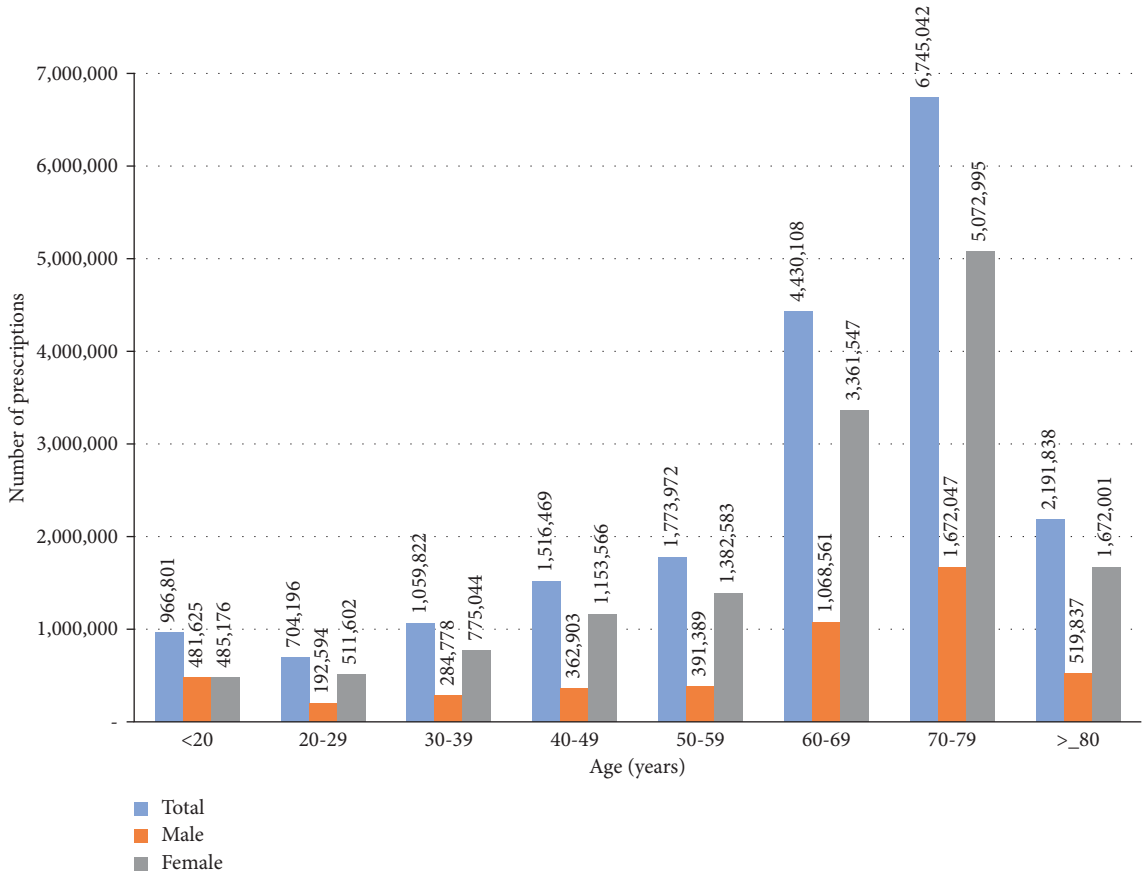

Figure 1: Number of herbal medicine prescriptions for functional dyspepsia based on sex- and age-stratified analyses.

elderly population is expanding in Korea is rapidly progressing [15], this trend is expected to continue. In particular, between 2010 and 2011, the number of prescriptions for patients aged 60 and older increased sharply, which may be attributable to the upward revision of the Korean elderly outpatient copayment system (age ≥65 years) in 2011 that has significantly influenced the medical behavior of Korean medicine practitioners and the number of herbal medicine prescriptions among older adults [16, 17].

Although FD is a chronic disease, the average herbal medicine prescription period was as short as 1.68 days. For FD treatment, in addition to herbal medicine, acupuncture and moxibustion are usually performed once a day and up to three times a week [18]; therefore, the short duration of the prescriptions may be due to the fact that patients frequently visit medical institutions and not only receive herbal medicine prescriptions for short periods but also acupuncture and moxibustion. However, as this

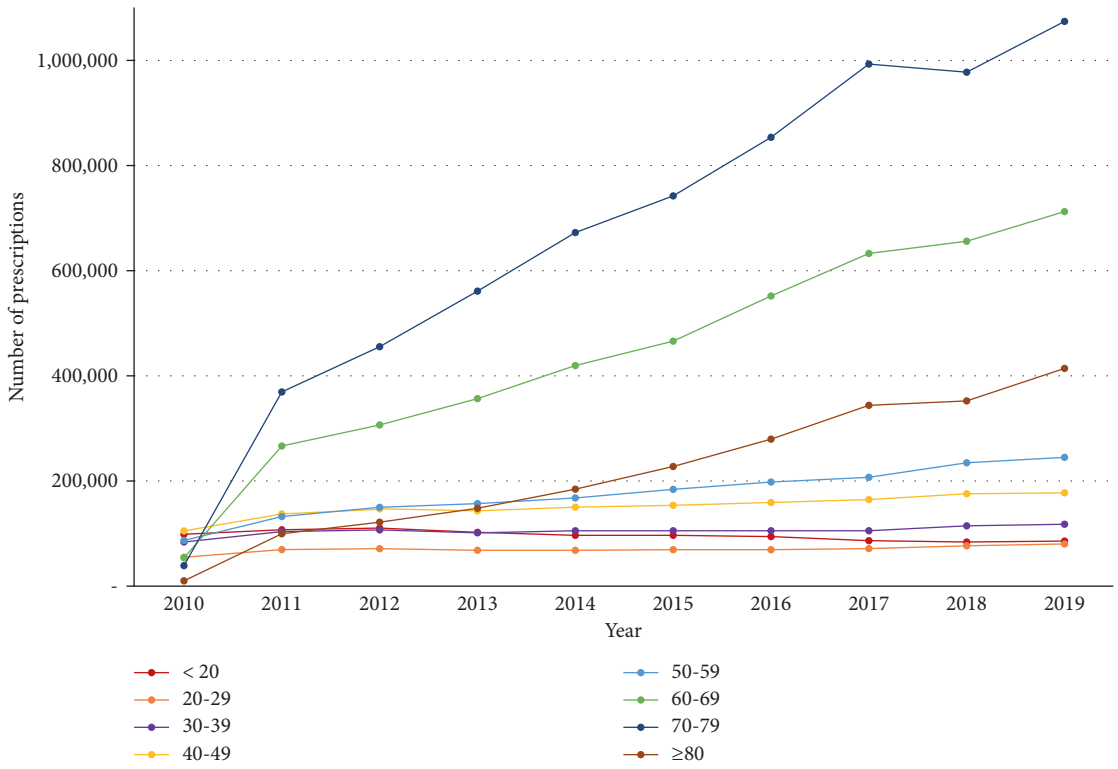

Figure 2: Number of herbal medicine prescriptions for functional dyspepsia based on the year.

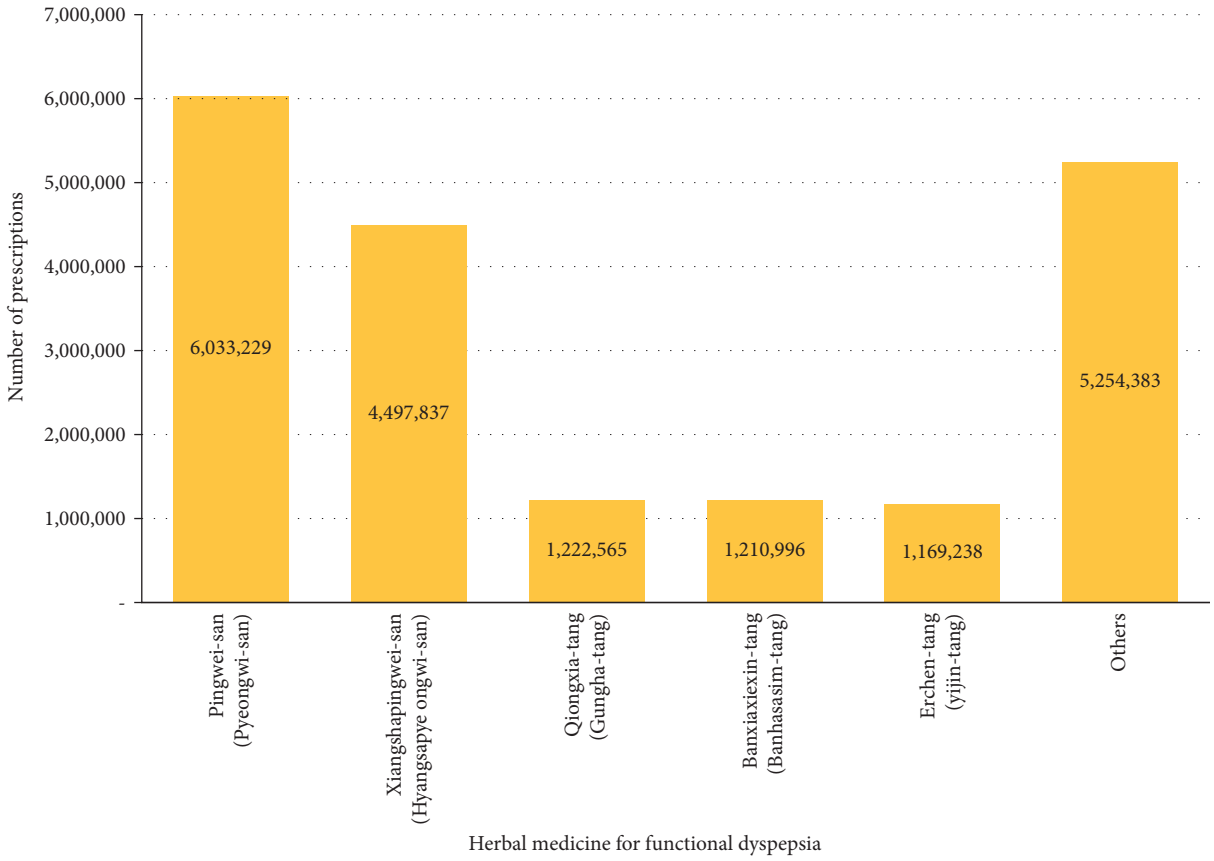

Figure 3: Number of frequently prescribed herbal medicines for functional dyspepsia.

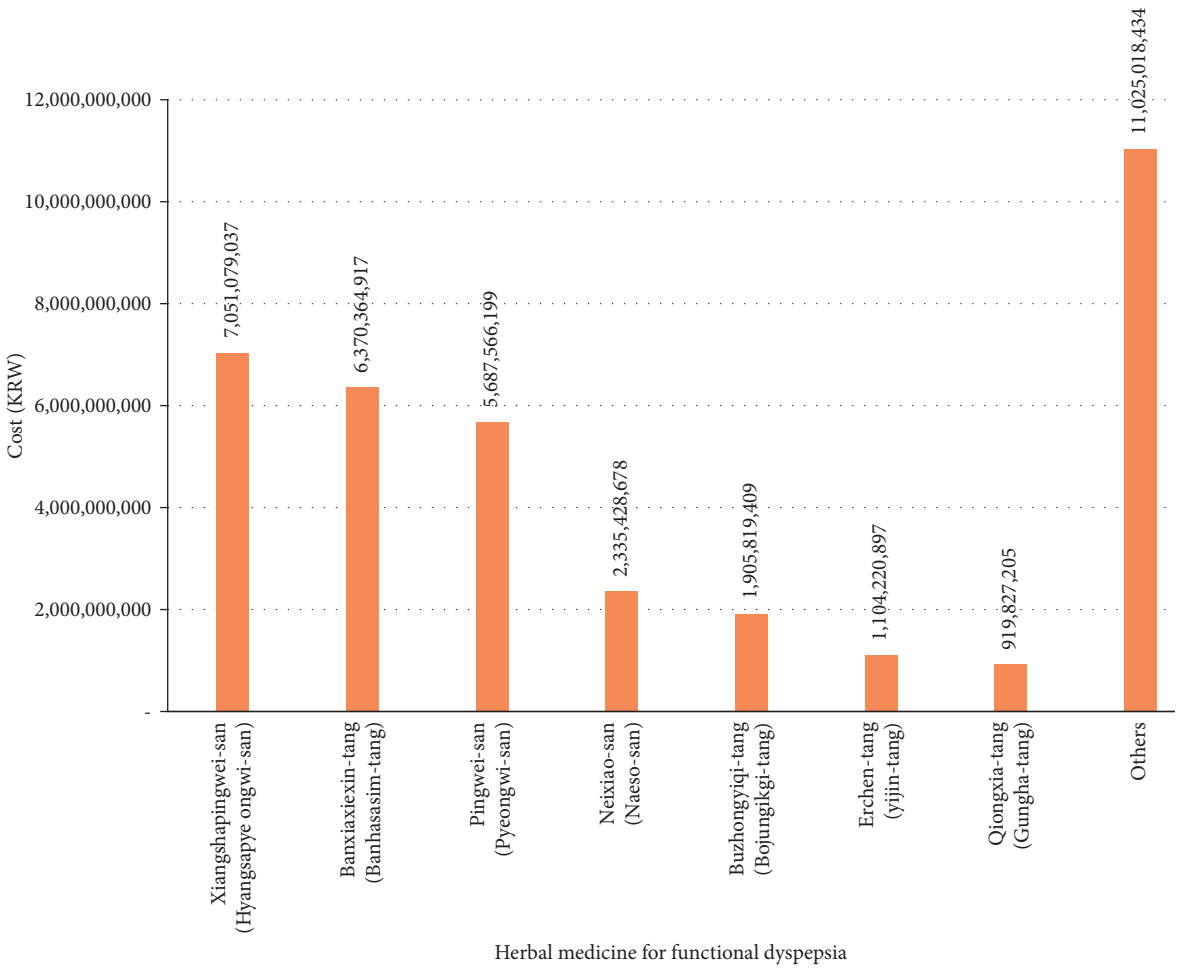

Figure 4: Cost of frequently prescribed herbal medicines for functional dyspepsia.

study only targeted the number of herbal medicine prescriptions, the results should be interpreted cautiously, because no data are available regarding to the total number and duration of treatment per patient or for the prescription pattern of other treatments, such as acupuncture and moxibustion.

Our analysis showed that, among the herbal medicines prescribed, *Pingwei-san* (*Pyeongwi-san*) was the most prescribed, followed by *Xiangshapingwei-san* (*Hyangsapyeongwi-san*), *Qiongxia-tang* (*Gungha-tang*), *Banxiaxiexin-tang* (*Banhasasim-tang*), and *Erchen-tang* (*Yijin-tang*). These results are similar to those used in the order of *Pingwei-san* (*Pyeongwi-san*; 30%) and *Banxiaxiexin-tang* (*Banhasasim-tang*; 27%) for FD treatment in a survey conducted among 349 Korean medicine doctors in 2017 [11]. In particular, *Pingwei-san* (*Pyeongwi-san*) comprises six herbs: *Cangzhu* (*Atractylodis Rhizoma*), *Chenpi* (*Citri Unshius Pericarpium*), *Houpu* (*Magnoliae Cortex*), *Gancao* (*Glycyrrhizae Radix et Rhizoma*), *Shengjiang* (*Zingiberis Rhizoma Recens*), and *Dazao* (*Zizyphi Fructus*). In animal models, *Pingwei-san* (*Pyeongwi-san*) has been reported to regulate gastric secretion and gastrointestinal motility and protect the gastrointestinal mucosa [19, 20]; its effect on FD treatment has been confirmed in clinical studies [21, 22].

The total cost of herbal medicine prescriptions that were claimed to the NHI for FD treatment during the 10-year study period was ₩36,399,342,776 KRW, and the cost-based rankings of individual prescriptions were as follows: *Xiangshapingwei-san* (*Hyangsapyeongwi-san*), *Banxiaxiexin-tang* (*Banhasasim-tang*), and *Pingwei-san* (*Pyeongwi-san*). In particular, *Pingwei-san* (*Pyeongwi-san*), *Qiongxia-tang* (*Gungha-tang*), and *Erchen-tang* (*Yijin-tang*), which were the first, third, and fifth most prescribed herbal medicines, ranked third, ninth, and 10th, respectively, in terms of total prescription costs. This is because the maximum price for individual herbal medicines is set according to Regulation for Criteria for Providing Reimbursed Services in the NHI in Korea, and the order of the prescription amount and total cost may differ due to differences in the standard pricing of individual herbal medicines.

Most of the frequent comorbidities of FD were identified mainly with regard to the KCD M code, and lower back pain, myalgia, muscle strain, and joint pain were the commonest comorbidities among them. As the majority of this study population were older patients, it can be assumed that musculoskeletal disorders, which often afflict the elderly, were reported frequently [23, 24]. In addition, various comorbidities such as headache, dizziness, common cold,

Table 2: Frequent comorbidities associated with functional dyspepsia.

	Diagnosis code	*N*	%
M (diseases of the musculoskeletal system and connective tissue)	M545 (low back pain)	3,225,059	26.64
	M791 (myalgia)	1,390,267	11.48
	M626 (muscle strain)	1,118,574	9.24
	M255 (pain in joint)	870,202	7.19
	M544 (lumbago with sciatica)	692,076	5.72
Subtotal		12,420,825	—
R (symptoms, signs, and abnormal clinical and laboratory findings, not elsewhere classified)	R101 (pain localized to the upper abdomen)	796,848	33.10
	R51 (headache)	360,327	14.97
	R42 (dizziness and giddiness)	291,311	12.10
	R104 (other and unspecified abdominal pain)	223,702	9.29
	R05 (cough)	116,030	4.82
Subtotal		2,479,230	—
S (injury, poisoning, and other consequences from external causes)	S335 (sprain and strain of the lumbar spine)	435,071	20.59
	S934 (sprain and strain of the ankle)	206,398	9.77
	S836 (sprain and strain of other and unspecified parts of the knee)	205,873	9.74
	S337 (sprain and strain of other and unspecified parts of lumbar spine and pelvis)	203,042	9.61
	S434 (sprain and strain of the shoulder joint)	198,715	9.40
Subtotal		2,137,678	—
U (codes for special purposes)	U303 (neck-stiffness disorder)	215,162	12.49
	U680 (spleen *qi*-deficiency pattern)	134,750	7.82
	U234 (sequela of wind-stroke disorder)	115,626	6.71
	U238 (joint impediment disorders)	96,877	5.62
	U280 (Food-retention disorder)	90,571	5.26
Subtotal		1,757,326	—
G (diseases of the nervous system)	G442 (tension-type headache)	182,199	19.00
	G439 (migraine, unspecified)	132,424	13.81
	G470 (disorders of initiating and maintaining sleep (insomnias))	125,029	13.04
	G510 (Bell's palsy)	89,117	9.29
	G438 (other migraine)	56,505	5.89
Subtotal		977,695	—
J (diseases of the respiratory system)	J00 (acute nasopharyngitis (common cold))	549,195	70.09
	J310 (chronic rhinitis)	56,617	7.23
	J069 (acute upper respiratory infection, unspecified)	29,135	3.72
	J304 (allergic rhinitis, unspecified)	27,911	3.56
	J303 (other allergic rhinitis)	16,310	2.08
Subtotal		847,865	—
K (diseases of the digestive system)	K590 (constipation)	99,555	27.43
	K591 (functional diarrhea)	60,018	16.54
	K297 (gastritis, unspecified)	31,770	8.75
	K210 (gastroesophageal reflux disease with esophagitis)	22,201	6.12
	K076 (temporomandibular joint disorders)	17,004	4.69
Subtotal		380,691	—

chronic rhinitis, and constipation were reported. Herbal medicine is specifically a typical multitarget multicomponent agent and, thus, has the potential to simultaneously treat various comorbidities. Therefore, it will be meaningful to confirm whether not only FD, but also the accompanying symptoms/comorbidities are improved by herbal medicine treatment through prospective clinical studies.

FD is a chronic disease that significantly impairs quality of life and work productivity [4, 5] and is difficult to treat due to its diverse symptoms and variable course [6, 7]. In this situation, herbal medicine has multicomponent and multitarget characteristics that can target the various pathological mechanisms and symptoms of FD, and studies on the effects of herbal medicines in FD treatment have been actively conducted [25]. Additionally, the present study shows that herbal medicine treatment is being actively administered in actual clinical practice for the treatment of FD, and the prescription amounts increase every year. However, compared to other East Asian countries, the NHI benefit rate for traditional medicine, including herbal medicine, in Korea is relatively low [26, 27], which increases the private medical expenses and disease burden and, consequently, socioeconomic costs. Accordingly, there is increasing demand for the need to expand the items covered by the NHI in Korea. The NHI needs to establish appropriate policies to expand the coverage of traditional medicine by expanding research on the safety and efficacy of herbal

medicines and by recognizing the reality that the demand for herbal medicines for FD is increasing in Korea.

Meanwhile, for the treatment of FD, in addition to the 56 herbal medicines covered by the NHI in Korea, *Liujunzi-tang* (*Yukgunja-tang*), *Zhishixiaopi-wan* (*Jisilsobi-hwan*), and various crude herbal decoctions have been actively used, despite not being covered by the NHI in Korea [11]; their effectiveness has been verified through many clinical trials [28–31]. Nonetheless, their economic evaluation has not yet been undertaken, and when setting a control group for economic evaluation, a frequently used treatment with the same indication should be used [32]. Therefore, when specifying a control group for the economic evaluation of the herbal medicines used in FD treatment that are not covered under insurance, based on the results of this study, this can consist of the frequently used herbal medicines that are covered by the NHI such as *Pingwei-san* (*Pyeongwi-san*) and *Xiangshapingwei-san* (*Hyangsapyeongwi-san*). These studies provide important fundamental data to support decision-making that enables policymakers to allocate limited resources both efficiently and fairly.

Our study has the following limitations. As this study only targeted herbal medicine prescriptions for FD, it was not possible to confirm the prescription patterns of other interventions such as acupuncture and moxibustion, which can be used for FD in clinical settings. In real-world clinical practice, acupuncture, moxibustion, and *chuna* are actively used alongside herbal medicine to treat FD. In addition, as only 56 herbal medicines (mixed-extract powders) covered by the NHI were analyzed, the treatment pattern of crude herbal decoctions, which are widely used and not covered by the NHI, could not be confirmed [33]. Therefore, the medical expenditures identified in this study comprise only a part of the actual medical expenses. It would be meaningful to investigate medical behaviors and expenses using surveys and electronic medical record data in the future.

Despite the abovementioned limitations, to the best of our knowledge, this is the first study to use large-scale NHI claim data to investigate the disease burden and actual prescription pattern of herbal medicine, one of the most commonly used interventions in clinical Korean medicine. A 10-year retrospective long-term observation analysis was performed for all herbal medicines covered under the NHI. In the future, based on this study, we hope that evidence-based clinical research will be actively carried out, and related healthcare policies will be established to strengthen the insurance coverage of Korean medicine treatment.

5. Disclosure

The funding source played no role in the interpretation of the study results or the decision to submit these results for publication.

Data Availability

The data that support the findings of this study are available from the Healthcare Big Data Hub of the HIRA. However, restrictions apply with regard to availability as they were used under license for research in the current study; therefore, these data are not publicly available. However, the study-related data are available from the co-author (EKA) upon reasonable request.

Ethical Approval

The study protocol was exempted from ethical review by the Institutional Review Board of the Korea Institute of Oriental Medicine (I-2010/008-005).

Conflicts of Interest

The authors declare that there are no conflicts of interest regarding the publication of this paper.

Authors' Contributions

Conceptualization was done by BL. Methodology was done by BL and EKA. The original draft was written by BL. Review and editing were done by EKA and CY. Funding was acquired by CY. Supervision was done by CY.

Acknowledgments

This work was supported by the Korea Institute of Oriental Medicine (KSN2021210).

Supplementary Materials

Supplement 1. List of the 56 herbal medicines used to treat functional dyspepsia in Korea. *Supplement 2.* Number of prescriptions and cost of 56 herbal medicines by year. *Supplement 3.* Frequent comorbidities associated with functional dyspepsia when the K30 code was the primary diagnosis. (*Supplementary Materials*)

References

[1] V. Stanghellini, F. K. L. Chan, W. L. Hasler et al., "Gastroduodenal disorders," *Gastroenterology*, vol. 150, no. 6, pp. 1380–1392, 2016.

[2] I. Aziz, O. S. Palsson, H. Törnblom, A. D. Sperber, W. E. Whitehead, and M. Simrén, "Epidemiology, clinical characteristics, and associations for symptom-based Rome IV functional dyspepsia in adults in the USA, Canada, and the UK: a cross-sectional population-based study," *The Lancet Gastroenterology and Hepatology*, vol. 3, no. 4, pp. 252–262, 2018.

[3] A. C. Ford, A. Marwaha, R. Sood, and P. Moayyedi, "Global prevalence of, and risk factors for, uninvestigated dyspepsia: a meta-analysis," *Gut*, vol. 64, no. 7, pp. 1049–1057, 2015.

[4] I. F. Hantoro, A. F. Syam, E. Mudjaddid, S. Setiati, and M. Abdullah, "Factors associated with health-related quality of life in patients with functional dyspepsia," *Health Qual Life Outcomes*, vol. 16, no. 1, p. 83, 2018.

[5] G. B. Sander, L. E. Mazzoleni, C. F. Francesconi et al., "Influence of organic and functional dyspepsia on work productivity: the HEROES-DIP study," *Value in Health*, vol. 14, no. 5, pp. S126–S129, 2011.

[6] N. J. Talley and A. C. Ford, "Functional dyspepsia," *New England Journal of Medicine*, vol. 373, no. 19, pp. 1853–1863, 2020.

[7] L. B. Olafsdottir, H. Gudjonsson, H. H. Jonsdottir, E. Bjornsson, and B. Thjodleifsson, "Natural history of functional gastrointestinal disorders: comparison of two longitudinal population-based studies," *Digestive and Liver Disease*, vol. 44, no. 3, pp. 211–217, 2012.

[8] G. Chiarioni, M. Pesce, A. Fantin, and G. Sarnelli, "Complementary and alternative treatment in functional dyspepsia," *United European Gastroenterol Journal*, vol. 6, no. 1, pp. 5–12, 2018.

[9] Health Insurance Review & Assessment Service, "Healthcare Bigdata Hub. Statistics of frequent diseases," 2021, https://opendata.hira.or.kr/op/opc/olapHifrqSickInfo.do.

[10] L. Kim, J. Sakong, and Y. Kim, "Developing the inpatient sample for the National Health Insurance claims data," *Health Policy and Management*, vol. 23, no. 2, pp. 152–161, 2013.

[11] National Institute for Korean Medicine Development and The Society of Internal Korean Medicine, "Korean medicine clinical practice guideline for functional dyspepsia," vol. 11-14, p. 32, 2020, https://nikom.or.kr/nckm/module/practiceGuide/view.do?guide_idx=154&menu_idx=14.

[12] S. E. Kim, N. Kim, and J. Y. Lee, "Prevalence and risk factors of functional dyspepsia in health check-up population: a nationwide multicenter prospective study," *Journal of Neurogastroenterology and Motility*, vol. 24, no. 4, pp. 603–613, 2018.

[13] S. Kwon, S. Heo, D. Kim, S. Kang, and J. M. Woo, "Changes in trust and the use of Korean medicine in South Korea: a comparison of surveys in 2011 and 2014," *BMC Complementary and Alternative Medicine*, vol. 17, no. 1, p. 463, 2017.

[14] K. Sackett, M. Carter, and M. Stanton, "Elders' use of folk medicine and complementary and alternative therapies: an integrative review with implications for case managers," *Professional Case Management*, vol. 19, no. 3, pp. 113–123, 2014.

[15] I. Y. Jang, H. Y. Lee, and E. Lee, "Geriatrics fact sheet in Korea 2018 from national statistics," *Annals of Geriatric Medicine and Research*, vol. 23, no. 2, pp. 50–53, 2019.

[16] D. B. Jeong, "Analysis of the behavior of Korean medical doctors before and after upward revision of elderly outpatients copayment system," Master's Thesis, The Graduate School of Seoul National University., Seoul, South Korea, 2017.

[17] H. Kim, J. Y. Choi, M. Hong, and H. S. Suh, "Traditional medicine for the treatment of common cold in Korean adults: A nationwide population-based study," *Integrative Medicine Research*, vol. 10, no. 1, Article ID 100458, 2021.

[18] C. Y. Kwon, S. J. Ko, B. Lee, J. M. Cha, J. Y. Yoon, and J. W. Park, "Acupuncture as an add-on treatment for functional dyspepsia: a systematic review and meta-analysis," *Frontiers of Medicine*, vol. 8, Article ID 682783, 2021.

[19] M. C. Lee, J. R. Park, J. H. Shim, T. S. Ahn, and B. J. Kim, "Effects of traditional Chinese herbal medicine Shengmai-san and Pyungwi-san on gastrointestinal motility in mice," *Journal of Korean Medicine for Obesity Research*, vol. 15, no. 2, pp. 68–74, 2015.

[20] I. K. Chang and I. M. Heu, "Experimental studies on the efficacy of Pyungwee-san, Hyangsapyungwee-san And Bylwhangumchunggl-san," *Kyung Hee Unicersity Oriental Medical Journal*, vol. 13, pp. 427–461, 1990.

[21] B. Yuan, "Effect of Pingwei powder on gastric dynamics of intractable functional dyspepsia," *Clinical Journal of Anhui Traditional Chinese Medicne*, vol. 15, no. 5, pp. 396-397, 2003.

[22] S. Y. Kim and S. H. Yoon, "A selective effect of combined treatment of electroacupuncture at Zusanli(ST36), manual acupuncture, and Pyengwisan in function dyspepsia patients with pyloric valve disturbance and hypoactivity of gastric vagus nerve," *The Korean Journal of Internal Medicine*, vol. 30, no. 1, pp. 191–199, 2009.

[23] R. F. Loeser, "Age-related changes in the musculoskeletal system and the development of osteoarthritis," *Clinics in Geriatric Medicine*, vol. 26, no. 3, pp. 371–386, 2010.

[24] R. D. Meucci, A. G. Fassa, and N. M. X. Faria, "Prevalence of chronic low back pain: systematic review," *Revista de Saúde Pública*, vol. 49, p. 1, 2015.

[25] M. H. K. Chu, I. X. Y. Wu, R. S. T. Ho et al., "Chinese herbal medicine for functional dyspepsia: systematic review of systematic reviews," *Therapeutic Advances in Gastroenterology*, vol. 11, Article ID 1756284818785573, 2018.

[26] C. W. Huang, I. H. Hwang, Y. H. Yun et al., "Population-based comparison of traditional medicine use in adult patients with allergic rhinitis between South Korea and Taiwan," *Journal of the Chinese Medical Association*, vol. 81, no. 8, pp. 708–713, 2018.

[27] H. L. Park, H. S. Lee, B. C. Shin et al., "Traditional medicine in China, Korea, and Japan: a brief introduction and comparison," *Evidence-Based Complementary and Alternative Medicine*, vol. 2012, Article ID 429103, 2012.

[28] S. Zhang, L. Zhao, H. Wang et al., "Efficacy of modified LiuJunZi decoction on functional dyspepsia of spleen-deficiency and qi-stagnation syndrome: a randomized controlled trial," *BMC Complementary and Alternative Medicine*, vol. 13, p. 54, 2013.

[29] H. Kusunoki, K. Haruma, and J. Hata, "Efficacy of Rikkunshito, a traditional Japanese medicine (Kampo), in treating functional dyspepsia," *Internal Medicine*, vol. 49, no. 20, pp. 2195–2202, 2010.

[30] H. Suzuki, J. Matsuzaki, and Y. Fukushima, "Randomized clinical trial: rikkunshito in the treatment of functional dyspepsia--a multicenter, double-blind, randomized, placebo-controlled study," *Neuro-Gastroenterology and Motility*, vol. 26, no. 7, pp. 950–961, 2014.

[31] K. Tominaga, Y. Sakata, and H. Kusunoki, "Rikkunshito simultaneously improves dyspepsia correlated with anxiety in patients with functional dyspepsia: a randomized clinical trial (the DREAM study)," *Neuro-Gastroenterology and Motility*, vol. 30, no. 7, Article ID e13319, 2018.

[32] J. H. Kim, H. Y. Kwon, J. H. Hong, and T. J. Lee, *A Guideline for Economic Evaluation of Korean Medicine*, Guideline center for Korean Medicine, Seoul, South Korea, 2018.

[33] B. Lim, "Korean medicine coverage in the National health insurance in Korea: present situation and critical issues," *Integrative Medicine Research*, vol. 2, no. 3, pp. 81–88, 2013.

Hindawi
Evidence-Based Complementary and Alternative Medicine
Volume 2022, Article ID 3793946, 10 pages
https://doi.org/10.1155/2022/3793946

Research Article

RNA Sequencing Analysis of Gene Expression by Electroacupuncture in Guinea Pig Gallstone Models

Mingyao Hao,[1] Zhiqiang Dou,[2] Luyao Xu,[2] Zongchen Shao,[2] Hongwei Sun,[3] and Zhaofeng Li[2]

[1]*External Treatment Center of Traditional Chinese Medicine, Affiliated Hospital of Shandong University of Traditional Chinese Medicine, Jinan 250014, China*
[2]*College of Acupuncture and Moxibustion, Shandong University of Traditional Chinese Medicine, Jinan 250355, China*
[3]*Institute of Acupuncture and Moxibustion, Shandong University of Traditional Chinese Medicine, Jinan 250355, China*

Correspondence should be addressed to Zhaofeng Li; qdlzfcmd@126.com

Received 3 November 2021; Accepted 14 December 2021; Published 7 January 2022

Academic Editor: Zhaohui Liang

Background. Clinical studies have shown that electroacupuncture (EA) promotes gallbladder motility and alleviates gallstone. However, the mechanism underlying the effects of EA on gallstone is poorly understood. In this study, the mRNA transcriptome analysis was used to study the possible therapeutic targets of EA. *Methods*. Hartley SPF guinea pigs were employed for the gallstone models. Illumina NovaSeq 6000 platform was used for the RNA sequencing of guinea pig gallbladders in the normal group (Normal), gallstone model group (Model), and EA-treated group (EA). Differently expressed genes (DEGs) were examined separately in Model vs. Normal and EA vs. Model. DEGs reversed by EA were selected by comparing the DEGs of Model vs. Normal and EA vs. Model. Biological functions were enriched by gene ontology (GO) analysis. The protein-protein interaction (PPI) network was analyzed. *Results*. After 2 weeks of EA, 257 DEGs in Model vs. Normal and 1704 DEGs in EA vs. Model were identified. 94 DEGs reversed by EA were identified among these DEGs, including 28 reversed upregulated DEGs and 66 reversed downregulated DEGs. By PPI network analysis, 10 hub genes were found by Cytohubba plugin of Cytoscape. Quantitative real-time PCR (qRT-PCR) verified the changes. *Conclusion*. We identified a few GOs and genes that might play key roles in the treatment of gallstone. This study may help understand the therapeutic mechanism of EA for gallstone.

1. Introduction

Gallstone disease affects 4% to 20% of the population [1, 2]. More than 80% of gallstones were cholesterol stones [3, 4]. Though approximately 3/4 of the patients are asymptomatic, the major burden generates when symptoms or complications occur [5]. Therefore, it has gained attention worldwide [2, 6]. Cholecystectomy is recommended to be offered to patients with symptomatic gallbladder stones [7]. However, patients hesitate or are unwilling to consider cholecystectomy because of the fear of potential risks and the concern for postoperative complications. The pursuit of physical integrity in some cultural backgrounds also limits its application. Although gallbladder-preserving cholelithotomy preserves gallbladder function and reduces surgical complications, the problem of stone recurrence is still an unsolvable problem.

The mechanisms of the pathogenesis of gallstone are multifaceted, including lithogenic genes, altered bile lipid composition, intestinal absorption of cholesterol, gut microbiota, defective gallbladder motility, dietary factors, and lifestyles [3, 5, 8]. Diet style has been considered one of the risk factors of gallstone disease. A high-lipid diet or fat consumption from meat or fried foods increases the likelihood of gallstones [8, 9]. While diet patterns, such as vegetarian diet, alternate Mediterranean diet, Alternate Healthy Eating Index diet, and Dietary Approaches to Stop Hypertension, may act as protective factors against the formation of gallstones [8, 10, 11]. Hence, a lithogenic diet is used as a common method to form gallstone animal models.

Studies have found that some genes, such as mucin genes and lith genes, were associated with gallstone formation [12–15]. Recently, gut microbiome studies have shown that they have a close correlation with many disease conditions. Hence, great attention has been gained to the involvement of the gut microbiome in gallstone pathogenesis. The gut microbiome promotes the formation of gallstones by affecting gallbladder motility, affecting cholesterol metabolism and secretion, affecting bile acid metabolism, and eliciting chronic inflammation [16]. 16S rRNA gene sequencing analysis found that gallstone mice models displayed reduced microbiota richness. Lower Firmicutes level and decreased Firmicutes/Bacteroidetes ratio might be significant factors for the gallstone formation [17].

The hypomotility of the gallbladder is also believed to be one of the key causes of gallstones [18, 19]. Gallbladder hypomotility delays emptying, increases residual volume, and reduces its response to CCK, resulting in cholestasis, bile cholesterol supersaturation, the further aggravation of gallbladder hypomotility, and the promotion of the formation of gallstones [20]. Studies have shown that postprandial hypomotility of the gallbladder is an independent risk factor for gallstone recurrence after lithotripsy [18]. Therefore, improving gallbladder motility may be the key to the treatment of gallstones. The previous studies [21, 22] of our research team showed that the gallbladder relaxed on a large scale after accepting acupuncture. The clinical trials and animal studies suggest that acupuncture on Yanglingquan (GB34), Qimen (LR14), and Yidan (CO11) is an effective method for regulating gallbladder motility [23, 24]. Yet, the underlying mechanisms of acupuncture for gallstones remain largely unclear.

High-throughput RNA sequencing (RNA-seq) has been widely used to explore the mechanisms of a series of diseases. However, only a few studies have been carried out on gallstone gene expression. Therefore, the present study was carried out to explore the potential complicated molecular mechanisms of EA in gallstone by RNA-seq to identify key genes. We generated a gallstone guinea pig model and performed RNA-seq to analyze mRNA profiles in the gallbladder tissues of the guinea pigs from the Normal group, Model group, and EA group. DEGs were investigated in the Model vs. Normal and EA vs. Model separately. Enrichment analysis and PPI analysis were performed to explore the potential mechanism in gallstone. Hub genes were selected to verify RNA expression by qRT-PCR.

2. Materials and Methods

2.1. Animal Experiments. 30 male SPF Hartley guinea pigs (250 g to 300 g, 4 to 5 weeks) were purchased from Qingdao Kangda Biotechnology Co., Ltd (Certification No. SCXK 20160002). The Ethical Committee for Research involving Animals of SDUTCM approved all procedures (20190125001). All animals were maintained in the Animal Experiment Center of the Affiliated Hospital of Shandong University of Traditional Chinese Medicine. After 1 week of acclimation and normal diet feeding, they were randomly divided into 3 groups ($n = 10$), namely (1) Normal group, (2) Model group, and (3) EA group. The Normal group was fed with a normal diet, while the Model group and EA group were fed with a lithogenic diet (purchased from Jiangsu Xietong Pharmaceutical Bioengineering Co., Ltd) for 6 weeks. After modeling, the gallbladder of all guinea pigs in the Model group and the EA group were observed under ultrasound examination (M5Vet, Mindray, Shenzhen, China) to verify the success of the gallstone model.

2.2. EA Treatment. EA treatment was provided for guinea pigs in the EA group after the gallstone model was established. Stainless steel acupuncture needles (Hwato, 0.25 mm × 13 mm, 200242) were inserted at a depth of 2 mm on both Yanglingquan (GB34) acupoints in the EA group. Then, the two acupuncture needles were connected with an EA stimulator (Hwato, SDZ-V) at an intensity range from 0.4 to 0.6 mA, a frequency of 20 Hz, and the continuous wave for 20 minutes once daily for 2 weeks (Figure 1(a)).

2.3. Sample Collection and Sequencing. All guinea pigs were sacrificed at the end of the EA treatment, and the gallbladders were collected. The samples were quickly put into liquid nitrogen for temporary storage and removed to a −80°C refrigerator for long-term storage. 3 gallbladders were randomly chosen from each group to do RNA-seq analysis. Total RNA was extracted by TRIzol (Invitrogen, United States). RNA samples were further purified with magnetic oligo (dT) beads after denaturation. Purified mRNA samples were reverse transcribed to first-strand cDNA, and a second cDNA was further synthesized. Fragmented DNA samples were blunt-ended and adenylated at the 3′ ends. Adaptors were ligated to construct a library. DNA was quantified by Qubit (Invitrogen). After cBot cluster generation, DNA samples were sequenced using Illumina NovaSeq 6000 (Illumina, San Diego, CA, United States) from Genergy Bio Technology (Shanghai, China).

2.4. RNA-Seq Analysis. Raw data were converted to Fastq format. Quality control (QC) was performed by FastQC (version 0.11.5) (https://www.bioinformatics.babraham.ac.uk/projects/fastqc/). STAR [25] (2.5.3a) (https://github.com/alexdobin/STAR) was used to map the clean reads to the reference genome (ftp://ftp.ensembl.org/pub/release99/fasta/cavia_porcellus/dna/Cavia_porcellus.Cavpor3.0.dna.toplevel.fa.gz). StringTie [26] (https://ccb.jhu.edu/software/stringtie/) was used to assess the expression levels of mRNAs by calculating FPKM. DESeq2 software [27] (v1.16.1) (https://bioconductor.org/packages/release/bioc/html/DESeq2.html) was used to calculate DEGs between different samples with $P < 0.05$ and $|\log2FC| \geq 1$ as the threshold. DEGs reversed by EA were identified. DEGs upregulated in Model vs. Normal but downregulated in EA vs. Model were defined as DEGs reversed downregulated (Reversed DOWN DEGs), and DEGs downregulated in Model vs. Normal but upregulated in EA vs. Model were defined as DEGs reversed upregulated (Reversed UP DEGs). Reversed UP DEGs and Reversed DOWN DEGs were defined as EA reversed DEGs.

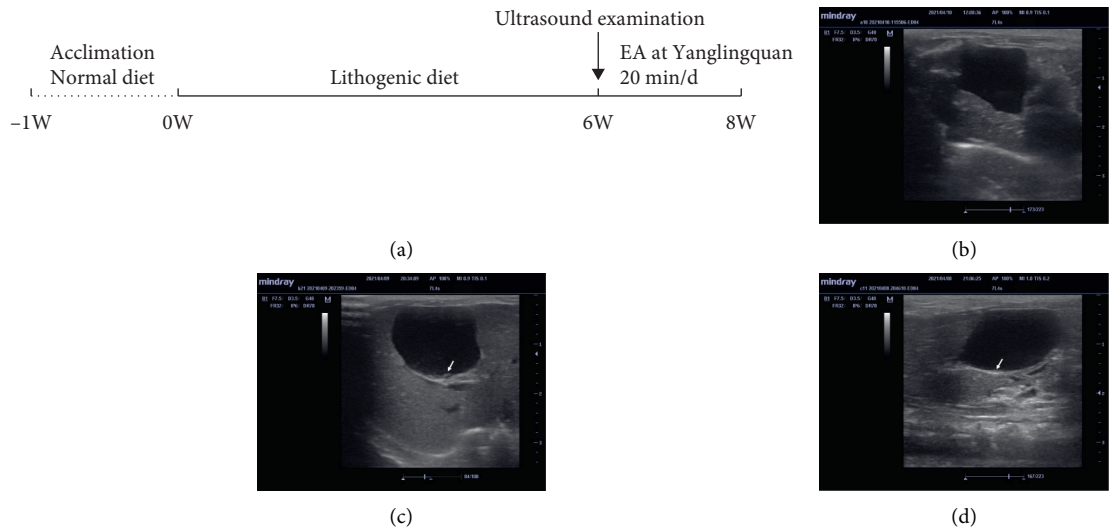

Figure 1: Representation of the flow chart (a) and the ultrasound examinations of guinea pig gallbladders from the Normal group (b), the Model group (c), and the EA group (d) separately after 6 weeks of lithogenic diet feeding. The arrow in (c) and (d) shows gallstones in gallbladder. EA: electroacupuncture.

2.5. Bioinformatics Analysis. GO enrichment was analyzed in EA reversed DEGs by the DAVID database [28,29] (https://david.ncifcrf.gov/home.jsp). The PPI network of EA-reversed DEGs was predicted and constructed using the STRING online database [30] (https://string-db.org). Then, Cytoscape software [31] (v3.8.1) (https://cytoscape.org/) was applied to visualize the network and distinguish the hub genes.

2.6. Quantitative Real-Time PCR. Total RNA was extracted from the samples of gallbladders with TRIzol (Invitrogen, United States) according to the manufacturer's instructions. Then RNA was converted to cDNA using *EasyScript*® One-Step gDNA Removal and cDNA Synthesis SuperMix (AE311-02, TransGen Biotech, Beijing, China). The level of transcripts was determined by qRT-PCR using the *PerfectStart*® Green qPCR SuperMix (AQ601-02, TransGen Biotech, Beijing, China) on an Applied Biosystems QuantStudio™ 5 Real-Time PCR Instrument (Thermo Fisher Scientific, United States). Primers were obtained from Sangong Biotech (Shanghai, China). The sequences of E2F1 are GCAGCAACTGGACCACCTAA (Forward primer) and AAGACATCGATGGGGCCTTG (Reverse primer). The sequences of GAPDH are GCTGATGCCCCTATGTTCGT (forward primer) and TGATGGCATGGACTGTGGTC (reverse primer).

2.7. Statistical Analysis. The data of qRT-PCR were presented as mean ± standard deviation (SD) and were analyzed with one-way ANOVA followed by Tukey's multiple comparisons tests in GraphPad Prism 8.4.2. The value of $P < 0.05$ was considered statistically significant.

3. Results

3.1. Model Identification of Gallstone. The gallstone guinea pig model was established by lithogenic diet. Abdominal ultrasound examination showed gallstones in the Model group and the EA group after 6 weeks of lithogenic diet (see Figures 1(b)–1(d)).

3.2. Quality Assessment. More than 30 million reads of each sample were obtained, and the percentages of Q20 and Q 30 were above 97% and 93%, respectively, in each sample. These results indicated that the quality of the sequencing was acceptable. More than 70% of clean reads were mapped onto the reference genome (see Table 1).

3.3. Identification of DEGs. We used Illumina NovaSeq 6000 to analyze the gallbladder tissues of guinea pigs after 2-week electroacupuncture. The data were analyzed and DEGs were selected according to the threshold of $P < 0.05$ and $|\log2FC| \geq 1$. 257 DEGs were identified in Model vs. Normal, with 176 upregulated genes and 81 downregulated genes (see Figure 2(a), Figure 2(c), and Table S1). 1704 DEGs were found in EA vs. Model, with 270 upregulated DEGs and 1434 downregulated DEGs (see Figures 2(b), 2(d), and Table S2). Among these DEGs, 94 EA-reversed DEGs were identified, including 28 reversed UP DEGs and 66 reversed DOWN DEGs (see Figure 2(e), Figure 2(f), and Table S3).

3.4. Go Enrichment Analysis of 94 EA Reversed DEGs. GO enrichment analysis (including BP, biological process; CC, cellular component; MF, molecular function) was performed to predict the underlying biological functions of 94 EA

Table 1: Quality assessment of the RNA-seq.

Sample	Raw reads	Clean reads	Clean reads (%)	Q20 (%)	Q30 (%)	Total mapped	Mapped ratio (%)
Normal 2	34014866	33102392	97.32	98.00	94.20	30576715	92.40
Normal 4	36119610	35112328	97.21	97.95	94.15	32305432	92.00
Normal 8	36385004	35490310	97.54	97.80	93.80	30009483	84.60
Model 6	32884164	31919142	97.07	98.00	94.15	29430412	92.20
Model 29	35567182	34572958	97.20	97.90	93.95	32029940	92.60
Model 38	32026472	30888052	96.45	97.85	93.90	28575186	92.50
EA 13	33984346	33147418	97.54	97.80	93.65	26207366	79.10
EA 14	36185162	34789908	96.14	97.95	94.15	24475529	70.40
EA 19	43398886	41221630	94.98	97.80	93.85	32803154	79.60

Q20: quality score of 20; Q30: quality score of 30; Normal: the normal group; Model: the model group; EA: the electroacupuncture group.

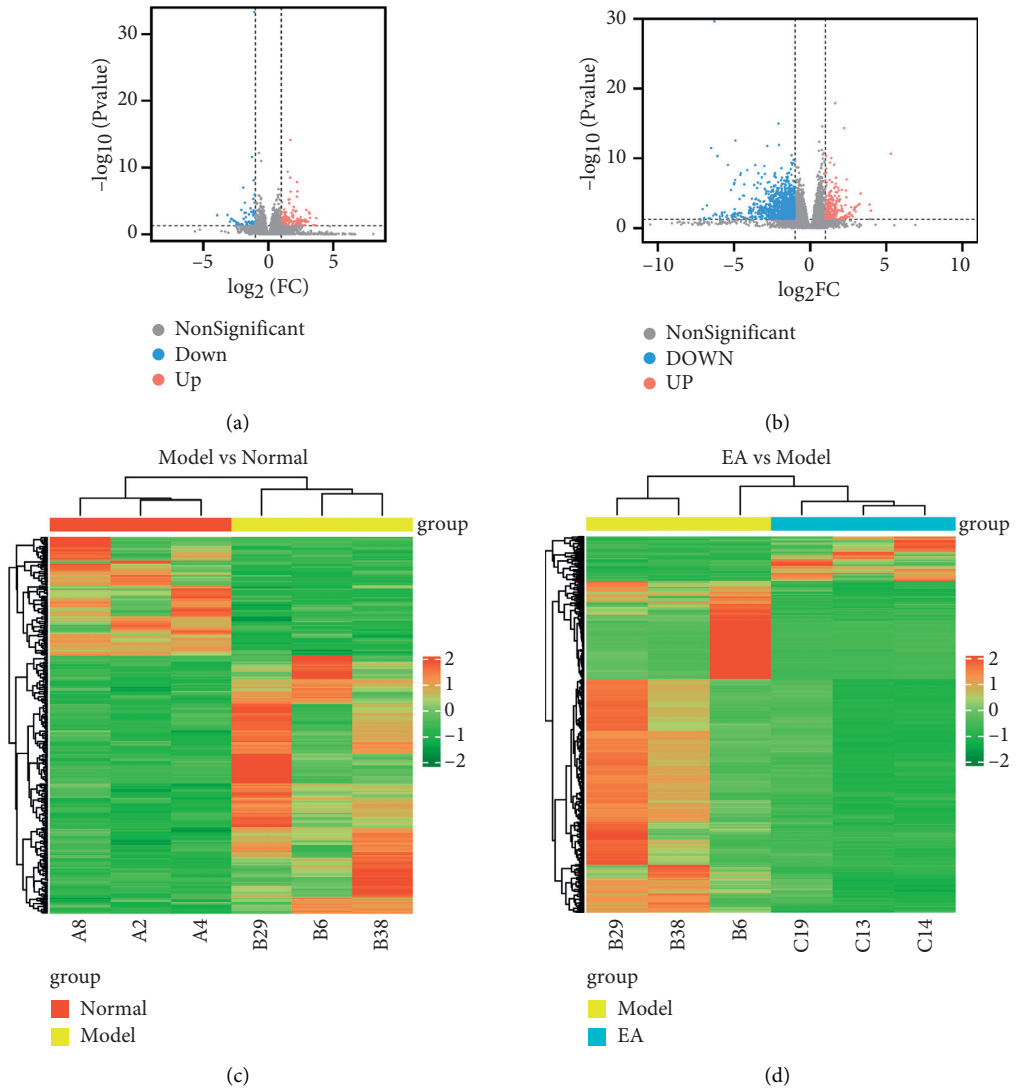

Figure 2: Continued.

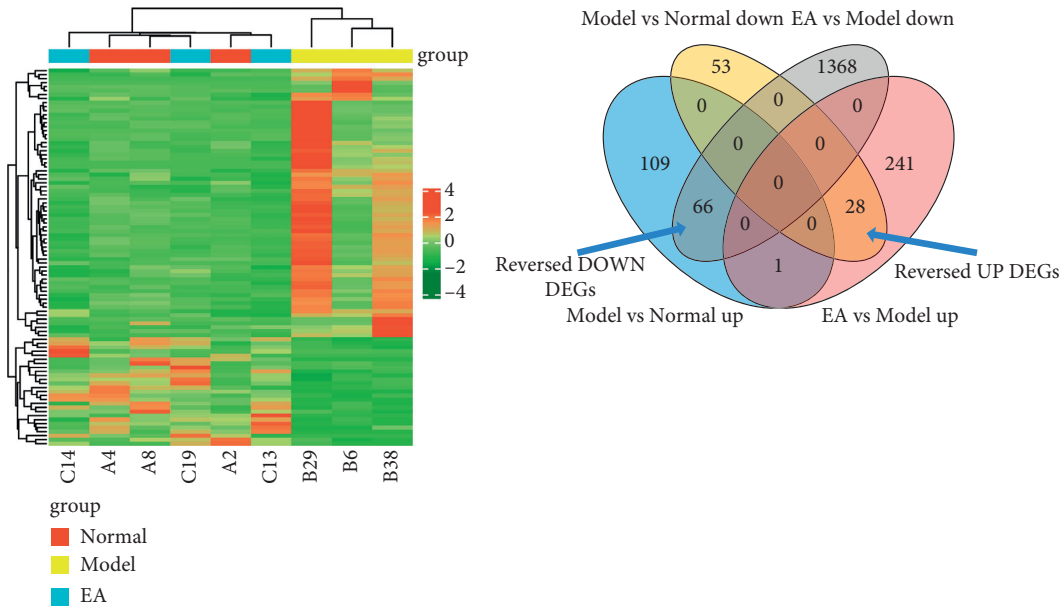

(e) (f)

Figure 2: DEGs identified: volcano plots (a) and heatmap (c) of 257 DEGs in Model vs. Normal, with 176 upregulated DEGs and 81 downregulated DEGs. Volcano plots (b) and heatmap (d) of 1704 DEGs in EA vs. Model, with 270 upregulated DEGs and 1434 downregulated DEGs. A heatmap of 94 reversed DEGs (e). Venn diagram of EA reversed DEGs (f). Normal: the normal group, model: the model group, EA: the electroacupuncture group, DEGs: differently expressed genes, reversed DOWN DEGs: electroacupuncture-reversed downregulated differently expressed genes, and reversed UP DEGs: electroacupuncture-reversed upregulated differently expressed genes.

reversed DEGs. The DEGs were enriched to 15 GO terms, including 2 BPs, 3 CCs, and 10 MFs ($P < 0.05$). The 2 BPs were positive regulation of transferase activity, and positive regulation of macromolecule biosynthetic process. The 3 CCs were cell projection, cytoskeletal part, and cell projection part. The 10 MFs were cation transmembrane transporter activity, ion transmembrane transporter activity, cation channel activity, substrate-specific transmembrane transporter activity, transmembrane transporter activity, ion channel activity, substrate-specific transporter activity, substrate-specific channel activity, channel activity, and passive transmembrane transporter activity as shown in Table 2 and Figure 3.

3.5. Construction of the PPI Network and Identification of Hub Genes. 94 EA-reversed DEGs were used to construct the PPI network based on the STRING database to identify the hub genes that may play key roles in the EA effect of gallstones. 59 nodes and 98 edges were established in the PPI network with score >0.150 (Figure 4(a)), and 46 nodes and 95 edges were analyzed. Cytohubba plugin was used to find the hub genes. The top 10 hub genes were CDC6, CDC45, MYB, E2F1, UBE2NL, UBE2T, UHRF1, MDM4, NHLRC1, and MAP3K2 (see Figure 4(b)).

3.6. Gene Validation. We randomly selected the E2F1 gene and performed qRT-PCR analysis to validate the expression of genes to confirm the key genes identified above. E2F1 was downregulated in Model vs. Normal and upregulated in EA vs. Model ($P < 0.05$), which validated the same trend in sequencing (see Figure 5).

4. Discussion

Lithogenic diet has been used widely in inducing animal gallstone models [32–34]. After successfully inducing the guinea pig gallstone models, we used high throughput RNA-seq to analyze the mRNA expression in guinea pig gallbladders of the Normal, Model, and EA groups. 257 DEGs and 1704 DEGs were separately identified in Model vs. Normal and in EA vs. Model. Among these DEGs, there are 94 EA-reversed genes, including 28 reversed UP DEGs and 66 reversed DOWN DEGs. We also predicted the potential functions of these EA-reversed DEGs using GO and PPI network analysis. Go enrichment analysis revealed that EA mainly regulated several GO-MF terms about the transmembrane transporter activities and channel activities.

Transporters are expressed in many tissues within the body and play important roles in human physiology, pharmacology, pathology, and toxicology [35]. EA involves multiple pathways and produces multitarget effects. In gallstone formation, cholesterol and its membrane transports were considered major pathogenic factors [5, 36]. Therefore, EA may involve in the transmembrane transporter activities of cholesterol and the regulation of glucose and lipid to reduce the gallstones. In our results, hub genes E2F1, UBE2T, UBE2NL, and UHRF1 involve in several important bioprocesses, including cell cycle progression, membrane transporting, regulation of cholesterol, glucose, lipid, etc.

Table 2: GO terms of EA-reversed DEGs.

GO ID	GO term	GO category	*P* value
GO:0051347	Positive regulation of transferase activity	BP	0.03526
GO:0010557	Positive regulation of macromolecule biosynthetic process	BP	0.04364
GO:0042995	Cell projection	CC	0.00410
GO:0044430	Cytoskeletal part	CC	0.02518
GO:0044463	Cell projection part	CC	0.03979
GO:0008324	Cation transmembrane transporter activity	MF	0.00937
GO:0015075	Ion transmembrane transporter activity	MF	0.01942
GO:0005261	Cation channel activity	MF	0.01998
GO:0022891	Substrate-specific transmembrane transporter activity	MF	0.02899
GO:0022857	Transmembrane transporter activity	MF	0.03767
GO:0005216	Ion channel activity	MF	0.03837
GO:0022892	Substrate-specific transporter activity	MF	0.04042
GO:0022838	Substrate-specific channel activity	MF	0.04162
GO:0015267	Channel activity	MF	0.04441
GO:0022803	Passive transmembrane transporter activity	MF	0.04441

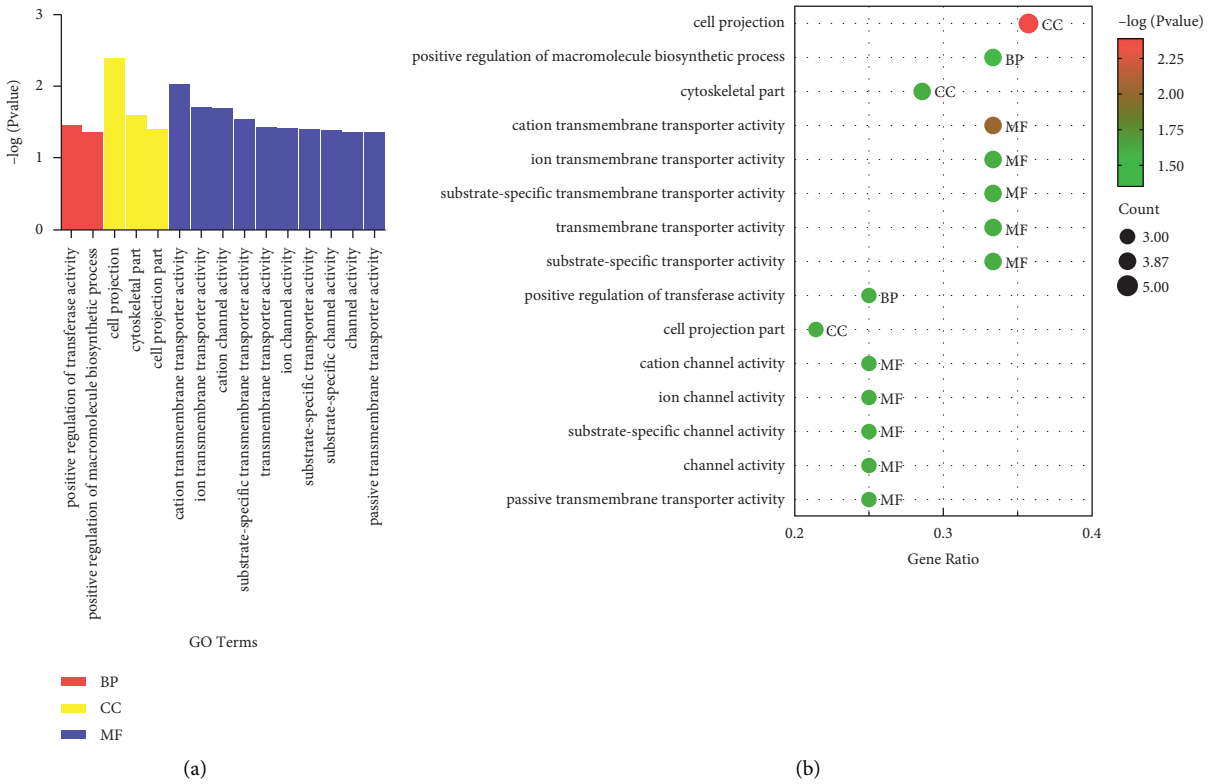

Figure 3: GO analysis of 94 EA reversed DEGs. Bar plot (a) of EA-reversed DEGs showed an enrichment score (-log(*P* value)) of the significant enrichment terms involving all 2 BPs, 3 CCs, and 10 MFs. Each bubble in the bubble plot (b) represents different -log(*P* value). GO: gene ontology; DEGs: differently expressed genes; BP: biological process; CC: cellular component; MF: molecular function.

E2F1 is a transcription factor that involves in cell cycle progression, DNA-damage response, and apoptosis [37, 38]. It also participates in the regulation of metabolism. The loss of E2F1 leads to abnormal cholesterol accumulation in the liver and the development of fibrosis in response to a high-cholesterol diet [39]. E2F1 regulates cholesterol uptake. By enhancing the expression of PCSK9, a negative regulator of cholesterol uptake, E2F1 increased cholesterol uptake [38, 39]. Cholesterol uptake is considered one of the factors for gallstones [5]. In our study, E2F1 expression was reduced in the Model group. However, it could be reversed to increase in the EA group. The result suggested that E2F1 might be correlated with the mechanism of gallstone, and it might be a possible therapeutic target of EA.

Research has shown that UBE2T, as a member of the E2 family in the ubiquitin-proteasome pathway, was key in protein ubiquitination. Ubiquitination controls diverse biological processes, including inflammation, immune

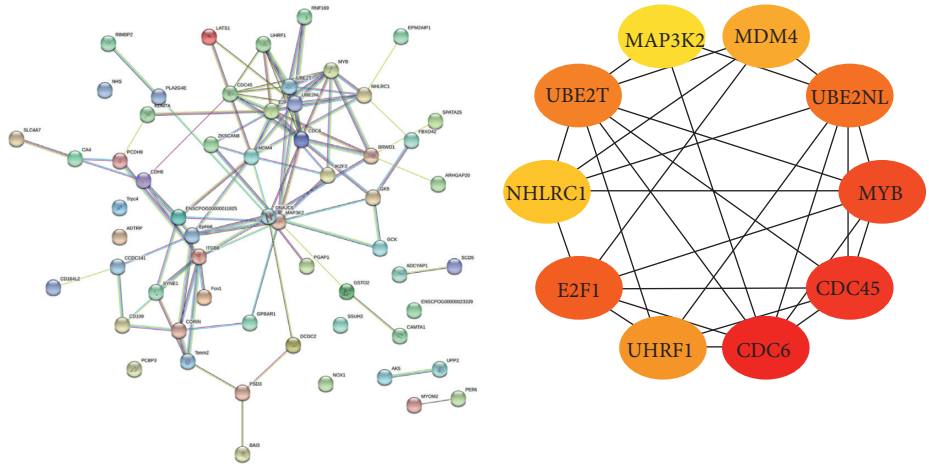

Figure 4: PPI network of 94 EA reversed DEGs (a) with a score >0.150, and the top 10 hub genes of EA-reversed DEGs by the cytohubba plugin (b). Each node stands for a gene or a protein, and the edges represent the interactions between the nodes. PPI: protein-protein interaction; DEGs: differently expressed genes.

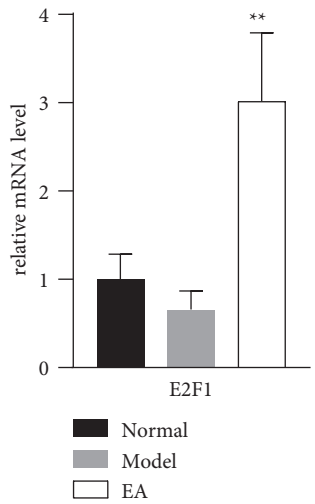

Figure 5: E2F1 mRNA expression using qRT-PCR. Statistical analysis was performed with one-way analysis of variance (ANOVA) and Tukey's multiple comparisons tests by GraphPad Prism 8.4.2. Compared with the Model group, $^{**}P < 0.01$.

response, cell differentiation, cell proliferation, etc. [40–45]. Dysregulated ubiquitin system may lead to a variety of diseases, such as various types of cancer, neurodegeneration, and metabolic disorders [46, 47]. In ubiquitination, E1, E2, and E3 enzymes sequentially activate, conjugate, and ligate ubiquitin to substrate proteins [48]. The E2s accept ubiquitin from the E1 complex and catalyze its covalent attachment to other proteins, involving in the change of protein stability, cellular localization, and biological activity. Hence, the E2 family is crucial in a wide range of biological processes, such as controlling the cell cycle, transducing signals, and inducing tumors, and it may provide an understanding of the pathogenesis of diseases [49]. As a member of the E2 family, UBE2T can induce cell cycle arrest at the G2/M phase and increase cell apoptosis. It has been reported to have a close relationship with the gallbladder. By analyzing microarray data, UBE2T was considered a hub gene in patients with gallbladder cancer, and it might serve as a biomarker for gallbladder cancer [50]. Through the PI3K/Akt signaling pathway and the Akt/GSK3β/β-catenin pathway, UBE2T is involved in the cell proliferation, migration, and invasion of cancer cells [51–53]. UBE2NL, also a ubiquitin-conjugating enzyme E2 family member, is related to the ubiquitination process [54]. It binds to ubiquitin-conjugating enzyme E2V2 [55–57] and interacts with E3 ubiquitin ligase in the poly-ubiquitination reaction and cell cycle progression [58]. UBE2NL has been found to be a novel type 2 diabetes relevant gene [59] and a novel candidate gene in familial gastroschisis [60]. It also expresses in the brain and participates in parkin-mediated mitophagy as a genetic risk factor for sporadic Alzheimer's disease [54].

UHRF1 is an E3 ubiquitin ligase that plays a key role in DNA methylation, DNA-damage repair, and cell proliferation [61]. UHRF1 is a key regulator of DNA double-strand break repair that directly participates in the interplay between VRCA1 and 53BP1 [62]. UHRF1 is important in epigenetics. During DNA replication, UHRF1 inherits DNA methylation. By binding either H3K9me2/3 or hemi-methylated CpG, UHRF1 is required in the recruitment of DNMT1 to DNA methylation sites. It also maintains DNA methylation at genomic sites containing methylated H3K9 [63–65]. As an epigenetic regulator, UHRF1 is significant in vascular smooth muscle cell plasticity. By promoting proliferation and differentiation, UHRF1 regulates the VSMC phenotype, and it may hold therapeutic potential in vascular pathologies [66]. Silencing UHRF1 inhibits cell proliferation and promotes cell apoptosis in retinoblastoma through the PI3K/Akt signaling pathway [67]. UHRF1 is highly expressed in proliferating and cancer cells, and it has been identified as a novel AMPK gate-keeper in cellular metabolism by interacting with AMPK and suppressing its activity. UHRF1 is physiologically significant in the regulation of glucose and lipid [68], and thereby, it is involved in the

regulation of liver metabolism. The liver overexpression of the UHRF1 mice model showed increasing blood glucose level, reducing glucose tolerance, reducing insulin sensitivity, and accumulating lipid droplets in the liver tissues. Gluconeogenesis, glycogen synthesis, and triglyceride synthesis-related gene upregulation is caused by overexpression [69].

The involvement of hub genes in the cholesterol, glucose and lipid metabolism gives a hint that EA may treat gallstone by regulating the metabolism. And it needs further design relevant experiments to verify these hypotheses. And There are limitations in this study. Due to lack of KEGG pathway of guinea pig in DAVID database, the KEGG enrichment analysis has not been carried out. And it also lacks the control group of sham acupuncture group. In the clinical practice, not only Yanglingquan (GB34) selected for the treatment of gallstone, but for the reason of standardization, we only use Yanglingquan (GB34) as the acupoint for EA. We have identified hub genes involved in the EA treatment of gallstone and may help to understand the therapeutic mechanism of EA. However, Further experiments need to be carried to study the expressions and interactions.

5. Conclusions

We analyzed the mRNA expression in gallbladders of guinea pigs in the Normal group, Model group, and EA group by high throughput RNA-seq. A number of key genes and GO terms were involved. These findings provide a clue to understand the possible therapeutic mechanism of EA on gallstone.

Data Availability

The raw data can be available from the corresponding author on reasonable request.

Conflicts of Interest

The authors have no conflicts of interest to declare.

Authors' Contributions

Mingyao Hao and Zhiqiang Dou contributed equally to this article.

Acknowledgments

The authors are grateful to Mr. Da Zhang (Mindray Bio-Medical Electronics, Shenzhen, China) for providing help in ultrasound examination. RNA-seq experiments were performed by Genergy Bio Technology, Shanghai, China. This work was supported by the National Natural Science Foundation of China (81804201), Meridian (Acupoint)—Viscera Regulation and Application Scientific Research Innovation Team, Shandong University of Traditional Chinese Medicine (220315), Acupoint-Viscera Correlation Study Youth Scientific Research Innovation Team, Shandong University of Traditional Chinese Medicine (22202110), Key project of Excellent Youth Science Fund of Shandong University of Traditional Chinese Medicine (2018zk05), and SRT Project of Shandong University of Traditional Chinese Medicine (S202010441004).

Supplementary Materials

Supplementary tables are provided. See Table S1 for the list of 257 DEGs in Model vs. Normal. See Table S2 for the list of 1704 DEGs in EA vs. Model. See Table S3 for 94 EA reversed DEGs. (*Supplementary Materials*)

References

[1] Q. Zeng, Y. He, D. C. Qiang, and L. X. Wu, "Prevalence and epidemiological pattern of gallstones in urban residents in China," *European Journal of Gastroenterology and Hepatology*, vol. 24, no. 12, pp. 1459-1460, 2012.

[2] European association for the study of the liver (EASL), "EASL clinical practice guidelines on the prevention, diagnosis and treatment of gallstones," *Journal of Hepatology European*, vol. 65, no. 1, pp. 146–181, 2016.

[3] A. di Ciaula and P. Portincasa, "Recent advances in understanding and managing cholesterol gallstone," *F1000Res*, vol. 7, no. F1000, Faculty Rev, pp. 1529, 2018.

[4] Y. Wang, M. Qi, C. Qin, and J. Hong, "Role of the biliary microbiome in gallstone disease," *Expert Review of Gastroenterology & Hepatology*, vol. 12, no. 12, pp. 1193–1205, 2018.

[5] A. Di Ciaula, D. Q. Wang, and P. Portincasa, "An update on the pathogenesis of cholesterol gallstone disease," *Current Opinion Gastroenterology*, vol. 34, no. 2, pp. 71–80, 2018.

[6] F. Lammert, "Gallstone disease: scientific understanding and future treatment," *In: G. Hirschfield, D. Adams, and E. Liaskou, "Biliary Disease: From Science to Clinic"*, Springer International Publishing, New York, NY, USA, pp. 229–241, 2017.

[7] Internal Clinical Guidelines Team (UK), *Gallstone Disease: Diagnosis and Management of Cholelithiasis, Cholecystitis and Choledocholithiasis*, National Institute for Health and Care Excellence (UK), London, UK, 2014.

[8] A. Di Ciaula, G. Garruti, G. Frühbeck et al., "The Role of diet in the pathogenesis of cholesterol gallstones," *Current Medicinal Chemistry*, vol. 26, no. 19, pp. 3620–3638, 2019.

[9] Y. Park, D. Kim, J. S. Lee et al., "Association between diet and gallstones of cholesterol and pigment among patients with cholecystectomy: a case-control study in Korea," *Journal of Health, Population, and Nutrition*, vol. 36, no. 1, p. 39, 2017.

[10] C. M. Chang, T. Chiu, C. C. Chang, M. N. Lin, and C. L. Lin, "Plant-based diet, cholesterol, and risk of gallstone disease: a prospective study," *Nutrients*, vol. 11, no. 2, p. 335, 2019.

[11] J. Wirth, M. Song, T. T. Fung et al., "Diet-quality scores and the risk of symptomatic gallstone disease: a prospective cohort study of male US health professionals," *International Journal of Epidemiology*, vol. 47, no. 6, pp. 1938–1946, 2018.

[12] V. Goral, "Gallstone etiopathogenesis, lith and mucin genes and new treatment approaches," *Asian Pacific Journal of Cancer Prevention*, vol. 17, no. 2, pp. 467–471, 2016.

[13] S. C. Chuang, E. His, and K. T. Lee, "Mucin genes in gallstone disease," *Clinica Chimica Acta*, vol. 413, no. 19-20, pp. 1466–1471, 2012.

[14] H. H. Wang, P. Portincasa, M. Liu, P. Tso, and D. Q. Wang, "An update on the lithogenic mechanisms of cholecystokinin a receptor (CCKAR), an important gallstone gene for lith13," *Genes*, vol. 11, no. 12, p. 1438, 2020.

[15] K. S. Yoo, H. S. Choi, D. W. Jun et al., "MUC expression in gallbladder epithelial tissues in cholesterol-associated gallbladder disease," *Gut and Liver*, vol. 10, no. 5, pp. 851–858, 2016.

[16] I. N. Grigor'eva and T. I. Romanova, "Gallstone disease and microbiome," *Microorganisms*, vol. 8, no. 6, p. 835, 2020.

[17] Q. Wang, L. Jiao, C. He et al., "Alteration of gut microbiota in association with cholesterol gallstone formation in mice," *BMC Gastroenterology*, vol. 17, no. 1, p. 74, 2017.

[18] N. G. Venneman and K. J. van Erpecum, "Pathogenesis of gallstones," *Gastroenterology Clinical of North America*, vol. 39, no. 2, pp. 171–183, 2010.

[19] Q. Hu and Z. Wang, "Research development of kinetic mechanism of gallstone formation," *China Journal of Modern Medicine*, vol. 20, no. 21, pp. 3303–3308, 2010.

[20] Y. Chen, J. Kong, and W. Su, "Cholesterol gallstone disease: focusing on the role of gallbladder," *Laboratory Investigation*, vol. 95, no. 2, pp. 124–131, 2015.

[21] Z. Guo, Q. Xu, S. Chen, and Y. Chen, "Influence of Acupuncture at pancreas-gallbladder point in auricular therapy on gallbladder dynamics of chronic cholecystitis patients," *Journal of Traditional Chinese Medicine*, vol. 52, no. 20, pp. 1755–1758, 2011.

[22] S. Chen, L. Wei, and S. Guo, "Preliminary observation of time-effect relationship on gallbladder dynamics of chronic cholecystitis with low tension by electroacupuncture at yanglingquan," *Journal of Clinical Acupuncture and Moxibustion*, vol. 29, no. 9, pp. 35–37, 2013.

[23] J. Zhao, Y. Yu, M. Luo, L. Li, and P. Rong, "Bi-directional regulation of acupuncture on extrahepatic biliary system: an approach in guinea pigs," *Scientific Reports*, vol. 7, no. 1, Article ID 14066, 2017.

[24] L. Wei, S. Du, and S. Chen, "Preliminary observation of acupuncture at qimen and yanglingquan on time-effect rule of influence on low tension gallbladder's movement," *Liaoning Journal of Traditional Chinese Medicine*, vol. 41, no. 6, pp. 1264-1265, 2014.

[25] A. Dobin, C. A. Davis, F. Schlesinger et al., "STAR: ultrafast universal RNA-seq aligner," *Bioinformatics*, vol. 29, no. 1, pp. 15–21, 2013.

[26] M. Pertea, G. M. Pertea, C. M. Antonescu, T. C. Chang, J. T. Mendell, and S. L. Salzberg, "StringTie enables improved reconstruction of a transcriptome from RNA-seq reads," *Nature Biotechnology*, vol. 33, pp. 290–295, 2015.

[27] M. I. Love, W. Huber, and S. Anders, "Moderated estimation of fold change and dispersion for RNA-seq data with DESeq2," *Genome Biology*, vol. 15, no. 12, p. 550, 2014.

[28] D. W. Huang, B. T. Sherman, and R. A. Lempicki, "Systematic and integrative analysis of large gene lists using DAVID bioinformatics resources," *Nature Protocols*, vol. 4, no. 1, pp. 44–57, 2009.

[29] D. W. Huang, B. T. Sherman, and R. A. Lempicki, "Bioinformatics enrichment tools: paths toward the comprehensive functional analysis of large gene lists," *Nucleic Acids Research*, vol. 37, no. 1, pp. 1–13, 2009.

[30] L. J. Jensen, M. Kuhn, M. Stark et al., "STRING 8-a global view on proteins and their functional interactions in 630 organisms," *Nucleic Acids Research*, no. 37, pp. D412–D416, 2009, (Database issue).

[31] P. Shannon, A. Markiel, O. Ozier et al., "Cytoscape: a software environment for integrated models of biomolecular interaction networks," *Genome Research*, vol. 13, no. 11, pp. 2498–2504, 2003.

[32] K. M. Tharp, A. Khalifeh-Soltani, H. M. Park et al., "Prevention of gallbladder hypomotility via FATP2 inhibition protects from lithogenic diet-induced cholelithiasis," *American Journal of Physiology Gastrointestinal Liver Physiology*, vol. 310, pp. G855–G864, 2016.

[33] M. Liu, C. Liu, H. Chen et al., "Prevention of cholesterol gallstone disease by schaftoside in lithogenic diet-induced C57BL/6 mouse model," *European Journal of Pharmacology*, vol. 815, pp. 1–9, 2017.

[34] L. Huang, C. Ding, and X. Si, "Changes in the interstitial cells of cajal in the gallbladder of guinea pigs fed a lithogenic diet," *Experimental and Therapeutic Medicine*, vol. 22, no. 2, p. 823, 2021.

[35] C. D. Klaassen and L. M. Aleksunes, "Xenobiotic, bile acid, and cholesterol transporters: function and regulation," *Pharmacological Review*, vol. 62, no. 1, pp. 1–96, 2010.

[36] F. Lammert, K. Gurusamy, C. W. Ko et al., "Gallstones," *Nature Review Disease Primers*, vol. 2, Article ID 16024, 2016.

[37] M. G. Ertosun, F. Z. Hapil, and O. Osman Nidai, "E2F1 transcription factor and its impact on growth factor and cytokine signaling," *Cytokine & Growth Factor Reviews*, vol. 31, pp. 17–25, 2016.

[38] P. D. Denechaud, L. Fajas, and A. Giralt, "E2F1, a novel regulator of metabolism," *Frontiers in Endocrinology*, vol. 8, p. 311, 2017.

[39] Q. Lai, A. Giralt, C. Le May et al., "E2F1 inhibits circulating cholesterol clearance by regulating Pcsk9 expression in the liver," *JCI Insight*, vol. 2, no. 10, Article ID e89729, 2017.

[40] D. S. Hewings, J. Heideker, T. P. Ma et al., "Reactive-site-centric chemoproteomics identifies a distinct class of deubiquitinase enzymes," *Nature Communications*, vol. 9, no. 1, p. 1162, 2018.

[41] X. Zhou, J. Yu, X. Cheng et al., "The deubiquitinase Otub1 controls the activation of CD8+ T cells and NK cells by regulating IL-15-mediated priming," *Nature Immunology*, vol. 20, no. 7, pp. 879–889, 2019.

[42] L. Yang, W. Guo, S. Zhang, and G. Wang, "Ubiquitination-proteasome system: a new player in the pathogenesis of psoriasis and clinical implications," *Journal of Dermatology Science*, vol. 89, no. 3, pp. 219–225, 2018.

[43] J. Qiu, M. J. Sheedlo, K. Yu et al., "Ubiquitination independent of E1 and E2 enzymes by bacterial effectors," *Nature*, vol. 533, no. 7601, pp. 120–124, 2016.

[44] S. H. Kao, H. T. Wu, and K. J. Wu, "Ubiquitination by HUWE1 in tumorigenesis and beyond," *Journal of Biomedical Science*, vol. 25, no. 1, p. 67, 2018.

[45] A. F. Alpi, V. Chaugule, and H. Walden, "Mechanism and disease association of E2-conjugating enzymes: lessons from UBE2T and UBE2L3," *Biochemical Journal*, vol. 473, no. 20, pp. 3401–3419, 2016.

[46] X. Huang and V. M. Dixit, "Drugging the undruggables: exploring the ubiquitin system for drug development," *Cell Research*, vol. 26, no. 4, pp. 484–498, 2016.

[47] Y. S. Choo and Z. Zhang, "Detection of protein ubiquitination," *Journal of Visualized Experiments: JoVE*, vol. 30, no. 1293, 2009.

[48] L. Song and Z. Q. Luo, "Post-translational regulation of ubiquitin signaling," *The Journal of Cell Biology*, vol. 218, no. 6, pp. 1776–1786, 2019.

[49] G. Markson, C. Kiel, R. Hyde et al., "Analysis of the human E2 ubiquitin conjugating enzyme protein interaction network," *Genome Research*, vol. 19, no. 10, pp. 1905–1911, 2009.

[50] X. Zhu, T. Li, T. X. Niu, L. Chen, and C. Ge, "Identification of UBE2T as an independent prognostic biomarker for gallbladder cancer," *Oncology Letters*, vol. 20, no. 4, p. 44, 2020.
[51] Y. Wang, H. Leng, H. Chen et al., "Knockdown of UBE2T inhibits osteosarcoma cell proliferation, migration, and invasion by suppressing the PI3K/Akt signaling pathway," *Oncology Research*, vol. 24, no. 5, pp. 361–369, 2016.
[52] J. Guo, M. Wang, J. P. Wang, and C. X. Wu, "Ubiquitin-conjugating enzyme E2T knockdown suppresses hepatocellular tumorigenesis via inducing cell cycle arrest and apoptosis," *World Journal of Gastroenterology*, vol. 25, no. 43, pp. 6386–6403, 2019.
[53] D. Zhang, J. Liu, T. Xie et al., "Oleate acid-stimulated HMMR expression by CEBPα is associated with nonalcoholic steatohepatitis and hepatocellular carcinoma," *International Journal of Biological Sciences*, vol. 16, no. 15, pp. 2812–2827, 2020.
[54] A. Gómez-Ramos, P. Podlesniy, E. Soriano, and J. Avila, "Distinct X-chromosome SNVs from some sporadic AD samples," *Scientific Reports*, vol. 5, no. 18012, 2015.
[55] G. Nalepa, M. Rofle, and W. J. Harper, "Drug discovery in the ubiquitin-proteasome system. Nature reviews," *Nature Reviews Drug Discovery*, vol. 5, no. 7, pp. 596–613, 2006.
[56] A. Ciechnover, "The unravelling of the ubiquitin system," *Nature Reviews Molecular Cell Biology*, vol. 16, no. 5, pp. 322–324, 2015.
[57] F. T. Moraes, R. A. Edwards, S. McKenna et al., "Crystal structure of the human ubiquitin conjugating enzyme complex, hMms2-hUbc13," *Nature Structural Biology*, vol. 8, no. 8, pp. 669–673, 2001.
[58] M. Argentini, N. Barboulem, and B. Wasylyk, "The contribution of the RING finger domain of MDM2 to cell cycle progression," *Oncogene*, vol. 19, no. 34, pp. 3849–3857, 2000.
[59] J. Flannick, J. M. Mercader, C. Fuchsberger et al., "Exome sequencing of 20,791 cases of type 2 diabetes and 24,440 controls," *Nature*, vol. 570, no. 7759, pp. 71–76, 2019.
[60] V. M. Salinas-Torres, H. L. Gallardo-Blanco, R. A. Salinas-Torres et al., "Whole exome sequencing identifies multiple novel candidate genes in familial gastroschisis," *Molecular Genetics & Genomic Medicine*, vol. 8, no. 5, Article ID e1176, 2020.
[61] R. M. Vaughan, B. M. Dickson, E. M. Cornett, J. S. Harrison, B. Kuhlman, and S. B. Rothbart, "Comparative biochemical analysis of UHRF proteins reveals molecular mechanisms that uncouple UHRF2 from DNA methylation maintenance," *Nucleic Acids Research*, vol. 46, no. 9, pp. 4405–4416, 2018.
[62] H. Zhang, H. Liu, Y. Chen et al., "A cell cycle-dependent BRCA1-UHRF1 cascade regulates DNA double-strand break repair pathway choice," *Nature Communications*, vol. 7, Article ID 10201, 2016.
[63] X. Liu, Q. Gao, P. Li et al., "UHRF1 targets DNMT1 for DNA methylation through cooperative binding of hemi-methylated DNA and methylated H3K9," *Nature Communication*, vol. 4, p. 1563, 2013.
[64] G. Auclair, J. Borgel, L. A. Sanz et al., "EHMT2 directs DNA methylation for efficient gene silencing in mouse embryos," *Genome Research*, vol. 26, no. 2, pp. 192–202, 2016.
[65] C. Bronner, M. Alhosin, A. Hamiche, and M. Mousli, "Coordinated dialogue between UHRF1 and DNMT1 to ensure faithful inheritance of methylated DNA patterns," *Genes (Basel)*, vol. 10, no. 1, p. 65, 2019.
[66] L. Elia, P. Kunderfranco, P. Carullo et al., "UHRF1 epigenetically orchestrates smooth muscle cell plasticity in arterial disease," *The Journal of Clinical Investigation*, vol. 128, no. 6, pp. 2473–2486, 2018.
[67] Y. Liu, G. Liang, T. Zhou, and Z. Liu, "Silencing UHRF1 Inhibits cell proliferation and promotes cell apoptosis in retinoblastoma via the PI3K/Akt signalling pathway," *Pathology and Oncology Research*, vol. 26, no. 2, pp. 1079–1088, 2020.
[68] X. Xu, G. Ding, C. Liu et al., "Nuclear UHRF1 is a gate-keeper of cellular AMPK activity and function," *Cell Research*, 2021.
[69] X. Chen, *Study the Function of UHRF Protein Family by Liver Specific Overexpression Mouse Model*, Dissertation of East China Normal University, Shanghai, China, 2020.

Hindawi
Evidence-Based Complementary and Alternative Medicine
Volume 2021, Article ID 5088129, 7 pages
https://doi.org/10.1155/2021/5088129

Review Article

Research Status Quo in Traditional Mongolian Medicine: A Bibliometric Analysis on Research Documents in the Web of Science Database

Tae-Hun Kim[1] **and Jung Won Kang**[2]

[1]*Korean Medicine Clinical Trial Center, College of Korean Medicine, Kyung Hee University, 23 Kyungheedae-ro, Dongdaemun-gu, Seoul 02447, Republic of Korea*
[2]*Department of Acupuncture & Moxibustion, College of Korean Medicine, Kyung Hee University, 23 Kyungheedae-ro, Dongdaemun-gu, Seoul 02447, Republic of Korea*

Correspondence should be addressed to Tae-Hun Kim; rockandmineral@gmail.com

Received 21 October 2021; Accepted 16 December 2021; Published 28 December 2021

Academic Editor: Zhaohui Liang

Objective. In this study, the current state of research on traditional Mongolian medicine (TMM) through a bibliometric analysis of research documents located in the Web of Science (WoS) database was assessed. *Methods*. The WoS database was searched on September 2021 with the keywords "traditional Mongolian medicine." Publications on TMM scientific research were included in this study, without any language limitations. Bibliometric data from such publications were retrieved from the WoS database. Full records with cited reference lists were descriptively analyzed. To assess trends in TMM research topics, authors' keywords were analyzed. A thematic evolution map based on coword analysis was suggested. To analyze research networks among co-authors, affiliations, or countries of the authors, collaboration networks were evaluated. The Bibliometrix R package (3.1) was used for the analysis. *Results*. A total of 234 scientific publications were included in the analysis. The top three countries of origin of the corresponding authors were China ($n = 153$), Japan ($n = 28$), and South Korea ($n = 9$). The top three relevant affiliations of the authors in the included publications were "Inner Mongolia Medical University," "Inner Mongolia University of Nationalities," and "National University of Mongolia." "Flavonoids," "cytotoxicity," "NMR," and "Tibetan medicine" were the most frequently used keywords in the included documents. Most publications focused on the chemical analysis and mechanism of effects of Mongolian herbal medications. There were few publications on nonpharmacological interventions such as bloodletting or TMM diagnostics, which should be promoted in future publications. *Conclusion*. There were only a limited number of publications on TMM identified through a search of the WoS database, using the keywords "Traditional Mongolian medicine." More improved strategy for searching for TMM publications must be established. Research publications on TMM, especially regarding non-pharmacological interventions, need to be promoted. In addition, collaboration with researchers worldwide needs to be encouraged in the future.

1. Introduction

Traditional medicine is defined as a system of medicine established based on specific cultural beliefs that pass on from generation to generation [1]. It is usually classified as a complementary health approach, but is used in clinical practice as mainstream medicine in some countries [2]. Research on traditional medicine can provide evidence on the effectiveness and safety of its interventions in the local areas where it is used and offers guidance on novel drug development processes to global pharmaceutical companies [3]. In this sense, research publications on traditional medicine must be identifiable and accessible outside the local region.

Bibliometrics is a subfield of research in information science and can be defined, according to Paul Otlet, as the

measurement and analysis of relevant items around published books or documents [4]. Along with the contents of the research publications, metadata such as authors, institutions, year of publication, and reference lists are the subjects of interest in bibliometric analysis. To study research trends and collaboration in a specific field, these data are analyzed using mathematical calculation methods, and the results are generally suggested as figures or network graphs, which provide a basic clue as the first step to understanding the current research status in the corresponding field [5].

Traditional Mongolian medicine (TMM) is assumed to have over a 5,000-year-long history, and it has specific features such as bone art, balneotherapy, and DOM therapy developed and practiced by the Mongolian nomads, along with the adoption of extrinsic medical theory and remedies from abroad, such as Tibetan Medicine, Ayurveda, or traditional Chinese medicine (TCM) [6]. However, research on TMM is not well known outside of Mongolia, and there is not enough information to understand the current research status through the eyes of foreign researchers. In the PubMed, MeSH term for TMM, "Medicine, Mongolian Traditional" was introduced in 2010, but only a small number of literature are found using this term, which reflects the current information deficiency [7]. From this viewpoint, a brief bibliometric analysis of TMM through a search of the Web of Science (WoS) database was conducted to evaluate the current research status of TMM.

2. Methods

2.1. Literature Search and Selection of the Literature. For this study, the literature on TMM was identified through an electronic database search. The WoS, which includes extensive research literature with detailed information on the authors, institutions, countries of the authors, and reference lists, was searched, and any literature identified until September 2021 was included in this study. The purpose of this study was to evaluate the current status of research on TMM worldwide; therefore, reports, books, or journals that were available only in Mongolia were not included. The search strategy for the WoS is as follows.

#1 traditional Mongolian medicine

#2 TMM and Mongol

#3 Mongolian medicine

#4 #1 OR #2 OR #3

The following inclusion criteria were adopted for this bibliometric analysis:

(i) Literature type: all research articles (papers), conference proceedings, or data papers, regardless of the sources of the literature, were included in this study. No limitations were imposed in terms of the type of literature if it was searched in the WoS database. There were no linguistic limitations in this study.

(ii) Publication period: all literature between the years 1991 and 2021 was included.

(iii) Topics of the literature: any literature that dealt with research on TMM was included in this study. TMM was defined as "medicinal practice which is indigenous to Mongolian population and was established based on the tradition and beliefs of Mongolian people," according to the explanation of MeSH terminology in PubMed [8]. Any research types including cell or animal experiments of various interventions of TMM, clinical studies, epidemiologic studies, reviews, and surveys of TMM practitioners were included in this study. Studies that were not related to TMM were excluded from analysis.

The titles and abstracts of each article were reviewed by two authors. Full texts were also assessed if there was insufficient information regarding the selection process. Two authors (T-HK and JWK) screened the articles individually, and decisions were made through discussion.

2.2. Data Extraction and Bibliometric Analysis Method. Bibliometric data from the included publications were retrieved from the WoS database. Full records with cited reference lists for each publication were exported as a plain text file that provided detailed information on all the included documents such as authors, document titles, publication source (or journal title), document types, keywords of the publications, KeyWords Plus®, which is a specific index term for each document and is generated using the title of the article by the WoS, country of the authors, abstract, year of publication, and reference lists [9]. The type of studies, number of authors for each document, country of the corresponding authors, most relevant affiliations, most cited documents, and sources (journal) of the documents were analyzed.

To assess trends in TMM research, authors' keywords and KeyWords Plus® were analyzed in a descriptive way. A thematic evolution map using keywords was suggested to present changes in research topics according to temporal changes. Coword analysis on the keywords of different documents was presented in a low-dimensional space based on the different periods of each publication, which was based on Cobo's method [10].

To analyze the research network among co-authors, affiliations, or countries of the authors, collaboration networks were obtained using the following formula:

Bcoll = A' x A, where A is a document x author matrix in the author collaboration network, a document x affiliation matrix in the affiliation collaboration network, and a document × country matrix in the country collaboration network. Each element in the matrix suggests the number of collaborations between two authors (institutions or countries) among the included publications [9,11]. The closeness centrality of each node was calculated by measuring the total distance from other nodes in the collaboration network plot, and the betweenness centrality was calculated by assessing the number of shortest paths from other nodes to a specific node [12]. The Bibliometrix package for R (Ver 3.1) was used in this bibliometric analysis.

3. Results

3.1. Summary of the Included Documents. From the 4,625 records identified from the WoS search, only 234 documents were included in this study (Figure 1). The average time from publication to 2021 was 5.68 years, and the average number of citations per document was 6.363. The total number of references was 6,426, and the number of all authors was 1,050. The number of co-authors per documents was 6.28. The most common types of documents such as articles ($n = 202$), reviews ($n = 11$), meeting abstracts ($n = 13$), editorial materials ($n = 2$), and notes ($n = 1$) were followed (Supplementary file 1). The number of annual publications has been increased gradually between 1991 and 2021 (Supplementary file 2). The number of average total article citations per year also showed gradual increase between 1991 and 2021 (Supplementary file 3).

3.2. Analysis of the Authors. Among the included 6,407 authors, Wang Q. H. (number of documents = 19), Batkhuu J. (number of documents = 10), Bao L. D. (number of documents = 9), and Glasl S. (number of documents = 9) were the most active authors and among the top 4 (Supplementary file 4). The most cited authors were Glasl S. (number of documents = 20), Kletter C. (number of documents = 19), Narantuya S. (number of documents = 19), Purevsuren S. (number of documents = 17), and Obmann A. (number of documents = 16). The most influential authors with the highest *h*-index were Glasl S. (7), Narantuya S. (7), Purevsuren S. (7), Batkhuu J. (6), Kletter C. (6), and Zehl M. (6) (Table 1).

3.3. Analysis of the Institutions and Countries. Institutions that included the most active authors in this study were identified, and Inner Mongolia Medical University was the most relevant one ($n = 71$). The Inner Mongolia University of Nationalities came second ($n = 61$), and the National University of Mongolia was the third institution ($n = 16$) (Table 2). Countries where the corresponding authors were from were analyzed, and the top five countries of the corresponding authors were China ($n = 153$), Japan ($n = 28$), South Korea ($n = 9$), Austria ($n = 8$), and Russia ($n = 7$). Mongolia had only 4 corresponding authors (Table 3).

3.4. Analysis of Journals and Cited Documents. The five most relevant journals that published documents related to TMM were the Journal of Ethnopharmacology ($n = 24$), Spectroscopy and Spectral Analysis ($n = 16$), Natural Product Research ($n = 15$), Journal of Natural Medicine ($n = 8$), Evidence-Based Complementary and Alternative Medicine ($n = 6$), and Planta Medica ($n = 6$) (Supplementary file 5). The most frequently cited document was "Protective effects of probiotic *Lactobacillus casei* Zhang against endotoxin and d-galactosamine-induced liver injury in rats via anti-oxidative and anti-inflammatory capacities" by Wang 2013 (Supplementary file 6) [13].

3.5. Analysis of Research Topic. When the frequency of the author's keywords in each document was assessed, the most frequently used keywords were "flavonoids" ($n = 12$), "cytotoxicity" ($n = 8$), "NMR" ($n = 8$), "Tibetan medicine" ($n = 7$), "insomnia" ($n = 6$), and "trace elements" ($n = 6$). The most frequently used KeyWords Plus® were "constituents" ($n = 17$), "expression" ($n = 16$), "activation" ($n = 15$), "extract" ($n = 11$), and "inhibition" ($n = 11$) (Table 4). From the thematic evolution map, through keywords analysis, research topics changed from "antimicrobial activity," "flavonoids," "insomnia," and "Iridaceae" (1991–2017) to "insomnia," "flavonoids," "anti-inflammatory activity," "NMR," "oxidative stress," and "*Saposhnikovia divaricata*" (Figure 2). When assessing the network of keywords used in the publications, prominent co-occurrence was observed among different keywords such as "flavonoids" and "chemical constituents," "NMR" and "Chinese minority traditional medicine," and "Tibetan medicine" and "Warm acupuncture" (Supplementary file 7).

3.6. Collaboration Networks for Co-Authors, Institutions, and Countries. In the collaboration network of the authors, Wang QH showed the highest betweenness centrality (score = 17), but most authors exhibited very low betweenness centrality. On the closeness centrality score, most authors showed similar closeness centrality (Supplementary file 8). In the collaboration network of the institutions, Inner Mongolia University (score = 66), National University of Mongolia (score = 61), and Peking University (score = 56) showed the highest betweenness centrality among the included institutions (Supplementary file 9). However, closeness centrality had similar scores among the institutions. From these results, a very loose collaboration between authors can be identified. In the collaboration network of the countries, Mongolia and China showed the highest betweenness centrality (score = 15.82 in Mongolia and 1.18 in China) and closeness centrality (score = 0.14 in Mongolia and 0.11 in China). Therefore, the two countries can be assumed to be the core of the collaboration network in TMM research (Supplementary file 10).

4. Discussion

In this study, only a small number of research publications were identified through the WoS search ($n = 229$). The leading countries that the corresponding authors belonged to were China, Japan, and South Korea. From the analysis of research collaboration among countries, Mongolia and China showed the highest centrality scores for betweenness and closeness. The most actively used keywords were "flavonoids," "cytotoxicity," and "NMR." Research topics from the included publications were mainly related to the chemical analysis of medicinal herbs or herbal products. Nonpharmacological interventions or TMM diagnostics have not been frequently evaluated.

This is the first bibliometric analysis on TMM in a global database, the WoS. An extensive search of literature on TMM was conducted, and appropriate publications were

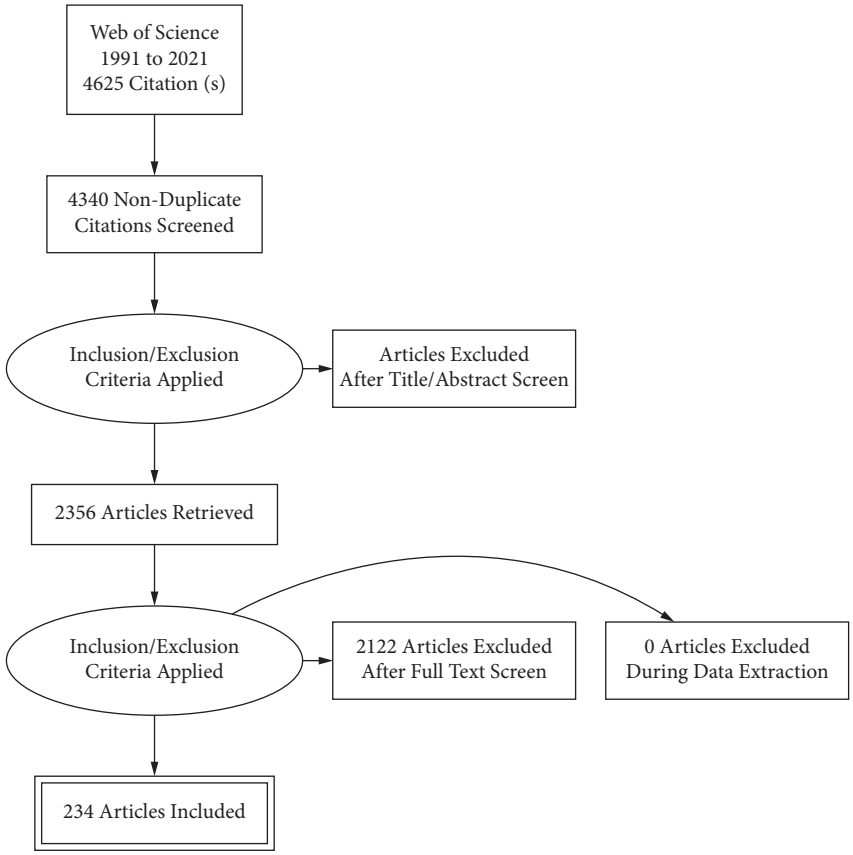

Figure 1: Study flow diagram.

Table 1: Top 10 most cited authors.

Author	Local citations*	*H*-index
Glasl S.	20	7
Kletter C.	19	6
Narantuya S.	19	7
Purevsuren S.	17	7
Obmann A.	16	5
Batkhuu J.	14	6
Zehl M.	13	6
Murata T.	12	5
Sasaki K.	11	4
Suganuma K.	11	4

*Local citations were counted from the included references.

Table 2: Most relevant affiliations (top 20 institutions).

Affiliations	Articles
Inner Mongolia Medical University	71
Inner Mongolia University of Nationalities	63
National University of Mongolia	18
Mongolian National University of Medical Science	15
Obihiro University of Agriculture and Veterinary Medicine	15
Baotou Medical College	14
Minzu University of China	14
Beijing University of Chinese Medicine	13
Institute of Chemistry and Chemical Technology	12

Table 2: Continued.

Affiliations	Articles
Inner Mongolia Normal University	11
University of Vienna	10
Health Sciences University of Mongolia	9
Taipei Medical University	9
Inner Mongolia University	8
Inner Mongolia Agricultural University	7
Institute for Mongolian Buddhist and Tibetan Studies	7
Jilin University	7
Peking University	7
Tohoku Medical and Pharmaceutical University	7
Shenyang Pharmaceutical University	6

Table 3: List of the corresponding authors' countries.

Country	Articles (%)
China	153 (68)
Japan	28 (12.4)
South Korea	9 (4)
Austria	8 (3.6)
Russia	7 (3.1)
Germany	5 (2.2)
Mongolia	4 (1.8)
USA	4 (1.8)
Australia	1 (0.4)
Canada	1 (0.4)
Hungary	1 (0.4)
India	1 (0.4)
Spain	1 (0.4)
Sweden	1 (0.4)
Thailand	1 (0.4)

Table 4: Most frequently used keywords and KeyWords Plus® (top 20).

Words assessed by authors' keywords	Occurrences	Words assessed by KeyWords Plus	Occurrences
Flavonoids	12	Constituents	17
Cytotoxicity	8	Expression	16
NMR	8	Activation	15
Tibetan medicine	7	Extract	11
Insomnia	6	Inhibition	11
Trace elements	6	Acid	10
ICP-AES	5	Apoptosis	10
Oxidative stress	5	Derivatives	9
Syringa pinnatifolia	5	Identification	9
Traditional medicine	5	Glycosides	8
Apoptosis	4	Oxidative stress	8
Dianthus versicolor	4	Rats	8
Hyperlipidemia	4	Mechanisms	7
Sesquiterpene	4	Cells	6
Spectroscopic methods	4	Extracts	6
Warm acupuncture	4	Flavonoids	6
Anti-inflammatory	3	Mice	6
Anti-inflammatory activity	3	Pathway	6
Antimicrobial activity	3	Roots	6
Antioxidant activity	3	Cancer	5

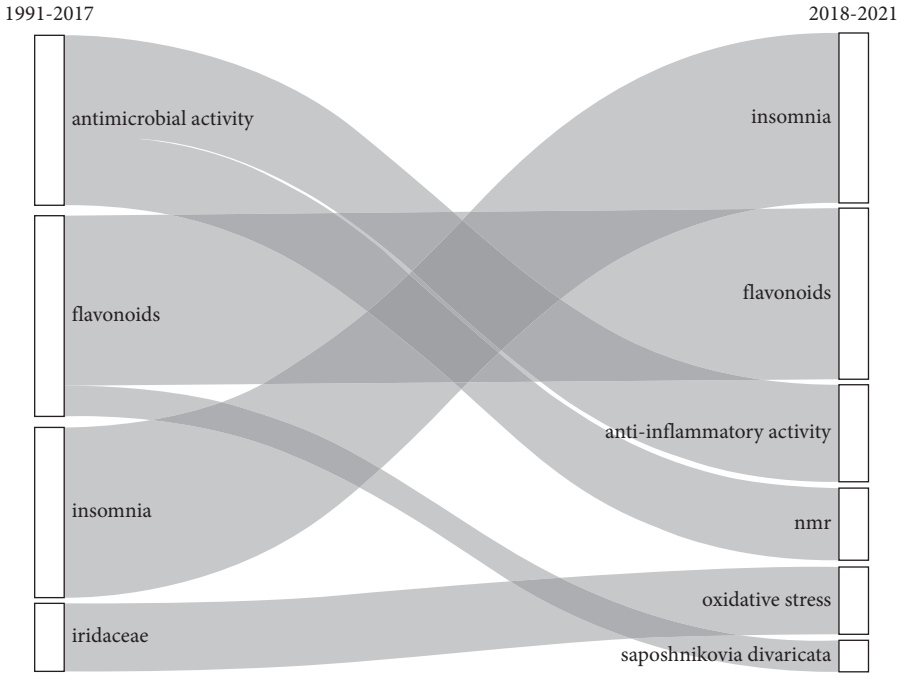

Figure 2: The thematic evolution map.

included based on predefined selection criteria. Although qualitative analysis of publication status was the main research methodology, collaboration networks were accessed by calculating the betweenness centrality and closeness centrality and suggested a thematically changing map through a coword analysis of keywords. The results of this study can provide a brief map of the current status of research on TMM among the publications available worldwide.

This study has several limitations that originate from the research methodologies used. First, the WoS was used only to search for relevant publications and extract data. The WoS is a widely used database that covers research publications and citations [14]. Because the WoS supplies various metadata, including document information (title and publication date), author information (author's name and information), and citation information (reference lists and citation numbers), users can export these metadata, which enables researchers to easily conduct a bibliometric analysis [15]. However, empirical evidence suggests that the WoS database has considerable errors that originate from the transcription procedure, such as mistyping or omission of authors and titles or incomplete (omitted) cited reference lists. In addition, online publications can introduce errors, which can double count the same publication or reduce the time it takes for a study to be published after being accepted, possibly distorting the influence on the citation of the study [16]. Another issue is related to the limited range of journals included in the WoS database [17]. From this perspective, it is acknowledged that there may have been errors in the selection and analysis of literature. Second, the search strategy may have been biased. Keywords such as "Traditional Mongolian medicine" and "Mongolian medicine" were used to identify publications in the WoS. If any document that had been classified as TMM research did not use these keywords in the title, abstract, or keywords, the search could not locate these publications. Although TMM is included in the MeSH's vocabulary, the omission of keywords or phrases allows for a limited literature search in PubMed, which is another reason why a specially developed search filter or strategy for TMM is necessary in the future [7].

From this study, it was found that the results of pharmacological studies have only been published actively by researchers in China and Mongolia. Like acupuncture in traditional Chinese medicine and Korean medicine, TMM has a variety of nonpharmacological interventions such as bloodletting therapy [18] and moxibustion therapy [19]. It has principles in the physiology and pathology of medical theory, distinguished from traditional medicine in other neighboring countries, which offers a different picture or clinical practice in TMM [20]. Therefore, balanced research on the various components of TMM should be encouraged.

5. Conclusion

There are not many publications on TMM, and research topics focus on the mechanism studies of herbs or botanical products in TMM. Nonpharmacological interventions or TMM diagnostics should be promoted in future studies. In addition, global research collaboration needs to be encouraged beyond China and Mongolia.

Data Availability

The data used to support the findings of this study are available from the corresponding author upon request.

Disclosure

The part of this study' results was presented at the International Symposium of Traditional Mongolian Integrative Medicine: Development Achievement, Trends, and Prospects in Ulaanbaatar, Mongolia, 2021.

Conflicts of Interest

The authors declare that they have no conflicts of interest.

Authors' Contributions

T-HK and JWK conceived study design, conducted literature searching and bibliometric analysis, and wrote the final draft of this manuscript.

Supplementary Materials

Supplementary file 1. Summary of the included research literature between 1991 and 2021. Supplementary file 2. Changes in the number of publications by year. Supplementary file 3. Average total article citations per year. Supplementary file 4. Most active authors (top 20). Supplementary file 5. Most relevant journal lists (top 20). Supplementary file 6. Most global cited documents. Supplementary file 7. Co-occurrence network of keywords. Supplementary file 8. Collaboration network of the authors in the literatures. Supplementary file 9. Collaboration network of the institutions in the literatures. Supplementary file 10. Collaboration network between countries. (*Supplementary Materials*)

References

[1] 2021 https://www.ncbi.nlm.nih.gov/mesh/68008519.

[2] 2021 https://www.nccih.nih.gov/health/complementary-alternative-or-integrative-health-whats-in-a-name.

[3] V. Fønnebø, S. Grimsgaard, H. Walach et al., "Researching complementary and alternative treatments–the gatekeepers are not at home," *BMC Medical Research Methodology*, vol. 7, no. 1, pp. 1–6, 2007.

[4] R. Rousseau, "Forgotten founder of bibliometrics," *Nature*, vol. 510, no. 7504, p. 218, 2014.

[5] M. J. Kurtz and J. Bollen, "Usage bibliometrics," arXiv: 110228912011, 2011.

[6] B. Sh, *Brief History and Development of Traditional Mongolian Medicine*World Intellectual Property Organization, Geneva, Switzerland, 2016.

[7] 2021 https://www.ncbi.nlm.nih.gov/mesh/?term=Medicine%2C+Mongolian+Traditional.

[8] 2021 https://www.ncbi.nlm.nih.gov/mesh/?term=traditional+Mongolian+medicine.

[9] M. Aria and C. Cuccurullo, "Bibliometrix: an R-tool for comprehensive science mapping analysis," *Journal of informetrics*, vol. 11, no. 4, pp. 959–975, 2017.

[10] M. J. Cobo, A. G. López-Herrera, E. Herrera-Viedma, and F. Herrera, "An approach for detecting, quantifying, and visualizing the evolution of a research field: a practical application to the fuzzy sets theory field," *Journal of informetrics*, vol. 5, no. 1, pp. 146–166, 2011.

[11] W. Glänzel and A. Schubert, "Analysing scientific networks through co-authorship," in *Handbook of Quantitative Science and Technology Research*, pp. 257–276, Springer, Berlin, Germany, 2004.

[12] H. Hou, H. Kretschmer, and Z. Liu, "The structure of scientific collaboration networks in Scientometrics," *Scientometrics*, vol. 75, no. 2, pp. 189–202, 2008.

[13] Y. Wang, Y. Li, J. Xie et al., "Protective effects of probiotic *Lactobacillus casei* Zhang against endotoxin- and D-galactosamine-induced liver injury in rats via anti-oxidative and anti-inflammatory capacities," *International Immunopharmacology*, vol. 15, no. 1, pp. 30–37, 2013.

[14] C. Birkle, D. A. Pendlebury, J. Schnell, and J. Adams, "Web of Science as a data source for research on scientific and scholarly activity," *Quantitative Science Studies*, vol. 1, no. 1, pp. 363–376, 2020.

[15] C. Analytics, "Web of Science core collection field tags," *Scientometrics*, vol. 103, no. 2, 2019.

[16] F. Franceschini, D. Maisano, and L. Mastrogiacomo, "Empirical analysis and classification of database errors in Scopus and Web of Science," *Journal of informetrics*, vol. 10, no. 4, pp. 933–953, 2016.

[17] P. Mongeon and A. Paul-Hus, "The journal coverage of Web of Science and Scopus: a comparative analysis," *Scientometrics*, vol. 106, no. 1, pp. 213–228, 2016.

[18] T.-H. Kim and S.-Y. Jung, "Mongolian traditional-style bloodletting therapy," *Journal of Alternative & Complementary Medicine*, vol. 19, no. 12, pp. 921–924, 2013.

[19] T.-H. Kim, D.-H. Kim, and S. G. Lee, "Moxibustion therapy in traditional Mongolian medicine," *Chinese Journal of Integrative Medicine*, vol. 24, no. 9, pp. 707–712, 2018.

[20] T.-H. Kim, B. Luvsannaym, J.-I. Kim, J.-Y. Choi, and S.-M. Choi, "An introduction of febrile disease in Mongolian traditional medicine," *Journal of Acupuncture Research*, vol. 26, no. 4, pp. 91–98, 2009.

Hindawi
Evidence-Based Complementary and Alternative Medicine
Volume 2021, Article ID 8628182, 15 pages
https://doi.org/10.1155/2021/8628182

Research Article

Meta-Analysis of Elderly Lower Body Strength: Different Effects of Tai Chi Exercise on the Knee Joint-Related Muscle Groups

Yuan Yang,[1,2] **Jia-hui Li**,[1] **Nan-Jun Xu**,[1] **Wei-Yi Yang**,[1] **and Jun Liu**[1,2]

[1]*The Second Affiliated Hospital of Guangzhou University of Chinese Medicine, Guangzhou, China*
[2]*Bone and Joint Research Team of Degeneration and Injury, Guangdong Provincial Academy of Chinese Medical Sciences, Guangzhou, China*

Correspondence should be addressed to Wei-Yi Yang; czyangwy@163.com and Jun Liu; gjtb@gzucm.edu.cn

Received 20 August 2021; Accepted 9 November 2021; Published 22 December 2021

Academic Editor: Mozaniel De Oliveira

Importance. Tai Chi exercise mostly involves muscle fitness with biological, biomechanical, and psychosomatic medicine in elderly rehabilitation. Increased incidents related to elderly muscle fitness deficiency tend to be an urgent public health issue. However, there is a controversy on the effects of Tai Chi exercise on muscle fitness, especially the lower body strength of the elderly. *Objective*. To determine whether lower body strength such as keen extension and flexion strength may be improved by Tai Chi exercise in older adults from the perspective of evidence-based medicine. *Methods*. Databases of PubMed, Embase, and Cochrane Library were searched up to July 1, 2021. Randomized clinical trials are adopted to compare Tai Chi exercise with sedentary behavior or other low intensity exercise in terms of influence on lower body strength rehabilitation, especially keen extension and flexion strength in people aged over 60. A meta-analysis was performed to discuss outcomes of lower body strength, knee muscle strength, and knee extension/flexion strength. *Results*. A total of 25 randomized trials involving 1995 participants fulfilled the inclusion criteria. (1) Tai Chi exercise significantly improved elderly lower body strength (−0.54, [−0.81, −0.28], $p < 0.00001$, $I^2 = 74\%$), but there was no differential improvement in the strength of the knee joints (0.10, [−0.02, 0.23], $p = 0.11$, $I^2 = 34\%$). (2) Elderly individual lower body strength declined with age, while this trend was suppressed by Tai Chi exercise (−0.35, [0.14, 0.56], $p = 0.001$, $I^2 = 70\%$). (3) Although Tai Chi exercise did no significantly improve the large muscle group of knee joint extensor like quadriceps femoris (3.15, [−0.69, 6.99], $p = 0.24$, $I^2 = 26\%$), it showed marked enhancement to the strength of deep small muscle group of knee joint flexor (10.25, [6.90, 13.61], $p < 0.00001$, $I^2 = 0\%$). The heterogeneity might be caused by distinguished measurements of muscle strength. Therefore, Tai Chi exercise specifically enhanced some certain muscle strength of knee joints and improved muscle fitness rehabilitation as well as function activity for elderly. *Conclusions*. In this RCT meta-analysis, Tai Chi exercise has positive effects on lower body strength of elderly. Although no obvious improvement on the knee extensor is observed, it may be used as a rehabilitation treatment for training stable deep muscle groups to improve the knee flexion strength significantly.

1. Introduction

Tai Chi exercise is considered of high clinical value to rehabilitation of diseases. Combined with the latest research in bioinformatics and health informatics, it mostly involves the biological, biomechanical, and psychosomatic medicine in the elderly healthy research [1]. Classically, deficiency in lower muscle fitness in elderly individuals makes them vulnerable to muscle fatigue, mobility disorder, and physical injury [2]. However, whether Tai Chi can improve elderly muscular strength is still controversial. Experts hold distinguished attitudes towards the effects of Tai Chi exercise on lower body strength of the elderly. The argument focuses mainly on the following aspects: (1) Is it possible that the external force stimulation of Tai Chi actions causes changes of "functional adaptability" to bone tissue or muscular strength? (2) Is physiological mechanism of Tai Chi, compared with other physical activities, characteristically concentrated on its energy efficiency of local bone and lower body muscle tissue? (3) Do prescription factors such as the

duration or frequency of Tai Chi exercise affect the function on lower body muscle strength or not?

As a low-moderate intensity traditional exercise, Tai Chi is likely to prevent falls and enhance walking ability of elderly. A meta-analysis [3] shows persuasive evidence of improved exercise ability such as balance, movement, gait speed, and muscle fitness of elderly life. Zhou et al. [4, 5] believe that Tai Chi effectively postpones the decline of muscle strength caused by aging, and there was a significant improvement in lower body muscle strength for elder Tai Chi practitioners. Yang and Liu [6] collected 66 studies and found that Tai Chi may improve health fitness indicators of middle-aged and elderly people. Research of multiple sclerosis patients [7, 8] shows that Tai Chi has a positive regulatory effect on balance, coordination ability, walking ability, and muscle fitness. It also emphasizes that the improvement on lower body muscle strength by Tai Chi is related to the adjustment of knee joint strength and range of motion. Another meta-analysis [9] of 31 studies points out that Tai Chi improves muscle strength and reduce the risk of falls by enhancing the elderly's cardiopulmonary function, immune capacity, mental control, flexibility, and balance control.

However, other reports confirm that Tai Chi mainly improves muscle flexibility, dynamic balance, and joint stiffness rather than muscle strength or endurance [10, 11]. For example, the New Tai Chi Rehabilitation Program [12, 13] is shown to have no significant effect on the lower body strength of female elderly patients with knee osteoarthritis. Song et al. [14] also argue that there is no significant difference in knee joint strength of elderly women with osteoarthritis after 12 weeks of 12-form Sun style Tai Chi exercise. Since Tai Chi exercise relies heavily on horse stance or single leg, knee joints are in a state of weight bearing for a long time. Practitioners with insufficient lower body muscle strength are highly likely to suffer from severe strain in their own knee joints and lower limb muscles, which harms patients' rehabilitation [15].

In summary, the effect of Tai Chi exercise on the lower body strength is inconsistent in different research works. These conclusions cannot be supported or proved as systematic and medical evidence. Consequently, whether Tai Chi exercise can improve muscle strength in the elderly needs further research from the perspective of physical fitness. Here, we analyzed the related literature in recent years to explain the influence of Tai Chi on the lower body strength of the elderly, which may provide scientific guide and practical reference for health promotion.

2. Methods

Our meta-analysis was performed according to the Cochrane Handbook.

2.1. Search Trials. We searched the databases of PubMed, Embase, and Cochrane Library up to July 1, 2021. The keywords of "Tai Chi," "muscular strength," "keen extension," and "keen flexion" were used to identify published systematic reviews or meta-analyses evaluating the association between Tai Chi exercise and the change of lower body strength, keen extension, and flexion strength. Searching strategy for this meta-analysis is available in 3.1. The language was restricted to English, and the search was restricted to systematic reviews or meta-analyses published from January 1, 2000, to July 1, 2021. We identified original randomized clinical trials (RCTs) included in the systematic reviews or meta-analyses.

2.2. Inclusion Criteria. Inclusion criteria were as follows: (1) All studies were RCTs including keywords such as "random," "randomized," and "control." (2) Trials enrolled adults older than 60 years without limitation to their gender, race, or health condition. (3) Intervention measure of the experimental group is Tai Chi exercise without limitation to style, learning methods, or training sites. For the control group, the intervention measures were none, low intensity exercise, routine treatment, health education, routine exercise, etc. (4) Trials provided data of quadriceps femoris and other lower body muscles strength. (5) All articles are in English. *Exclusion criteria* were as follows: (1) randomized trials without a control group; (2) repeated publication literature; (3) ambiguous results or data and failure to contact the author; (4) unavailable full text; (5) reviews, animal experiments, conference abstracts, case reports, etc.

2.3. Risk of Bias Assessments. According to the Cochrane Collaboration Network, the bias in each trial was evaluated by 7 items as follows: the randomization sequence generation, allocation concealment, blinding of participants and personnel, blinding of outcome assessment, incomplete outcome data, selective reporting, and other bias. We defined other bias as trials of muscle strength measured by unauthorized methods and trials in which baseline characteristics were not similar between different intervention groups.

2.4. Data Extraction. Two researchers (Yuan Yang, Jia-hui Li) independently extracted the following information from each study: lead author; publication year; country of origin; participant characteristics; type, time, and intensity of Tai Chi exercise; interventions of control group; baseline of lower body strength; and trial duration. Disagreements were resolved by consensus. If the trials had more than 2 groups or factorial designs and permitted multiple comparisons, we extracted only the information and data of interest reported in the original articles. If a meta-analysis provided data that we did not retrieve, we extracted those fracture data from forest plots of the meta-analysis and reviewed original articles to confirm whether the trials met our inclusion criteria. When those data were our outcomes of interest, we pooled them with the data from primary trials.

The lower body strength of participants was the primary outcome because lower body strength might lead to more serious consequences than other elderly muscle strength. The secondary outcomes were the knee muscle strength,

keen extension, and flexion strength. Knee muscle strength was defined as total knee joints muscles when they occurred at all sites or when trials did not describe the types of muscles in detail. If a trial only reported the strength of participants with certain type of muscles, such as keen extension and flexion strength, we did not consider it to be knee muscle strength.

2.5. Statistical Analysis. In this study, RevMan 5.3 software (provided by Cochrane Collaboration Network) was used for data analysis. Mean ± SD were used to process the included data obtained by the same measurement method. Standard mean difference (SMD) and 95% confidence interval (95% CI) were used to process the data obtained by different methods of measurement or units. Estimates for HRs were weighted by ANOVA variance and computed by random effects modeling. Statistical heterogeneity was assessed using I^2 statistics. The appropriate effect model for the research indicators was selected, the combined effect statistics were analyzed, and then the forest plot was drawn. The risk of publication bias was assessed by the funnel plot.

Solutions to heterogeneity in this analysis process are as follows: firstly, checking the original data and confirming that the fixed effect model converts into a random effect model with high heterogeneity; then, removing the original data items one by one or excluding the lower quality literature for sensitivity analysis to find the possible source of heterogeneity; lastly, carrying out subgroup analysis according to different muscle strength measurement methods and different parts of muscle strength index.

3. Results

3.1. Retrieved Studies. As shown in Figure 1, 252 unrepeated articles were reviewed according to the searching strategy (*searching strategy: PubMed ["tai ji" OR "t'ai ji" OR "tai chi" OR "t'ai chi" OR "tai chi chuan" AND ("muscular strength" OR "muscular endurance" or "flexibility")] (142 articles)/ Embase [("tai ji"/exp OR "tai ji" OR "tai chi"/exp OR "tai chi" OR "tai chi chuan"*/exp *OR "tai chi chuan") AND ("muscular strength"/exp OR "muscular strength" OR "muscular endurance" OR "flexibility"/exp OR "flexibility") (172 articles)/ manual retrieval with the articles closely related]*). Titles and abstracts of these records were screened for inclusion, and 154 articles which had nothing to do with the outcomes of this study were excluded. Full texts of 98 records were read, and 64 articles were deleted. Among these articles, 19 did not have their data collected by persuasive test (30 s chair stand test/heel rise test/spring gauge test), 30 mostly mentioned grip strength or upper body strength, and 15 did not meet the age of >60. 10 of the remaining 35 readings were not analyzed with baseline or control data. Four articles have missing data (Day et al. [16] with incomplete data of quad strength and no significant difference between left and right knee, Guo et al. [17] with incomplete baseline data of quadriceps extensors and hamstring flexor, Wolf et al. [18] with no data of limited changes of lower body strength, and Zhang et al. [19] with incomplete data of lower body strength). 21 RCTs with complete data were included for further analysis from the final 25 trials.

3.2. Characteristics of Included Studies. The relevant characteristics of 25 articles were listed according to the publication time sequence, as shown in Table 1, including 4 articles that did not carry out meta-analyses but included systematic reviews. Most trials did not group the participants by sex, and only a few focused on older women [14, 20–22]. All the training programs of Tai Chi exercise were set at ≥20 min, ≥2 days/week, and ≥6 weeks, most of which were set at 60 min/day and 2–4 days/week. In addition, the control group did sedentary or other low intensity exercise such as stretching and walking. Three methods (30 s chair stand test, spring gauge test, and isokinetic dynamometer test) were mentioned to detect muscle strength, which might be one of the factors evaluating the outcome indicators.

3.3. Outcomes of Literature Quality Assessment. Figure 2 shows the assessment of the risk of bias. All studies were randomized. In addition, since this study mainly discussed the intervention effect of Tai Chi, which is a relatively popular traditional exercise in China, among the documents included in this searching, there are 12 trials from China. We have sorted out the main information for reference in Table 1. According to the risk assessment shown in Section 2.3, literature quality of these trials was evaluated and divided into three levels: "low risk," "unclear," and "high risk." As shown in Figure 2, 20 trials described an adequate random sequence generation process, while other literature (Kasim et al. [23], Day et al. [16], Li et al. [5], Huang and Lin [24]) did not specify the random allocation method. As the intervention approach was Tai Chi exercise, it was difficult to achieve double-blind trials, so the risk bias of the whole assessment was high. While 17 trials described the methods used for allocation concealment, 5 trials (Audette et al. [22], Choi et al. [25], Guo et al. [17], Buto and Li [3], song et al. [14]) had incomplete outcome indicators with missing data of baseline testing or postintervention testing. In addition, there are unspecific descriptions of the withdrawal and missing visits in the trials (Day et al. [16], Woo et al. [26], Wolf et al. [18], Guo et al. [17], Li et al. [5], Song et al. [14], Xu et al. [20], Yip et al. [27]). To sum up, 4 trials (Day et al. [16], Wolf et al. [18], Xu et al. [20], Yip et al. [27]) were of low quality, 6 trials (Liu et al. [28], Song et al. [21], Sungkarat et al. [29], Taylor et al. [30], Woo et al. [26], Zhuang et al. [31]) were of high quality, and the others were of moderate quality.

3.4. Tai Chi Exercise and Lower Body Strength Risk

3.4.1. Analysis of the Effects before and after Tai Chi Exercise on Lower Body Strength. Excluding 5 trials without baseline data and 5 with incomplete data about the effect after Tai Chi exercise, we analyzed a total of 14 distinguished studies to compare the effect before and after Tai Chi exercise on lower

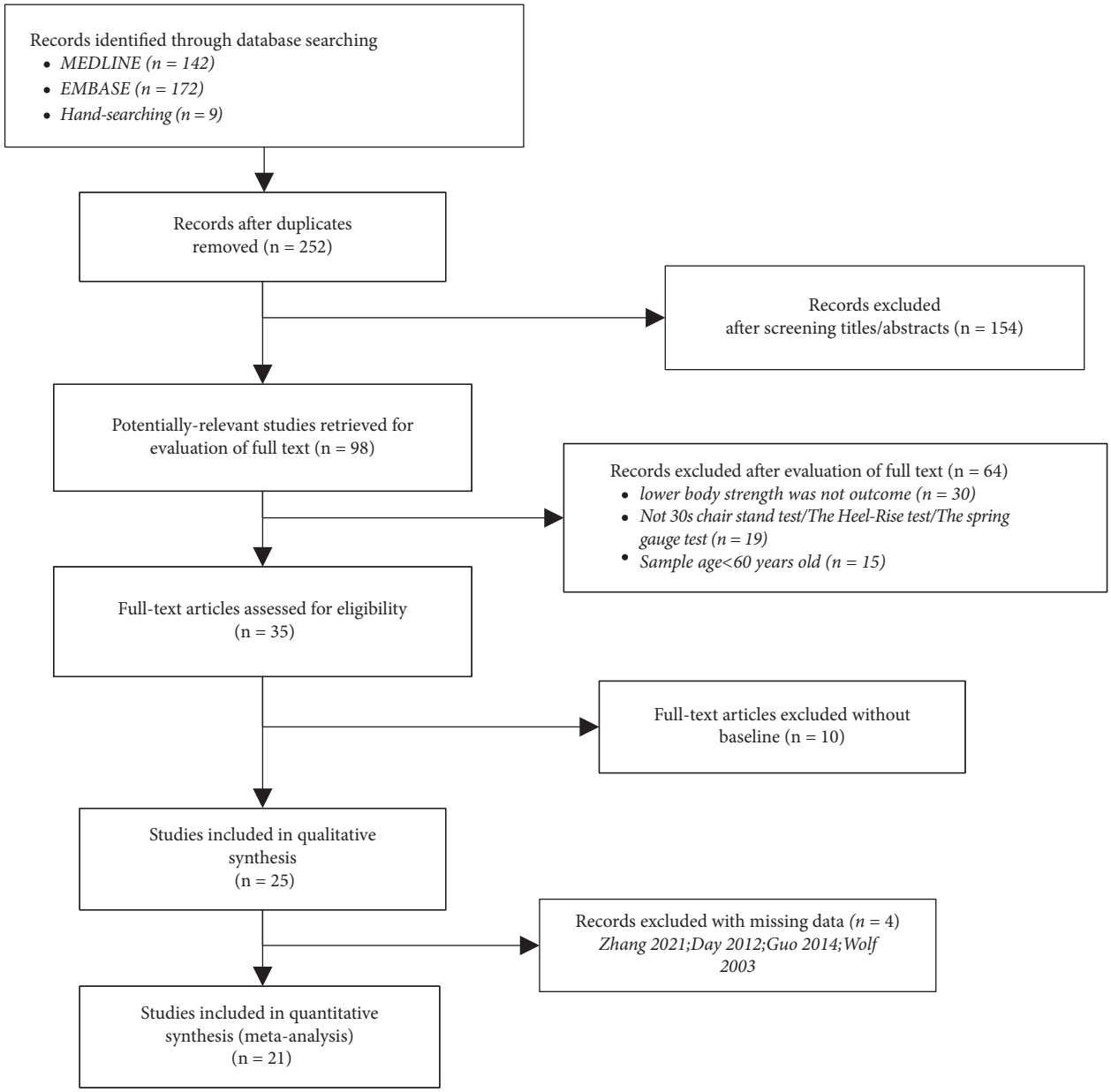

Figure 1: Study flow diagram of Tai Chi intervention on elderly muscular strength.

body strength. There was statistically significant improvement in lower body strength after Tai Chi exercise with high heterogeneity by a fixed effect model. Random effect model was then adopted for analysis, and there was still highly heterogeneity in this sequence (−0.54, 95% CI [−0.81, −0.28], $p < 0.00001$, $I^2 = 74\%$) in Figure 3(a). Sensitivity analysis and subgroup analysis were then used to evaluate the following:

(1) The method of sequential exclusion from the analysis was used to evaluate whether it had an impact on the heterogeneity and outcome index. As shown in Table 2, after removing each trial in turn, the heterogeneity was still large ($p < 0.001$, $I^2 > 60\%$), which suggested that the source was not from one certain trial. (2) Three papers which may have publication bias were excluded (Liu et al. [28], Song et al. [32], Zhang et al. [19]) after being checked by funnel plot analysis as indicated in Figure 3(b). It was shown in Appendix S1 that the heterogeneity was decreased significantly ($p = 0.85$, $I^2 = 0\%$). However, 2 papers (Liu et al. [28], Zhang et al. [19]) were evaluated with high quality, which might arouse doubts about the weight of publication bias. (3) As distinguished methods might contribute to the factor of great heterogeneity in Figure 3(a), subgroup analysis was carried out according to the methods of common 30 s chair stand test and other tests. After checking the 14 included trials, 8 studies were using the 30 s chair stand test method. As shown in Figures 4(a) and 4(b), based on the random effect model analysis, the trend was consistent with Figure 3(a), while it was suggested that the use of different methods ($I^2 = 81\%$, $p = 0.01$; $I^2 = 77\%$, $p = 0.003$) was supposed to be one of the reasons for the great heterogeneity.

To sum up, there was a significant difference in lower body strength before and after Tai Chi exercise, especially in

Table 1: Study characteristics of the 25 included RCTs.

Study	Objects, y	Num. (pre/post)		Training program		Control	Assessment methods	Outcomes
		Tai Chi	Control	Intervention	Frequency			
Zhang et al. [19]	Elderly, ≥60	18	18	Tai Chi	16 w	—	—	Knee flexion/extension
Kasim et al. [23]	Elderly, 65~75	11	10	Tai Chi	60 min/time, 3 times/w, 12 w	Zumba Gold	30 s chair stand test	Lower body strength
Adcock et al. [39]	Elderly, ≥65	18/15	19/16	Home training including Tai Chi-inspired exercises	30–40 min/time, 3 times/w, 16 w	—	30 s chair stand test	Lower body strength
Sungkarat et al. [29]	Amnestic mild cognitive impairment, ≥60	33	33	Tai Chi	50 min/time, 3 times/w, 15 w	—	Spring gauge test	Knee extension strength
Takeshima et al. [40]	Elderly, 67–79	35	34	Tai Chi	60 min/day, 2 days/week, 12 w	—	30 s chair stand test	Lower body strength
Noradechanunt et al. [41]	Elderly, ≥60	13	13	Tai Chi	90 min/time, 2 times/w, 12 w	—	30 s chair stand test	Lower body strength
Huang and Lin [24]	Elderly	48	47	Tai Chi	—	—	30 s chair stand test/manual muscle tester	Lower body strength/keen extension strength
Xu et al. [20]	Obese elderly women, ≥60	29	9	Tai Chi plus a behavioral weight loss program	45 min/day, 2 days/week, 16 w	—	Manual muscle dynamometer	Knee extensor torque
Guo et al. [17]	Elderly	16	9	Tai Chi	—	—	Isokinetic dynamometer test	Knee flexion/extension
Song et al. [32]	Elderly women	31	30	Tai Chi	40 min/day, 6 days/week, 12 m	Walking	Isokinetic dynamometer test	Knee extension strength
Zhuang et al. [31]	Elderly, 60–80	22	28	Combined exercise including 8-form Yang style Tai Chi	60 min/day, 3 days/week, 16 w	—	30 s chair stand test/isokinetic dynamometer test	Knee flexor extensors
Day et al. [16]	Preclinically disabled elderly, ≥70	171	190	Modified Sun style Tai Chi	60 min/day, 2 days/week, 24 w	—	30 s chair stand test/spring gauge test	Lower body strength/quad strength
Day et al. [16]	Parkinson elderly	65	65	Tai Chi	60 min/day, 2 days/week, 24 w	Stretching	Isokinetic dynamometer test	Knee extensors and flexors
Liu et al. [28]	Elderly, 60–85	15	17	Tai Chi	45 min/day, 2 days/week, 16 w	—	Biodex System 3 dynamometer	Plantar flexion and dorsiflexion
Taylor et al. [30]	Community residing elderly	220	231	Modified 10-form Sun style Tai Chi	60 min/day, 2 days/week, 20 w	Low-level exercise	30 s chair stand test	Lower limb strength
Song et al. [21]	OA elderly women	30	35	Tai Chi	55–65 min/w with instructors, 20 min/day/w by self, 6 m	—	Isokinetic dynamometer test	Knee flexor/extensor
Li et al. [5]	Community-based elderly, ≥60	22	18	24-form Tai Chi	60 min/time, 4 times/w, 6 w; 60 min/day/w, 10 w	—	Isokinetic dynamometer test	Knee flexion/extension

Table 1: Continued.

Study	Objects, y	Num. (pre/post)		Training program		Control	Assessment methods	Outcomes
		Tai Chi	Control	Intervention	Frequency			
Frye et al. [42]	Elderly	31/23	23/21	Tai Chi	60 min/time, 3 times/w, 12 w	—	30 s chair stand test	Lower body strength
Buto et al. [3]	Community-dwelling seniors	11	9	24-form Yang style Tai Chi	60 min/time, 1 time/w, 12 m	—	Heel rise test	Lower limbs strength
Woo et al. [26]	Community-based Elderly, 65–74	30	30/29	Yang style with 24 forms of Tai Chi (TC)	3 times/w, 12 m		A quadriceps device	Strength of quadriceps
Audette et al. [22]	Elderly women, ≥65	11	8	Tai Chi	60 min/time, 3 times/w, 12 w	Brisk walking	A BTE work simulator	Knee extensor strength
Choi et al. [25]	Fall-prone elderly	29	30	12 forms of Sun style Tai Chi	35 min/time, 3 times/w, 12 w	—	Manual muscle tester	Knees extension and flexion
Yip et al. [27]	Osteoarthritis elderly	21	16	Arthritis self-management program including Tai Chi	120 min/time, 6 times/w, 16 w	—	A score of "5" assessment	Hamstring strength/ quadriceps strength
Song et al. [14]	OA elderly women	22	21	12 forms of Sun style Tai Chi	20 min/time, ≥3 times/w, 12 w	—	Isokinetic dynamometer teat	Knee muscle strength
Wolf et al. [18]	Community-based elderly	72	64	Tai Chi and balance training	15 w	—	Nicholas MMT 0116 muscle tester	Hip, knee, or ankle strength

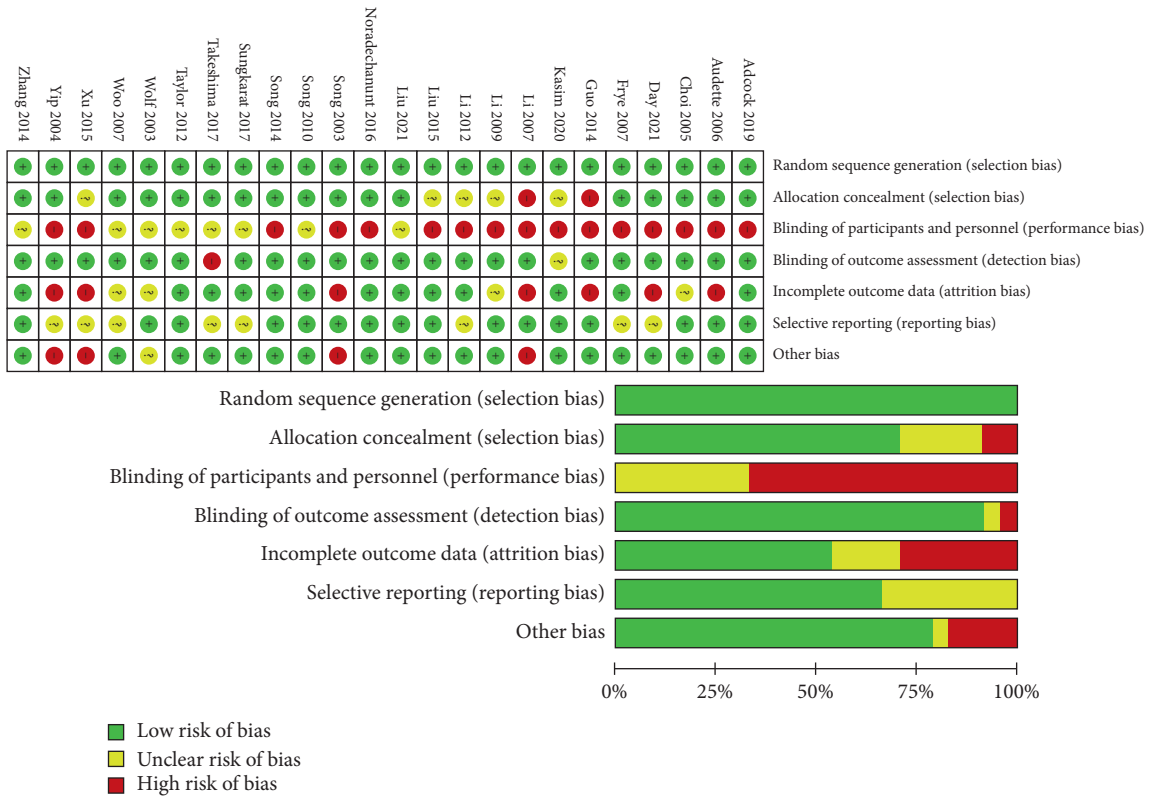

Figure 2: Risk of bias graph. We reviewed authors' judgements about each risk of bias item presented as percentages across all included studies. We defined other bias as trials of muscle strength measured by unauthorized methods and trials in which baseline characteristics were not similar between different intervention groups.

Study or Subgroup	Pre–Taichi exercise			Post–Taichi exercise			Weight (%)	Std. Mean Difference	Std. Mean Difference
	Mean	SD	Total	Mean	SD	Total		IV, Random, 95% CI	IV, Random, 95% CI
Adcock 2019	13.9075	3.6805	15	13.9075	2.0447	15	6.1	0.00 [−0.72, 0.72]	
Frye 2007	12.4	3.93	31	13.8	4.47	23	7.5	−0.33 [−0.87, 0.21]	
Kasim 2020	13.5	2.8	11	15.9	4.4	11	5.1	−0.63 [−1.49, 0.23]	
Li 2007	68	35	11	63	33	11	5.3	0.1 4 [−0.70, 0.98]	
Li 2012	47.2	29.8007	65	56.7	35.9394	65	9.2	−0.29 [−0.63, 0.06]	
Lin 2015	18.2	3.9	48	19.7	4.3	48	8.7	−0.36 [−0.77, 0.04]	
Liu 2012	49.48	6.8626	15	60.34	7.2075	15	5.4	−1.50 [−2.33, −0.68]	
Noradechanunt 2016	14.6	3.5	13	15.7	2.1	13	5.7	−0.37 [−1.15, 0.41]	
Song 2010	171.3	72.9501	30	181	75.4589	30	7.8	−0.13 [−0.64, 0.38]	
Song 2014	179.35	29.01	31	225.79	27.92	31	7.2	−1.61 [−2.19, −1.03]	
Sungkaral 2017	26.7	5.9	33	30.3	6	33	7.9	−0.60 [−1.09, −0.10]	
Takeshima 2017	32.4	4.6	25	32.5	4.7	25	7.4	−0.02 [−0.58, 0.53]	
Taylor 2012	11	3.5	220	12.3	3.7	220	10.3	−0.36 [−0.55, −0.17]	
Zhuang 2014	17.52	4.71	28	27.16	5.08	22	6.3	−1.95 [−2.63, −1.26]	
Total (95% CI)			*576*			*562*	*100.0*	*−0.54 [−0.81, −0.28]*	

Heterogeneity: tau^2 = 0.17; chi^2 = 50.00, *df* = 13 (*P* < 0.00001); I^2 = 74%

Test for overall effect: *Z* = 3.99 (*P* < 0.0001)

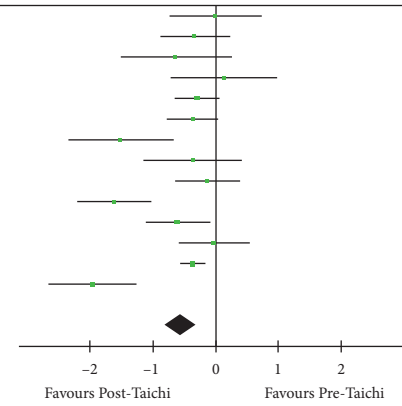

(a)

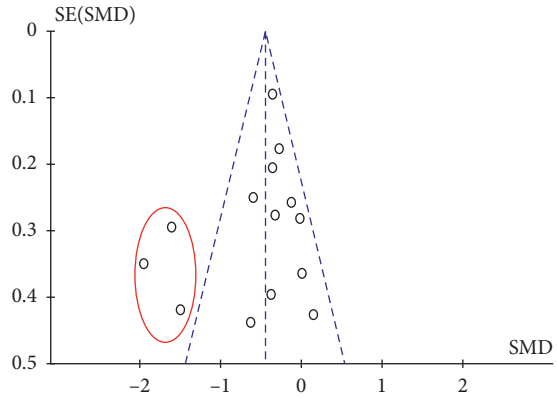

(b)

Study or Subgroup	Taichi			Control			Weight (%)	Std. Mean Difference	Std. Mean Difference
	Mean	SD	Total	Mean	SD	Total		IV, Random, 95% CI	IV, Random, 95% CI
Adcock 2019	0	4.2103	15	−1.181	6.8968	16	4.2	0.20 [−0.51 , 0.91]	
Audette 2006	8.17	8.0619	11	2.95	9.5825	8	3.1	0.57 [−0.36, 1.51]	
Choi 2005	5.35	3.24	29	2.09	4.71	30	5.4	0.79 [0.26, 1.32]	
Frye 2007	1.4	5.6073	23	0.6	4.7975	21	4.9	0.15 [−0.44, 0.74]	
Kasim 2020	2.4	5.2154	11	3.1	7.2862	10	3.5	−0.11 [−0.96, 0.75]	
Li 2007	−5	48.104	11	−13	67.683	9	3.3	0.13 [−0. 75, 1.02]	
Li 2009	10.665	13.7764	22	6.94	14.4898	18	4.7	0.26 [−0.37, 0.88]	
Li 2012	9.5	46.6877	65	−1.05	44.3061	65	6.7	0.23 [−0.11, 0.58]	
Lin 2015	1.5	5.8051	48	0.8	7.2862	47	6.3	0.11 [−0.30, 0.51]	
Liu 2012	10.86	9.952	15	−2.34	5.1452	17	3.6	1.66 [0.84, 2.47]	
Noradechanunt 2016	1.1	4.0818	13	0.3	5.8727	13	3.9	0.15 [−0.62, 0.92]	
Song 2003	6.75	8.9	22	4.25	6.6	21	4.9	0.31 [−0.29, 0.91]	
Song 2010	9.7	104.9562	30	3.15	99.4114	35	5.7	0.06 [−0.42, 0.55]	
Song 2014	46.44	40.2627	31	26.61	82.3282	30	5.5	0.30 [−0.20, 0.81]	
Sungkarat 2017	3.6	8.4146	33	1.3	7.7465	33	5.7	0.28 [−0.20, 0. 77]	
Takeshima 2017	0.1	7.7814	35	0.5	9.2578	34	5.8	−0.05 [−0.52, 0.43]	
Taylor 2012	1.3	5.0934	220	1.3	5.163	231	7.7	0.00 [−0.18, 0.18]	
Woo 2007	1.6428	4.1755	58	2.0792	0.8035	59	6.6	−0.14 [−0.51, 0.22]	
Yip 2004	1.24	1.2587	21	0.125	1.0361	16	4.4	0.93 [0.25, 1.62]	
Zhuang 2014	9.64	5.0802	22	−0.05	3.54	28	4.2	2.23 [1.51, 2.95]	
Total (95% CI)			*735*			*741*	*100.0*	*0.35 [0.14, 0.56]*	

Heterogeneity: tau^2 = 0.14; chi^2 = 62.92, *df* = 19 (*P* < 0.00001); I^2 = 70%

Test for overall effect: *Z* = 3.27 (*P* = 0.001)

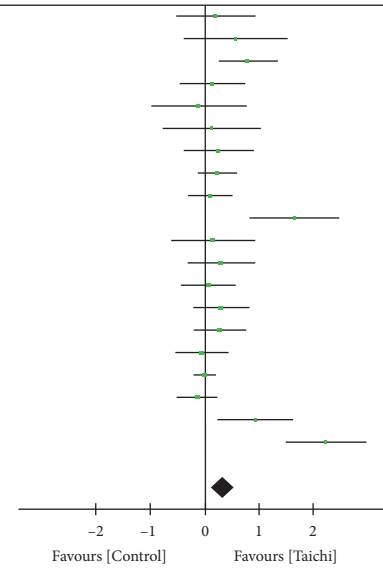

(c)

Figure 3: Continued.

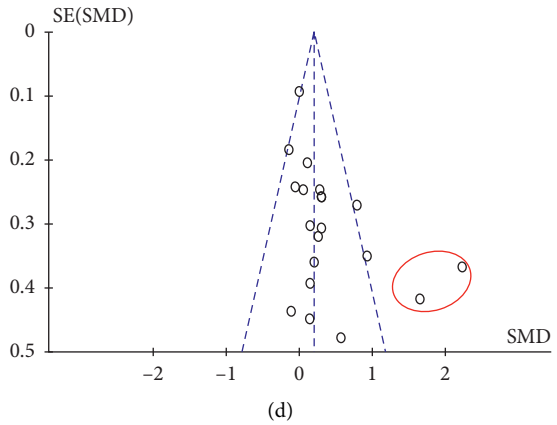

(d)

Figure 3: Forest plot of total data comparison. (a) Outcome of lower body strength before and after Tai Chi exercise. (b) Funnel plot of lower body strength before and after Tai Chi exercise. (c) Outcome of lower body strength in Tai Chi and control groups. (d) Funnel plot of lower body strength in Tai Chi and control groups.

Table 2: Sensitivity analysis of lower body strength before and after Tai Chi exercise.

Study excluded	SMD	95% CI	I^2 (%)	p (heterogeneity)
Adcock et al., 2019	−0.58	−0.86, −0.30	75	<0.00001
Frye et al., 2007	−0.56	−0.85, −0.28	76	<0.00001
Kasim et al., 2020	−0.54	−0.82, −0.26	76	<0.00001
Buto et al., 2007	−0.58	−0.86, −0.31	75	<0.00001
Li et al., 2012	−0.57	−0.87, −0.28	76	<0.00001
Huang and Lin, 2015	−0.56	−0.86, −0.27	76	<0.00001
Liu et al., 2012	−0.49	−0.75, −0.23	72	<0.0001
Noradechanunt et al., 2016	−0.56	−0.84, −0.28	76	<0.00001
Song et al., 2010	−0.58	−0.87, −0.30	75	<0.00001
Song et al., 2014	−0.45	−0.69, −0.21	64	0.0008
Sungkarat et al., 2017	−0.54	−0.83, −0.25	76	<0.00001
Takeshima et al., 2017	−0.59	−0.87, −0.31	75	<0.00001
Taylor et al., 2012	−0.57	−0.90, −0.25	75	<0.00001
Zhuang et al., 2014	−0.67, −0.22	−0.67, −0.22	61	0.002

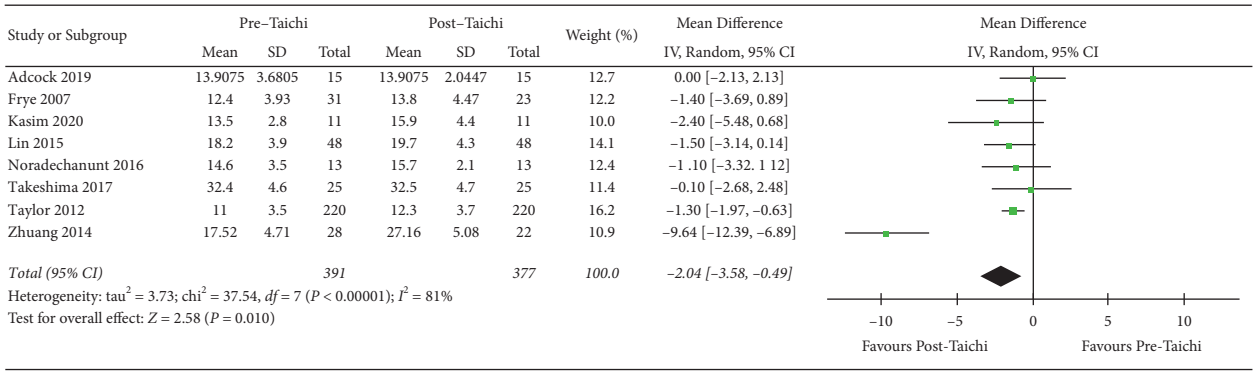

(a)

Figure 4: Continued.

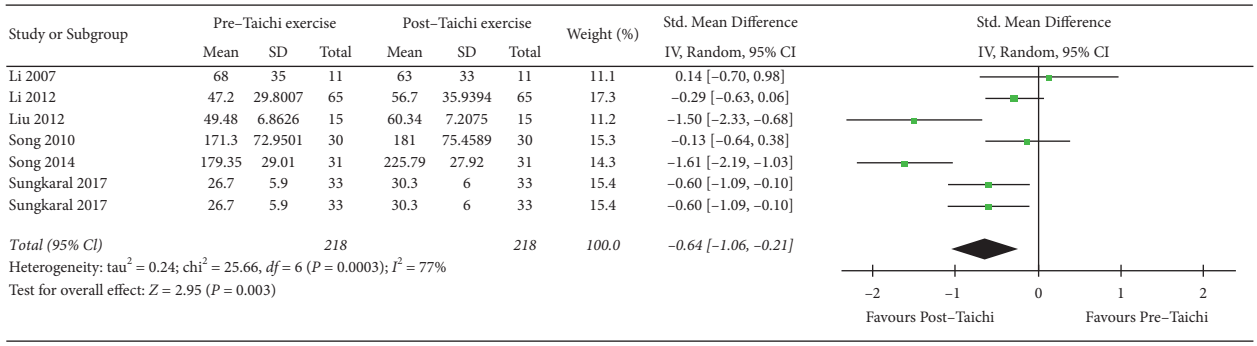

(b)

Figure 4: Forest plot of comparison. Subgroup outcome of forest plot in Figure 3(a). (a) 30 s chair stand test method. (b) Other test methods.

the research of Liu et al. [28], Song et al. [32], and Zhang et al. [19]. Even though there was great heterogeneity among these 14 trials, mainly caused by publication bias analysis and subgroup analysis, the same results were obtained. Namely, Tai Chi exercise clearly increases the lower body strength of the elderly.

3.4.2. Analysis of the Comparison of Tai Chi Exercise Group and Control Group in Enhancing Lower Body Strength. Excluding 4 studies with incomplete data, we included a total of 20 articles in the meta-analysis. As shown in Figure 3(c), there was a statistically significant difference in lower body strength between Tai Chi exercise and control group (SMD = −0.35, 95% CI [0.14, 0.56], $p = 0.001$). Random effect model was adopted for analysis, and there was great heterogeneity in this sequence ($p < 0.00001$, $I^2 = 70\%$). Sensitivity analysis and subgroup analysis were also used to evaluate the potential sources of heterogeneity and the stability of the results: (1) The method of sequential exclusion from the analysis was used to evaluate whether it had an impact on the heterogeneity and outcome index. As shown in Table 3, after removing each trial, the heterogeneity was decreased ($p = 0.02$, $I^2 = 44\%$), which suggested that the trial of Zhuang et al. [31] was probably one factor of high heterogeneity from the analysis. (2) As is seen in Figure 3(d), besides the trial of Zhuang et al. [31], we excluded the other trial that might also have publication bias (Liu et al. [28]). Heterogeneity decreased significantly ($p = 0.34$, $I^2 = 10\%$) in Appendix S2, which suggested that the source of the greater heterogeneity in Figure 3(c) might be related to the publication bias. However, these 2 trials were evaluated with high quality, which revealed that Tai Chi exercise, compared to sedentary or low intensity exercise, indeed increased the lower body strength of the elderly. Therefore, the results of this study are relatively stable. (3) Subgroup analysis was carried out according to the methods of common 30 s chair stand test and other tests. A total of 8 articles with the 30 s chair stand test method and 12 articles with other test methods are included in Figures 5(a) and 5(b). The trend of the first subgroup ($p = 0.22$) was inconsistent with the trend in Figure 3(c). It was suggested that 30 s chair stand test method ($p < 0.00001$, $I^2 = 86\%$) was more likely related to the great heterogeneity in this analysis.

To sum up, there was a significant difference in lower body strength with Tai Chi exercise, especially in the research of Zhuang et al. [31] and Liu et al. [28] which contributed vital weight but high heterogeneity to the conclusion. It revealed that the significant effects of Tai Chi exercise compared with control group should be reconsidered with high heterogeneity by containing measurements such as 30 s chair stand test.

3.5. Tai Chi Exercise and Knee Muscle Strength Risk

3.5.1. Analysis of Tai Chi Exercise/Control Group in Knee Muscle Strength. As the effect of Tai Chi is different on different joint muscles, the results of high heterogeneity should be discussed in terms of subgroup analysis of mainly functioning muscle groups. A total of 13 studies were included in the subgroup analysis between Tai Chi exercise and control group in knee muscle strength in Figure 6(a). It was suggested that the knee muscle strength of elderly individuals with Tai Chi exercise is significantly higher than that of the control group ($p = 0.0008$). Meanwhile, there was great heterogeneity ($p < 0.00001$, $I^2 = 76\%$) in this analysis, which was probably caused by the difference in sample size, measurement, and publication bias. We excluded 1 trial which had obvious publication bias (Zhuang et al. [31]) according to funnel plot analysis in Appendix S3 and showed no significant improvement to knee strength in Tai Chi exercise group compared with control group (0.10, [−0.02, 0.23], $p = 0.11$). The decreased heterogeneity ($p = 0.11$, $I^2 = 34\%$) indicated that the source of greater heterogeneity might be related to different outcomes of muscle groups. While Choi et al. [25], Yip et al. [27], and Zhuang et al. [31] pointed out that Tai Chi exercise evidently improved knee muscle strength compared with the control group, other included studies proved that there was no statistical difference. To sum up, Tai Chi exercise showed no significant improvement on knee muscle strength after decreasing the high heterogeneity.

Table 3: Sensitivity analysis of lower body strength between Tai Chi exercise and control group.

Study excluded	SMD	95% CI	I^2 (%)	p (heterogeneity)
Adcock et al., 2019	0.36	0.14, 0.58	71	<0.00001
Audette et al., 2006	0.34	0.13, 0.56	71	<0.00001
Choi et al., 2005	0.32	0.11, 0.54	69	<0.00001
Frye et al., 2007	0.36	0.14, 0.58	71	<0.00001
Kasim et al., 2020	0.37	0.15, 0.58	71	<0.00001
Buto et al., 2007	0.36	0.14, 0.58	71	<0.00001
Li et al., 2009	0.36	0.14, 0.58	71	<0.00001
Li et al., 2012	0.36	0.14, 0.59	71	<0.00001
Huang and Lin, 2015	0.37	0.15, 0.60	71	<0.00001
Liu et al., 2012	0.29	0.10, 0.49	64	<0.0001
Noradechanunt et al., 2016	0.36	0.14, 0.58	71	<0.00001
Song et al., 2003	0.35	0.13, 0.57	71	<0.00001
Song et al., 2010	0.37	0.15, 0.59	71	<0.00001
Song et al., 2014	0.36	0.13, 0.58	71	<0.00001
Sungkarat et al., 2017	0.36	0.14, 0.58	71	<0.00001
Takeshima et al., 2017	0.38	0.16, 0.60	71	<0.00001
Taylor et al., 2012	0.38	0.15, 0.62	68	<0.00001
Woo et al., 2007	0.39	0.17, 0.61	70	<0.00001
Yip et al., 2004	0.32	0.11, 0.53	69	<0.00001
Zhuang et al., 2014	0.24	0.08, 0.39	44	0.02

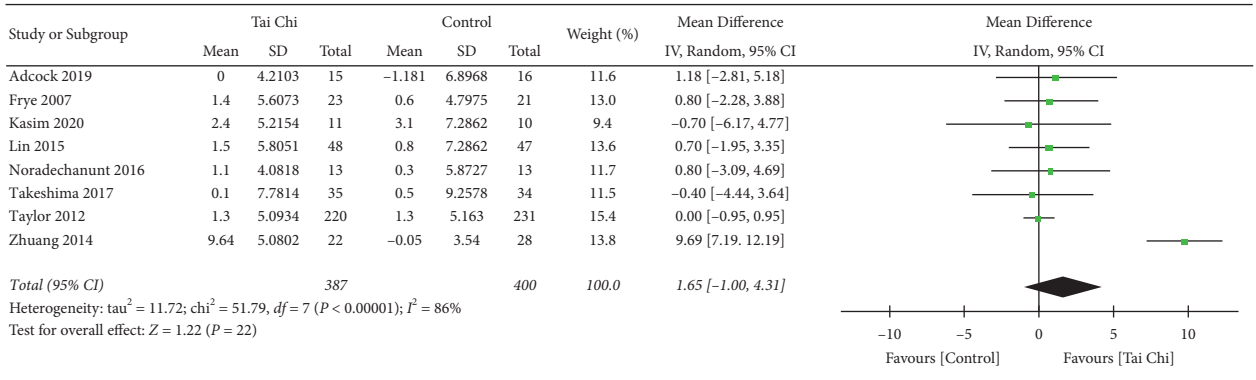

(a)

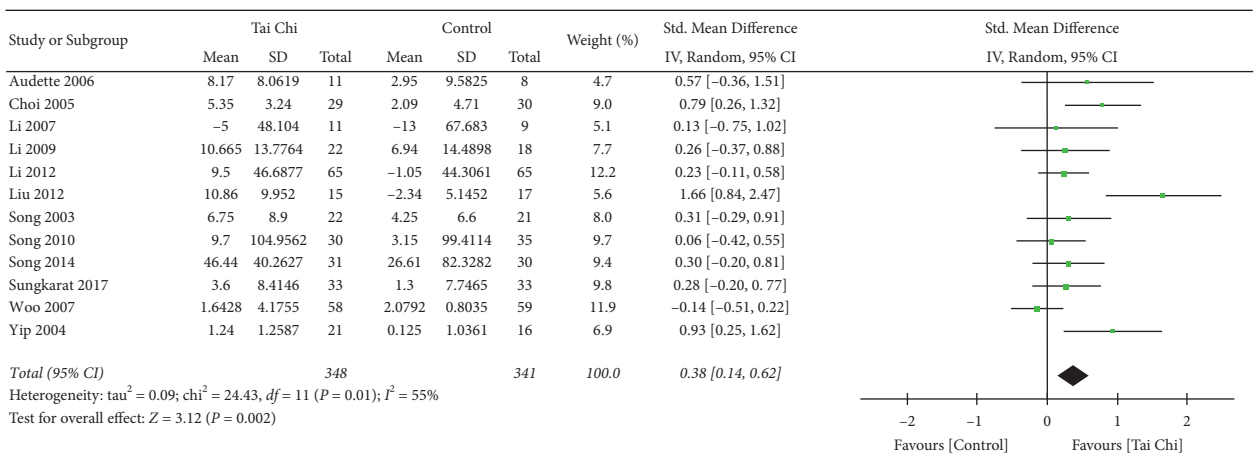

(b)

Figure 5: Forest plot of comparison. Subgroup outcome of forest plot in Figure 3(c). (a) 30 s chair stand test method. (b) Other test methods.

Study or Subgroup	Tai Chi Mean	Tai Chi SD	Tai Chi Total	Control Mean	Control SD	Control Total	Weight (%)	Std. Mean Difference IV, Fixed, 95% CI
Adcock 2019	0	4.2103	15	−1.181	6.8968	16	2.9	0.20 [−0.51 , 0.91]
Choi 2005	5.35	3.24	29	2.09	4.71	30	5.1	0.79 [0.26, 1.32]
Frye 2007	1.4	5.6073	23	0.6	4.7975	21	4.1	0.15 [−0.44, 0.74]
Kasim 2020	2.4	5.2154	11	3.1	7.2862	10	1.9	−0.11 [−0.96, 0.75]
Lin 2015	1.5	5.8051	48	0.8	7.2862	47	8.8	0.11 [−0.30, 0.51]
Noradechanunt 2016	1.1	4.0818	13	0.3	5.8727	13	2.4	0.15 [−0.62, 0.92]
Song 2003	6.75	8.9	22	4.25	6.6	21	3.9	0.31 [−0.29, 0.91]
Sungkarat 2017	3.6	8.4146	33	1.3	7.7465	33	6.1	0.28 [−0.20, 0. 77]
Takeshima 2017	0.1	7.7814	35	0.5	9.2578	34	6.4	−0.05 [−0.52, 0.43]
Taylor 2012	1.3	5.0934	220	1.3	5.163	231	41.9	0.00 [−0.18, 0.18]
Woo 2007	1.6428	4.1755	58	2.0792	0.8035	59	10.8	−0.14 [−0.51, 0.22]
Yip 2004	1.24	1.2587	21	0.125	1.0361	16	3.0	0.93 [0.25, 1.62]
Zhuang 2014	9.64	5.0802	22	−0.05	3.54	28	2.8	2.23 [1.51, 2.95]
Total (95% CI)			*550*			*559*	*100.0*	*0.16 [0.04, 0.28]*

Heterogeneity: chi^2 = 49.22, df = 12 (P < 0.00001); I^2 = 76%
Test for overall effect: Z = 2.67 (P = 0.008)

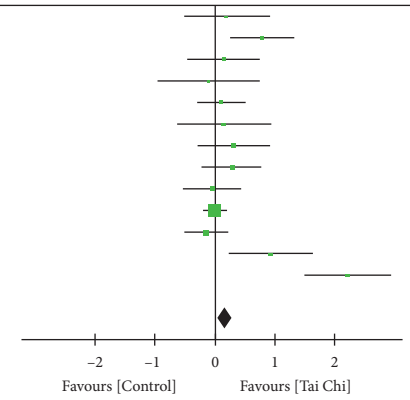

(a)

Study or Subgroup	Tai Chi Mean	Tai Chi SD	Tai Chi Total	Control Mean	Control SD	Control Total	Weight (%)	Mean Difference IV, Random, 95% CI
Choi 2005	5.35	3.24	29	2.09	4.71	30	24.5	3.26 [1.20, 5.32]
Lin 2015	1.25	7.8164	48	−1.8	8.233	47	18.3	3.05 [−0.18, 6.28]
Song 2003	6.75	8.9	22	4.25	6.6	21	12.4	2.50 [−2.17, 7.17]
Sungkarat 2017	3.6	8.4146	33	1.3	7.7465	33	15.2	2.30 [−1.60, 6.20]
Woo 2007	1.6428	4.1755	58	2.0792	0.8035	59	29.5	−0.44 [−1.53, 0.66]
Total (95% CI)			*190*			*190*	*100.0*	*1.89 [−0.21, 3.99]*

Heterogeneity: tau^2 = 3.58; chi^2 = 13.33, df = 4 (P = 0.010); I^2 = 70%
Test for overall effect: Z = 1.76 (P = 0.08)

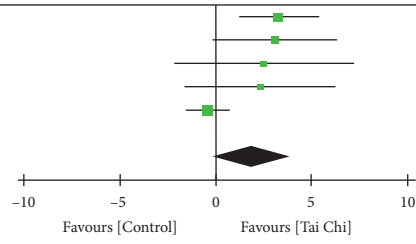

(b)

Study or Subgroup	Tai Chi Mean	Tai Chi SD	Tai Chi Total	Control Mean	Control SD	Control Total	Weight (%)	Std. Mean Difference IV, Random, 95% CI
Audette 2006	8.17	8.0619	11	2.95	9.5825	8	16.1	5.22 [−2.95, 13.39]
Li 2009	6.21	13.92	22	6.76	16.92	18	12.3	−0.58 [−10.32, 9.16]
Li 2012	13.9	49.8989	65	0.5	48.4501	65	4.8	13.40 [−3.51' 30.31]
Song 2010	10.	92.7935	30	−0.7	78.869	35	0.8	10.70 [−31.55, 52.95]
Yip 2004	1.24	1.2522	21	0.19	1.0697	16	58.0	1.05 [0.30, 1.80]
Zhuang 2014	11.88	23.4741	22	−1.13	21.2988	28	8.1	13.01 [0.42, 25.60]
Total (95% CI)			*171*			*170*	*100.0*	*3.15 [−0.69, 6.99]*

Heterogeneity: tau^2 = 6.49; chi^2 = 6.76, df = 5 (P = 0.24); I^2 = 26%
Test for overall effect: Z = 1.61 (P = 0.11)

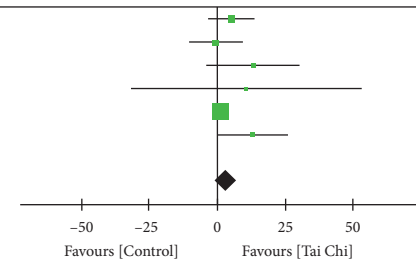

Study or Subgroup	Tai Chi Mean	Tai Chi SD	Tai Chi Total	Control Mean	Control SD	Control Total	Weight (%)	Std. Mean Difference IV, Random, 95% CI
Li 2009	15.12	12.38	22	7.09	12.08	18	17.1	8.03 [0.42, 15.64[]
Li 2012	5.1	27.1529	65	−2.6	25.6702	65	15.2	7.70 [−1.38, 16.78]
Liu 2012	10.86	9.952	15	−2.34	5.1452	17	19.7	13.20 [7.60, 18.80]
Song 2010	9.4	53.7557	30	7	39.1644	35	5.0	2.40 [−20.80, 25.60]
Yip 2004	1.24	1.22961	21	0.06	1.0322	16	24.1	1.19 [0.45, 1.91]
Zhuang 2014	8.74	10.5609	22	−1.12	11.8794	28	18.9	9.86 [3.63, 16.09]
Total (95% CI)			*175*			*179*	*100.0*	*7.42 [1.62, 13.21]*

Heterogeneity: tau^2 = 36.16; chi^2 = 28.99, df = 5 (P < 0.0001); I^2 = 83%
Test for overall effect: Z = 2.51 (P = 0.01)

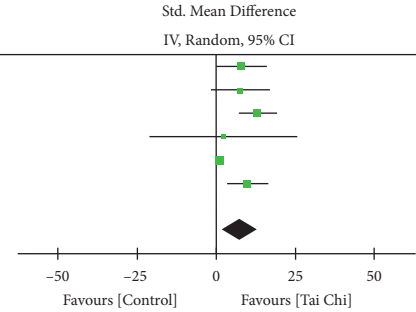

(c)

Figure 6: Forest plot of comparison. Outcome of Tai Chi and control knee strength. (a) Outcome of Tai Chi and control knee strength. (b) Knee strength with spring gauge test. (c) Knee extension/flexion strength with isokinetic dynamometer test.

3.5.2. Subgroup Analysis of the Effects of Tai Chi Exercise on Lower Body Muscle Strength by Various Test Methods

(1) Spring Gauge Test. The spring gauge test is used to assess the maximum strength to complete resistance to evaluate the effect of exercise on overall knee muscle strength. 5 articles with this method were included in the subgroup analysis with greater heterogeneity ($p = 0.08$, $I^2 = 70\%$) in Figure 6(b). This indicates that data obtained by this method may be one of the reasons for the great heterogeneity of Figure 6(a). However, after removing the data obtained by this method, the results still showed high heterogeneity ($p = 0.02$, $I^2 = 78\%$), and regression analysis was needed. It also revealed that the main reason for the large heterogeneity in Figure 6(a) is the publication bias mentioned rather than different detection methods. To sum up, measuring knee strength by spring gauge test may generate heterogeneity in outcomes, which indicates that Tai Chi has no significant improvement on knee joint muscle strength.

(2) The Isokinetic Dynamometer. The isokinetic dynamometer test is mainly used to measure the effects of exercise on knee flexion and extension strength. The analysis of knee extension strength and knee flexion strength in Figure 6(c) is shown as follows: according to the subgroup analysis of knee muscle strength, it was found specifically that Tai Chi had no obvious effect on knee extension strength (3.15, [−0.69, 6.99], $p = 0.24$, $I^2 = 26\%$) but had a significant effect on knee flexion strength ($p = 0.01$, $I^2 = 83\%$). Further sensitivity analysis and regression analysis were conducted. After excluding the low quality studies, we found that there was no statistical difference in knee extension strength between the Tai Chi and control groups, and the heterogeneity ($p = 0.08$, $I^2 = 19\%$) was reduced more than before. However, there is a significant difference in knee flexion strength between the Tai Chi and control groups, and the heterogeneity (10.25, [6.90, 13.61], $p < 0.00001$, $I^2 = 0\%$) was dramatically reduced. It is indicated that the reasons for heterogeneity in Figure 6(a) may be related to RB.

To sum up, different measurements may be one of the reasons for the great heterogeneity in the analysis of difference knee muscle strength between Tai Chi exercise and control group. Compared with knee extension strength, knee flexion strength by isokinetic dynamometer may generate heterogeneity in outcomes and proved that there exists statistical difference between Tai Chi and control group. Namely, while there is no significant improvement on knee extension strength, Tai Chi has a significant improvement on knee flexion strength.

4. Discussion

The decrease of muscle fitness, especially lower body strength, is the major inducement to affect the daily life of the elderly. We have also reached the conclusion that there is a significant improvement on the lower body strength of the elderly after Tai Chi exercise. However, the results of this meta-analysis showed that Tai Chi exercise has no significant improvement on overall knee muscle strength. The high heterogeneity in our analysis may originate from the publication bias and diversity of detective methods. Further subgroup analysis showed that although there was no significant improvement in knee extension strength, knee flexion strength was indeed improved. Sensitivity analysis showed that subgroup analysis had high homogeneity after excluding low quality literature data. Therefore, the effect of Tai Chi on lower body muscle strength of the elderly should be positive. Although Tai Chi has no obvious effect on the knee joint, it is helpful to improve the muscle fitness of knee flexion. Combined with the characteristics of Tai Chi exercise, the reason why it works might be the practice of knee/hip bending and single-leg standing which effectively increase lower body strength and optimize the normal biomechanical mechanism around knee joints [1, 33]. Therefore, Tai Chi exercise can be used as a rehabilitation treatment for training the stable deep muscle group, which effectively stimulates the deep muscle group of lower body, improves the muscle strength of knee joint, enhances the flexibility of joint, and then reduces the risk of related diseases caused by insufficient lower body strength of elderly.

Previous studies of Tai Chi exercise and muscle fitness are mainly focused on the elderly, including healthy individuals as well as chronic patients. Results of this meta-analysis showed that there are 31 studies on Tai Chi and muscle strength, mainly involving fibromyalgia, disability, KOA, Parkinson, menopause, cancer, arthritis, osteoporosis, and COPD. However, few researchers studied the overall regulation of Tai Chi on muscle strength, muscle endurance, flexibility, and other muscle fitness. Various nonrandomized controlled trials also emphasize muscle fitness and muscle strength and even deeply search for the distinguished effects of lower body muscle strength. Zhou et al. [4] found in a cross-sectional study that the muscle strength improvement degree is different in iliopsoas, quadriceps femoris, hamstring muscle, and tibial anterior muscle for elderly with 3 to 30 years of Tai Chi experience. Another evaluated method-surface electromyography of the anterior tibialis and lateral gastrocnemius muscles was recorded and showed that lower extremity muscle cocontraction plays a role in the observed benefit of longer-term Tai Chi training on gait and postural control [34]. Lu et al. [35] pointed out that at least three years of Tai Chi exercise caused different changes in knee joint strength for the elderly, particularly in extension and flexion. Tsang and Hui-Chan [36] found that the strength of knee extension ($p = 0.004$), knee flexion ($p = 0.021$), eccentric knee extension ($p = 0.049$), and knee flexion ($p = 0.007$) was significantly improved in the elderly with 3-year Tai Chi exercise. Wu et al. [37] found that only the knee extension strength of the elderly who had been practicing in Tai Chi for 3 years was significantly improved ($p < 0.013$). The result showed that the strength of quadriceps femoris in Tai Chi was significantly increased after 6 months of Tai Chi exercise, with lower body muscle strength being mainly reflected in the hip, knee, and ankle joint activities related muscle strength. Generally, muscle strength is supposed to be evaluated by isokinetic or isometric movement of related muscle groups [38]. Due to lack of relevant literature, the

muscle fitness of knee joint extension and flexion is mainly selected in this study, which needs to be discussed for further research.

This study has several limitations as follows: (1) The control group does not include other types of exercise and different intensities (e.g., resistance exercise, water sports) to comprehensively evaluate the advantages and disadvantages of Tai Chi in improving lower body muscle fitness. (2) Lower quality papers should be excluded when heterogeneity occurs in the risk assessment. Even though we did not analyze all outcomes in the analysis process, relevant characteristics of these original literature were still shown in the literature feature, Table 3) We have not consider different physiology characteristics in different genders; exercise load and Tai Chi style may influence the effects on muscle fitness. In addition, the test of lower body muscle strength also tends to be replaced by other detection methods such as 3/5 chair combat strength test and heel rise test which are not included in the study. The above factors may have publication bias in the analysis of the results.

5. Conclusions

As a complementary and alternative rehabilitation method, Tai Chi exercise has been widely accepted by clinical researchers as well as elderly people with chronic diseases. Our study reveals that Tai Chi can improve lower body strength but has no significant effect on the knee joint-related muscle groups. Furthermore, the lower body muscle strength of the elderly decreased with age, and Tai Chi did not aggravate the declining trend. Therefore, Tai Chi exercise is likely to be used as a rehabilitation treatment for the training of stable deep muscle group, which effectively stimulates the deep muscle group of lower body, thus indirectly enhancing joint activity, improving muscle fitness, and improving functional activities of elderly individuals.

Data Availability

The data we used to support the findings of this study can be accessed from the paper by searching the database according to our protocol which is elaborated clearly in the manuscript.

Disclosure

The content is solely the responsibility of the authors and does not necessarily represent the official views of the National Institutes of Health.

Conflicts of Interest

The authors declare no conflicts of interest with respect to the design of the study; the collection, analysis, or interpretation of data; the writing of the manuscript; or the decision to publish the results.

Authors' Contributions

Yuan Yang, Jia-hui Li, and Nan-Jun Xu contributed equally to this work.

Acknowledgments

Thanks are due to Joanna Li (Wuhan City College, China) and Wang Feng (Faculty of Education, University of Malaya, Malaysia) for providing language help and to Professor Ou Aihua (The Second Affiliated Hospital of Guangzhou University of Chinese Medicine, China) for assistance with the data analysis. This work was funded by the National Natural Science Foundation of China (Nos. 82004383, 82004386, 81873314, and 81974574), China Postdoctoral Science Foundation (No. 2018M633036), Medical Science Research Foundation of Guangdong Province (No. B2019091), Science and Technology Planning Project of Guangdong Province (No. 2020A1414050050), Science and Technology Program of Guangzhou (No. 202102010273), Project of Guangdong Provincial Department of Finance (Nos. [2014]157, [2018] 8), Key Scientific Research Platforms and Research Projects of Universities in Guangdong Province (No. 2018KQNCX041), and Science and Technology Research Project of Guangdong Provincial Hospital of Chinese Medicine (Nos. YN2019ML08 and YN2015MS15).

Supplementary Materials

The fixed forest plots of lower body strength before and after Tai Chi exercise, lower body strength in Tai Chi and control groups, and knee strength in Tai Chi and control groups are shown, respectively, in Appendices S1–3. The heterogeneity in Appendix S1 was decreased significantly ($I^2 = 0\%$, $p = 0.85$). However, 2 trials (Liu et al. [28], Zhang et al. [19]) were evaluated with high quality, which aroused doubts about the weight of publication bias. In Appendix S2, the heterogeneity decreased significantly ($p = 0.34$, $I^2 = 10\%$), which suggested that the source of greater heterogeneity in Figure 3(c) might be related to the publication bias. One trial with obvious publication bias (Zhuang et al. [31]) was excluded in Appendix S3; it showed no significant improvement to knee strength in Tai Chi exercise group compared with control group ($p = 0.09$). (*Supplementary Materials*)

References

[1] L. Zeng, W. Yang, D. Guo et al., "Systematic evaluation of the effect of traditional exercise therapy on pain improvement and joint function in knee osteoarthritis patients," *Chinese Journal of Chinese Medicine*, vol. 33, no. 5, pp. 2132–2139, 2018.

[2] L. Zou, T. Xiao, C. Cao et al., "Tai chi for chronic illness management: synthesizing current evidence from meta-analyses of randomized controlled trials," *The American Journal of Medicine*, vol. 134, no. 2, pp. 194–205, 2021.

[3] M. S. D. S. Buto, M. P. B. de Oliveira, C. Carvalho, V. Vassimon-Barroso, and A. C. d. M. Takahashi, "Effect of complementary therapies on functional capacity and quality of life among prefrail and frail older adults: a systematic review of randomized controlled trials," *Archives of Gerontology and Geriatrics*, vol. 91, 2020.

[4] M. Zhou, N. Peng, Q. Dai, H.-W. Li, R.-G. Shi, and W. Huang, "Effect of tai chi on muscle strength of the lower extremities in

the elderly," *Chinese Journal of Integrative Medicine*, vol. 22, no. 11, pp. 861–866, 2016.

[5] J. X. Li, D. Q. Xu, and Y. Hong, "Changes in muscle strength, endurance, and reaction of the lower extremities with tai chi intervention," *Journal of Biomechanics*, vol. 42, no. 8, pp. 967–971, 2009.

[6] F. Yang and W. Liu, "Biomechanical mechanism of tai-chi gait for preventing falls: a pilot study," *Journal of Biomechanics*, vol. 105, Article ID 109769, 2020.

[7] S. Charron, K. A. McKay, and H. Tremlett, "Physical activity and disability outcomes in multiple sclerosis: a systematic review (2011–2016)," *Multiple Sclerosis and Related Disorders*, vol. 20, pp. 169–177, 2018.

[8] L. Zou, H. Wang, Z. Xiao et al., "Tai chi for health benefits in patients with multiple sclerosis: a systematic review," *PLoS One*, vol. 12, no. 2, Article ID e0170212, 2017.

[9] J. X. Li, Y. Hong, and K. M. Chan, "Tai chi: physiological characteristics and beneficial effects on health," *British Journal of Sports Medicine*, vol. 35, no. 3, pp. 148–156, 2001.

[10] A. C. Lee, W. F. Harvey, X. Han et al., "Pain and functional trajectories in symptomatic knee osteoarthritis over up to 12 weeks of exercise exposure," *Osteoarthritis and Cartilage*, vol. 26, no. 4, pp. 501–512, 2018.

[11] R. Solianik, D. Mickevičienė, L. Žlibinaitė, and A. Čekanauskaitė, "Tai chi improves psychoemotional state, cognition, and motor learning in older adults during the COVID-19 pandemic," *Experimental Gerontology*, vol. 150, Article ID 111363, 2021.

[12] X. Pan, L. Huang, J. Lv, X. Wu, W. Niu, and Y. Liu, "Effect of new type taijiquan on lower limb muscle strength and dynamic balance in elderly women with knee osteoarthritis," *Sports Science and Technology*, vol. 38, no. 1, pp. 68–71, 2017.

[13] L. Huang, *Effect of Taijiquan Intervention on Clinical Rehabilitation and Gait Biomechanics in Elderly Patients with Knee Osteoarthritis*, Shanghai University Of Sport, Shanghai, China, 2015.

[14] R. Song, E. O. Lee, P. Lam, and S. C Bae, "Effects of tai chi exercise on pain, balance, muscle strength, and perceived difficulties in physical functioning in older women with osteoarthritis: a randomized clinical trial," *Journal of Rheumatology*, vol. 30, no. 9, pp. 2039–2044, 2003.

[15] Y.-W. Chen, M. A. Hunt, K. L. Campbell, K. Peill, and W. D. Reid, "The effect of tai chi on four chronic conditions-cancer, osteoarthritis, heart failure and chronic obstructive pulmonary disease: a systematic review and meta-analyses," *British Journal of Sports Medicine*, vol. 50, no. 7, pp. 397–407, 2016.

[16] L. Day, K. D. Hill, D. Jolley, F. Cicuttini, L. Flicker, and L. Segal, "Impact of tai chi on impairment, functional limitation, and disability among preclinically disabled older people: a randomized controlled trial," *Archives of Physical Medicine and Rehabilitation*, vol. 93, no. 8, pp. 1400–1407, 2012.

[17] L.-Y. Guo, C.-P. Yang, Y.-L. You et al., "Underlying mechanisms of tai-chi-chuan training for improving balance ability in the elders," *Chinese Journal of Integrative Medicine*, vol. 20, no. 6, pp. 409–415, 2014.

[18] S. L. Wolf, H. X. Barnhart, N. G. Kutner, E. Mcneely, C. Coogler, and T. Xu, "Selected as the best paper in the 1990s: reducing frailty and falls in older persons: an investigation of tai chi and computerized balance training," *Journal of the American Geriatrics Society*, vol. 51, no. 12, pp. 1794–1803, 2003.

[19] T. Zhang, M. Mao, W. Sun et al., "Effects of a 16-week tai chi intervention on cutaneous sensitivity and proprioception among older adults with and without sensory loss," *Research in Sports Medicine*, vol. 29, no. 4, pp. 406–416, 2021.

[20] F. Xu, J. Letendre, J. Bekke et al., "Impact of a program of tai chi plus behaviorally based dietary weight loss on physical functioning and coronary heart disease risk factors: a community-based study in obese older women," *Journal of Nutrition in Gerontology and Geriatrics*, vol. 34, no. 1, pp. 50–65, 2015.

[21] R. Song, B. L. Roberts, E.-O. Lee, P. Lam, and S.-C. Bae, "A randomized study of the effects of t'ai chion muscle strength, bone mineral density, and fear of falling in women with osteoarthritis," *Journal of Alternative & Complementary Medicine*, vol. 16, no. 3, pp. 227–233, 2010.

[22] J. F. Audette, Y. S. Jin, R. Newcomer, L. Stein, G. Duncan, and W. R. Frontera, "Tai chi versus brisk walking in elderly women," *Age and Ageing*, vol. 35, no. 4, pp. 388–393, 2006.

[23] N. F. Kasim, J. Veldhuijzen van Zanten, and S. Aldred, "Tai chi is an effective form of exercise to reduce markers of frailty in older age," *Experimental Gerontology*, vol. 135, Article ID 110925, 2020.

[24] Y. Huang and X. Liu, "Improvement of balance control ability and flexibility in the elderly tai chi chuan (TCC) practitioners: a systematic review and meta-analysis," *Archives of Gerontology and Geriatrics*, vol. 60, no. 2, pp. 233–238, 2015.

[25] J. H. Choi, J.-S. Moon, and R. Song, "Effects of Sun-style tai chi exercise on physical fitness and fall prevention in fall-prone older adults," *Journal of Advanced Nursing*, vol. 51, no. 2, pp. 150–157, 2005.

[26] J. Woo, A. Hong, E. Lau, and H. Lynn, "A randomised controlled trial of tai chi and resistance exercise on bone health, muscle strength and balance in community-living elderly people," *Age and Ageing*, vol. 36, no. 3, pp. 262–268, 2007.

[27] Y. Yip, J. Sit, and D. Wong, "A quasi-experimental study on improving arthritis self-management for residents of an aged people's home in Hong Kong," *Psychology Health & Medicine*, vol. 9, no. 2, pp. 235–246, 2004.

[28] J. Liu, X. Q. Wang, J. J. Zheng et al., "Effects of tai chi versus proprioception exercise program on neuromuscular function of the ankle in elderly people: a randomized controlled trial," *Evidence-Based Complementary and Alternative Medicine*, vol. 2012, Article ID 265486, 8 pages, 2012.

[29] S. Sungkarat, S. Boripuntakul, N. Chattipakorn, K. Watcharasaksilp, and S. R. Lord, "Effects of tai chi on cognition and fall risk in older adults with mild cognitive impairment: a randomized controlled trial," *Journal of the American Geriatrics Society*, vol. 65, no. 4, pp. 721–727, 2017.

[30] D. Taylor, L. Hale, P. Schluter et al., "Effectiveness of tai chi as a community-based falls prevention intervention: a randomized controlled trial," *Journal of the American Geriatrics Society*, vol. 60, no. 5, pp. 841–848, 2012.

[31] J. Zhuang, L. Huang, Y. Wu, and Y. Zhang, "The effectiveness of a combined exercise intervention on physical fitness factors related to falls in community-dwelling older adults," *Clinical Interventions in Aging*, vol. 9, pp. 131–140, 2014.

[32] Q. H. Song, Q. H. Zhang, and R. M. Xu, "Effect of tai-chi exercise on lower limb muscle strength, bone mineral density and balance function of elderly women," *International Journal of Clinical and Experimental Medicine*, vol. 7, no. 6, pp. 1569–1576, 2014.

[33] M. Roig, K. O'Brien, G. Kirk et al., "The effects of eccentric versus concentric resistance training on muscle strength and mass in healthy adults: a systematic review with meta-analysis," *British Journal of Sports Medicine*, vol. 43, no. 8, pp. 556–568, 2009.

[34] P. M. Wayne, B. J. Gow, F. Hou et al., "Tai chi training's effect on lower extremity muscle co-contraction during single- and dual-task gait: cross-sectional and randomized trial studies," *PLoS One*, vol. 16, no. 1, Article ID e0242963, 2021.

[35] X. Lu, C. W. Hui-Chan, and W. W. Tsang, "Tai chi, arterial compliance, and muscle strength in older adults," *European Journal of Preventive Cardiology*, vol. 20, no. 4, pp. 613–619, 2013.

[36] W. W. N. Tsang and C. W. Y. Hui-Chan, "Comparison of muscle torque, balance, and confidence in older tai chi and healthy adults," *Medicine & Science in Sports & Exercise*, vol. 37, no. 2, pp. 280–289, 2005.

[37] G. Wu, F. Zhao, X. Zhou, and L. Wei, "Improvement of isokinetic knee extensor strength and reduction of postural sway in the elderly from long-term tai chi exercise," *Archives of Physical Medicine and Rehabilitation*, vol. 83, no. 10, pp. 1364–1369, 2002.

[38] C. Lan, J.-S. Lai, S.-Y. Chen, and M.-K. Wong, "Tai chi chuan to improve muscular strength and endurance in elderly individuals: a pilot study," *Archives of Physical Medicine and Rehabilitation*, vol. 81, no. 5, pp. 604–607, 2000.

[39] M. Adcock, M. Fankhauser, J. Post et al., "Effects of an in-home multicomponent exergame training on physical functions, cognition, and brain volume of older adults: a randomized controlled trial," *Frontiers of Medicine*, vol. 6, p. 321, 2019.

[40] N. Takeshima, M. M. Islam, Y. Kato et al., "Effects of 12 weeks of tai chi chuan training on balance and functional fitness in older Japanese adults," *Sports*, vol. 5, no. 2, 2017.

[41] C. Noradechanunt, A. Worsley, and H. Groeller, "Thai yoga improves physical function and well-being in older adults: a randomised controlled trial," *Journal of Science and Medicine in Sport*, vol. 20, no. 5, pp. 494–501, 2016.

[42] B. Frye, S. Scheinthal, T. Kemarskaya, and R. Pruchno, "Tai chi and low impact exercise: effects on the physical functioning and psychological well-being of older people," *Journal of Applied Gerontology*, vol. 26, no. 5, pp. 433–453, 2007.

Hindawi
Evidence-Based Complementary and Alternative Medicine
Volume 2021, Article ID 2903543, 14 pages
https://doi.org/10.1155/2021/2903543

Research Article

Predictive Biomarkers for Postmyocardial Infarction Heart Failure Using Machine Learning: A Secondary Analysis of a Cohort Study

Feng Li,[1] Jin-Yu Sun,[2] Li-Da Wu,[1] Qiang Qu,[2] Zhen-Ye Zhang,[1] Xu-Fei Chen,[1] Jun-Yan Kan,[2] Chao Wang,[3] and Ru-Xing Wang[1]

[1]*Department of Cardiology, Wuxi People's Hospital, Nanjing Medical University, Wuxi 214023, China*
[2]*Department of Cardiology, The First Affiliated Hospital of Nanjing Medical University, Nanjing 210029, China*
[3]*Department of Cardiology, The First Affiliated Hospital of Guangxi Medical University, Nanning 530021, China*

Correspondence should be addressed to Ru-Xing Wang; ruxingw@aliyun.com

Received 22 August 2021; Accepted 17 November 2021; Published 13 December 2021

Academic Editor: Zhaohui Liang

Background. There are few biomarkers with an excellent predictive value for postacute myocardial infarction (MI) patients who developed heart failure (HF). This study aimed to screen candidate biomarkers to predict post-MI HF. *Methods*. This is a secondary analysis of a single-center cohort study including nine post-MI HF patients and eight post-MI patients who remained HF-free over a 6-month follow-up. Transcriptional profiling was analyzed using the whole blood samples collected at admission, discharge, and 1-month follow-up. We screened differentially expressed genes and identified key modules using weighted gene coexpression network analysis. We confirmed the candidate biomarkers using the developed external datasets on post-MI HF. The receiver operating characteristic curves were created to evaluate the predictive value of these candidate biomarkers. *Results*. A total of 6,778, 1,136, and 1,974 genes (dataset 1) were differently expressed at admission, discharge, and 1-month follow-up, respectively. The white and royal blue modules were most significantly correlated with post-MI HF (dataset 2). After overlapping dataset 1, dataset 2, and external datasets (dataset 3), we identified five candidate biomarkers, including *FCGR2A*, *GSDMB*, *MIR330*, *MED1*, and *SQSTM1*. When *GSDMB* and *SQSTM1* were combined, the area under the curve achieved 1.00, 0.85, and 0.89 in admission, discharge, and 1-month follow-up, respectively. *Conclusions*. This study demonstrates that *FCGR2A*, *GSDMB*, *MIR330*, *MED1*, and *SQSTM1* are the candidate predictive biomarker genes for post-MI HF, and the combination of *GSDMB* and *SQSTM1* has a high predictive value.

1. Introduction

Heart failure (HF) is one of the primary long-term complications of acute myocardial infarction (MI). Meanwhile, post-MI HF has been identified as a time-dependent variable significantly related to mortality with a hazard ratio of 3.31 [1–3]. Screening the post-MI HF genes served as novel candidate biomarkers facilitates exactly diagnosis and timely intervention. However, despite many proposed biomarkers involving post-MI HF, few of them have gained widespread acceptance and application in clinical practice [4].

We analyzed the gene expression profile of post-MI HF patients and those who remained HF-free over a 6-month follow-up using plasma samples collected at admission, discharge, and 1-month follow-up. Differential expression analysis and weighted gene coexpression network analysis (WGCNA) were combined to screen the top-ranked circulating candidates. In addition, we performed enrichment analysis to illustrate the potential influence on progression from MI to HF using functional annotation algorithms. Moreover, we confirmed the differentially expressed genes (DEGs) and key modules using external datasets from 2 different acute MI patient cohorts, 4 single-cardiac cell

transcriptomic studies [5], and 12 ischemic cardiomyopathy patients' expression profiles [6]. This study aimed to identify circulating biomarkers to predict post-MI HF using machine learning methods.

2. Methods

2.1. Data Acquisition. A total of 64 samples from patients with ST-elevation MI were enrolled from the First Chair and Department of Cardiology of the Medical University of Warsaw, with the approval of the Ethics Committee of the Ain Shams the Faculty of Medicine [7]. All 17 patients were indicated for direct percutaneous coronary intervention. Coronary angiography, angioplasty of the infarct-related artery, and pharmacological therapy were performed following the 2008 European Society of Cardiology guidelines for acute myocardial infarction [8]. Whole blood samples were collected at the time point of admission (first day of MI), discharge (4 to 6 days after MI), and 1-month follow-up, respectively. According to the manufacturer's instructions, the transcriptional profiling was analyzed using Human Gene 1.0 ST Array (Affymetrix, Santa Clara, CA, USA; Platform GPL6244). The involvement of this study did not influence treatment. All participants were provided written informed consent following the Declaration of Helsinki. This study was a secondary data analysis on publicly available data, and the raw data were acquired from the Gene Expression Omnibus database (https://www.ncbi.nlm.nih.gov/geo/) [7]. Figure 1 shows a flow diagram summarizing the entire study design.

2.2. Data Processing and Probe Reannotation. Log_2-transformation, background correction, and quantile normalization were performed on the raw gene expression profiles using the linear models for the microarray data (limma) algorithm. Then, the probe serial numbers were converted into gene symbols according to the annotation file provided by the manufacturer. When a single gene was mapped by more than one probe, the average expression level of this gene was calculated. Finally, the expression profile containing 23,307 genes was further processed.

2.3. Clustering Analysis and Visualization. Clustering analysis is a powerful tool to perform molecular classification among samples and identify subtype characterization [9–11]. Among the many clustering algorithms, hierarchical cluster analysis and k-means clustering are the two prominent representatives, whereas t-distributed stochastic neighbor embedding analysis and principal component analysis are widely used unsupervised methods to reduce dimensions of expression data.

The processed expression data were first analyzed by the k-means cluster method and visualized using a heatmap. Then, we performed an unsupervised hierarchical cluster analysis with a scale-free network and topological overlaps. Meanwhile, hierarchical cluster analysis is a cluster analysis method to create a hierarchy of clusters and thus group patients with similar gene expressions into the same clusters [12,13]. Additionally, we ran the discriminant analysis using t-distributed stochastic neighbor embedding analysis, a nonlinear dimensionality reduction algorithm well-suited for visualizing high-dimensional data [14,15]. In this study, hierarchical cluster and t-distributed stochastic neighbor embedding analysis were performed on the full set (all the four time points) of detected genes, which aimed to illustrate the general difference in expression patterner between the post-MI HF and non-HF groups.

Moreover, we performed principal component analysis on the expression data of admission, discharge, and 1-month follow-up, respectively. The principal component analysis is a widely used distance-based statistical algorithm that reduces the dimensionality of complex datasets, increases interpretability, and minimizes information loss [14–19]. An appropriate time point with good distinguishing ability will be selected based on the expression parameter revealed by principal component analysis.

2.4. Screening Differentially Expressed Genes (DEGs). Fold change is a univariate filter method to compare the absolute expression value change between two groups, and it has been widely used as a threshold for screening possible biomarkers. We analyzed the gene expression profile acquired at three time points (admission, discharge, and 1-month follow-up) and screened DEGs between the post-MI HF and non-HF groups based on $\log_2$ fold change expression using the limma method [20]. We assumed that the difference in blood samples might be smaller compared with tissue samples (like heart tissue). Therefore, to avoid eliminating excessive candidate biomarkers, we set a lower threshold of fold change >1.1 and P value < 0.05. The DEGs were visualized as a volcano plot and heatmap using the "ggplot2" and "pheatmap" package in R.

2.5. Construction of WGCNA. WGCNA is a bioinformatics algorithm to explore the transcriptome expression patterns across genes, identify gene modules associated with complex disease features, and reveal the biologically functional interpretations of network modules [21–24]. Based on the time-series gene expression profiles, we used the one-step network construction function of the "WGCNA" package (version 1.60) for constructing the coexpression network and identifying key modules. Scale independence and mean connectivity were calculated using a gradient method with a range of 1 to 20, and the power value was selected with a threshold of independence degree >0.8. The minimal module size and the merge cut height were set as 30 and 0.3, respectively. After module construction, we summarized the module eigengene according to the first module principal component to evaluate the significance of each module, and the module-trait relationships were assessed based on the correlation between module eigengenes and clinical traits. Furthermore, we calculated all genes' average absolute gene significance within one module and evaluated the correlation strength accordingly. In addition, the gene significance value was defined by log10-transformed P value in the linear regression between expression and clinical traits. The

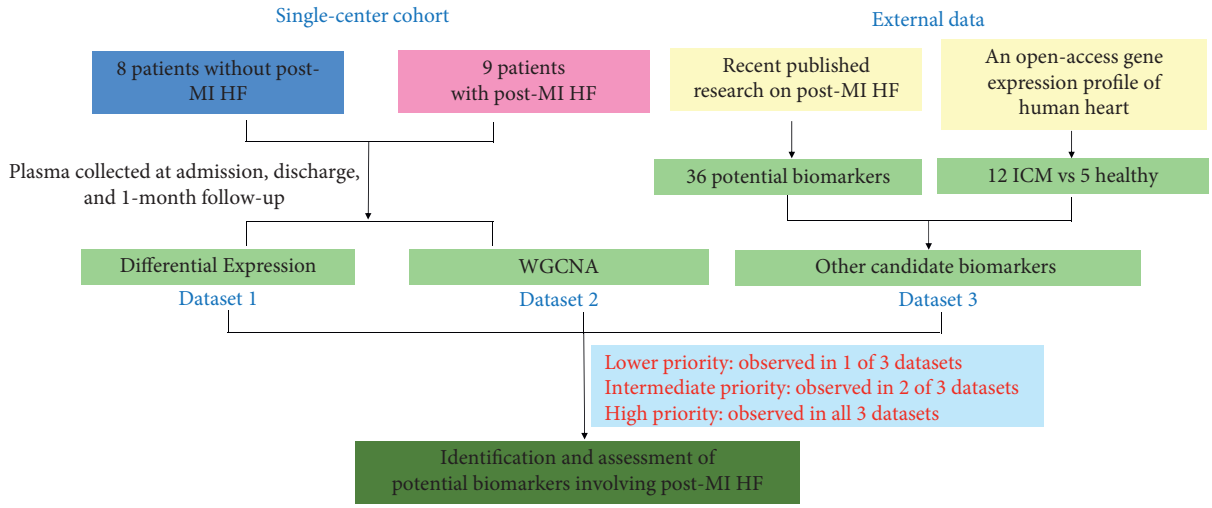

Figure 1: Study workflow diagram summarizing the entire study design. MI: myocardial infarction; HF: heart failure; ICM: ischemic cardiomyopathy; WGCNA: weighted gene coexpression network analysis.

modules with the highest MS values were considered as the key modules [21].

After constructing coexpression networks, we further evaluated the preservation levels of key modules using module preservation analysis, which summarizes different preservation statistics into one single overall measure of preservation (i.e., Zsummary value). Zsummary is a statistic value composed of multiple statistics related to density connectivity [25]. Generally, a higher Zsummary value suggested the more substantial evidence that a module should be preserved: Zsummary value less than 2 indicated "no evidence," Zsummary value between 2 and 10 indicated "weak evidence," and Zsummary value higher than 10 indicated strong evidence. However, the Zsummary value tends to increase with the rise of module size, and therefore, it is unappropriated to use the Zsummary value to perform preservation analysis on modules with distinct sizes. In that case, medianRank, which is calculated based on the observed preservation statistics and not affected by module size, should also be applied [26]. A module with a lower medianRank value is more preserved than those with a higher medianRank.

2.6. Enrichment Analysis and Protein-Protein Interaction (PPI) Network. To reveal the roles of key modules in the progression of post-MI HF, we ran gene ontology (GO) enrichment analysis using the "clusterProfiler" package. Moreover, we performed association and enrichment analysis based on DisGeNET [27] database and visualized using Metascape, which was a tool to systematically analyze and interpret OMICs-based research [28]. DisGeNET, a gene-disease associations database, contains publicly available collections of genes and human disease-associated variants [27]. In addition, we ran a PPI enrichment analysis on genes from key modules and created an interaction network. The molecular complex detection algorithm was also applied to detect densely connected network components [29].

2.7. Identification of Potential Biomarkers and Expression Analysis. To identify potential biomarkers for post-MI HF, DEGs (dataset 1) were cross-referenced with genes from key modules (dataset 2). We considered the biomarkers would be reproducible if they were identified by both expression analysis and coexpression network analysis at the same time. In parallel, we included other candidate biomarkers from external datasets (dataset 3): (1) a recently published research combining aptamer-based proteomics from 2 different acute MI patient cohorts and 4 single-cardiac cell transcriptomic studies, which identified 36 potential circulating biomarkers [5]; (2) an open-access gene expression profile of human heart evaluating the influence of heart failure on human nucleocytoplasmic transport-related genes: 12 samples from ischemic cardiomyopathy and 5 samples from control hearts [6]. Then, we ranked biomarkers according to 3 priorities: lower priority (observed in 1 of 3 datasets), intermediate priority (observed in 2 of 3 datasets), and high priority (observed in all three datasets).

2.8. Statistical Analysis. Continuous variables were represented as mean ± standard deviation (normal distribution) or median + interquartile range (skewed distribution). Categorical variables were presented as percentages. The one-way ANOVA test, Kruskal–Wallis test, and chi-square test were used to determine statistical differences, as appropriate. The receiver operating characteristic (ROC) curves were created, and the area under the curve (AUC) was calculated to assess the predictive value of these possible biomarkers. All statistical analysis was performed by R software version 3.6.1 (R Foundation for Statistical Computing, Vienna). $P < 0.05$ was considered as statistical significance.

3. Results

3.1. Clinical Characteristics of the Study Population. This study included 17 patients with myocardial infarction who volunteered for a six-month visit. All these patients

were diagnosed with STEMI and received coronary angiography, angioplasty, and pharmacological treatment following current guidelines [8]. After six months, 9 patients were diagnosed with HF (post-MI HF group), and the other 8 individuals were grouped into the post-MI non-HF group. No significant difference was observed in age, sex, body mass index, hypertension, diabetes, smoking, hypercholesterolemia, anterior myocardial infarction, and medications (beta-blockers, aspirin, clopidogrel, statins, and angiotensin-converting enzyme inhibitors) at baseline (all $P > 0.05$). However, the post-MI HF group showed higher NT-proBNP (918.3 ± 848.5 *vs.* 62 ± 14.1 pg/mL, $P < 0.001$), lower LVEF (39.3 ± 8.4 *vs.* $66.8 \pm 1.9\%$, $P = 0.001$), and more administration of diuretics (7 *vs.* 1, $P = 0.015$) compared with the non-HF group. Baseline demographic and clinical characteristics have been summarized in the parent study [7].

3.2. Clustering Analysis and Visualization. K-means cluster analysis indicated a distinct expression patterner between the HF and non-HF groups, although only limited expression similarity was observed in samples from the same time point (Figure 2(a)). Consistently, hierarchical cluster and t-distributed stochastic neighbor embedding analysis suggested that post-MI HF patients showed a different expression patterner compared with non-HF patients (Figures 2(b) and 2(c)). Principal component analysis on the expression data of three time points showed that the expression at admission and discharge might be appropriate time points with a good distinguishing ability (Figures 2(d)–2(f)).

3.3. Differential Gene Expression Profiling in HF and Non-HF Groups. For the expression data acquired at admission, 3,556 genes were significantly upregulated, whereas 3,222 genes were significantly downregulated (Figures 3(a) and 3(b)). At the time point of discharge, differential expression analysis identified a total of 1,136 genes associated with post-MI HF events (519 up- and 617 downregulated in HF patients; Figures 3(c) and 3(d)). However, 1,974 genes were differently expressed at 1 month (950 up- and 1024 downregulated in HF patients; Figures 3(e)and 3(f)).

3.4. Weighted Coexpression Network Construction and Key Modules Identification. The soft-thresholding power of 8 was selected according to the scale-free topology criterion (scale-free $R^2 = 0.81$, Figures 4(a) and 4(b)), and 28 modules were created (Figure 4(c)). All the genes that could not be put into any other modules were included in the grey module, and the grey module was excluded from the following research. Next, we analyzed the association between modules and clinical traits, including the diagnosis of HF and follow-up time (Figures 4(d) and 4(e)). The white and royal blue modules were most significantly positively or negatively correlated with post-MI HF, respectively. Accordingly, white and royal blue modules were identified as the key modules. A total of 40 and 105 genes were included in the white and royal blue modules, respectively. In Figures 4(f) and 4(g), we illustrated the correlation between module membership and gene significance in white (correlation coefficient = 0.91, $P <$ 1e-200) and royal blue module (correlation coefficient = 0.74, $P =$ 1.8e-111). Figure 4(h) shows the module preservation statistics, and the $Z_{summary}$ values of both white and royal blue modules were more than 10. Additionally, Figure 4(i) illustrates the medianRank score analysis of different modules.

3.5. Enrichment Analysis of Key Modules and Interaction Network. We ran enrichment analysis on the key modules using the Gene Ontology database. As shown in Figure 5(a), enriched biological processes were mainly involved in autophagy, a process utilizing autophagic mechanism, negative regulation of ubiquitin-dependent protein catabolic process, negative regulation of proteolysis involved in cellular protein catabolic process, and positive regulation of RNA splicing. The cellular components were mainly enriched in nuclear chromatin, inclusion body, mediator complex, clathrin-coated endocytic vesicle membrane, and nuclear pore nuclear basket. Enriched molecular functions mainly involved nuclear hormone receptor binding, hormone receptor binding, histone binding, vitamin D receptor binding, and thyroid hormone receptor binding. Additionally, Figure 5(b) shows the gene network of GO analysis, and the network of enriched terms is shown in Figure 5(c). Moreover, the enrichment analysis in DisGeNET revealed that genes in the key modules were associated with sleep disturbances, multiple congenital anomalies, delayed speech and language development, bulbous nose, and neurodevelopmental disorders (Figure 5(d)). Furthermore, the PPI network was illustrated in Figure 5(e), and 2 cluster subnetworks (including *SMARCC1*, *NR3C1*, *RNF2*, *NCOR1*, *MED1*, *MED14*, *TNRC6A*, *APP*, *PTBP3*, and *BCL7C*) were created using the molecular complex detection algorithm.

3.6. Identification of Potential Biomarkers and Expression Analysis. Dataset 1 included 200 DEGs from 3 time points, and dataset 2 included 145 genes from key modules. After overlapping dataset 1 and dataset 2, a total of 5 genes were acquired, including *OR7E14P*, *GSDMB*, *TAX1BP3*, *SQSTM1,* and *KAT6B*. The detailed cross-reference information was provided in Figure 6(a). Moreover, 9 genes were found in all three datasets and considered high-priority candidates, including *FCGR2A*, *RQCD1*, *IRF8*, *RELL1*, *GPR21*, *PTBP3*, *CYB5R1*, *ICA1*, and *CPNE8* (Figure 6(b)). Based on a literature search, we identified 5 genes that might most effectively differentiate the post-MI HF patients from those without HF: *FCGR2A*, *GSDMB*, *MIR330*, *MED1*, and *SQSTM1*. Figures 6(c)–6(e) shows the expression level of these genes at admission, discharge, and 1 month after discharge, respectively.

3.7. Accuracy of Biomarkers for Predicting Post-MI HF. To evaluate the predictive value of the 5 biomarkers, we created ROC curves and calculated the AUC at all 3 time points,

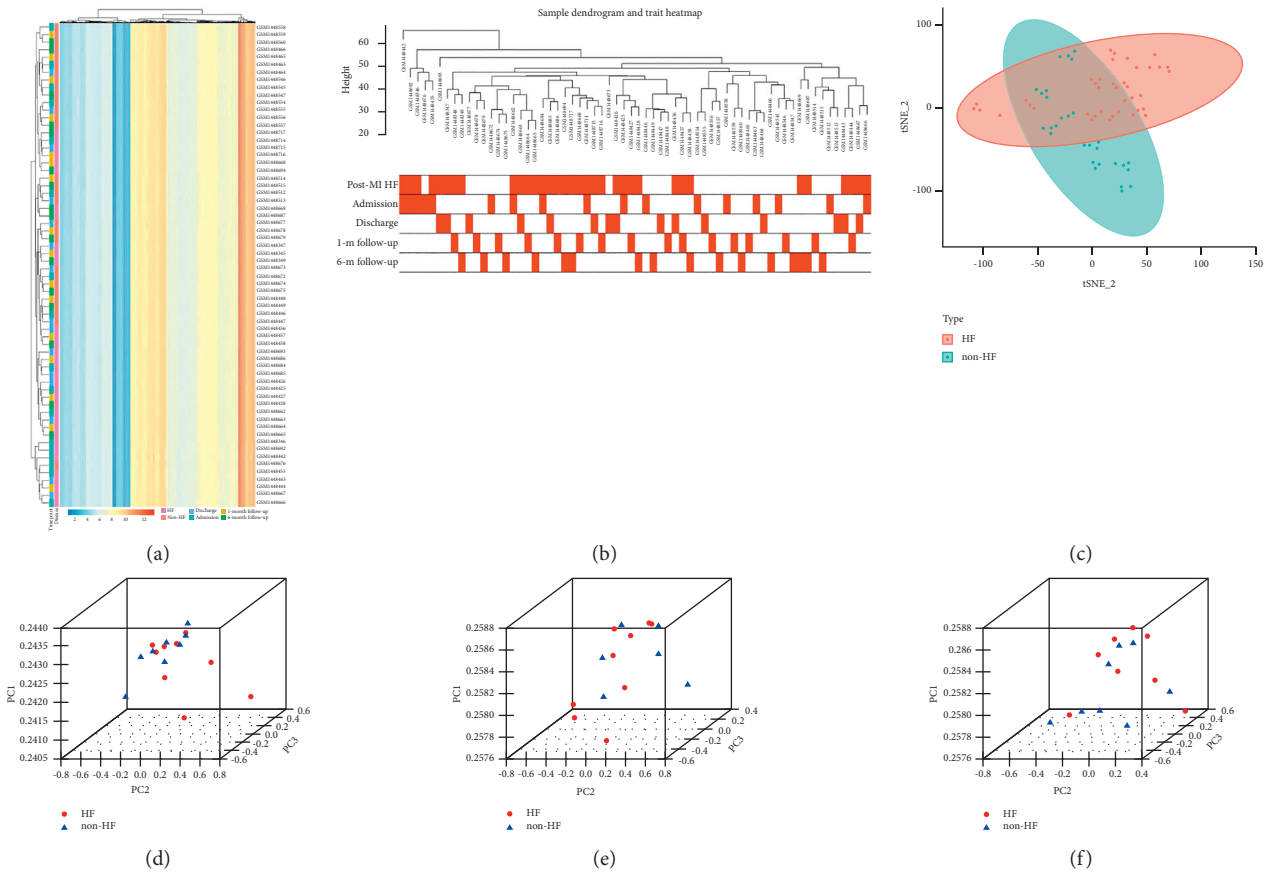

Figure 2: Clustering analysis of the expression profile. (a) K-means clustering, (b) hierarchical cluster, and (c) t-distributed stochastic neighbor embedding analysis. Principal component analysis on the sample collected at (d) admission, (e) discharge, and (f) 1-month follow-up. HF: heart failure; PC: principal component.

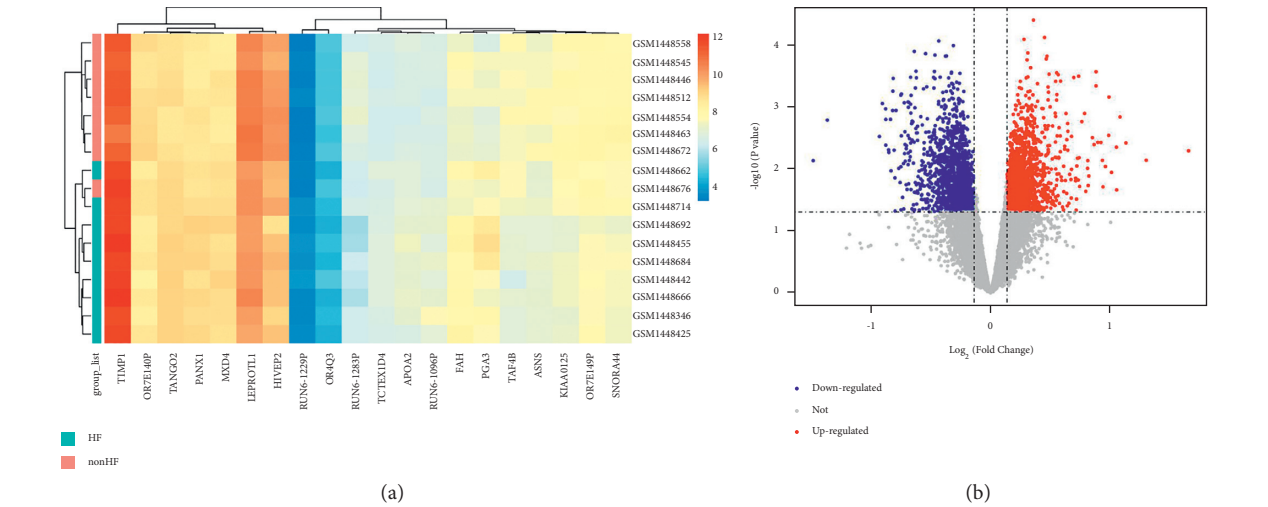

Figure 3: Continued.

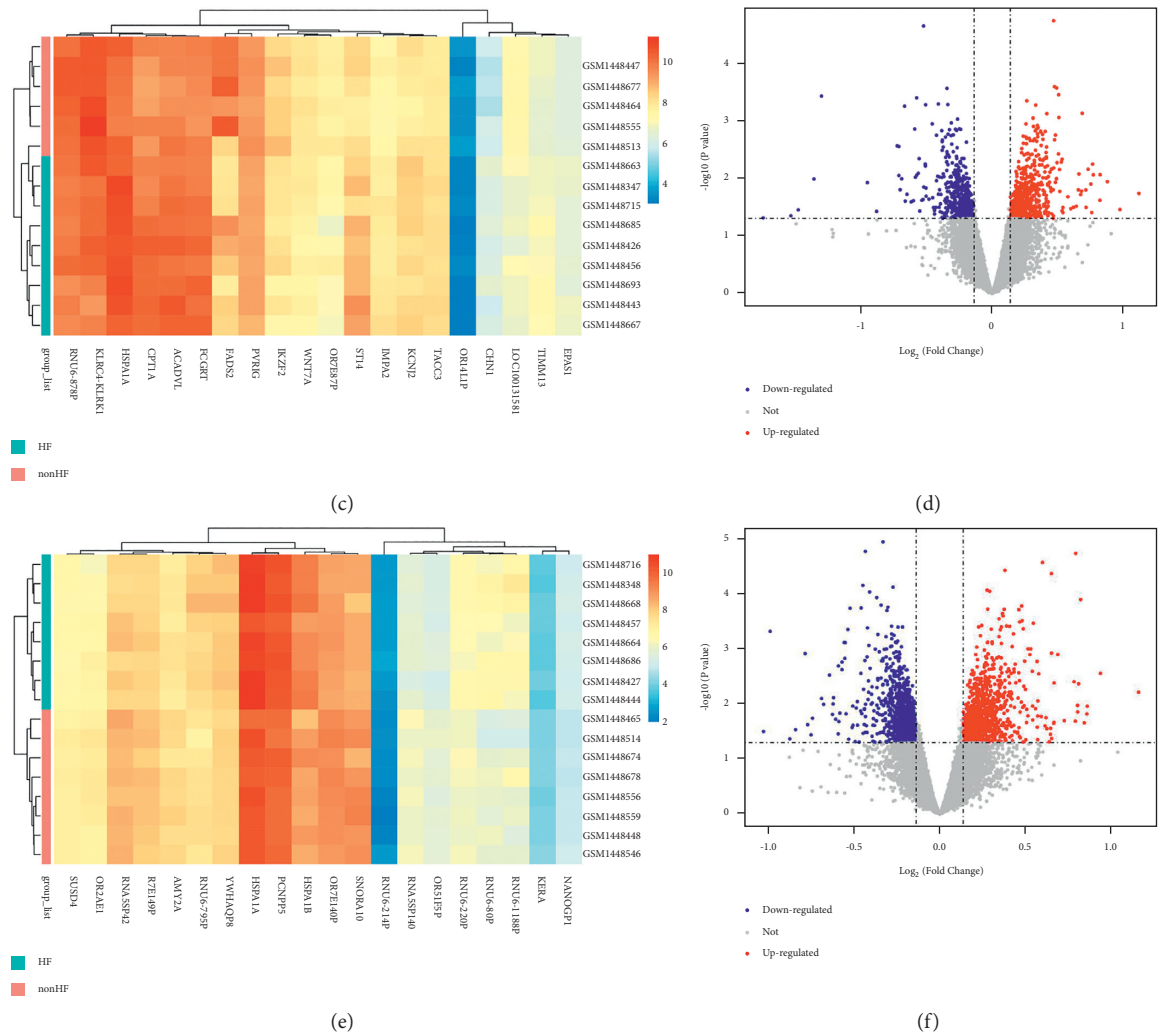

Figure 3: The expression heatmap and volcanic plots of the differential gene expression between post-MI HF and non-HF patients. The analysis was performed on the sample collected at (a, b) admission, (c, d) discharge, and (e, f) 1-month follow-up, respectively. MI: myocardial infarction; HF: heart failure.

respectively (Table 1). When combining *GSDMB* and *SQSTM1*, the AUCs achieved 1.00, 0.85, and 0.89 in admission, discharge, and 1-month follow-up, respectively.

4. Discussions

In this study, we performed a secondary analysis of a cohort study using machine learning including nine post-MI HF patients and eight post-MI patients who remained HF-free over a 6-month follow-up. The main findings are as follows. (1) Five candidate biomarkers (including *FCGR2A*, *GSDMB*, *MIR330*, *MED1,* and *SQSTM1*) were identified, which might most effectively differentiate the post-MI HF patients from those without HF. (2) When combining *GSDMB* and *SQSTM1*, the AUC achieved as high as 1.00, 0.85, and 0.89 in admission, discharge, and 1-month follow-up, respectively, indicating a high predictive value for post-MI HF.

FCGR2A, also named FcγRIIa, is a low-affinity receptor for the constant fragment of immunoglobulin G, mainly expressed on platelets' surface. Calverley et al. [30] reported an increased level of *FCGR2A* in patients with myocardial infarction, unstable angina, and ischemic stroke. Schneider et al. [31] analyzed the expression level of *FCGR2A* in post-MI patients and found a 4-fold greater risk of subsequent MI, stroke, and death in those with higher platelet *FCGR2A* expression. In our study, we revealed that *FCGR2A* was significantly upregulated in post-MI HF patients. Engagement of *FCGR2A* on platelets by immune complexes will trigger intracellular signaling events and lead to platelet activation and aggregation. Multiple studies have revealed that HF was significantly associated with abnormal platelet morphology and function [32, 33]. In addition, HF patients have higher mean platelet volume [34], increased whole blood aggregation [35], and elevated platelet-derived adhesion molecules [36]. Potential mechanisms include hemodynamic and vascular factors, secretion of cytokines like C-C chemokines, and renin-angiotensin system activation [32].

Gasdermins (*GSDMs*) are a family of functionally diverse proteins expressed in various cell types and tissues, and

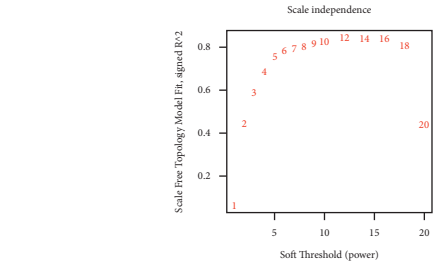

(a)

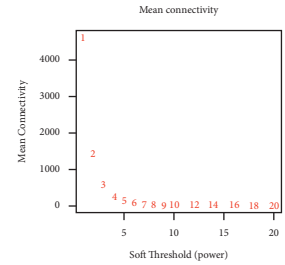

(b)

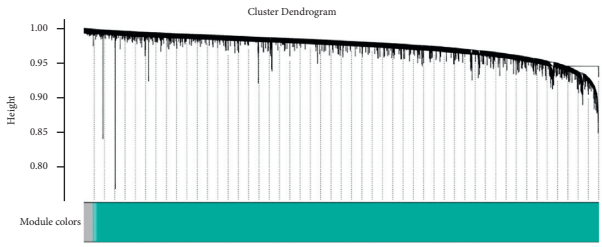

(c)

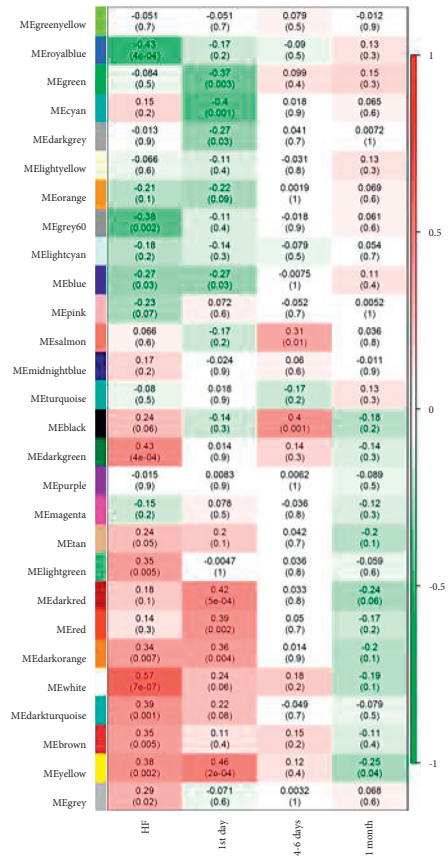

(d)

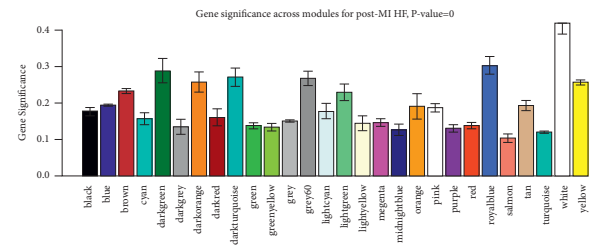

(e)

(f)

Figure 4: Continued.

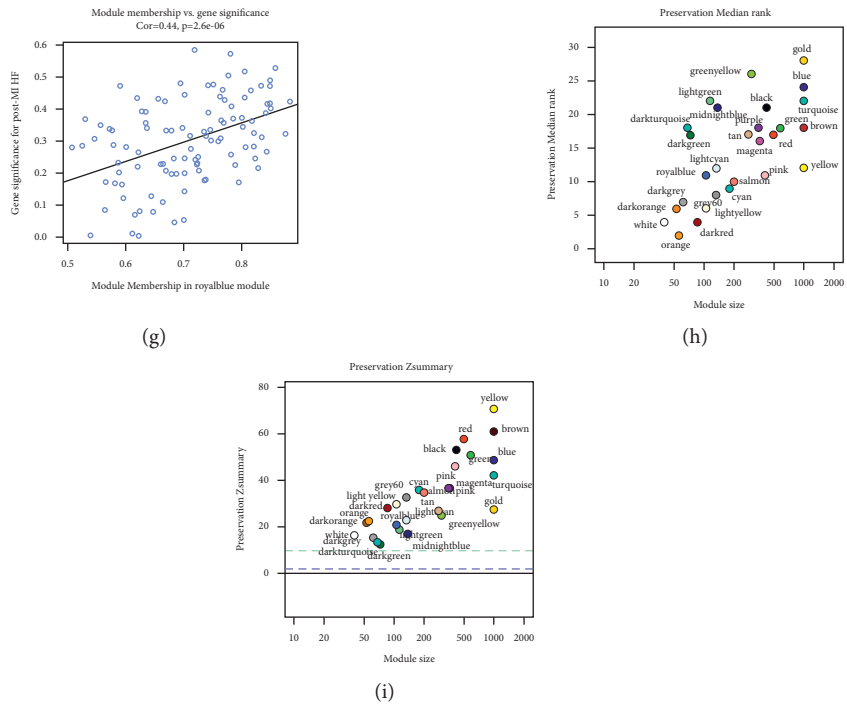

Figure 4: Network construction and analysis of the weighted coexpressed genes. (a) Analysis of the scale-free fit index and (b) the mean connectivity for various soft-thresholding powers. The soft-thresholding power of 8 was selected based on the scale-free topology criterion. (c) Dendrogram clustered using a dissimilarity measure (1-TOM). Each color in the dendrogram indicates one coexpression module, and every branch stands for a signal gene. (d) Heatmap of the correlation between module eigengenes and the disease status of post-MI HF. (e) Distribution of gene significance in the modules associated with post-MI HF. The white and royal blue modules were most significantly positively or negatively correlated with post-MI HF, respectively. Scatter plot of module eigengenes in the (f) white module and (g) royal blue module. (h) Module preservation analysis based on Zsummary. Each point represents a module, and the dashed blue and green lines indicate the threshold of 2 and 10, respectively. A module with Zsummary of <5 would be considered as nonpreserved. (i) MedianRank score analysis of different modules. MI: myocardial infarction; HF: heart failure.

GSDMs have been well demonstrated to be involved in pyroptosis, a proinflammatory type of regular cell death [37]. It has been reported that *GSDMB* promotes noncanonical pyroptosis by enhancing caspase-4 activity and *GSDMD* cleavage [38]. With the deepening understanding of HF and chronic inflammation, pyroptosis has been revealed as having an important role in HF [39]. The pyroptosis of myocardial cells leads to the irreversible loss of cardiomyocytes, whereas pyroptosis of cardiac fibroblasts results in myocardial fibrosis and cardiac hypertrophy, which leads to the adverse change in cardiac structure and function and will eventually result in HF. Moreover, accumulating studies revealed that sleep disturbances significantly increased cellular stress, inflammation, and myoblast pyroptosis, leading to the development of HF [40–42]. Interestingly, our results revealed that *GSDMB* was differently expressed in all three time points and included in key modules showing high similarity with sleep disturbances-associated genes, suggesting its important role in the development of post-MI HF.

SQSTM1 (also known as p62), a multifunctional protein consisting of a series of domains, acts in concert with binding partners to regulate the cellular process, especially autophagy [43]. As an autophagy receptor, *SQSTM1* has been recognized as an autophagy marker [44]. Autophagy is a self-degradative process for delivering aggregating proteins and damaged organelles to lysosomes for degradation, protecting cells from intracellular stress, and providing essential energy for starving cells [45]. However, the exact mechanisms between autophagy and HF remain largely vague despite the many studies. Current evidence indicates the key role of autophagy in protecting myocardial cells against HF, while overactivation of autophagy will contribute to the progress of HF [46,47]. In the early stage of HF, activated autophagy increases protein degradation, reduces myocardial hypertrophy, and antagonizes ventricular hypertrophy. On the contrary, autophagy promotes cardiomyocyte death and accelerates the deteriorating progression of HF. In our study, the expression of *SQSTM1* was significantly increased in post-MI HF, which suggested that excessive autophagy with MI might contribute to the development of HF. In addition, our results showed that the combination of *GSDMB* and *SQSTM1* had a high predictive value for post-MI HF, indicating that pyroptosis and autophagy played a jointly promoting role in the development of post-MI HF.

Mediator, a multisubunit nuclear complex, is a major component of eukaryotic transcription machinery that

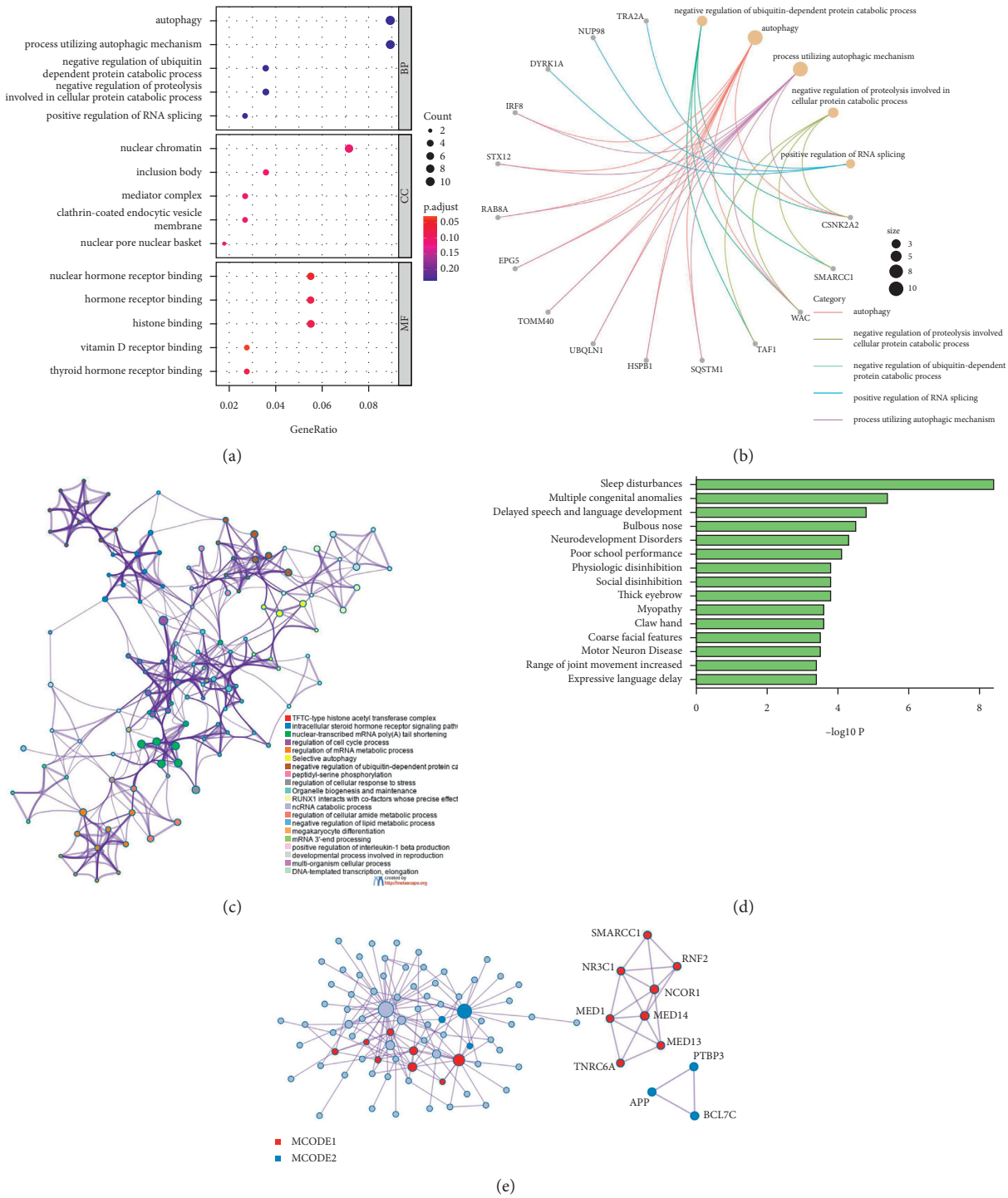

FIGURE 5: Enrichment analysis of key modules and interaction network. (a) GO analysis on white and royal blue modules. The significance of enrichment gradually increases from blue to red, and the size of the dots indicates the number of genes contained in the corresponding pathway. (b) Gene network of GO analysis. (c) The network of enriched terms. Each node represents an enriched term and is colored by cluster ID. Nodes sharing the same cluster ID are typically close to each other. (d) Summary of enrichment analysis in DisGeNET. (e) The PPI network of the genes in key modules. GO: Gene Ontology; PPI: protein-protein interaction.

served as a bridge between transcription factors and RNA polymerase II [48]. Studies have demonstrated that Med1 (a subunit of mediator) plays an important role in regulating vital cardiac gene expression and maintaining normal heart function. Reportedly, deletion of *Med1* may lead to cardiac function abnormalities, including left ventricular dilation, decreased ejection fraction, and pathological ventricular remodeling [49,50]. Hall et al. [51] revealed that deletion of *Med1* in cardiomyocytes deregulated more than 5000 genes and promoted the development of acute HF.

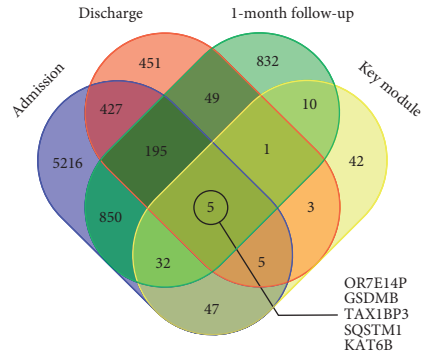

(a)

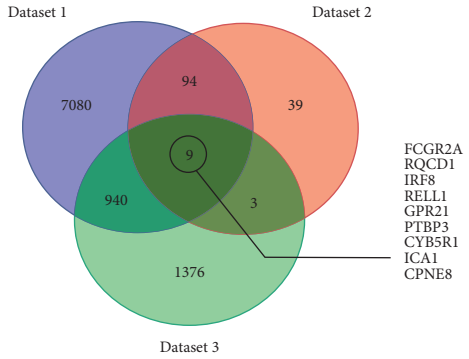

(b)

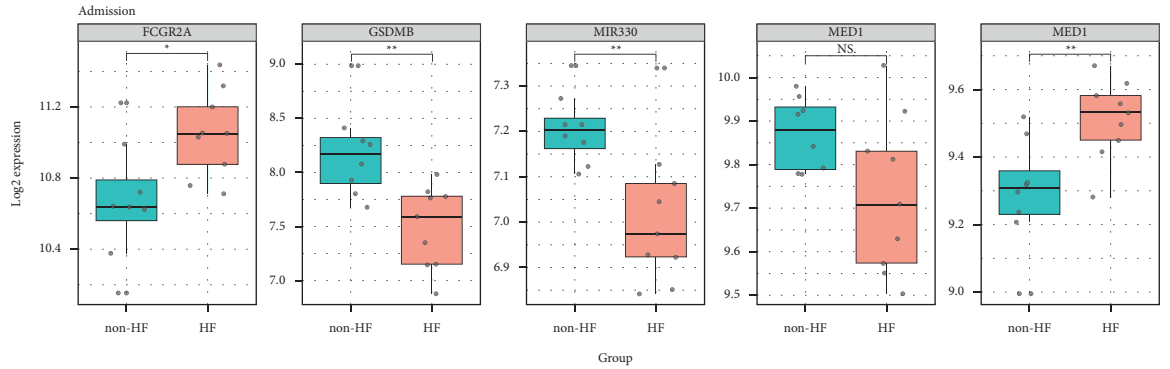

(c)

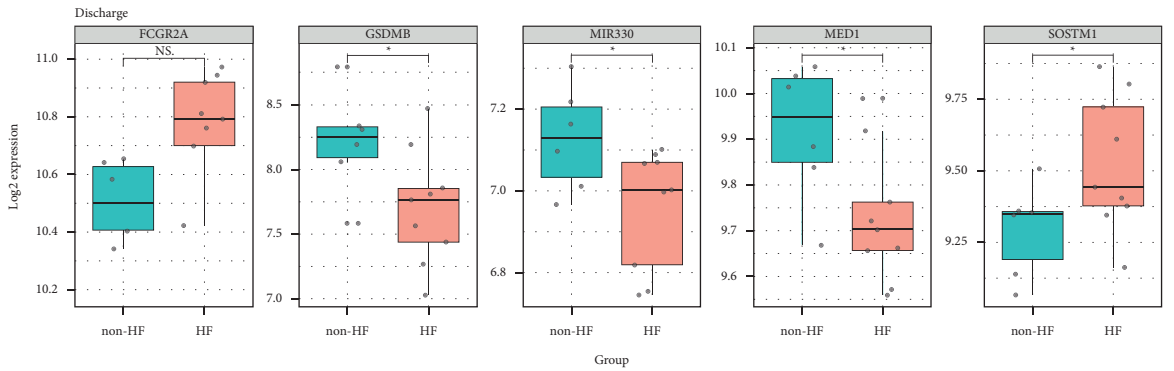

(d)

Figure 6: Continued.

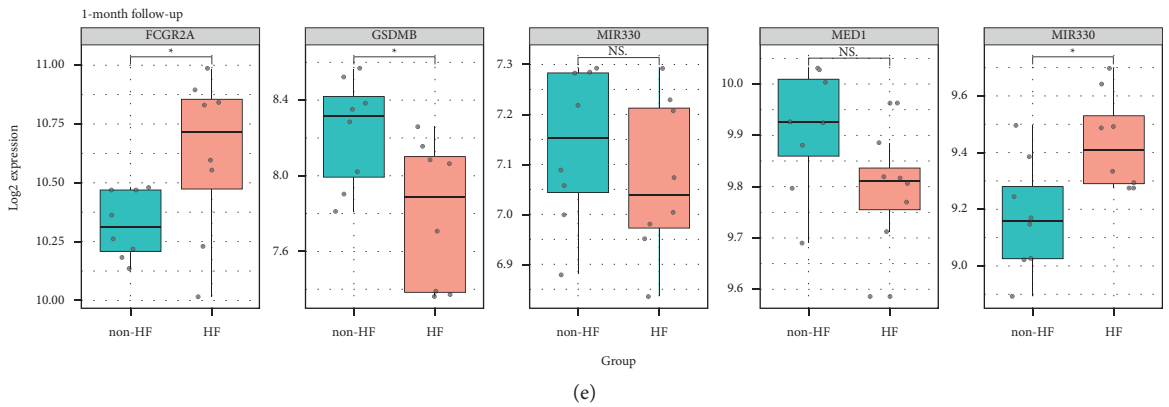

(e)

Figure 6: Identification of potential biomarkers and expression analysis for post-MI HF. (a) The Venn diagram of genes from the blue and yellow modules and DEGs from samples acquired at admission, discharge, and 1-month follow-up. (b) The Venn diagram of genes from dataset 1, dataset 2, and dataset 3. The expression levels of the 5 candidate genes in post-MI HF and non-HF patients at (c) admission, (d) discharge, and (e) 1-month follow-up. MI: myocardial infarction; HF: heart failure; DEGs: differentially expressed genes; NS: no significance. $^{*}P < 0.05$; $^{**}P < 0.01$; $^{***}P < 0.001$.

Table 1: The value of AUC for five candidate biomarkers of post-MI HF at all three time points.

	Admission	Discharge	1-month follow-up
FCGR2A	0.8472	0.8333	0.7969
GSDMB	0.9028	0.8148	0.8125
MIR330	0.8750	0.7963	0.6406
MED1	0.7361	0.8333	0.7500
SQSTM1	0.8611	0.7963	0.8438

AUC: the area under the curve; MI: myocardial infarction; HF: heart failure.

Underlying mechanisms may be involved in the deregulated expression of genes in calcium signaling, cardiac muscle contraction, and mitochondrial metabolic functions, accompanied by the downregulated expression of *Med1* [52]. Interestingly, Bai et al. [53] had reported that *Med1* in macrophages has an antiatherosclerotic role by suppressing the expression of proinflammatory genes via PPARγ-regulated transactivation [54, 55], suggesting its protective role in the cardiovascular system. Similarly, our study showed that *Med1* was significantly downregulated in patients with post-MI HF, indicating it may be served as an effective biomarker for HF.

MiRNAs are a class of small noncoding RNAs, which function as regulators of gene expression at the post-transcriptional level [56]. Ren et al. [57] demonstrated that overexpression of *MIR330* in acute coronary syndrome alleviated acute coronary syndrome by suppressing atherosclerotic plaque formation and enhancing vascular endothelial cell proliferation through the WNT signaling pathway. Moreover, Wei et al. [58] reported that upregulated *MIR330* might lead to stable carotid plaques by targeting Talin-1 in symptomatic carotid stenosis patients. However, in another research [59], overexpression of *MIR-330* was reported to promote left ventricular remodeling, increase myocardial infarction sizes, and aggravate myocardial ischemia-reperfusion injury during coronary recanalization. Different downstream pathways exert distinct biological effects, and the role of *MIR330* in post-MI HF remains to be further studied.

5. Limitation

Several limitations should be highlighted in our study. First, our study belongs to a secondary analysis of a cohort study. In the parent study [7], the study group and validation group were created, and microarrays were used to identify a set of genes associated with post-MI development HF in the early phase of MI, especially on admission. Differently, in our study, we focused on the study group of the parent study and performed a more in-depth analysis of the whole blood samples collected at admission, discharge, and 1-month follow-up to screen candidate biomarkers to predict post-MI HF in the early stage using differential expression analysis and WGCNA. More importantly, the developed external datasets on post-MI HF were introduced to confirm the candidate biomarkers, which facilitated increasing sample sizes and improving the reliability of results. Second, the datasets contained different cardiac models and pathologies and failed to include a strictly post-MI HF disease [5, 6], which posed a risk of introducing false positives and false negatives. However, these pathologies shared many underlying features and were likely to exhibit similar biomarker profiles [5]. Moreover, despite included external

datasets, our study still had relatively smaller sample sizes, which may have an effect on the stability of results, reduce the test efficiency, and cause possible bias to the research results; accordingly, external validation with a larger cohort is still required to demonstrate their reliability, and meanwhile, further studies should be required to elucidate the underlying mechanisms. In addition, our screening tools have their limitations; therefore, candidate biomarkers need further validation in clinical and experimental studies.

6. Conclusions

This study demonstrates that *FCGR2A*, *GSDMB*, *MIR330*, *MED1*, and *SQSTM1* are the candidate biomarkers for the progression of HF after MI, and the combination of *GSDMB* and *SQSTM1* has the highest predictive value. Following studies are required to further validate the predictive accuracy and clarify the underlying mechanisms.

Data Availability

All the data generated or analyzed during this study include the available Gene Expression Omnibus (GEO) database (Accession nos. GSE59867 and GSE42955) and a published article (DOI: 10.1161/CIRCULATIONAHA.119.045158).

Conflicts of Interest

The authors declare no conflicts of interest.

References

[1] P. G. Steg, O. H. Dabbous, L. J. Feldman et al., "Determinants and prognostic impact of heart failure complicating acute coronary syndromes," *Circulation*, vol. 109, no. 4, pp. 494–499, 2004.

[2] M. F. Minicucci, P. S. Azevedo, B. F. Polegato, S. A. R. Paiva, and L. A. M. Zornoff, "Heart failure after myocardial infarction: clinical implications and treatment," *Clinical Cardiology*, vol. 34, no. 7, pp. 410–414, 2011.

[3] Y. Gerber, S. A. Weston, M. Enriquez-Sarano et al., "Mortality associated with heart failure after myocardial infarction: a contemporary community perspective," *Circulation. Heart Failure*, vol. 9, no. 1, Article ID e002460, 2016.

[4] N. E. Ibrahim and J. L. Januzzi Jr., "Established and emerging roles of biomarkers in heart failure," *Circulation Research*, vol. 123, no. 5, pp. 614–629, 2018.

[5] M. Y. Chan, M. Efthymios, S. H. Tan et al., "Prioritizing candidates of post-myocardial infarction heart failure using plasma proteomics and single-cell transcriptomics," *Circulation*, vol. 142, no. 15, pp. 1408–1421, 2020.

[6] M. M. Molina-Navarro, E. Roselló-Lletí, A. Ortega et al., "Differential gene expression of cardiac ion channels in human dilated cardiomyopathy," *PLoS One*, vol. 8, no. 12, Article ID e79792, 2013.

[7] A. Maciejak, M. Kiliszek, M. Michalak et al., "Gene expression profiling reveals potential prognostic biomarkers associated with the progression of heart failure," *Genome Medicine*, vol. 7, no. 1, p. 26, 2015.

[8] F. Van de Werf, J. Bax, A. Betriu et al., "Management of acute myocardial infarction in patients presenting with persistent ST-segment elevation: the task force on the management of ST-segment elevation acute myocardial Infarction of the european society of cardiology," *European Heart Journal*, vol. 29, no. 23, pp. 2909–2945, 2008.

[9] N. M. Griffin, J. Yu, F. Long et al., "Label-free, normalized quantification of complex mass spectrometry data for proteomic analysis," *Nature Biotechnology*, vol. 28, no. 1, pp. 83–89, 2010.

[10] X. Han, R. Wang, Y. Zhou et al., "Mapping the mouse cell atlas by microwell-seq," *Cell*, vol. 172, no. 5, pp. 1091–1107, 2018.

[11] J. Tang, Y. Wang, Y. Luo et al., "Computational advances of tumor marker selection and sample classification in cancer proteomics," *Computational and Structural Biotechnology Journal*, vol. 18, pp. 2012–2025, 2020.

[12] B. Hervier, H. Devilliers, R. Stanciu et al., "Hierarchical cluster and survival analyses of antisynthetase syndrome: phenotype and outcome are correlated with anti-tRNA synthetase antibody specificity," *Autoimmunity Reviews*, vol. 12, no. 2, pp. 210–217, 2012.

[13] V. S. Hahn, H. Knutsdottir, X. Luo et al., "Myocardial gene expression signatures in human heart failure with preserved ejection fraction," *Circulation*, vol. 143, no. 2, pp. 120–134, 2021.

[14] A. Reinhardt, D. Stichel, D. Schrimpf et al., "Anaplastic astrocytoma with piloid features, a novel molecular class of IDH wildtype glioma with recurrent MAPK pathway, CDKN2A/B and ATRX alterations," *Acta Neuropathologica*, vol. 136, no. 2, pp. 273–291, 2018.

[15] G. C. Linderman, M. Rachh, J. G. Hoskins, S. Steinerberger, and Y. Kluger, "Fast interpolation-based t-SNE for improved visualization of single-cell RNA-seq data," *Nature Methods*, vol. 16, no. 3, pp. 243–245, 2019.

[16] M. Ringnér, "What is principal component analysis?" *Nature Biotechnology*, vol. 26, no. 3, pp. 303-304, 2008.

[17] S. Stewart, M. A. Ivy, and E. V. Anslyn, "The use of principal component analysis and discriminant analysis in differential sensing routines," *Chemical Society Reviews*, vol. 43, no. 1, pp. 70–84, 2014.

[18] Y. Song, J. A. Westerhuis, N. Aben, M. Michaut, L. F. A. Wessels, and A. K. Smilde, "Principal component analysis of binary genomics data," *Briefings in Bioinformatics*, vol. 20, no. 1, pp. 317–329, 2019.

[19] K. Tsuyuzaki, H. Sato, K. Sato, and I. Nikaido, "Benchmarking principal component analysis for large-scale single-cell RNA-sequencing," *Genome Biology*, vol. 21, no. 1, p. 9, 2020.

[20] M. E. Ritchie, B. Phipson, D. Wu et al., "Limma powers differential expression analyses for RNA-sequencing and microarray studies," *Nucleic Acids Research*, vol. 43, no. 7, p. e47, 2015.

[21] P. Langfelder and S. Horvath, "WGCNA: an R package for weighted correlation network analysis," *BMC Bioinformatics*, vol. 9, no. 1, p. 559, 2008.

[22] G. Wang, J. Yu, Y. Yang et al., "Whole-transcriptome sequencing uncovers core regulatory modules and gene signatures of human fetal growth restriction," *Clinical and Translational Medicine*, vol. 9, no. 1, p. 9, 2020.

[23] G. M. Wittenberg, J. Greene, P. E. Vértes, W. C. Drevets, and E. T. Bullmore, "Major depressive disorder is associated with differential expression of innate immune and neutrophil-related gene networks in peripheral blood: a quantitative review of whole-genome transcriptional data from case-control studies," *Biological Psychiatry*, vol. 88, no. 8, pp. 625–637, 2020.

[24] H. Furusawa, J. H. Cardwell, T. Okamoto et al., "Chronic hypersensitivity pneumonitis, an interstitial lung disease with distinct molecular signatures," *American Journal of Respiratory and Critical Care Medicine*, vol. 202, no. 10, pp. 1430–1444, 2020.

[25] L. Peña-Castillo, R. G. Mercer, A. Gurinovich et al., "Gene co-expression network analysis in Rhodobacter capsulatus and application to comparative expression analysis of Rhodobacter sphaeroides," *BMC Genomics*, vol. 15, no. 1, p. 730, 2014.

[26] M. R. Bakhtiarizadeh, B. Hosseinpour, M. Shahhoseini, A. Korte, and P. Gifani, "Weighted gene Co-expression network analysis of endometriosis and identification of functional modules associated with its main hallmarks," *Frontiers in Genetics*, vol. 9, p. 453, 2018.

[27] J. Piñero, À. Bravo, N. Queralt-Rosinach et al., "DisGeNET: a comprehensive platform integrating information on human disease-associated genes and variants," *Nucleic Acids Research*, vol. 45, no. D1, pp. D833–D839, 2017.

[28] Y. Zhou, B. Zhou, L. Pache et al., "Metascape provides a biologist-oriented resource for the analysis of systems-level datasets," *Nature Communications*, vol. 10, no. 1, p. 1523, 2019.

[29] G. D. Bader and C. W. Hogue, "An automated method for finding molecular complexes in large protein interaction networks," *BMC Bioinformatics*, vol. 4, no. 1, p. 2, 2003.

[30] D. C. Calverley, E. Brass, M. R. Hacker et al., "Potential role of platelet FcγRIIA in collagen-mediated platelet activation associated with atherothrombosis," *Atherosclerosis*, vol. 164, no. 2, pp. 261–267, 2002.

[31] D. J. Schneider, S. R. McMahon, G. L. Ehle, S. Chava, H. S. Taatjes-Sommer, and S. Meagher, "Assessment of cardiovascular risk by the combination of clinical risk scores plus platelet expression of FcγRIIa," *The American Journal of Cardiology*, vol. 125, no. 5, pp. 670–672, 2020.

[32] I. Chung and G. Y. H. Lip, "Platelets and heart failure," *European Heart Journal*, vol. 27, no. 22, pp. 2623–2631, 2006.

[33] Y. Sato, A. Yoshihisa, K. Watanabe et al., "Association between platelet distribution width and prognosis in patients with heart failure," *PLoS One*, vol. 15, no. 12, Article ID e0244608, 2020.

[34] P. Erne, J. Wardle, K. Sanders, S. M. Lewis, and A. Maseri, "Mean platelet volume and size distribution and their sensitivity to agonists in patients with coronary artery disease and congestive heart failure," *Thrombosis and Haemostasis*, vol. 59, no. 2, pp. 259–263, 1988.

[35] V. L. Serebruany, M. E. McKenzie, A. F. Meister et al., "Whole blood impedance aggregometry for the assessment of platelet function in patients with congestive heart failure (EPCOT Trial)," *European Journal of Heart Failure*, vol. 4, no. 4, pp. 461–467, 2002.

[36] V. L. Serebruany, S. R. Murugesan, A. Pothula et al., "Increased soluble platelet/endothelial cellular adhesion molecule-1 and osteonectin levels in patients with severe congestive heart failure. Independence of disease etiology, and antecedent aspirin therapy," *European Journal of Heart Failure*, vol. 1, no. 3, pp. 243–249, 1999.

[37] S. Feng, D. Fox, and S. M. Man, "Mechanisms of gasdermin family members in inflammasome signaling and cell death," *Journal of Molecular Biology*, vol. 430, no. 18 Pt B, pp. 3068–3080, 2018.

[38] Q. Chen, P. Shi, Y. Wang et al., "GSDMB promotes non-canonical pyroptosis by enhancing caspase-4 activity," *Journal of Molecular Cell Biology*, vol. 11, no. 6, pp. 496–508, 2019.

[39] Q. Wang, J. Wu, Y. Zeng et al., "Pyroptosis: a pro-inflammatory type of cell death in cardiovascular disease," *Clinica Chimica Acta*, vol. 510, pp. 62–72, 2020.

[40] A. C. Coniglio and R. J. Mentz, "Sleep breathing disorders in heart failure," *Heart Failure Clinics*, vol. 16, no. 1, pp. 45–51, 2020.

[41] E. Lee, M. Ramsey, A. Malhotra et al., "Links between objective sleep and sleep variability measures and inflammatory markers in adults with bipolar disorder," *Journal of Psychiatric Research*, vol. 134, pp. 8–14, 2021.

[42] L. M. Yu, W. H. Zhang, X. X. Han et al., "Hypoxia-induced ROS contribute to myoblast pyroptosis during obstructive sleep apnea via the NF-κB/HIF-1α signaling pathway," *Oxidative Medicine and Cellular Longevity*, vol. 2019, Article ID 4596368, 2019.

[43] S.-J. Jeong, X. Zhang, A. Rodriguez-Velez, T. D. Evans, and B. Razani, "p62/SQSTM1 and selective autophagy in cardiometabolic diseases," *Antioxidants & Redox Signaling*, vol. 31, no. 6, pp. 458–471, 2019.

[44] T. Lamark, S. Svenning, and T. Johansen, "Regulation of selective autophagy: the p62/SQSTM1 paradigm," *Essays in Biochemistry*, vol. 61, no. 6, pp. 609–624, 2017.

[45] D. Glick, S. Barth, and K. F. Macleod, "Autophagy: cellular and molecular mechanisms," *The Journal of Pathology*, vol. 221, no. 1, pp. 3–12, 2010.

[46] J. M. Bravo-San Pedro, G. Kroemer, and L. Galluzzi, "Autophagy and mitophagy in cardiovascular disease," *Circulation Research*, vol. 120, no. 11, pp. 1812–1824, 2017.

[47] L. Zhan, J. Li, and B. Wei, "Autophagy in endometriosis: friend or foe?" *Biochemical and Biophysical Research Communications*, vol. 495, no. 1, pp. 60–63, 2018.

[48] R. D. Kornberg, "Mediator and the mechanism of transcriptional activation," *Trends in Biochemical Sciences*, vol. 30, no. 5, pp. 235–239, 2005.

[49] Y. Jia, H.-C. Chang, M. J. Schipma et al., "Cardiomyocyte-specific ablation of Med1 subunit of the mediator complex causes lethal dilated cardiomyopathy in mice," *PLoS One*, vol. 11, no. 8, Article ID e0160755, 2016.

[50] C. Napoli, C. Schiano, and A. Soricelli, "Increasing evidence of pathogenic role of the Mediator (MED) complex in the development of cardiovascular diseases," *Biochimie*, vol. 165, pp. 1–8, 2019.

[51] D. D. Hall, K. M. Spitler, and C. E. Grueter, "Disruption of cardiac Med1 inhibits RNA polymerase II promoter occupancy and promotes chromatin remodeling," *American Journal of Physiology-Heart and Circulatory Physiology*, vol. 316, no. 2, pp. H314–H325, 2019.

[52] K. M. Spitler, J. M. Ponce, G. Y. Oudit, D. D. Hall, and C. E. Grueter, "Cardiac Med1 deletion promotes early lethality, cardiac remodeling, and transcriptional reprogramming," *American Journal of Physiology-Heart and Circulatory Physiology*, vol. 312, no. 4, pp. H768–H780, 2017.

[53] L. Bai, Z. Li, Q. Li et al., "Mediator 1 is atherosclerosis protective by regulating macrophage polarization," *Arteriosclerosis, Thrombosis, and Vascular Biology*, vol. 37, no. 8, pp. 1470–1481, 2017.

[54] N. Wang, L. Verna, N.-G. Chen et al., "Constitutive activation of peroxisome proliferator-activated receptor-γ suppresses pro-inflammatory adhesion molecules in human vascular endothelial cells," *Journal of Biological Chemistry*, vol. 277, no. 37, pp. 34176–34181, 2002.

[55] X. Y. Yang, L. H. Wang, T. Chen et al., "Activation of human T lymphocytes is inhibited by peroxisome proliferator-activated receptor γ (PPARγ) agonists," *Journal of Biological Chemistry*, vol. 275, no. 7, pp. 4541–4544, 2000.

[56] Y. Zhou, Z. F. Wang, W. Li et al., "Retracted: protective effects of microRNA-330 on amyloid β-protein production, oxidative stress, and mitochondrial dysfunction in Alzheimer's disease by targeting VAV1 via the MAPK signaling pathway," *Journal of Cellular Biochemistry*, vol. 119, no. 7, pp. 5437–5448, 2018.

[57] J. Ren, R. Ma, Z. B. Zhang, Y. Li, P. Lei, and J. L. Men, "Retracted: effects of microRNA-330 on vulnerable atherosclerotic plaques formation and vascular endothelial cell proliferation through the WNT signaling pathway in acute coronary syndrome," *Journal of Cellular Biochemistry*, vol. 119, no. 6, pp. 4514–4527, 2018.

[58] X. Wei, Y. Sun, T. Han et al., "Upregulation of miR-330-5p is associated with carotid plaque's stability by targeting Talin-1 in symptomatic carotid stenosis patients," *BMC Cardiovascular Disorders*, vol. 19, no. 1, p. 149, 2019.

[59] Z. Y. Liu, H. W. Pan, Y. Cao et al., "Downregulated microRNA-330 suppresses left ventricular remodeling via the TGF-β1/Smad3 signaling pathway by targeting SRY in mice with myocardial ischemia-reperfusion injury," *Journal of Cellular Physiology*, vol. 234, no. 7, pp. 11440–11450, 2019.

Hindawi
Evidence-Based Complementary and Alternative Medicine
Volume 2021, Article ID 9639131, 10 pages
https://doi.org/10.1155/2021/9639131

Research Article

Electroacupuncture Reverses CUMS-Induced Depression-Like Behaviors and LTP Impairment in Hippocampus by Downregulating NR2B and CaMK II Expression

Shuo Jiang,[1] **Zui Shen**,[2] **and Wenlin Xu**[1]

[1]*The First Affiliated Hospital of Zhejiang University of Traditional Chinese Medicine, Hangzhou 310006, China*
[2]*Zhejiang University of Traditional Chinese Medicine, Hangzhou 310053, China*

Correspondence should be addressed to Wenlin Xu; 447812723@qq.com

Received 14 September 2021; Accepted 13 October 2021; Published 12 November 2021

Academic Editor: Zhaohui Liang

Objective. Depression is a global mental health problem with high disability rate, which brings a huge disease burden to the world. Electroacupuncture (EA) has been shown to be an effective method for the treatment of depression. However, the mechanism underling the antidepressant effect of EA has not been clearly clarified. The change of synaptic plasticity is the focus in the study of antidepressant mechanism. This study will observe the effect of EA on LTP of hippocampal synaptic plasticity and explore its possible mechanism. *Methods*. The depression-like behavior rat model was established by chronic unpredictable mild stress (CUMS). EA stimulation (Hegu and Taichong) was used to treat the depressed rats. The depression-like behavior of rats was tested by weight measurement, open field test, depression preference test, and novelty suppressed feeding test. Long-term potentiation (LTP) was recorded at CA1 synapses in hippocampal slices by electrophysiological method. N-methyl-D-aspartate receptor subunit 2B (NR2B) and calmodulin-dependent protein kinase II (CaMK II) protein levels were examined by using western blot. *Results*. After the establishment of CUMS-induced depression model, the weight gain rate, sucrose preference rate, line crossing number, and rearing times of rats decreased, and feeding time increased. At the same time, the LTP in hippocampus was impaired, and the expressions of NR2B and CaMK II were upregulated. After EA treatment, the depression-like behavior of rats was improved, the impairment of LTP was reversed, and the expression levels of NR2B and CaMK II protein were downregulated. *Conclusion*. EA can ameliorate depression-like behaviors by restoring LTP induction, downregulating NR2B and CaMK II expression in CUMS model rats, which might be part of the mechanism of EA antidepressant.

1. Introduction

Depression is a major global mental health problem with high prevalence, recurrence rate, disability rate, and suicide risk. According to the WHO statistics, about 350 million people worldwide suffer from depression [1]. At present, depression has become the main cause of disability in the world and the second largest disease burden after ischemic heart disease [2,3]. The pathogenesis of depression is complex and unclear. Due to the lack of accurate and effective treatment targets, the curative effect of modern medicine in the treatment of depression is poor [4].

At present, the pathogenesis of depression is diverse, such as the regulation of monoamine neurotransmitters and their receptors in the brain, neuroendocrine disorders, neurotrophin malnutrition and nerve regeneration, changes in hippocampal neurons, cell signal transduction, and immune function [5]. In recent years, neural plasticity has gradually become a research hotspot [6–9]. More and more evidence shows that the regional specific changes of synaptic morphology and function are the result of chronic stress and depression. As the embodiment of system reorganization, neural plasticity continues through the normal development, maturation, and degradation of the nervous system. In

order to understand the essence of neurological or mental diseases, neuroplasticity is an important aspect that cannot be ignored [10, 11].

Long-term potentiation (LTP) is a form of synaptic plasticity. The intensity of LTP is related to synaptic activity [12, 13]. LTP is a phenomenon such that the intensity of synaptic response increases for a long time after short series of high-frequency stimulation. LTP is generally considered to be the physiological basis of brain learning and long-term memory processes [14]. In recent years, scholars have found that hippocampal LTP abnormalities not only affect learning and memory functions, but also may be related to the occurrence of psychological and behavioral abnormalities such as anxiety and depression [15]. When a large amount of Ca^{2+} flows into the postsynaptic membrane from cells, LTP can be induced and can last for hours to days [16]. Compared with healthy people, LTP plasticity in patients with depression was significantly impaired. This attenuation of synaptic plasticity is restored after remission of depressive state [17]. The impaired LTP plasticity was a potential pathomechanism and treatment target of depression.

The most critical factor in the initiation of synaptic plasticity is calcium (Ca^{2+}) influx through NMDA receptors [18]. Calcium influx triggers the activation of calcium/calmodulin-dependent protein kinase II (CaMK II) [19]. CaMK II can be regarded as an indicator of intracellular calcium level [20]. It is worth noting that when excess glutamate binds to NR2B, the overactivated extrasynaptic NR2B (inducing glutamate excitotoxicity) has strong calcium permeability [21]. In previous studies, we found that chronic unpredictable mild stress (CUMS) can lead to the overactivation of postsynaptic glutamate NMDA pathway in rat hippocampal astrocytes, resulting in the accumulation of glutamate and a large amount of Ca^{2+} flowing into neurons and astrocytes, resulting in intracellular calcium overload. NMDA receptor subunit NR2B plays an important role [22]. In CUMS-induced depressive rats, with the gradual aggravation of depressive symptoms, the expression of NR2B increased significantly and the content of intracellular calcium increased.

Electroacupuncture has a good antidepressant effect [23–25]. The mechanisms of electroacupuncture antidepressant include regulating neuropeptides and neurotransmitters [26], inhibiting HPA axis hyperactivity and inflammation [27], and restoring hippocampal synaptic plasticity [28]. Synaptic plasticity is the focus of electroacupuncture antidepressant research. Whether the effect of electroacupuncture on synaptic plasticity is related to NR2B is unclear. In this study, we explored the antidepressant effect of electroacupuncture and its possible mechanism by studying the effects of EA on hippocampal synaptic plasticity and NR2B protein level in CUMS rat models.

2. Materials and Methods

2.1. Animals. Healthy adult female Sprague Dawley (SD) rats (7-8 weeks old, weighing 220-250 g) were used in the experiment. All animals were obtained from Shanghai Experimental Animal Center, Chinese Academy of Sciences. Before further experiments, the rats were housed under a new environment (room temperature: $24 \pm 1^{\circ}C$; relative humidity: $45 \pm 15\%$; 12/12 h light/dark cycle) for one week. Study procedures were conducted according to the National Institutes of Health Guide for the Care and Use of Laboratory Animals. The research program and animal care followed the Committee's guidelines. 45 rats were randomly divided into three groups: control group ($n = 15$), CUMS group ($n = 15$), and CUMS + EA group ($n = 15$).

2.2. Chronic Unpredictable Mild Stress. Rats with depression-like behaviors were prepared by exposing the rats to chronic unpredictable mild stress [22]. The animals were isolated in separate cages and subjected to various stressors for 4 weeks. The stressors used in this study were water deprivation (24 hours), food deprivation (24 hours), tail pinch (1 minute), cold swim (4°C, 5 minutes), thermal stimulation (45°C, 5 minutes), foot shock (50 mV shock every 10 seconds for 30 seconds, a total of 15 shocks), and horizontal shaking (10 minutes). The animals were given a random stimulus at a random time every day and the same stressor was not applied consecutively over two days to ensure that the timing and manner of the stimulus occurrence were unpredictable. Rats in the CUMS group and CUMS + EA group were exposed to CUMS when rats in the control group received no other intervention except normal feeding (Figure 1).

2.3. Interventions. Rats in the CUMS + EA group received EA treatment after the establishment of rat depression model, while rats in CUMS group and the control group received grasping without other intervention (Figure 1). The rats were treated with electroacupuncture at the Siguan points including LI4 (Hegu) and LR3 (Taichong) on both sides for 3 weeks [24,29]. LI4 is located at the radial midpoint of the second metacarpal, and LR3 is located in the depression anterior to the junction of the first and second metatarsal.

Stainless steel needles of 0.18 mm diameter and 15 mm length (Suzhou Medical Appliance Factory, Suzhou, China) were inserted to a depth of approximately 2 mm of 4 acupuncture points. The electrical stimulation apparatus G6805-II (Qingdao Xinsheng Industrial Co., Ltd., Qingdao, China) was connected to needles at a 15 Hz continuous wave for 30 min each time. EA was performed once a day for the fifth week and once every other day for the sixth and seventh week.

2.4. Behavioral Tests. Behavioral tests were used to evaluate the establishment of the model and the efficacy of the antidepressant effects, including weight measurements, the open field test, the novelty suppressed feeding test, and the sucrose preference test. Record every week (days 0, 7, 14, 21, 28, 35, 42, and 49) to observe the physiological state during CUMS modeling.

2.4.1. Weight Measurement. The weight of the rats in each group was measured every week and the weight gain rate of the rats was calculated as follows: (weight increase ratio = (body weight at measurement - body weight on the first day)/body weight on the first day ×100%).

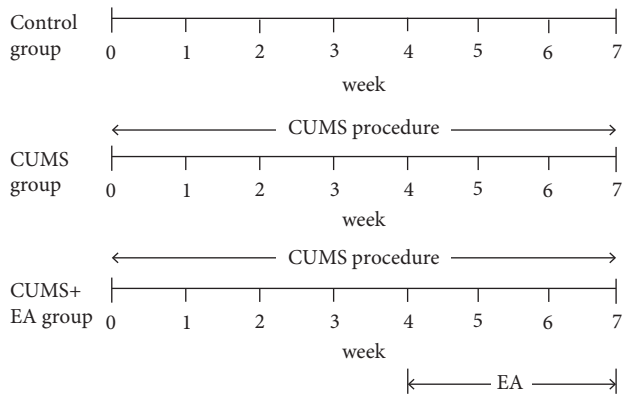

Figure 1: Experimental procedure.

2.4.2. Open Field Test (OFT). The apparatus was an 80 cm × 80 cm × 40 cm square wooden box, with black all around and covering the bottom. The box was placed in a soundproof room. The floor of the box was separated by white lines into 25 squares of equal size (each 16 cm × 16 cm).

Each animal was placed in the center of the box bottom, and a camera was used to observe and record the number of line crossings and number of rearings. After the behavior experiment of one rat, the feces and other residues in the box were cleaned immediately, and an alcohol cotton ball (75%) was used to wipe away the odor left by the previous rat to avoid interfering with the behavior of the next rat. Scoring: ① the number of line crossings: when more than three claws stepped into one square or the center of gravity fell into one square, the score was 1; ② number of rearings: when the forelimb left the horizontal ground, the score was 1.

2.4.3. Sucrose Preference Test. ① Preparation stage: two identical water bottles were placed in each cage at the same time. In the first 24 hours, two bottles of the same weight containing 1% sucrose water were used; in the second 24 hours, one bottle of 1% sucrose water and the other bottle of pure water of the same weight were used. Then, fasting and water prohibition were carried out for 24 hours. ② Experimental stage: each rat was given a bottle of 1% sucrose water and a bottle of purified water at the same time. After 24 hours, the consumption amounts of sucrose water and purified water were measured, and the preference rate of sucrose water was calculated as follows: (preference rate of sucrose water = consumption of sucrose water/(consumption of purified water + consumption of sugar water) ×100%).

2.4.4. Novelty Suppressed Feeding Test. After 24 hours of fasting, rats were placed in an open field made of plexiglass (76.5 × 76.5 × 40 cm). A small amount of food was placed in the center of the open field. During the experiment, the rats were magnified from any corner into the open field, and each rat was placed in the open field for 6 minutes. The whole process was recorded on a computer by a video camera above the open field. The time of the first bite was recorded to the exact second. If the rat did not eat the food in 6 minutes, the result was recorded as no bite.

2.5. Western Blot. At the end of the seven weeks, rats were anesthetized by intraperitoneal injection with sodium pentobarbital (40 mg/kg) and decapitated. The hippocampi were homogenized in ice-cold RIPA lysis buffer and were centrifuged. The supernatant was resolved and separated by sodium dodecyl sulfate-polyacrylamide gel electrophoresis (10% gel) and transferred onto polyvinylidene fluoride (PVDF) membranes. Next, the membranes were blocked with 5% skimmed milk at room temperature for two hours and incubated overnight at 4 °C with primary antibodies at a dilution of mouse anti-CaMK II 1 : 2000 (Affbiotech, Changzhou, China). After washing with phosphate-buffered solution, the membranes were incubated with the horseradish peroxidase-conjugated goat anti-mouse immunoglobulin G secondary antibody 1 : 2000 (SA00001-15, Protein-tech, USA) for one hour, followed by extensive washing. Proteins were analyzed with an enhanced chemiluminescence system (ECL). Optical densities were measured by ImageJ software (National Institutes of Health, Bethesda, MD, USA). GAPDH was used as the loading control.

2.6. Immunofluorescence. Brain tissues were cut into 35 μm thick slices until the entire structure of the hippocampus was detected. The slices were washed three times with 0.1 M phosphate-buffered saline (PBS) and incubated at room temperature for 20 minutes in 5% bovine serum albumin. Primary (overnight, 4°C) and secondary antibody incubations (one hour, room temperature) were carried out. The slices were washed three times with PBS after each incubation. Primary antibody was mouse anti-NR2B 1 : 200 (ab93610, Abcam). Secondary antibody was goat anti-mouse immunoglobulin G (Alexa Fluor 488) 1 : 2000 (ab150157, Abcam). Slices were coverslipped with a water-based mounting medium containing 4′,6-diamidino-2-phenylindole (DAPI) (KeyGEN BioTECH, Jiangsu, China). Stained sections were then observed by fluorescence microscopy (Olympus) and processed with ImageJ Software.

2.7. Long-Term Potentiation. At the end of the seven weeks, rats were anesthetized by intraperitoneal injection with sodium pentobarbital (40 mg/kg). After skin preparation, the rats were fixed on a stereotactic apparatus, then the hippocampus was drilled into them according to the coordinates (the position of stimulating electrode, P: -4.2 mm, R: 3.8 mm, and the position of recording electrode, P: -3.4 mm, R: 2.5 mm). The concentric circle stimulating electrode and metal recording electrode were gently inserted into the sites (Schaffer and CA1) of the hippocampus. The tip of the stimulating electrode was located in the hippocampal Schaffer collateral branches, and the tip of the recording electrode was located in the radiation layer of the CA1 area (located in hippocampal gyrus). When approaching the

predetermined position, the insertion depth of the stimulating electrode and recording electrode in the subcortical area was slowly and precisely adjusted. At the same time, a direct current test stimulation with a width of 100 μS and an intensity of 150 μA was given every 10 seconds until the best field excitatory postsynaptic response (fEPSP) was reached. Then, the position of the electrode was fixed, the stimulation intensity of the basic fEPSP was recorded at 30–40% of the maximum response, and the electrode was recorded for 20 minutes to ensure the stability of the basic synaptic transmission. The high-frequency stimulation (HFS) to induce LTP was 200 Hz. Each stimulation consisted of 20 pulses with a total of 3 stimulation strings and an interval of 30 s. LTP was induced by HFS and recorded for 60 minutes to observe the LTP characteristics. The recorded signals were collected and amplified with an MP150 16-channel multichannel electrophysiological signal acquisition and processing system and displayed and stored on a multimedia computer. The experimental data and images were processed by SigmaPlot software.

2.8. Statistics. Statistical Product and Service Solutions (SPSS) 24.0 was adopted for data analysis. The results are presented as the mean ± standard error of the mean (SEM). Data normality was assessed by the Kolmogorov-Smirnov test. For statistical analyses of the behavioral tests within each group, a paired *t*-test was employed. One-way ANOVA and Tukey–Kramer's post hoc test were used for LTP statistical analysis. A P value < 0.05 was considered statistically significant.

3. Results

3.1. Behavioral Tests. After modeling (on week 4), compared to the control group, the weight increase ratio of the rats in CUMS group and CUMS + EA group decreased significantly ($^{***}P < 0.001$, Figure 2(a)). During the treatment stage (from week 5 to week 7), the weight increase ratio of the rats in CUMS group decreased constantly (compared to the control group, $^{***}P < 0.001$; compared to the CUMS + EA group, $^{\#\#\#}P < 0.001$, Figure 2(a)). In contrast, this ratio in the rats in the CUMS + EA group increased constantly (compared to the CUMS group, $^{\#\#\#}P < 0.001$, Figure 2(a)). At week 7, there was a significant difference between the control group and the CUMS + EA group ($^{*}P < 0.05$, Figure 2(a)). The weight increase ratios of the rats in the CUMS + EA group were higher than that in the control group.

The line crossing number was not significantly different between groups on day 1. After modeling, the number of line crossings of rats in CUMS group and CUMS + EA group significantly decreased. In weeks 4, 5, and 6, compared to the control group, the number of line crossings of rats in the CUMS group and CUMS + EA group decreased significantly ($^{***}P < 0.001$, Figure 2(b)). In week 6, compared to the CUMS group, the number of line crossings of the rats in the CUMS + EA group began to increase gradually ($^{\#\#\#}P < 0.001$, Figure 2(b)). In week 7, the number of line crossings of the rats in CUMS + EA group increased constantly (compared to control group, $^{*}P < 0.05$; compared to CUMS group, $^{\#\#\#}P < 0.001$, Figure 2(b)).

The increase in the number of rearing was not significantly different between each of the groups on day 1. From week 4 to week 7, there were significant differences between groups ($^{*}P < 0.05$, $^{***}P < 0.001$, $^{\#\#}P < 0.01$, $^{\#\#\#}P < 0.001$, Figure 2(c)). The rising number had a gradual increase from week 5 to week 7 in the CUMS + EA group (compared to the CUMS group, $^{\#\#}P < 0.01$, $^{\#\#\#}P < 0.001$, Figure 2(c)). There was a significant decrease in the CUMS group throughout the whole experiment.

The sucrose preference ratio was not significantly different between each of the groups on day 1. From week 4 to week 6, compared to the control group, there were significant decreases in sucrose preference in the CUMS group and CUMS + EA group ($^{*}P < 0.05$, $^{**}P < 0.01$, $^{***}P < 0.001$, Figure 2(d)). On week 6, the sucrose preference ratio of the rats in the CUMS + EA group began to increase gradually (compared to the CUMS group, $^{\#\#}P < 0.01$, Figure 2(d)). In week 7, the sucrose preference ratio of the rats in the CUMS + EA group increased constantly. There was no difference between the control group and the CUMS + EA group.

The time to first bite was not significantly different between each of the groups on day 1. Compared to the control group, the time to first bite of the rats in the CUMS group and CUMS + EA group increased significantly from week 4 to week 6 ($^{**}P < 0.01$, $^{***}P < 0.001$, Figure 2(e)). Compared to the CUMS group, there was a gradual recovery from the rats in the CUMS + EA group from week 5 to week 7 ($^{\#\#}P < 0.01$, $^{\#\#\#}P < 0.01$, Figure 2(e)). There was no difference between the control group and the CUMS + EA group at week 7. The time to first bite of the rats in the CUMS group was at a high level throughout the whole experiment.

3.2. Western Blot Results. Protein expression of CaMK II was upregulated after modeling. Compared with the control group, the relative densities of CaMK II in the CUMS group and CUMS + EA group both increased significantly ($^{**}P < 0.01$ and $^{***}P < 0.001$, Figure 3(b)). After EA treatment, the relative density of CaMK II decreased. There was a significant difference between the CUMS group and the CUMS + EA group ($^{\#\#\#}P < 0.001$, Figure 3(b)).

3.3. Immunofluorescence Results. Compared to the control group, the expression of NR2B in cells increased significantly in the CUMS group ($^{***}P < 0.001$, Figure 4(b)). There was no difference in the expression of NR2B in the hippocampal cells between the control group and the CUMS + EA group. Compared to the CUMS group, the expression of NR2B in hippocampal cells decreased significantly in the CUMS + EA group ($^{\#\#\#}P < 0.001$, Figure 4(b)).

The immunofluorescence results showed that the expression of NR2B in the hippocampi of depressed rats was significantly upregulated. After EA treatment, the expression of NR2B decreased significantly.

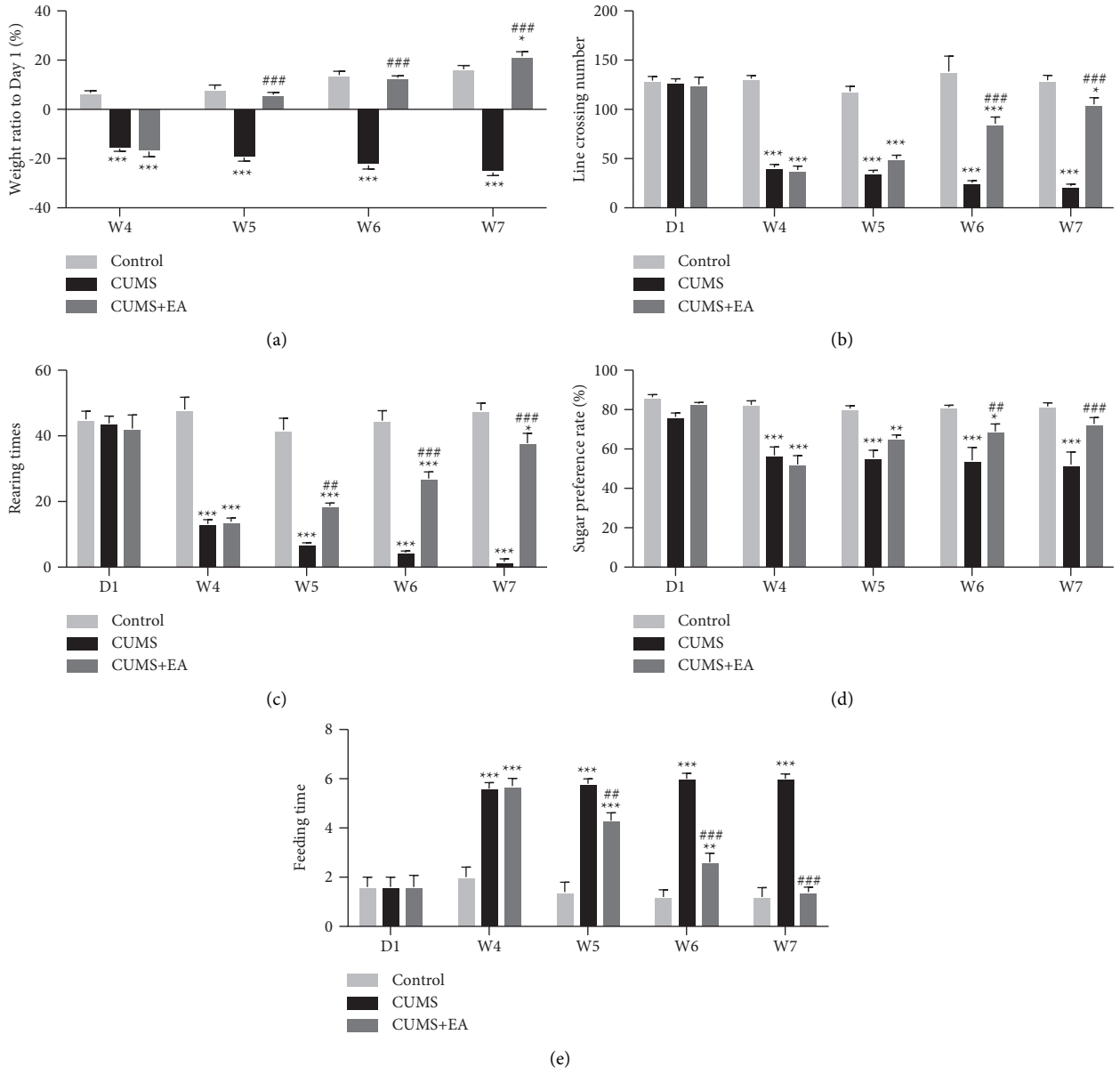

Figure 2: The effects of CUMS on body weight and behavior. (a) Body weight increase ratio of each group of rats at different time points ($W4$ = week 4, $W5$ = week 5, $W6$ = week 6, and $W7$ = week 7) relative to the ratio of the control group ($^{*}P < 0.05$, $^{***}P < 0.001$) and to the CUMS group ($^{\#\#\#}P < 0.001$). (b) Number of line crossings. (c) Number of rearings. (d) Sucrose preference rate. (e) Time to first bite for each group at different time points relative to the control group ($^{*}P < 0.05$, $^{**}P < 0.01$, and $^{***}P < 0.001$) and to the CUMS group ($^{\#\#}P < 0.01$ and $^{\#\#\#}P < 0.001$). Data are presented as the mean ± SEM, $n = 15$ for each group.

3.4. Long-Term Potentiation Results. We recorded evoked fEPSP in the stratum radiatum of the CA1 region in rats in the control group, CUMS group, and CUMS + EA group. High-frequency stimulation (HFS) induced stable reaction of LTP in high level in control rats and depression-like rats with EA. High-frequency stimulation (HFS) induced a weak reaction of LTP in depression-like rats. As time went on, the LTP of depression-like rats kept in a lower level than the rats in the other two groups. LTP was significantly restricted in depression-like rats (Figure 5(a)). Compared to the rats in the other two groups, the increase of fEPSP in rats' hippocampi in CUMS group was not obvious under the induction of short string high-frequency stimulation (HFS).

Figure 5(b) summarizes the change of fEPSP slope for three groups. There was a great difference between CUMS model rats and the other two groups ($^{***}P < 0.001$, $^{\#\#\#}P < 0.001$, Figure 5(b)). Compared to the control group, changes of fEPSP slope in CUMS group were smaller. Compared to CUMS group, the fEPSP slope in CUMS + EA group was significantly increased.

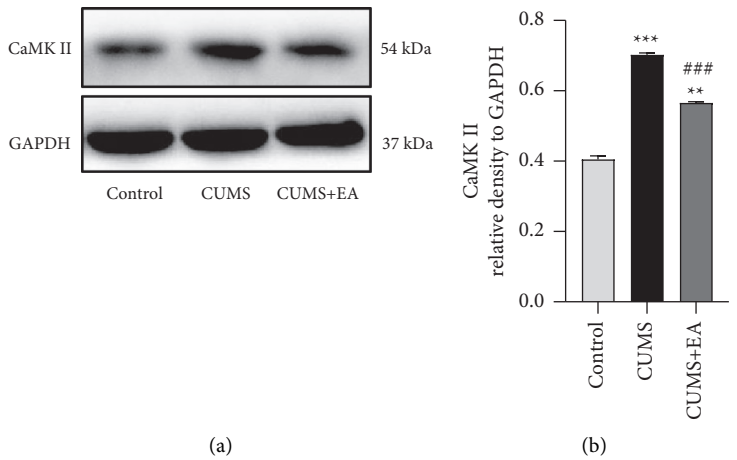

Figure 3: Expression of CaMK II in each group. (a) Western blot analyses of CaMK II protein levels in hippocampal homogenates. (b) Protein expression ratios relative to GAPDH. Data are given as the mean ± SEM, $n = 5$ for each group. $^{**}P < 0.01$ and $^{***}P < 0.001$ compared to the control group. $###P < 0.001$ versus the CUMS group.

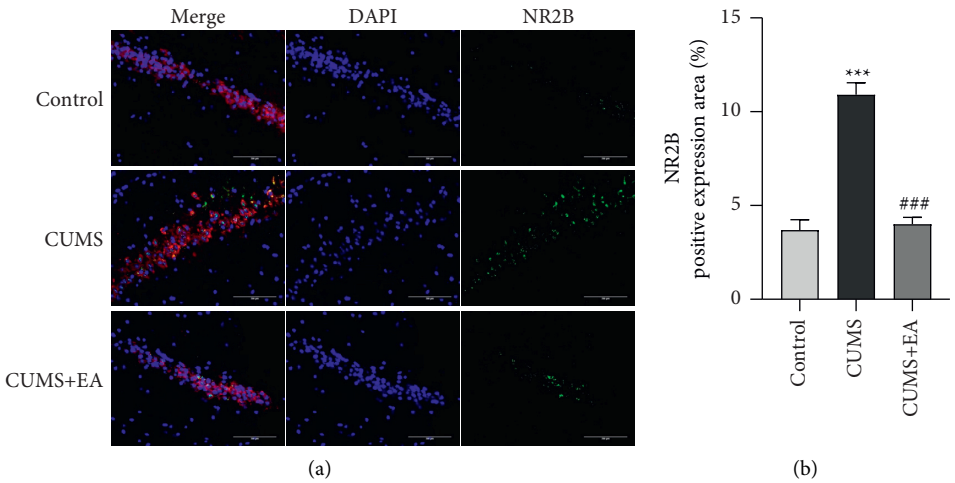

Figure 4: Expression of NR2B in each group. (a) Double-immunofluorescence micrographs showing NR2B-positive cells in the hippocampus of each group. (b) Positive expression area (%) of NR2B. Mean ± SEM, $n = 5$ for each group. $^{***}P < 0.001$ compared to the control group. $###P < 0.001$ compared to the CUMS group.

4. Discussion

In our former study, depression behavior (decreasing the weight gain rate, sucrose preference rate, line crossing number, and rearing times and increasing feeding time) was produced in CUMS-induced depressive rats. In our current study, the LTP in hippocampus was impaired, and the expressions of NR2B and CaMK II were upregulated in the CUMS-induced depression rats. After EA treatment, the depression-like behavior of rats was improved, and the change of LTP and the expression of NR2B and CaMK II were reversed. The results suggest that EA can improve depression-like behavior in model rats, which may be related to repairing LTP and downregulating NR2B and CaMK II.

Depression is a serious neurophysiological disorder with a complicated pathogenesis [5]. Most patients experience chronic stress for a long period of time. Some studies have shown that stressful life events, especially chronic agnostic stress events, are considered to be obvious predisposing factors of depression [30,31]. Chronic long-term stress has shown a dose-response relationship with depression. The more stressful life events there are, the higher the incidence rate of depression is, and the more severe the symptoms are [32]. Our team used CUMS to simulate the difficulties people encounter in real life, which is internationally recognized as an effective animal modeling method for depression [33]. The results showed that, with the extension of modeling time, compared with the control group, rats in the model group and treatment group showed decreases in their weight increase ratio, sucrose preference ratio, number of line crossings, and number of rearings. Moreover, the time to first bite in the open field of rats in the control group was reduced compared with that of the rats in the model and treatment groups.

Neurobiological studies have confirmed that the occurrence of depression is related to multiple brain regions [34,35], mainly the prefrontal cortex (PFC), anterior cingulate cortex (ACC), thalamus, hippocampus, amygdala,

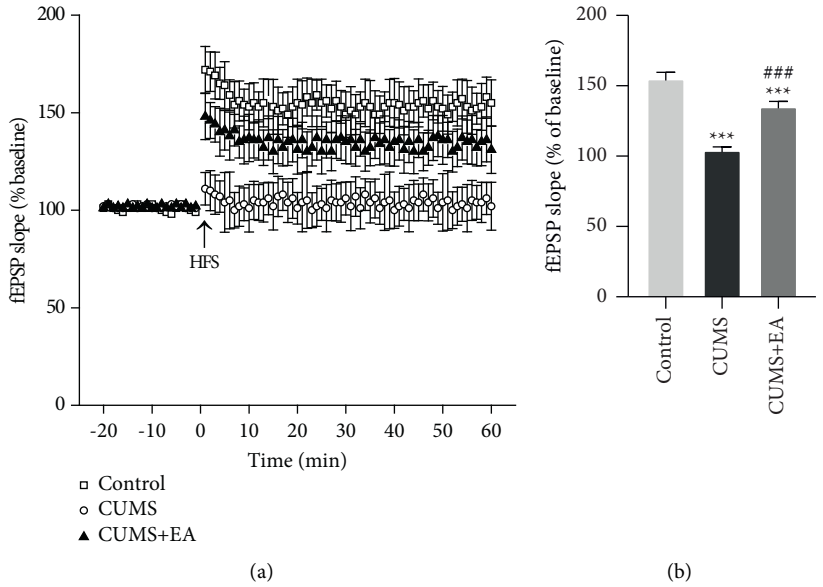

Figure 5: Induction of LTP in the hippocampal Schaffer collateral-CA1 in each group. (a) Time series plot of LTP in the three groups of rats. (b) Summarized data of the average slope change (normalized to the baseline value) from the three groups of rats. Means are shown and the SEM is displayed as error bars; $n = 5$ per group. $^{***}P < 0.001$ compared to the control group. $\#\#\#P < 0.001$ compared to the CUMS group. One-way ANOVA with Tukey–Kramer post hoc test.

and basal ganglia. Damage to the hippocampus is considered to be closely related to depression, posttraumatic stress disorder, and other mental diseases. The hippocampus is an important target for the study of excitatory-dependent synaptic plasticity in the mammalian brain [36]. Therefore, the current study of synaptic plasticity mainly focused on the hippocampus [37,38]. In this research, we also focused on the hippocampus to study the relationship between depression, synaptic plasticity, and EA treatment.

The antineuroplasticity changes in depression include decreased proliferation of neural stem cells, decreased survival of neuroblasts and immature neurons, damaged neural circuits, decreased neurotrophin levels, decreased spinal density, and dendritic retraction [39]. The impairment of LTP maintenance is mainly due to the dysfunction of protein synthesis and the formation of new neuronal structures [40]. Nerve spines, dendrites, and synapses are also missing in patients with depression or rodents [41], which provides a basis for LTP damage. In CUMS depressed rats, the LTP of CA3 - CA1 synapses induced by high-frequency stimulation decreased significantly, indicating that depression leads to LTP injury and cognitive decline [42]. Chronic stress can decrease the strength of this synapse and impairs LTP, while antidepressant treatment can reverse stress-induced changes [43]. This study shows that electroacupuncture can reverse LTP impairment in depressed rats. In the CUMS group, high-frequency stimulation failed to induce LTP, indicating that synaptic plasticity was impaired in CUMS-induced depression model rats. Compared with CUMS group, the fEPSP slope of CUMS + EA group was significantly increased and LTP was successfully induced, indicating that the damaged synaptic plasticity of depression rats after electroacupuncture treatment was restored.

LTP is a phenomenon such that the intensity of synaptic response increases for a long time after short series of high-frequency stimulation. When a large amount of Ca^{2+} flows into the postsynaptic membrane from cells, LTP can be induced for hours to days [16]. The occurrence of LTP requires the transport of intracellular calcium into the postsynaptic membrane, and a large number of Ca^{2+} receptor proteins are involved in the process of calcium transport [44], one of which is CaMK. CaMK is a protease that is highly expressed in brain tissue, especially in the hippocampus. It plays an important role in neural plasticity and memory formation. It is the most important Ca^{2+} receptor protein in neurons. Calcium influx triggers the activation of CaMK II [45]. CaMK II might be viewed as an indicator of intracellular calcium level [20]. There existed a close relationship between intracellular Ca^{2+} overload and cell death [46]. CaMK II plays an important role in synaptic plasticity, and it can connect with NMDARs.

Excitotoxicity induced by intracellular calcium overload caused by overexcitation of NMDA receptor is considered to be an important pathological mechanism of many nervous system diseases [47,48]. The most critical factor in the initiation of synaptic plasticity is Ca^{2+} influx through NMDA receptors [18]. NMDARs are known for their role in the induction of LTP [49]. Among the many subunits of NMDARs, NR2B is more important for inducing LTP. It is worth noting that when excess glutamate binds to NR2B, the overactivated extrasynaptic NR2B (inducing glutamate excitotoxicity) has strong calcium permeability [21]. The interaction between CaMK II and NR2B plays an important role in the formation of dendritic axons, the establishment of synaptic connections, and the formation and maturation of synapses. It is necessary for synaptic plasticity [50]. The

inhibition function of LTP and apoptosis of hippocampal neural cells were reversed with the decrease of NR2B and CaMK II protein levels [51]. In the current study, the relative ratio of CaMK II increased by CUMS and was reversed by EA.

The results showed that CaMK II and NR2B protein overexpression and LTP inhibition occurred in CUMS-induced depression model rats. After acupuncture treatment, LTP inhibition was effectively alleviated, and the expression levels of CaMK II and NR2B proteins were downregulated. These results suggest that the depression-like behavior of CUMS-induced depression rats is accompanied by the overexpression of CaMK II and NR2B proteins in hippocampus and the inhibition of LTP. Acupuncture and moxibustion can improve the above situation. The antidepressant mechanism of acupuncture may be related to inhibiting the overexpression of CaMK II and NR2B proteins, inducing stable LTP and improving synaptic plasticity.

5. Conclusion

EA can ameliorate depression-like behaviors by restoring LTP induction, downregulating NR2B and CaMK II expression in CUMS model rats, which might be part of the mechanism of EA antidepressant.

Data Availability

The raw data used to support the findings of this study are available from the corresponding author upon request.

Ethical Approval

The animal study was reviewed and approved by the Institutional Animal Care and Use Committee of Zhejiang Chinese Medical University.

Conflicts of Interest

The authors declare no conflicts of interest.

Authors' Contributions

SJ conceived and designed the experiments. ZS performed the experiments. WX analyzed the data and drafted the manuscript. All authors contributed to the article and approved the submitted version.

Acknowledgments

This work was supported by Natural Science Foundation of Zhejiang Province (grant no. LY18H270005), Guangdong Natural Science Foundation of Guangdong Province (grant no. 2019A1515012043), the National Natural Science Foundation of China (grant nos. 81503646, 81774411, and 82074522), and the Key-Area Research and Development Program of Guangdong Province (grant no. 2020B1111100007).

References

[1] K. Smith, "Mental health: a world of depression," *Nature*, vol. 515, no. 7526, p. 181, 2014.

[2] J. F. Greden, "The burden of recurrent depression: causes, consequences, and future prospects," *Journal of Clinical Psychiatry*, vol. 22, pp. 5–9, 2001.

[3] C. Holden, "Global survey examines impact of depression," *Science*, vol. 288, no. 5463, pp. 39-40, 2000.

[4] B. Metternich, D. Kosch, L. Kriston, M. Härter, and M. Hüll, "The effects of nonpharmacological interventions on subjective memory complaints: a systematic review and meta-analysis," *Psychotherapy and Psychosomatics*, vol. 79, no. 1, pp. 6–19, 2010.

[5] J. Dean and M. Keshavan, "The neurobiology of depression: an integrated view," *Asian Journal of Psychiatry*, vol. 27, pp. 101–111, 2017.

[6] T. Yang, Z. Nie, H. Shu et al., "The role of BDNF on neural plasticity in depression," *Frontiers in Cellular Neuroscience*, vol. 14, p. 82, 2020.

[7] W. Liu, T. Ge, Y. Leng et al., "The role of neural plasticity in depression: from Hippocampus to prefrontal cortex," *Neural Plasticity*, vol. 2017, Article ID 6871089, 9 pages, 2017.

[8] S. R. Wainwright and L. A. Galea, "The neural plasticity theory of depression: assessing the roles of adult neurogenesis and PSA-NCAM within the hippocampus," *Neural Plasticity*, vol. 2013, Article ID 805497, 11 pages, 2013.

[9] J. Wang, L. Jing, J.-C. Toledo-Salas, and L. Xu, "Rapid-onset antidepressant efficacy of glutamatergic system modulators: the neural plasticity hypothesis of depression," *Neuroscience Bulletin*, vol. 31, no. 1, pp. 75–86, 2015.

[10] A. May, "Experience-dependent structural plasticity in the adult human brain," *Trends in Cognitive Sciences*, vol. 15, no. 10, pp. 475–482, 2011.

[11] A. Pascual-Leone, A. Amedi, F. Fregni, and L. B. Merabet, "The plastic human brain cortex," *Annual Review of Neuroscience*, vol. 28, no. 1, pp. 377–401, 2005.

[12] J. Lisman, "Glutamatergic synapses are structurally and biochemically complex because of multiple plasticity processes: long-term potentiation, long-term depression, short-term potentiation and scaling," *Philosophical Transactions of the Royal Society of London - Series B: Biological Sciences*, vol. 372, no. 1715, 2017.

[13] R. Holderbach, K. Clark, J.-L. Moreau, J. Bischofberger, and C. Normann, "Enhanced long-term synaptic depression in an animal model of depression," *Biological Psychiatry*, vol. 62, no. 1, pp. 92–100, 2007.

[14] J. G. Howland and Y. T. Wang, "Chapter 8 Synaptic plasticity in learning and memory: stress effects in the hippocampus," *Progress in Brain Research*, vol. 169, pp. 145–158, 2008.

[15] S. Wang, Y. Yabuki, K. Matsuo et al., "T-type calcium channel enhancer SAK3 promotes dopamine and serotonin releases in the hippocampus in naive and amyloid precursor protein knock-in mice," *PLoS One*, vol. 13, no. 12, Article ID e0206986, 2018.

[16] T. Takeuchi, A. J. Duszkiewicz, and R. G. M. Morris, "The synaptic plasticity and memory hypothesis: encoding, storage and persistence," *Philosophical Transactions of the Royal Society B: Biological Sciences*, vol. 369, no. 1633, Article ID 20130288, 2014.

[17] M. Kuhn, F. Mainberger, B. Feige et al., "Erratum: state-dependent partial occlusion of cortical LTP-like plasticity in major depression," *Neuropsychopharmacology*, vol. 41, no. 11, p. 2794, 2016.

[18] W. N. Marsden, "Synaptic plasticity in depression: molecular, cellular and functional correlates," *Progress in Neuro-Psychopharmacology and Biological Psychiatry*, vol. 43, pp. 168–184, 2013.

[19] M. J. Byrne, J. A. Putkey, M. Neal Waxham, and Y. Kubota, "Dissecting cooperative calmodulin binding to CaM kinase II: a detailed stochastic model," *Journal of Computational Neuroscience*, vol. 27, no. 3, pp. 621–638, 2009.

[20] L. Li, M. I. Stefan, and N. Le Novère, "Calcium input frequency, duration and amplitude differentially modulate the relative activation of calcineurin and CaMKII," *PLoS One*, vol. 7, no. 9, Article ID e43810, 2012.

[21] Z. Zhang, C.-Z. Wang, X.-D. Wen, Y. Shoyama, and C.-S. Yuan, "Role of saffron and its constituents on cancer chemoprevention," *Pharmaceutical Biology*, vol. 51, no. 7, pp. 920–924, 2013.

[22] S. Jiang, Q. A. Zhang, Q. Guo, and Z. Di, "The glutamatergic system and astrocytic impairment in rat hippocampus: a comparative study of underlying etiology and pathophysiology of depression," *Journal of Integrative Neuroscience*, vol. 18, no. 4, pp. 387–392, 2019.

[23] X. Han, Y. Gao, X. Yin et al., "The mechanism of electroacupuncture for depression on basic research: a systematic review," *Chinese Medicine*, vol. 16, no. 1, p. 10, 2021.

[24] Q. Guo, X.-M. Lin, Z. Di, Q.-A. Zhang, and S. Jiang, "Electroacupuncture ameliorates CUMS-induced depression-like behavior: involvement of the glutamatergic system and apoptosis in rats," *Combinatorial Chemistry & High Throughput Screening*, vol. 24, no. 7, pp. 996–1004, 2021.

[25] H. Macpherson, B. Elliot, A. Hopton, H. Lansdown, and S. Richmond, "Acupuncture for depression: patterns of diagnosis and treatment within a randomised controlled trial," *Evidence-based Complementary and Alternative Medicine: eCAM*, vol. 2013, Article ID 286048, 11 pages, 2013.

[26] Y.-K. Kim, K.-S. Na, A.-M. Myint, and B. E. Leonard, "The role of pro-inflammatory cytokines in neuroinflammation, neurogenesis and the neuroendocrine system in major depression," *Progress in Neuro-Psychopharmacology and Biological Psychiatry*, vol. 64, pp. 277–284, 2016.

[27] X. Du and T. Y. Pang, "Is dysregulation of the HPA-Axis a core pathophysiology mediating Co-morbid depression in neurodegenerative diseases?" *Frontiers in Psychiatry*, vol. 6, p. 32, 2015.

[28] D. M. Bannerman, R. Sprengel, D. J. Sanderson et al., "Hippocampal synaptic plasticity, spatial memory and anxiety," *Nature Reviews Neuroscience*, vol. 15, no. 3, pp. 181–192, 2014.

[29] L. Jiang, H. Zhang, J. Zhou et al., "Involvement of hippocampal AMPA receptors in electroacupuncture attenuating depressive-like behaviors and regulating synaptic proteins in rats subjected to chronic unpredictable mild stress," *World Neurosurgery*, vol. 139, pp. e455–e462, 2020.

[30] C. Park, J. D. Rosenblat, E. Brietzke et al., "Stress, epigenetics and depression: a systematic review," *Neuroscience & Biobehavioral Reviews*, vol. 102, pp. 139–152, 2019.

[31] J. J. Strain, "The psychobiology of stress, depression, adjustment disorders and resilience," *World Journal of Biological Psychiatry*, vol. 19, no. 1, pp. S14–S20, 2018.

[32] Y. J. G. Karten, A. Olariu, and H. A. Cameron, "Stress in early life inhibits neurogenesis in adulthood," *Trends in Neurosciences*, vol. 28, no. 4, pp. 171-172, 2005.

[33] Y. Hao, H. Ge, M. Sun, and Y. Gao, "Selecting an appropriate animal model of depression," *International Journal of Molecular Sciences*, vol. 20, no. 19, 2019.

[34] E. Jesulola, C. F. Sharpley, and L. L. Agnew, "The effects of gender and depression severity on the association between alpha asymmetry and depression across four brain regions," *Behavioural Brain Research*, vol. 321, pp. 232–239, 2017.

[35] D. Szczepankiewicz, P. Celichowski, P. A. Kołodziejski et al., "Transcriptome changes in three brain regions during chronic lithium administration in the rat models of mania and depression," *International Journal of Molecular Sciences*, vol. 22, no. 3, 2021.

[36] T. V. P. Bliss and G. L. Collingridge, "A synaptic model of memory: long-term potentiation in the hippocampus," *Nature*, vol. 361, no. 6407, pp. 31–39, 1993.

[37] P. F. Smith, B. Truchet, F. A. Chaillan, Y. Zheng, and S. Besnard, "Vestibular modulation of long-term potentiation and NMDA receptor expression in the Hippocampus," *Frontiers in Molecular Neuroscience*, vol. 13, p. 140, 2020.

[38] R. A. J. Zwamborn, C. Snijders, N. An, A. Thomson, B. P. F. Rutten, and L. De Nijs, "Wnt signaling in the Hippocampus in relation to neurogenesis, neuroplasticity, stress and epigenetics," *Progress in Molecular Biology and Translational Science*, vol. 158, pp. 129–157, 2018.

[39] H. Eyre and B. T. Baune, "Neuroplastic changes in depression: a role for the immune system," *Psychoneuroendocrinology*, vol. 37, no. 9, pp. 1397–1416, 2012.

[40] H. Wang, B. Huang, W. Wang et al., "High urea induces depression and LTP impairment through mTOR signalling suppression caused by carbamylation," *EBioMedicine*, vol. 48, pp. 478–490, 2019.

[41] H. J. Kang, B. Voleti, T. Hajszan et al., "Decreased expression of synapse-related genes and loss of synapses in major depressive disorder," *Nature Medicine*, vol. 18, no. 9, pp. 1413–1417, 2012.

[42] F. Zhang, J. Luo, S. Min, L. Ren, and P. Qin, "Propofol alleviates electroconvulsive shock-induced memory impairment by modulating proBDNF/mBDNF ratio in depressive rats," *Brain Research*, vol. 1642, pp. 43–50, 2016.

[43] T. A. LeGates, M. D. Kvarta, J. R. Tooley et al., "Reward behaviour is regulated by the strength of hippocampus-nucleus accumbens synapses," *Nature*, vol. 564, no. 7735, pp. 258–262, 2018.

[44] N. Leresche and R. C. Lambert, "T-type calcium channels in synaptic plasticity," *Channels*, vol. 11, no. 2, pp. 121–139, 2017.

[45] S. Pepke, T. Kinzer-Ursem, S. Mihalas, and M. B. Kennedy, "A dynamic model of interactions of Ca^{2+}, calmodulin, and catalytic subunits of Ca2+/calmodulin-dependent protein kinase II," *PLoS Computational Biology*, vol. 6, no. 2, Article ID e1000675, 2010.

[46] S. Orrenius, V. Gogvadze, and B. Zhivotovsky, "Calcium and mitochondria in the regulation of cell death," *Biochemical and Biophysical Research Communications*, vol. 460, no. 1, pp. 72–81, 2015.

[47] A. Lau and M. Tymianski, "Glutamate receptors, neurotoxicity and neurodegeneration," *Pfluegers Archiv European Journal of Physiology*, vol. 460, no. 2, pp. 525–542, 2010.

[48] K. Szydlowska and M. Tymianski, "Calcium, ischemia and excitotoxicity," *Cell Calcium*, vol. 47, no. 2, pp. 122–129, 2010.

[49] M. Zeeman, X. Liu, O. Zhang, and J. Yan, "Role of N-methyl-d-aspartate receptor subunits GluN2A and GluN2B in auditory thalamocortical long-term potentiation in adult

mice," *Neuroscience Letters*, vol. 761, Article ID 136091, 2021.

[50] E. Nicholson and D. M. Kullmann, "T-type calcium channels contribute to NMDA receptor independent synaptic plasticity in hippocampal regular-spiking oriens-alveus interneurons," *The Journal of Physiology*, vol. 595, no. 11, pp. 3449–3458, 2017.

[51] L. Zhang, Z. W. Chen, S. F. Yang et al., "Retracted: micro RNA -219 decreases hippocampal long-term potentiation inhibition and hippocampal neuronal cell apoptosis in type 2 diabetes mellitus mice by suppressing the NMDAR signaling pathway," *CNS Neuroscience and Therapeutics*, vol. 25, no. 1, pp. 69–77, 2019.

Hindawi
Evidence-Based Complementary and Alternative Medicine
Volume 2021, Article ID 8475727, 7 pages
https://doi.org/10.1155/2021/8475727

Research Article

Effects of Chengqi Decoction on Complications and Prognosis of Patients with Pneumonia-Derived Sepsis: Retrospective Cohort Study

Zhipeng Huang,[1,2] Xiaoxin Cai,[2] Yao Lin,[2] Bojun Zheng,[3] Li Jian,[3] Yu Yi,[3] and Yang Guang[3]

[1]*Dongguan Hospital of Integrated Chinese and Western Medicine Affiliated to Guangzhou University of Traditional Chinese Medicine, Dongguan 523000, Guangdong, China*
[2]*Guangzhou University of Traditional Chinese Medicine, Guangzhou 510405, Guangdong, China*
[3]*Department of Critical Care Medicine, The Second Affiliated Hospital of Guangzhou University of Traditional Chinese Medicine, Guangzhou 510006, Guangdong, China*

Correspondence should be addressed to Li Jian; lijian426@gzucm.edu.cn, Yu Yi; yuyi27@mail2.sysu.edu.cn, and Yang Guang; yangguang@gzucm.edu.cn

Received 16 August 2021; Accepted 11 October 2021; Published 29 October 2021

Academic Editor: Zhaohui Liang

Purpose. A specific and efficacious method for treatment of pneumonia-derived sepsis is lacking. Chengqi decoction has been used for treatment of pneumonia-derived sepsis, but a clinical trial on patients with pneumonia-derived sepsis is lacking, a gap in the literature that we sought to fill. *Patients and Methods*. 282 patients with pneumonia-derived sepsis admitted to the intensive care unit of our hospital were selected. They were divided into the treatment group (141 cases) and control group (141 cases). Both groups underwent conventional treatment, but Chengqi decoction (in the form of enema) was given to the treatment group. Mortality, morbidity (abdominal distension and gastrointestinal bleeding), duration of antibiotic use, and use of vasoactive agents were documented 28 days after the drug was used. *Results*. The treatment group reduced mortality and morbidity (abdominal distension) ($P < 0.05$). After adjustment for significant covariates, 28-day survival was similar for the whole group (hazard ratio (HR): 0.48; 95% confidence interval (CI): 0.23–0.97; $P = 0.037$), for the subgroup ($n = 120$) with Acute Physiology and Chronic Health Evaluation II score ≥25 (HR: 0.180; 95% CI: 0.032–0.332; $P = 0.039$) and for the subgroup ($n = 66$) with N-terminal B-type natriuretic peptide <1800 (0.059, 0.004–0.979, and 0.019). There was no difference between the two groups for the duration of antibiotic use, major bleeding, or use of vasoactive drugs. *Conclusions*. Chengqi decoction improved 28-day survival and reduced the prevalence of abdominal distension in patients with pneumonia-derived sepsis.

1. Introduction

Sepsis is a clinical syndrome involving physiological, biological, and biochemical abnormalities and life-threatening organ dysfunction caused by a dysregulated inflammatory response to infection. Sepsis and septic shock are major healthcare problems [1]. Sepsis is considered a time-sensitive emergency because the best chance for a patient to survive is to be treated promptly [2]. However, the therapeutic effect of sepsis is not satisfactory, and the mortality rate is high [3].

Severe pneumonia is caused by infection by pathogenic microorganisms and is the main infection site of sepsis [4]. Unfortunately, patients suffering from severe sepsis often develop intestinal injury, which hampers treatment [5]. Therefore, exploration of any method that can cure both pneumonia and intestinal injury is rational and urgent.

Traditional Chinese medicine (TCM) theory dictates that diseases of the lung and those of the large intestine react with each other. The occurrence and development of sepsis is related to translocation of bacterial/endotoxins in the intestines [6, 7]. However, enemas containing TCM formulations have important roles in the immunomodulation of sepsis [8].

"Chengqi decoction" (CD) is a well-known TCM formulation used commonly in China. CD has an anti-inflammatory role in sepsis and prevents translocation of intestinal flora. TCM theory also states "Fei he da chang"—"the lung and the large intestine being interior-exteriorly related" [9]. If intestinal failure occurs, a large volume of toxins accumulates in the intestinal tract, so using enemas containing TCM formulations could become a new method of sepsis treatment [10].

We wished to ascertain if CD can be used to reduce the risk of death from pneumonia-derived sepsis (PDS), abdominal distension, gastrointestinal bleeding, use of vasoactive drugs, and duration of antibiotic use. We also sought to identify the characteristics of CD that could reduce the risk of death from PDS by 28 days by relieving gastrointestinal complications.

2. Patients and Materials

2.1. Study Design. We conducted a retrospective, observational cohort study and reported its results in accordance with Strengthening the Reporting of Observational Studies in Epidemiology (STROBE) guidelines [11].

2.2. Study Setting and Population. This study was conducted in a 15-bed intensive care unit (ICU) at a university-affiliated tertiary-care hospital. Patients admitted to the ICU between March 2014 and September 2019 were evaluated for study inclusion. For all patients, the characteristics documented at baseline were age, sex, weight, height, body mass index (BMI), diagnosis upon hospital admission, Sequential Organ Failure Assessment (SOFA) score, Acute Physiology and Chronic Health Evaluation II (APACHE II) score, heart rate, systolic blood pressure, diastolic blood pressure, mean arterial pressure, central venous pressure, white blood cell count, neutrophilic granulocyte percentage, pH, arterial partial pressure of oxygen (PaO_2), arterial partial pressure of carbon dioxide ($PaCO_2$), PaO_2/fraction of inspired oxygen (FiO_2), central (mixed) venous oxygen saturation ($ScvO_2$), as well as levels of lactate, N-terminal B-type natriuretic peptide (NT-proBNP), creatinine, blood urea nitrogen (BUN), C-reactive protein, and procalcitonin.

Patients (male or female) were aged >18 years. Patients were restricted to those with proven infections, defined as a positive blood culture or positive bronchoalveolar lavage fluid (BALF) culture and SOFA score ≥2; within 24 h of time, the culture was ordered [12]. Cultures positive for common contaminants (e.g., coagulase-negative staphylococci in one of two blood culture bottles and *Candida* species in BALF cultures) were excluded.

The control group comprised sepsis patients who had been in the ICU >7 days. Patients were excluded from the control group if they had a malignant tumor and advanced cachexia, had a tendency for severe bleeding or coagulation disorder, were pregnant or lactating, were infection of other systems, such as the urinary system and digestive tract infection, and had contraindications such as acute abdomen and severe cardiovascular diseases.

2.3. Variables. Mortality at 28 days was documented. "Abdominal distension" was defined as abdominal pressure >12 mmHg [13]. "Gastrointestinal bleeding" was defined as occult blood in feces or succus gastricus after exclusion of hemorrhoids or oral bleeding. The duration of antibiotic treatment and use of vasoactive agents were also documented.

2.4. Treatment. Conventional treatment (e.g., infection prevention, organ function support, resuscitation after shock, correction of disturbances in water and electrolyte balance, and maintenance of acid-base balance) and a lung-protective ventilation strategy (if necessary) were conducted for patients in both groups. On that basis, enema therapy using CD was added in the treatment group.

Rheum officinale, mirabilite, lobster sauce, Fructus Aurantii Immaturus, and *Magnolia officinalis* were the basic prescriptions for CD, with addition or subtraction of components as needed. Then, 200 mL of CD was fried strongly at 37°C. Enema containing CD was given once a day over 7 days.

2.5. Statistical Analyses. Patients were monitored after enrollment to 28 days or until death. Baseline characteristics were assessed within 24 h before enrollment. Data were analyzed using SPSS 25.0 (IBM, Armonk, NY, USA). Differences between the treatment group and control group were tested by analysis of an unpaired t-test, Wilcoxon's rank-sum test, x^2 test, or Fisher's exact test, as appropriate. Values are the mean ± SD. $P < 0.05$ was considered significant.

Univariate Cox regression was used to model the odds of 28-day mortality. For categorical variables, HRs reflected the increased odds of 28-day mortality for absence of the variables. For continuous variables, HRs reflected the increased odds of 28-day mortality for a one-unit increase in the baseline variable. The meaningful factors of single-factor analysis were introduced into the Cox multiple regression model. Factor screening was based on gradual introduction of a removal method to calculate the HR. In addition, we undertook multivariate Cox regression analysis to model the odds of 28-day mortality using the APACHE II score, NT-proBNP level, age, lactate level, PaO_2/FiO_2, $ScvO_2$, gastrointestinal bleeding, abdominal distension, and BMI as independent variables. A multivariate model using the APACHE II score, NT-proBNP level, and age was also used for analyses. Multivariate models reported HRs adjusted for all variables in the model. $P < 0.05$ was considered significant for all comparisons.

Table 1: Patient characteristics at baseline.

	Total	Chengqi decoction	Control	P
Patients (n)	282	141	141	—
Male (n (%))	162 (100)	75 (46.29)	87 (53.70)	0.223
Age (years)	67.00 (67.00–87.25)	67.00 (48.00–87.00)	67.00 (55.00–90.00)	0.484
BMI (kg/m^2)	23.66 (21.25–25.39)	24.22 (22.04–30.48)	23.31 (20.29–25.39)	0.006
APACHE II score	24.30 ± 7.20	25.23 ± 6.33	23.40 ± 8.00	0.222
SOFA score	12.00 (11.00–15.00)	13.00 (11.00–15.00)	12.00 (10.00–14.00)	0.189
HR (bpm)	94.00 (78.00–113.25)	88.00 (60.00–102.00)	97.00 (89.00–115.00)	0.010
SBP (mmHg)	115.00 (105.00–127.50)	115.00 (105.00–126.00)	111.00 (98.00–129.00)	0.803
DBP (mmHg)	49.50 (45.00–62.25)	50.00 (44.00–63.00)	49.00 (45.00–61.00)	0.771
MAP (mmHg)	72.00 (63.00–85.50)	72.00 (62.00–83.00)	72.00 (65.00–88.00)	0.688
CVP (mmHg)	8.95 ± 5.13	8.62 ± 5.52	8.28 ± 4.61	0.204
WBC	12.56 (4.19–23.90)	4.37 (3.72–23.90)	14.19 (7.19–23.90)	0.065
NG%	81.20 (80.10–87.68)	81.20 (79.10–87.30)	81.20 (80.10–89.90)	0.655
CRP (mg/L)	73.00 (45.75–85.00)	73.00 (34.00–89.00)	74.00 (54.00–84.00)	0.303
Procalcitonin (ng/mL)	5.11 (2.50–12.30)	3.12 (1.60–7.30)	8.10 (4.50–23.90)	≤0.001
PH	7.39 (7.30–7.44)	7.38 (7.29–7.43)	7.39 (7.30–7.46)	0.137
PaO_2	102.00 (91.00–126.00)	102.00 (91.00–126.00)	108.00 (90.40–126.00)	0.955
$PaCO_2$	46.90 (44.00–60.40)	45.80 (41.50–59.10)	46.90 (44.50–61.00)	0.101
PaO_2/FiO_2	232.77 ± 64.61	217.58 ± 63.68	247.95 ± 62.14	0.021
Lactate (mmol/L)	1.95 (1.30–3.30)	1.79 (1.30–2.60)	2.10 (1.30–4.00)	0.246
$ScvO_2$	64.31 ± 13.81	59.86 ± 13.79	68.69 ± 12.35	0.002
NT-proBNP (pg/mL)	5348.50 (2201.00–12180.00)	2392.00 (1569.00–7810.00)	7899.00 (3883.00–15015.00)	≤0.001
SCr (μmol/L)	184.39 (97.16–280.80)	113.39 (95.34–280.00)	188.00 (154.90–308.00)	0.106
BUN (mmol/L)	13.19 (8.80–16.41)	10.50 (7.58–15.20)	15.61 (12.00–19.66)	≤0.001

SOFA, sequential organ failure assessment; BMI, body mass index; APACHE, Acute Physiology and Chronic Health Evaluation; BUN, blood urea nitrogen; HR, heart rate; SBP, systolic blood pressure; DBP, diastolic blood pressure; MAP, mean arterial blood pressure; CVP, central venous pressure; WBC, white blood cell; NG%, neutrophilic granulocyte percentage; CRP, C-reactive protein; PaO_2, arterial partial pressure of oxygen; $PaCO_2$, arterial partial pressure of carbon dioxide; PaO_2/FiO_2, arterial partial pressure of oxygen/inspired oxygen fraction; $ScvO_2$, central (mixed) venous oxygen saturation; NT-proBNP, N-terminal B-type natriuretic peptide; SCr, serum creatinine.

Table 2: Primary and secondary outcomes.

	Total	Chengqi decoction	Control	P
Primary outcome				
Mortality (n (%))	96 (100)	33 (34.37)	63 (65.63)	0.03
Secondary outcomes				
Abdominal distension (n (%))	165 (100)	60 (36.36)	105 (63.64)	0.02
Gastrointestinal bleeding (n (%))	48 (100)	27 (56.25)	21 (43.75)	0.583
Duration of antibiotic use (days)	12.92 ± 5.31	13.23 ± 5.32	12.6 ± 5.23	0.332
Vasoactive agent (n (%))	180 (100)	84 (46.67)	96 (53.53)	0.391

3. Results

141 patients were enrolled in the CD group, and other 141 pneumonia-suffering patients were enrolled as controls. The characteristics of the two groups of patients at baseline are given in Table 1. The groups were well-matched, except for BMI ($P < 0.01$), heart rate ($P = 0.01$), procalcitonin level ($P < 0.01$), FiO_2/PaO_2 ($P = 0.02$), $ScvO_2$% ($P < 0.01$), NT-proBNP level ($P < 0.01$), and BUN level ($P < 0.01$) in the treatment group versus the control group.

Data for primary and secondary outcomes are given in Table 2. By day 28, the treatment group had a significant reduction in mortality (34.37% vs. 65.63%; $P = 0.03$) and prevalence of abdominal distension (36.36% vs. 63.64%; $P = 0.02$), as well as a nonsignificant increase in the prevalence of gastrointestinal bleeding (56.25% vs. 43.75%; $P = 0.58$). However, there was a nonsignificant reduction in use of vasoactive agents (46.67% vs. 53.53%; $P = 0.39$) and a nonsignificant decrease in duration of antibiotic use (13.23 ± 5.32 vs. 12.6 ± 5.23; $P = 0.33$).

The number of cases in our study was relatively small, so the survival rate at a given time could not be calculated, and Kaplan–Meier analysis was used. There was a significant difference in survival at 28 days between the two groups (Figure 1). Survival of the treatment group was significantly higher than that in the control group. The log-rank test was also carried out and also revealed a significant difference between the two groups ($P = 0.04$).

We studied the sum populations to determine the risk factors for death in each group. We applied univariate analysis of 10 potential risk factors with mortality as the dependent variable to each group (Figure 2), and the results are given in Table 3. We chose to include groups, the APACHE II score, NT-proBNP level, and age in the

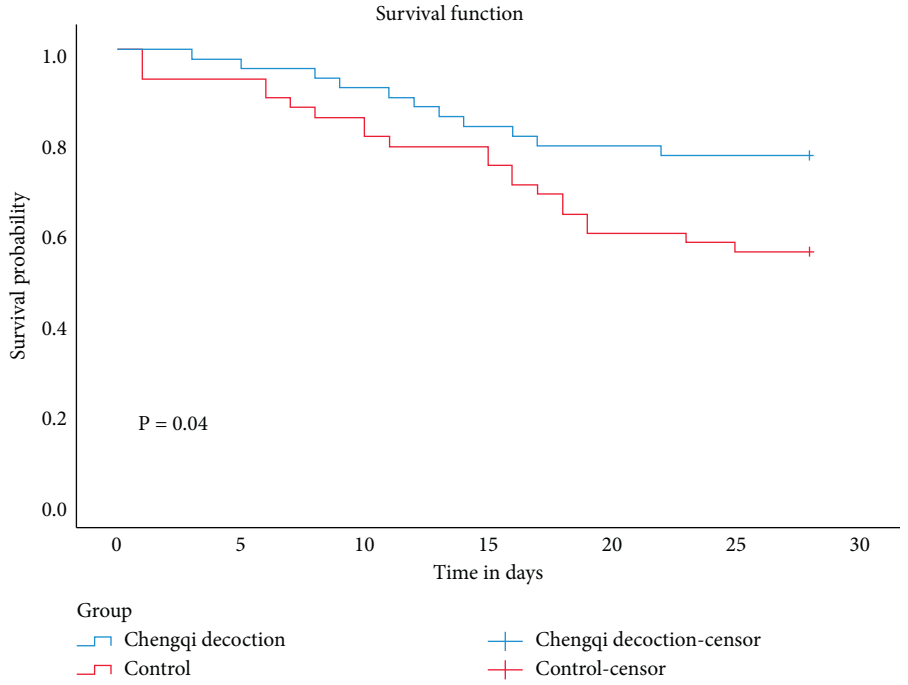

Figure 1: Kaplan–Meier estimate of survival on day 28 after adjustment by Cox regression analysis for the NT-proBNP level, age, and APACHE II score. The red line corresponds to the control group. The blue line corresponds to the Chengqi decoction group. The HR for probability of survival at 28 days was 0.48 (95% CI: 0.23–0.97; $P = 0.037$).

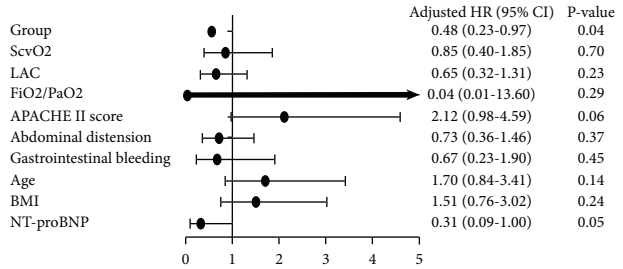

Figure 2: Univariate analysis of 10 potential risk factors for mortality as the dependent variable to each group.

Table 3: Univariate and multivariate models for overall survival on day 28.

Covariate at study entry	HR	95% CI	*P*
Univariate models			
NT-proBNP (pg/mL) (<1800 vs. ≥1800)	0.31	0.09–1.00	0.05
BMI (kg/m^2) (18–23 vs. >23 or <18)	1.51	0.76–3.02	0.24
Age (years) (≤65 vs. >65)	1.70	0.84–3.41	0.14
Gastrointestinal bleeding (present vs. absent)	0.67	0.23–1.90	0.44
Abdominal distension (present vs. absent)	0.73	0.36–1.46	0.37
APACHE II score (<25 vs. ≥25)	2.12	0.98–4.59	0.06
FiO_2/PaO_2 (<150 vs. ≥150)	0.04	0.01–13.60	0.29
Lactate (mmol/L) (<2 vs. ≥2)	0.65	0.32–1.31	0.23
$ScvO_2$ (%) (<75 vs. ≥75)	0.85	0.40–1.85	0.69
Group (Chengqi decoction vs. control)	0.48	0.23–0.97	0.04
Multivariate models			
Group (Chengqi decoction vs. control)	0.48	0.23–0.97	0.04*
APACHE II score (<25 vs. ≥25)	2.02	0.89–4.60	0.09
NT-proBNP (pg/mL) (<1800 vs. ≥1800)	0.34	0.09–1.19	0.09
Age (≤65 years vs. >65 years)	1.39	0.67–2.88	0.38

*Adjusted for: NT-proBNP, age, APACHE II score. HR, hazard ratio; NT-proBNP, N-terminal B-type natriuretic peptide; BMI, body mass index; FiO_2/PaO_2, inspired oxygen fraction/arterial partial pressure of oxygen; $ScvO_2$, central venous oxygen saturation; APACHE, Acute Physiology and Chronic Health Evaluation.

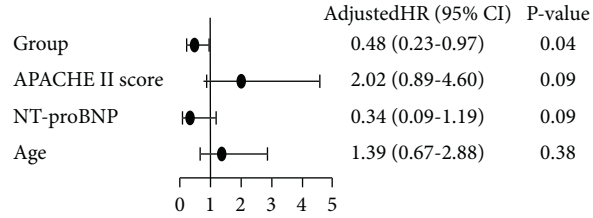

Figure 3: Multivariate analysis of four potential risk factors for mortality as the dependent variable to each group.

Table 4: Subgroup analyses of the risk of death in the Chengqi decoction group and control group at 28 days.

Subgroup	Chengqi decoction ($n = 141$)	Control ($n = 141$)	HR with Chengqi decoction (95% CI)	P
Age				
<65 years, *n*/total (%)	18/63	36/63	0.30 (0.08–1.08)	0.06
≥65 years, *n*/total (%)	15/78	27/78	0.45 (0.13–1.70)	0.21
APACHE II score				
<25, *n*/total (%)	27/78	42/84	0.53 (0.18–1.58)	0.25
≥25, *n*/total (%)	6/63	21/57	0.18 (0.03–1.02)	0.04
Lactate (mmol/L)				
<2, *n*/total (%)	15/81	24/60	0.34 (0.09–1.28)	0.10
≥2, *n*/total (%)	18/60	39/81	0.46 (0.14–1.56)	0.21
NT-proBNP (pg/mL)				
<1800, *n*/total (%)	3/54	6/12	0.06 (0.01–0.98)	0.02
≥1800, *n*/total (%)	30/87	57/129	0.67 (0.25–1.76)	0.41

HR, hazard ratio; APACHE, Acute Physiology and Chronic Health Evaluation.

multivariate model (Figure 3). After adjustment by univariable analysis, one covariate was found to be significant in the multivariate analysis, and the CD group showed a HR of 0.48 (95% confidence interval (CI): 0.23–0.97; $P = 0.04$).

Subgroup analyses for the HR of death at days 28 are given in Table 4. In the subgroup with an APACHE II score ≥25, the HR for probability of survival at 28 days was 0.18 (95% CI: 0.03–1.02; $P = 0.04$). In the subgroup with NT-proBNP <1800 npg/mL, the HR for the probability of survival at 28 days was 0.06 (95% CI: 0.01–0.98; $P = 0.02$).

4. Discussion

In recent years, understanding of sepsis and septic shock has gone from the tissue level to cellular and molecular levels, that is, from the theory of microcirculatory ischemia and hypoxia to the current theory of excessive release of inflammatory factors. Some scholars believe that the displacement of toxins is due to severe trauma, infection, shock, sepsis, and septic shock after surgery [14]. The pathogenesis and treatment of sepsis have been studied deeply [15, 16], but the incidence of sepsis and septic shock has not improved considerably. PDS remains a challenge in extracorporeal circuits for drug delivery in critically ill patients, and the mortality in this patient population is high [17]. However, TCM has obvious advantages over Western medicine in PDS treatment and conforms to the theory of treating pulmonary diseases through intestinal administration of drugs. Giving sepsis patients enema containing the CD formulation, combined with conventional treatment, could elicit the advantages of TCM and Western medicine [18, 19].

This was the first retrospective cohort trial investigating the effects of a 7-day course of CD treatment in patients with PDS. In this study, we chose to include groups, the APACHE II score, NT-proBNP level, and age which were filtered through single-factor analysis in the multivariate model. Meanwhile, we found that groups was the most important influencing factor, so we further analyzed the 28-day mortality between the CD group and control group. CD treatment relieved abdominal distension and led to a significant decrease in 28-day mortality. CD treatment did not increase the prevalence of gastrointestinal bleeding, duration of antibiotic use, or use of vasoactive agents. There was a significant decrease in 28-day mortality between the two groups, especially in the subgroup with an APACHE II score ≥25 and NT-proBNP <1800 pg/mL.

We demonstrated, through a retrospective cohort study, that CD could reduce 28-day mortality in patients with PDS. Improvement in the prognosis of patients with sepsis by CD has been demonstrated by several scholars [20–23]. In 2016, Mao et al. published a study on the effects of Xuan Bai Chengqi decoction (XCD) on lung compliance for patients with acute respiratory distress syndrome (ARDS). In that study, CD not only improved static compliance and dynamic compliance but also shortened the duration of parenteral nutrition and reduced the prevalence of complications and death [20]. CD also has a significant curative effect in severe pancreatitis, acute cholangitis, and myocardial ischemia [21–23].

Subgroup analyses revealed that patients with an APACHE II score ≥25 and NT-proBNP <1800 pg/mL were pronounced. These observations indicated that CD improved the prognosis of patients with PDS more significantly in the group with severe illness. In patients with good cardiac function, the effect of CD on the prognosis of patients with pneumonia and sepsis was more obvious and may have been associated with the increase of additional fluid in Chengqi decoction enema [24].

We found that CD could reduce the abdominal pressure of patients. This may have been related to the therapeutic characteristics of TCM formulations, which have multiple pathways, targets, and links. For example, Dachengqi decoction has been shown to be efficacious in ARDS treatment. Scholars have shown significant differences in the recovery time of intestinal sounds, anal exhaust time, regression of abdominal distension, as well as improvement in MODS and recovery time between two groups, indicating that Dachengqi decoction could improve the organ function of patients suffering from multiple-organ dysfunction syndrome [25–27]. Some scholars believe that TCM formulations have a good therapeutic effect on PDS and that they may act through the gastrointestinal tract. They have postulated that rhubarb can inhibit the activity of nitric oxide and inducible nitric oxide synthase to inhibit granulocyte aggregation and reduce free-radical production [28, 29]. Our study showed that CD may improve PDS through reduction of intraabdominal pressure without increasing the risk of gastrointestinal bleeding. The reduction in intraabdominal pressure may have been due to a reduction in the intestinal inflammatory response by CD.

Our study had three main limitations. First, it was conducted at a single institution. Second, the study cohort was small. Last, there was a potential selection bias to this retrospective study. Therefore, more prospective studies with larger cohorts are needed to support our findings.

5. Conclusion

In PDS, early administration of an enema containing CD for 7 days was safe and associated with improved survival without a significant increase in the risk of hemorrhage within the gastrointestinal tract. Our study was underpowered for an exploratory analysis to demonstrate survival benefit in patients with severe illness and good cardiac function.

Data Availability

The data used to support the findings of this study are included within the article.

Disclosure

Zhipeng Huang, Xiaoxin Cai, Yao Lin, and Bojun Zheng are the co-first authors..

Conflicts of Interest

The authors declare that they have no conflicts of interest.

Authors' Contributions

Bojun Zheng and Yu Yi designed the study. Zhipeng Huang, Xiaoxin Cai, and Yao Lin undertook the research and collected the data. Li Jian and Yang Guang analyzed the data. Li Jian wrote the manuscript. All authors contributed towards data analyses, drafting and revising the manuscript, and are accountable for all aspects of the work.

Acknowledgments

This work was supported by the Special Science and Technology Research of Guangdong Provincial Hospital of Traditional Chinese Medicine (YN 2014 PJR 203), the Guangdong Provincial Bureau of Traditional Chinese Medicine (20201157), the Guangdong Provincial Key Laboratory of Research on Emergency in TCM (2017B030314176), and the Science and Technology Planning Project of Guangdong Province of China (A2021100).

References

[1] M. Singer, C. S. Deutschman, C. W. Seymour, M. Shankar-Hari, D. Annane, and M. Bauer, "The third international consensus definitions for sepsis and septic shock (Sepsis-3)," *Journal of the American Medical Association*, vol. 315, no. 8, pp. 801–810, 2016.

[2] E. Abraham, "New definitions for sepsis and septic shock: continuing evolution but with much still to be done," *Journal of the American Medical Association*, vol. 315, no. 8, pp. 757–759, 2016.

[3] M. Cecconi, L. Evans, M. Levy, and A. Rhodes, "Sepsis and septic shock," *Lancet*, vol. 392, no. 10141, pp. 75–87, 2018.

[4] H. M. Ma, M. Ip, J. Woo et al., "Risk factors for drug-resistant bacterial pneumonia in older patients hospitalized with pneumonia in a Chinese population," *An International Journal of Medicine*, vol. 106, no. 9, pp. 823–829, 2013.

[5] S. A. Myers, L. Gobejishvili, S. Saraswat Ohri et al., "Following spinal cord injury, PDE4B drives an acute, local inflammatory response and a chronic, systemic response exacerbated by gut dysbiosis and endotoxemia," *Neurobiology of Disease*, vol. 124, pp. 353–363, 2019.

[6] B. H. Singer, R. P. Dickson, S. J. Denstaedt et al., "Bacterial dissemination to the brain in sepsis," *American Journal of Respiratory and Critical Care Medicine*, vol. 197, no. 6, pp. 747–756, 2018.

[7] B. W. Haak and W. J. Wiersinga, "The role of the gut microbiota in sepsis," *Lancet Gastroenterol Hepatol*, vol. 2, no. 2, pp. 135–143, 2017.

[8] T. B. Ahmad, L. Liu, M. Kotiw, and K. Benkendorff, "Review of anti-inflammatory, immune-modulatory and wound healing properties of molluscs," *Journal of Ethnopharmacology*, vol. 210, pp. 156–178, 2018.

[9] Q. Zhou and G. N. Verne, "Intestinal hyperpermeability: a gateway to multi-organ failure?" *Journal of Clinical Investigation*, vol. 128, no. 11, pp. 4764–4766, 2018.

[10] C. Smids, H. Talabur Horje, J. Drylewicz et al., "Intestinal T cell profiling in inflammatory bowel disease: linking T cell subsets to disease activity and disease course," *Journal of Crohn's and Colitis*, vol. 12, no. 4, pp. 465–475, 2018.

[11] E. Von Elm, D. G. Altman, M. Egger, S. J. Pocock, P. C. Gotzsche, and J. P. Vandenbroucke, "The strengthening the reporting of observational studies in epidemiology

(STROBE) statement: guidelines for reporting observational studies," *Annals of Internal Medicine*, vol. 147, no. 8, pp. 573–577, 2007.

[12] E. P. Raith, A. A. Udy, M. Bailey et al., "Prognostic accuracy of the SOFA score, SIRS criteria, and qSOFA score for in-hospital mortality among adults with suspected infection admitted to the intensive care unit," *Journal of the American Medical Association*, vol. 317, no. 3, pp. 290–300, 2017.

[13] M. L. N. G. Malbrain and I. E. De laet, "Intra-abdominal hypertension: evolving concepts," *Critical Care Nursing Clinics of North America*, vol. 24, no. 2, pp. 275–309, 2012.

[14] T. Van Der Poll, F. L. van de Veerdonk, B. P. Scicluna, and M. G. Netea, "The immunopathology of sepsis and potential therapeutic targets," *Nature Reviews Immunology*, vol. 17, no. 7, pp. 407–420, 2017.

[15] Y. Kakihana, O. Nishida, T. Taniguchi et al., "Efficacy and safety of landiolol, an ultra-short-acting beta 1-selective antagonist, for treatment of sepsis-related tachyarrhythmia (J-Land 3S): a multicentre, open-label, randomised controlled trial," *The Lancet Respiratory Medicine*, vol. 8, no. 9, pp. 863–872, 2020.

[16] K. E. Rudd, S. C. Johnson, K. M. Agesa et al., "Global, regional, and national sepsis incidence and mortality, 1990–2017: analysis for the global burden of disease study," *Lancet*, vol. 395, no. 10219, pp. 200–211, 2020.

[17] M. Hites, A. M. Dell'Anna, S. Scolletta, and F. S. Taccone, "The challenges of multiple organ dysfunction syndrome and extracorporeal circuits for drug delivery in critically ill patients," *Advanced Drug Delivery Reviews*, vol. 77, pp. 12–21, 2014.

[18] R. Zeng, Y. Zheng, R. Fan et al., "Si-ni-tang (a Chinese herbal formula) for improving immunofunction in sepsis: study protocol for a pilot randomized controlled trial," *Trials*, vol. 20, no. 1, p. 537, 2019.

[19] G. Z. Zhao, R. B. Chen, B. Li et al., "Clinical practice guideline on traditional Chinese medicine therapy alone or combined with antibiotics for sepsis," *Annals of Translational Medicine*, vol. 7, no. 6, p. 122, 2019.

[20] Z. Mao and H. Wang, "Effects of Xuanbai Chengqi decoction on lung compliance for patients with exogenous pulmonary acute respiratory distress syndrome," *Drug Design, Development and Therapy*, vol. 10, pp. 793–798, 2016.

[21] J. Guo, T. Jin, Z. Q. Lin et al., "Effect of Chaiqin Chengqi Decoction on cholecystokinin receptor 1-mediated signal transduction of pancreatic acinar cells in acute necrotizing pancreatitis rats," *Chinese Journal of Integrative Medicine*, vol. 21, no. 1, pp. 29–35, 2015.

[22] J. Guo, P. Xue, X. N. Yang et al., "The effect of Chaiqin Chengqi Decoction () on modulating serum matrix metalloproteinase 9 in patients with severe acute pancreatitis," *Chinese Journal of Integrative Medicine*, vol. 19, no. 12, pp. 913–917, 2013.

[23] L. Wang, Y. Li, Q. Ma et al., "Chaiqin Chengqi Decoction decreases IL-6 levels in patients with acute pancreatitis," *Journal of Zhejiang University-Science B*, vol. 12, no. 12, pp. 1034–1040, 2011.

[24] A. Kuriyama and S. Urushidani, "Continuous versus intermittent administration of furosemide in acute decompensated heart failure: a systematic review and meta-analysis," *Heart Failure Reviews*, vol. 24, no. 1, pp. 31–39, 2019.

[25] L. Y. Pan, Y. F. Chen, H. C. Li et al., "Dachengqi decoction attenuates intestinal vascular endothelial injury in severe acute pancreatitis in vitro and in vivo," *Cellular Physiology and Biochemistry: International Journal of Experimental Cellular Physiology, Biochemistry, and Pharmacology*, vol. 44, no. 6, pp. 2395–2406, 2017.

[26] M. Z. Xie, Q. H. Qi, S. L. Zhang, and M. M. Wei, "Effects of Dachengqi decoction () on morphological changes in enteric nerve system of rats with multiple organ dysfunction syndrome," *Chinese Journal of Integrative Medicine*, vol. 21, no. 8, pp. 624–629, 2015.

[27] J. Yang, M. Xiao, X. Wang et al., "Dachengqi decoction reduces the serum levels of mast cell tryptase and inflammatory cytokines in rabbits with post-cardiac arrest syndrome," *Xi Bao Yu Fen Zi Mian Yi Xue Za Zhi*, vol. 30, no. 10, pp. 1026–1029, 2014.

[28] S. L. Yang, Y. Jin, and L. Shen, "Effects of dachengqi decoction containing serum on the expressions of caveolin-1, eNOS, and NF-kappaB in lipopolysaccharide stimulated human bronchial epithelial cells," *Zhongguo Zhong Xi Yi Jie He Za Zhi*, vol. 32, no. 8, pp. 1088–1094, 2012.

[29] X. G. Sun, Q. Fan, and Q. R. Wang, "Effect of dachengqi decoction on expressions of TLR4 and TNF-alpha in the lung and the large intestine of mice with endotoxemia," *Zhongguo Zhong Xi Yi Jie He Za Zhi*, vol. 31, no. 2, pp. 244–248, 2011.

Hindawi
Evidence-Based Complementary and Alternative Medicine
Volume 2021, Article ID 5370214, 10 pages
https://doi.org/10.1155/2021/5370214

Research Article

Neuroprotective Effect of Moxibustion on Cerebral Ischemia/Reperfusion Injury in Rats by Downregulating NR2B Expression

Zhong Di,[1] **Qin Guo**,[1] **and Quanai Zhang**[2]

[1]*Department of Acupuncture and Moxibustion, The Third Affiliated Hospital of Zhejiang Chinese Medical University, Hangzhou, China*
[2]*Department of Acupuncture and Moxibustion, The Third School of Clinical Medicine, Zhejiang Chinese Medical University, Hangzhou, China*

Correspondence should be addressed to Quanai Zhang; tdcz2018@163.com

Received 30 August 2021; Revised 6 October 2021; Accepted 7 October 2021; Published 25 October 2021

Academic Editor: Zhaohui Liang

Objective. Stroke is a common and frequently occurring disease of the central nervous system, which is characterized by high mortality and a high disability rate. Moxibustion is a common method for treating stroke in traditional Chinese medicine, but its neuroprotective mechanism is unknown. N-Methyl-D-Aspartate Receptor Subunit 2B (NR2B) plays an important role in neuronal apoptosis. The objective of this study was to explore the mechanisms underlying the neuroprotective effect of moxibustion on cerebral ischemia/reperfusion (I/R) injury based on NR2B. *Methods*. Sprague–Dawley rats were randomly divided into 5 groups: the control group, I/R group, I/R + moxibustion group, I/R + Ro25-6981 (NR2B antagonist) group, and I/R + Ro25-6981 + moxibustion group. The cerebral ischemia/reperfusion model was induced by middle cerebral artery occlusion. Before the establishment of the model, the Ro25-6981 group received intraperitoneal injections of Ro25-6981, the moxibustion group received moxibustion, and the Ro25-6981 + moxibustion group received both interventions. The neurological dysfunction was evaluated by a neurological deficiency score (NDS). The infarct volume was examined by TTC (2,3,5-triphenyltetrazolium chloride) staining. The apoptosis rate of cerebral cells in the ischemic area was examined by TUNEL (terminal deoxynucleotidyl transferase-mediated dUTP nick end labeling) staining, and the expression of Bcl-2, Bax, and caspase-3 was observed by western blot. NR2B and JNK were also observed by western blot. *Results*. Compared with the I/R group, moxibustion significantly decreased the neurological deficiency score ($P < 0.05$) and the infarct rate ($P < 0.01$) in I/R rats which were similar to those in the Ro25-6981 group. After moxibustion treatment, there was a significant decrease in the apoptosis rate ($P < 0.001$) and the protein expression levels of Bax, caspase-3, and JNK ($P < 0.001$) and an increase in the expression of Bcl-2 ($P < 0.01$). Compared with the I/R group, moxibustion downregulated the expression of NR2B and decreased the activity of NR2B in the cerebral ischemia area ($P < 0.001$). *Conclusions*. Moxibustion can improve neurological dysfunction and decrease infarction area and neuronal apoptosis caused by cerebral ischemia/reperfusion in rats. Its neuroprotective mechanism may be related to downregulating the expression of NR2B.

1. Introduction

Stroke has a high mortality and disability rate [1, 2] and imposes huge economic burdens worldwide [3]. Among the types of stroke, ischemic stroke accounts for approximately 87% of cases [4]. Ischemia/reperfusion injury caused by cerebral ischemia or recanalization is an important cause of neurological deficits and neuronal apoptosis [5]. Cerebral ischemia/reperfusion injury involves a series of complex pathophysiological events, including inflammation, oxidative stress, abnormal energy metabolism, and synaptic and extrasynaptic glutamate accumulation, resulting in nerve cell death and neurological impairment. The important role of overactivated glutamate receptors, especially NMDA receptors, in cerebral ischemia/reperfusion injury has attracted wide attention [6, 7].

NMDA receptors are one of the three ionic receptors that mediate synaptic plasticity and contain multiple regulatory

subunits [8]. Among these subunits, NR2A and NR2B are considered to be the most important components of functional NMDA receptor ion channels. Because of the widespread expression of NR2A and NR2B in the brain, these subunits have received the most extensive research. NR2A and NR2B play opposite roles in regulating synaptic plasticity or neuronal survival and apoptosis [9, 10] and have different relationships with neuronal death and ischemic tolerance in the ischemic area [11]. Previous studies have shown that NR2B is more likely to promote neuronal death [12], while NR2A is beneficial for neuroprotection [9]. Therefore, it is critical to intervene with the NR2B receptor to reduce apoptosis caused by cerebral ischemia/reperfusion.

Inhibiting the NR2B-related neuronal apoptosis pathway through NR2B antagonists is a good choice. In many animal models of cerebral ischemia, NR2B antagonists, including ifenprodil, eliprodil, CP-101606, and Ro25-6981 [13], showed good neuroprotective effects. Fischer et al. performed electrophysiological experiments, toxicity experiments, intracellular Na^+, Ca^+ determination, and other experiments and showed that compared with ifenprodil, Ro25-6981 exhibited a better inhibitory effect [14]. Ro25-6981 is an activity-dependent, voltage-dependent, and noncompetitive antagonist of NR2B [15]. Preconditioning or postprocessing of NR2B antagonists can induce a protective effect on cerebral inflammation [16]. Ro25-6981 preconditioning could significantly increase the number of Bcl-2 cells and decrease the number of Bax cells in the brains of ischemic-hypoxic rats, reduce the death of hypoxic-ischemic cells, and enhance neuroprotective effects [17, 18].

Modern studies have shown that moxibustion has good protective effects on the brain and can reduce the inflammatory reaction and neuronal apoptosis induced by ischemia and hypoxia by reducing the synthesis and release of CO [19], increasing the activity of endogenous antioxidant enzymes [20], and inhibiting the activity of nitric oxide synthase [21]. In a rat model of middle cerebral artery occlusion (MCAO) induced cerebral ischemia, moxibustion could reduce the expression of caspase-9, caspase-3, and Bax and increase the expression of Bcl-2 in ischemic brain tissue to reduce the inflammatory reaction and neuronal apoptosis induced by ischemia and hypoxia [22, 23]. Moxibustion, as a nondrug therapy, can be combined with Ro25-6981 to reduce brain injury caused by cerebral ischemia/reperfusion and enhance neuroprotective effects, which is the starting point of this study.

In this study, the improved thread occlusion method was used to establish a rat model of middle cerebral artery occlusion. By comparing the effects of moxibustion and Ro25-6981 plus moxibustion on NR2B, JNK, Bax, Bcl-2, and caspase-3 in the cerebral ischemic area, we explored the neuroprotective effect of moxibustion on cerebral ischemia/reperfusion (I/R) injury and its possible mechanism.

2. Methods

2.1. Experimental Animals. Adult male Sprague Dawley rats weighing 200–220 g were obtained from the Animal Research Center of Zhejiang University of Traditional Chinese Medicine. Before further experiments, the rats were adapted to the new environment (room temperature: $23 \pm 2^{\circ}C$; relative humidity: $45 \pm 15\%$; light condition: 8 : 00 in the morning, light-dark cycle for 12 hours) for one week. The animals were kept in sterile propylene cages with aseptic shells, the shells were changed every day, and the rats received free water and food. All procedures in this study followed the guidelines for laboratory care and the use of animals at the National Institutes of Health. All the experimental methods were approved by the Animal Use and Nursing Committee of the Animal Research Center of Zhejiang University of Traditional Chinese Medicine. The research program and animal care followed the committee's guidelines.

2.2. Groups and Interventions. Eighty male SD rats were randomly divided into five groups: control group ($n = 16$), I/R group ($n = 16$), I/R + moxibustion group ($n = 16$), I/R + Ro25-6981 group ($n = 16$), and I/R + Ro25-6981 + moxibustion group ($n = 16$). The hair of the acupoint area was removed before treatment. In the I/R + moxibustion group and the I/R + Ro25-6981 + moxibustion group, the rats were fixed and treated with moxibustion. Rats in the other groups only underwent grasping stimulation.

Point selection was as follows: Baihui (GV 20), located at the top of the head near the midpoint of the line between the apex of the two ears, and Dazhui (GV 14), the posterior center between the 7^{th} cervical vertebra and the first thoracic vertebra.

Moxibustion was performed on fixed rats. Vaseline was applied to the point at which the hair was removed. Moxa strips with diameters of 4 mm were prepared. Light one end of the moxa strips. The ignition end of moxibustion was suspended at approximately 2 cm above the selected acupoint [24]. GV 20 was treated first, followed by GV 14. Moxibustion at each acupoint was performed for 15 minutes. Moxibustion treatment began 3 days before model induction and was performed once a day for 3 consecutive days.

Animals in the I/R + Ro25-6981 + moxibustion group and the I/R + Ro25-6981 group were given Ro25-6981 (5.0 mg/kg) (Sigma, R7150) dissolved in saline through the abdominal cavity (I.P.) [17]. The drug was given three times at intervals of 24 hours. Rats in the control group, ischemic model group, and moxibustion group were given the same amount of normal saline (1.0 ml/kg). The time and frequency of administration were the same as those in the Ro25-6981 group.

2.3. Animal Models. The cerebral ischemia model was established by middle cerebral artery occlusion (MCAO) [25]. The rats were anesthetized by intraperitoneal injection with sodium pentobarbital (40 mg/kg), the depth of anesthesia was evaluated by severe pain, and the rats had a slight reaction. In brief, after cervical skin preparation, a surgical incision was performed on the right neck. The right common carotid artery (CCA), external carotid artery (ECA), and

internal carotid artery (ICA) were separated. The proximal end of the ECA was cut and a nylon filament was inserted into the lumen of the ICA to block the origin of the middle cerebral artery (MCA). The average insertion depth of the thread occlusion was 18.5 ± 0.5 mm. After 2 hours, the thread was removed to establish reperfusion. In the control group, the operation procedure was the same as that in the I/R group, but no thread bolt was inserted, and the skin was sutured after disinfection.

Two hours after reperfusion, the neurological deficiency of rats was measured according to Zea Longa's scale [26]. Only animals with a score of 1 to 3 were considered successful.

2.4. Neurological Deficiency Score. The neurological deficiency score (NDS) was blindly evaluated at 6 h and 24 h after reperfusion. The NDS was based on a previously published scale [26] as follows: 0, no neurological deficit; 1, mild focal neurological deficit; 2, moderate focal neurological deficit; 3, severe focal deficit; and 4, lost consciousness or died. Only the animals with NDS of 1 to 3 at 2h after reperfusion were used in this study.

2.5. TTC Staining Measurement of the Infarct Region. Twenty-four hours after the operation, the animals were deeply anesthetized by an intraperitoneal injection of sodium pentobarbital (40 mg/kg). The rat brains were removed quickly and were sliced into 2.0 mm sections. TTC (1% w/V, Sigma, T8877) was prepared in PBS and water at 37°C until the TTC was dissolved. The slices were immersed in 10 ml of TTC solution and incubated at 37°C for 10 minutes. After TTC staining, normal tissue was red, and infarcted tissue was white. The infarct volume was measured by Image-Pro Plus 6.0. The infarct rate was calculated as follows: corrected infarct volume (%) = (contralateral hemispheric volume-ipsilateral noninfarct volume)/contralateral hemispheric volume × 100%.

2.6. TUNEL Staining to Detect Apoptosis in Rat Brains. The rat brain tissue was washed. Different concentrations of ethanol (50%, 70%, 85%, and 95% to anhydrous ethanol) were used to gradually dehydrate the tissue for 2 hours per stage. The tissue mass was made transparent, waxed, and embedded. Then, the tissue was sectioned to a thickness of 4–7 μm. The slices were dewaxed with xylene I for 10 minutes and xylene II for 10 minutes. The dewaxed slices were treated with 100% ethanol, 95% ethanol, 85% ethanol, 75% ethanol, and double-distilled water for 3 minutes each. Prepare TUNEL reaction solution (Beyotime, c1088) and add it to the sample. The antiquenching seals and DAPI (1 : 500 diluted) seals were stored at −20°C and photographed by fluorescence microscopy. The relevant parts of the samples were collected and analyzed by microscopy, and the apoptosis rate was calculated.

2.7. Western Blot Analysis. Appropriate amounts of rat brain tissue were lysed and homogenized, and the supernatant was collected. After SDS-PAGE, the proteins were transferred to NC membranes. The NC membrane was sealed with 5% skimmed milk powder. The membrane was incubated with the following primary antibodies in Tris-buffered saline plus Tween (TBST) at pH 7.4 overnight at 4°C : GAPDH (D16H11) XP Rabbit mAb (1 : 1000, CST, 5174), cleaved caspase-3 (1 : 1000, Affinity, AF7022), Bax/Bcl-2 (1 : 1000, Affinity, AF0120), JNK (1 : 1000, Affinity, AF6319), and p-JNK (1 : 1000, Affinity, AF3320). Sheep anti-rabbit HRP-labeled secondary antibody (1 : 1000, Beyotime, A0208) was diluted with a blocking solution containing 5% skimmed milk. The reaction proceeded for 2 hours at room temperature. After the secondary antibody reaction, the secondary antibody was recovered. Then, the membrane was washed with TBST 5–10 min 3 times. After ECL chemiluminescence treatment, the images were scanned by a Tanon-5200 imaging system.

2.8. Statistical Analysis. IBM SPSS 20.0 was used for statistical analysis. The data used in the figures are presented as the means ± standard error of the mean (mean ± SEM). Differences between multiple groups were compared by one-way analysis of variance (ANOVA). A paired t-test was used to compare the differences between the two groups. A value of $P < 0.05$ indicated that there was a difference in the comparison.

3. Results

3.1. Moxibustion Alleviated Neurological Deficits. Cerebral I/R injury led to disorders of neurological function, such as sensory and motor dysfunction. The NDS was evaluated according to the scoring criteria of Zea Longa. The higher the score, the more severe the dysfunction. The control group had no neurological deficit. Compared with the control group, the I/R group had obvious neurological deficits ($P < 0.05$). At 6 h after reperfusion, the NDS was not significantly different between the groups except for the control group. At 24 h after reperfusion, the NDS of I/R + moxibustion group was significantly lower compared with the I/R group ($P < 0.05$), and the I/R + Ro25-6981 group and I/R + Ro25-6981 + moxibustion group had similar results (Figure 1).

Figure 1 shows the neurological deficit score in each group. The higher the score, the more severe the dysfunction. $***P < 0.001$ compared to the control group; $^{\#}P < 0.05$ versus the I/R group.

3.2. Moxibustion Reduced the Brain Infarction. Due to the loss of dehydrogenase activity in the ischemic area, the TTC staining was pale, while normal tissue was crimson. As shown in Figure 2, the brain tissue in the control group was normal, and all the sections of each layer of brain tissue were dark red and infarcted; after ischemia/reperfusion in the I/R group, the color of the brain tissue on the nonischemic side was dark red, and the sections of each layer of brain tissue on the ischemic side showed pale areas of different sizes.

Compared with those in the I/R group, after I/R + moxibustion treatment, the pale area, total volume, and

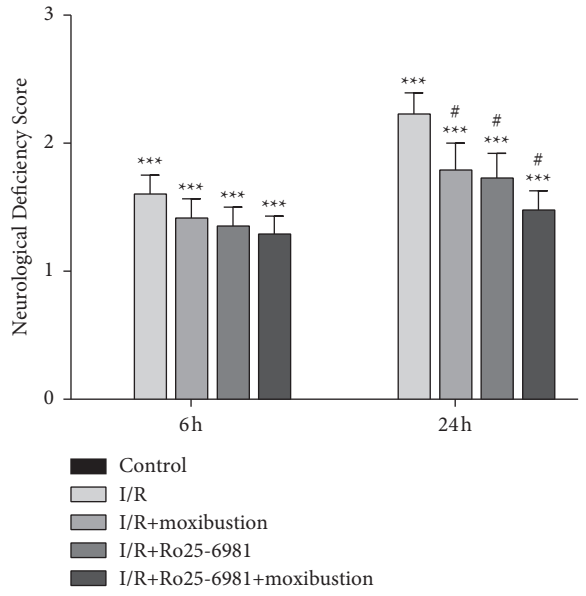

Figure 1: Neurological deficit score.

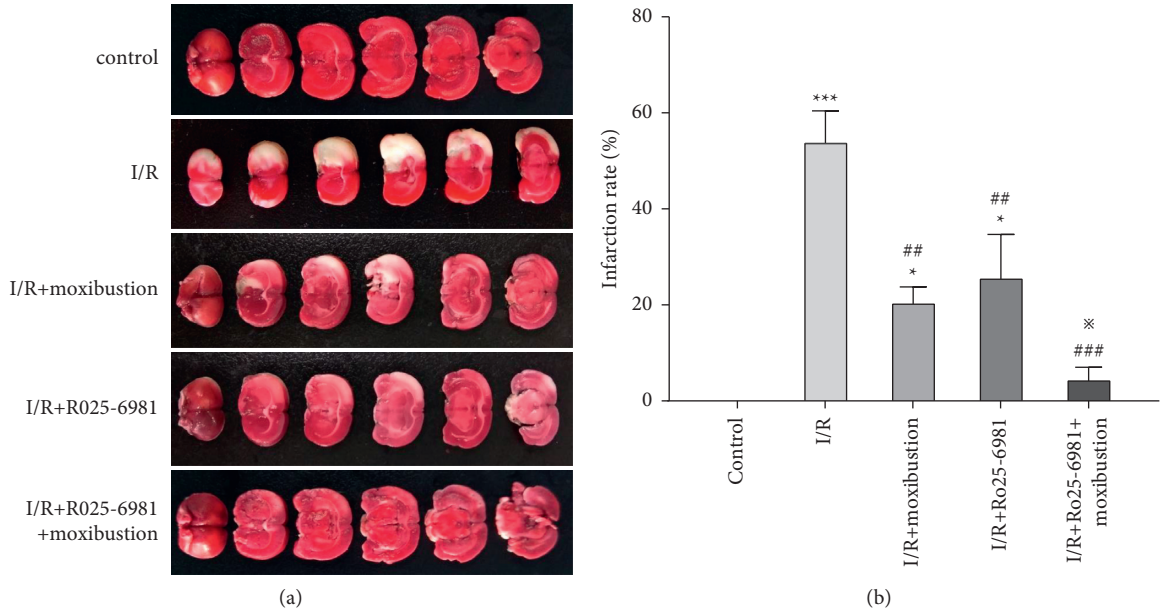

Figure 2: TTC staining of rat brain tissue in each group. (a) TTC staining of brain tissue in each group. The pink area is normal brain tissue, and the pale area is the ischemic infarcted area. (b) Cerebral infarction rates of rats in each group. $^{*}P < 0.05$ and $^{***}P < 0.001$ compared to the control group; $^{\#\#}P < 0.01$ and $^{\#\#\#}P < 0.001$ versus the I/R group; $^{※}P < 0.05$ versus the I/R + Ro25-6981 group.

infarction rates of ischemic lateral brain tissue were decreased ($P < 0.01$). Compared with I/R + Ro25-6981, after treatment with Ro25-6981 plus moxibustion, the pale area in each layer of ischemic brain tissue was significantly reduced, and the infarction rate was significantly decreased ($P < 0.05$).

3.3. Moxibustion Reduced Neuronal Apoptosis. The neuronal apoptosis induced by cerebral ischemia/reperfusion was examined by terminal deoxynucleotidyl transferase-mediated dUTP nick end labeling (TUNEL), which selectively labels apoptotic cells. Apoptotic cells were stained green by TUNEL, while normal cells were stained blue by DAPI. The results showed that there was no obvious apoptosis in the brain tissue of the control group, and the cells in the brain tissue sections were mainly blue. In the I/R group, the number of green cells increased significantly, suggesting that I/R led to a significant increase in the number of apoptotic cells on the ischemic side of the brain. The apoptosis rate in the ischemic area was significantly higher than that in the control group ($P < 0.001$) (Figure 3).

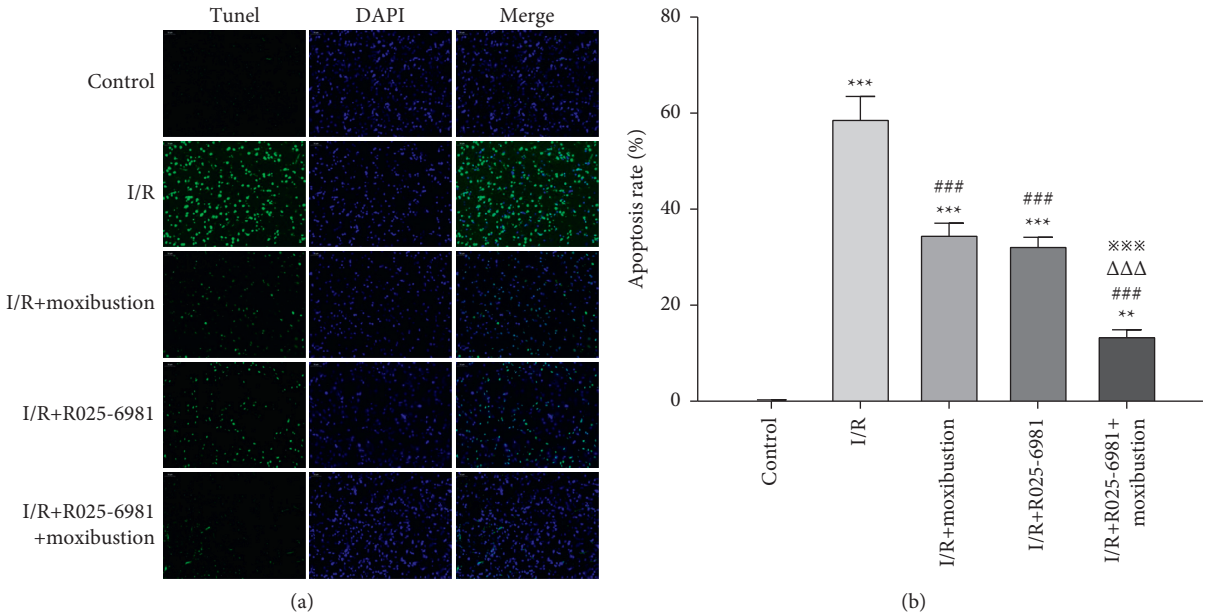

Figure 3: TUNEL staining of rat brain tissue in each group. (a) TUNEL staining results of brain tissue in each group. TUNEL staining showed green apoptotic cells while DAPI staining showed blue normal cells. The merged images included green apoptotic cells and blue normal cells. (b) Statistical analysis of the apoptosis rate on the injured side of the brain in each group. $^{**}P < 0.01$ and $^{***}P < 0.001$ compared to the control group; $^{\#\#\#}P < 0.001$ versus the I/R group; $^{\triangle\triangle\triangle}P < 0.001$ versus the I/R + moxibustion group; $^{※※※}P < 0.001$ versus the I/R + Ro25-6981 group.

Compared with that in the I/R group, the number of green cells in the I/R + Ro25-6981 group decreased, indicating that the number of apoptotic cells decreased and the apoptosis rate decreased ($P < 0.001$). Compared with I/R + Ro25-6981, after pretreatment with Ro25-6981 plus moxibustion, the number of green apoptotic cells decreased significantly, and the apoptosis rate decreased significantly ($P < 0.001$).

3.4. Moxibustion Upregulated the Protein Levels of Bcl-2 and Downregulated Bax and Caspase-3. After cerebral I/R injury, apoptosis-related factors are involved in the development of brain injury. Caspase-3 is involved in endogenous and exogenous apoptotic pathways. The Bcl-2 protein family is also involved in the process of apoptosis after cerebral ischemia, and there is a decrease in the antiapoptotic protein Bcl-2 and an increase in the proapoptotic protein Bax. The results showed that compared with the control group, the levels of caspase-3 and Bax in the I/R group increased significantly ($P < 0.001$), while the level of Bcl-2 decreased significantly ($P < 0.001$) (Figure 4).

Compared with the I/R group, the expression level of Bcl-2 in the I/R + moxibustion group increased significantly ($P < 0.01$), while the levels of caspase-3 and Bax decreased significantly ($P < 0.001$). Compared with the I/R group, the expression level of Bcl-2 in the I/R + Ro25-6981 group increased significantly ($P < 0.001$), while the levels of caspase-3 and Bax decreased significantly ($P < 0.001$). Compared with the I/R + Ro25-6981 group, the level of Bcl-2 in the I/R + moxibustion group increased more significantly ($P < 0.05$), and the expression level of caspase-3 decreased more significantly ($P < 0.01$). The level of Bax in the I/R + Ro25-6981 group decreased more significantly than that in the moxibustion group ($P < 0.001$).

3.5. Moxibustion Downregulated the Protein Levels of NR2B. NR2B is involved in the process of apoptosis in cerebral ischemia-reperfusion injury. The main subtypes of NMDA receptors include NR2A and NR2B. These subtypes play different roles in glutamate hyperstimulation. Excitotoxicity-dependent cell death is the result of overstimulation of NMDA receptors containing NR2B (rather than NR2A).

Figure 5 shows that compared with that in the control group, the gray value of NR2B in the I/R group increased, indicating that the expression of NR2B in brain tissue increased after I/R. The gray value of p-NR2B also increased significantly ($P < 0.001$), which indicated that the activity of NR2B increased significantly after I/R. Compared with that in the I/R group, the gray value of NR2B and p-NR2B in the I/R + moxibustion group decreased, indicating that the expression level of NR2B protein and activity of NR2B was downregulated after moxibustion treatment ($P < 0.001$). Compared with the I/R + moxibustion group, the gray value of NR2B and p-NR2B in the I/R + Ro25-6981 + moxibustion group decreased significantly, which indicated that the protein levels of NR2B and the activity of NR2B protein were downregulated significantly after Ro25-6981 + moxibustion treatment ($P < 0.001$).

3.6. Moxibustion Downregulated the Protein Levels of JNK. The c-Jun N-terminal kinase (JNK) signaling pathway plays an important role in cerebral ischemia/reperfusion injury

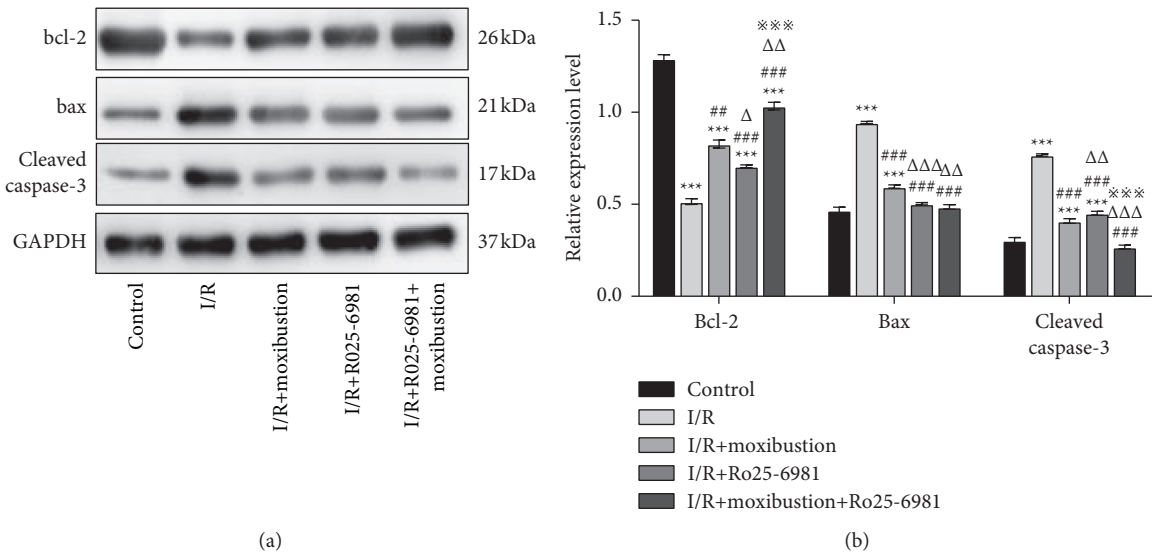

Figure 4: Analysis of the relative expression of apoptosis-related proteins in brain tissue in each group. (a) Protein expression of cleaved caspase-3, Bcl-2, and Bax on the ischemic side in each group. (b) Relative protein expression of Bcl-2, Bax, and cleaved caspase-3 on the ischemic side in each group. $^{***}P < 0.001$ compared to the control group; $^{\#\#}P < 0.01$ and $^{\#\#\#}P < 0.001$ versus the I/R group; $^{\triangle}P < 0.05$, $^{\triangle\triangle}P < 0.01$, and $^{\triangle\triangle\triangle}P < 0.001$ versus the I/R + moxibustion group; $^{※※※}P < 0.001$ versus the I/R+ Ro25-6981 group.

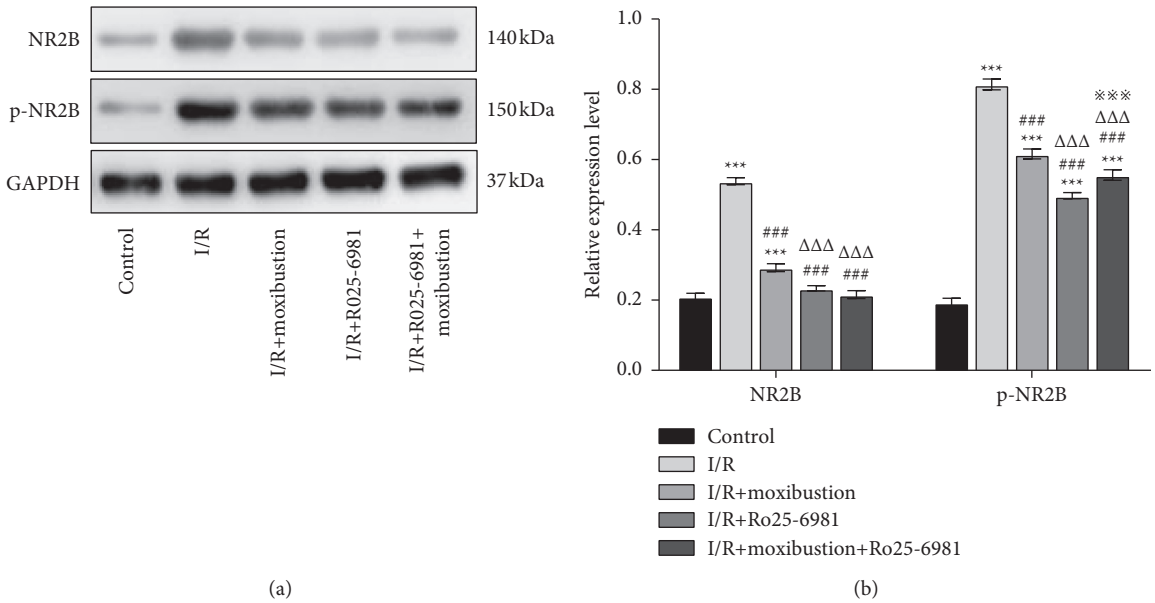

Figure 5: Relative expression of NR2B and p-NR2B protein in brain tissue of each group. (a) Protein expression of NR2B and p-NR2B in the injured brain tissue of each group. (b) Relative protein expression levels of NR2B and p-NR2B in the injured brain tissue of each group. $^{***}P < 0.001$ compared to the control group; $^{\#\#\#}P < 0.001$ versus the I/R group; $^{\triangle\triangle\triangle}P < 0.001$ versus the I/R + moxibustion group; $^{※※※}P < 0.001$ versus the I/R + Ro25-6981 group.

and neuronal apoptosis. Cerebral ischemia/reperfusion activates the JNK signaling pathway, which can control the differential expression of apoptosis-related genes [27].

Figure 6(a) shows that compared with that in the control group, the gray value of JNK and p-JNK in the I/R group increased, which indicated that the protein level of JNK and the activity of JNK increased significantly after I/R (($P < 0.001$). Compared with that in the I/R group, the gray value of JNK and p-JNK in the I/R + moxibustion group decreased, indicating that the expression level of JNK protein and activity of JNK were downregulated after moxibustion treatment ($P < 0.001$). Compared with the I/R + moxibustion group, the gray value of JNK increased and p-JNK decreased significantly in the I/R + Ro25-6981+moxibustion group, which indicated that the protein level of JNK increased ($P < 0.05$), but the activity of JNK protein was downregulated significantly after Ro25-6981 + moxibustion treatment ($P < 0.001$).

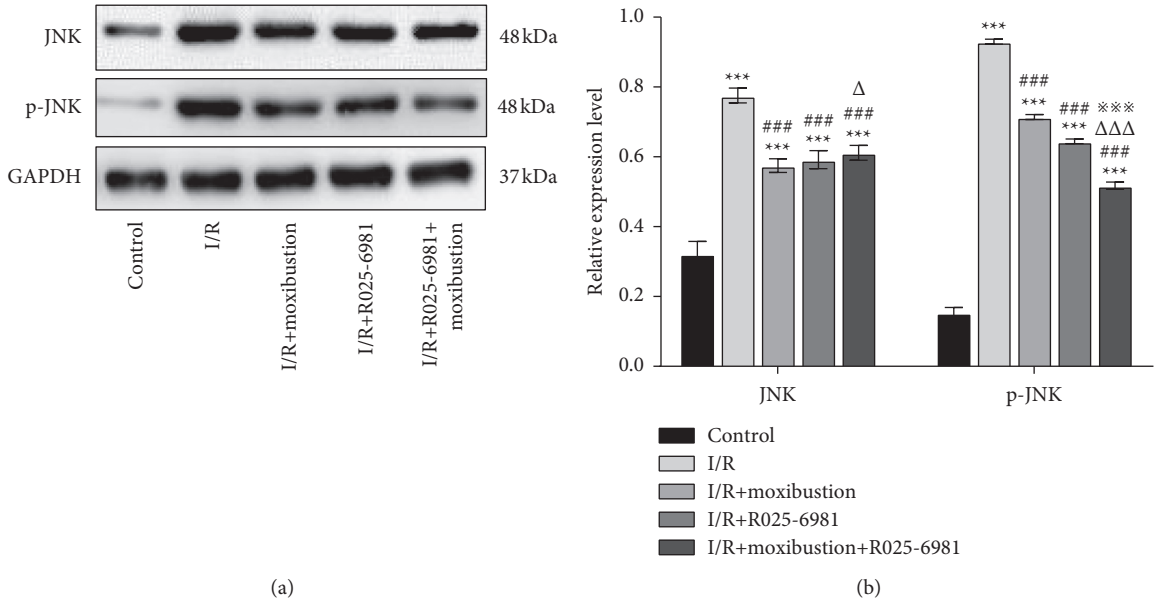

Figure 6: Relative protein expression of JNK and p-JNK in the brain tissues in the different groups. (a) Protein expression of JNK and p-JNK in the injured brain tissue of each group. (b) Relative protein expression levels of JNK and p-JNK in the injured brain tissue of each group. $^{***}P < 0.001$ compared to the control group; $^{\#\#\#}P < 0.001$ versus the I/R group; $^{\triangle}P < 0.05$ and $^{\triangle\triangle\triangle}P < 0.001$ versus the I/R + moxibustion group; $^{※※※}P < 0.001$ versus the I/*R* + Ro25-6981 group.

4. Discussion

The results of this study demonstrated that moxibustion can improve neurological dysfunction, decrease infarction area and neuronal apoptosis, downregulate the expression of NR2B and JNK, increase the level of Bcl-2, and decrease the level of caspase-3. Similarly, NR2B antagonist Ro25-6981 strengthened the improvements of neurological function, infarction area, neuronal apoptosis, and the changes of NR2B levels caused by I/R. Thus, moxibustion might exert a neuroprotective effect in the rat models of I/R injury by regulating the target of NR2B.

Nerve cell death and damage to the ischemic brain are a series of complicated pathological changes caused by limited blood flow in the ischemic area [28, 29]. Excitatory toxicity induced by the overexcitation of NMDA receptors is considered to be an important mechanism of apoptosis and brain injury after ischemia [30]. In the physiological state, NMDA receptors participate in high-level neural activities such as excitatory synaptic transmission, synaptic plasticity, learning, and memory, which are of great importance to the normal physiological activities of the nervous system [31]. Abnormal activation of NMDA receptors is important pathological pathogenesis of many nervous system diseases. NMDA receptors are gate-controlled ion channels. Among the NMDA receptor complexes, the subunits have been identified as NR1, NR2, and NR3, among which NR2 includes NR2A, NR2B, NR2C, NR2D, and other subunits. Among the various subunits of the NMDA receptor, NR2B is an important regulatory subunit [32]. Among these subunits, NR2A and NR2B have been widely studied because of their extensive expression in the brain [33]. In brain injury models such as cerebral ischemia, NR2A and NR2B participate in glutamate-mediated survival and death pathways in nerve cells, respectively. NR2B tends to promote neuronal death [12,34] while NR2A is associated with neuroprotection [9,35].

Activation of the c-Jun terminal kinase (JNK) signaling pathway is a key step in neuronal death in a variety of nervous system diseases and plays an important role in cerebral ischemia/reperfusion injury and neuronal apoptosis [36]. The JNK signaling pathway, also known as the stress-activated protein kinase signaling pathway, is an important component of serine protein kinase (MAPK) cascade activation. The MAPK signaling pathway plays an important role in the occurrence and development of cerebral ischemia [37]. Cerebral ischemia and hypoxia can activate MAPKs to regulate cell proliferation, differentiation, apoptosis, and other pathological changes, resulting in ischemic brain injury. The JNK signaling pathway is one of the three major MAPK pathways and is considered to be an important pathway for apoptosis. Activation of the JNK signaling pathway is a common factor in apoptosis induced by cerebral ischemia/reperfusion injury, oxidative stress, and inflammation [38,39]. Neuronal apoptosis induced by the JNK signaling pathway is related to the transcription and expression of bcl-2 gene family genes [40], especially Bcl-2 and Bax proteins [41]. The expression of Bcl-2 and Bax showed opposite trends. When the expression of Bcl-2 decreased and the expression of Bax increased, apoptosis was promoted, and when the expression of Bcl-2 increased and the expression of Bax decreased, apoptosis was inhibited [42]. The caspase family is the core of apoptosis, and active caspase-3 is the executor of apoptosis [43]. Caspase-3 induces a cascade reaction by cleaving other caspase substrates, which eventually leads to apoptosis. In this study,

after cerebral ischemia-reperfusion, with the loss of neurological function, the increase of cerebral infarction area and neuronal apoptosis rate, the expression of NR2B and JNK increased, Bax and caspase-3 increased, and Bcl-2 decreased. This finding is consistent with the results of previous studies [38].

JNKs can be activated through receptor tyrosine kinases, cytokine receptors, G protein-coupled receptors, and ligand-gated ion channels, including NMDA glutamate receptors [44]. Studies have shown that NMDA receptors are related to the activation of JNK, and glutamate can increase the level of p-JNK in primary nerve cells [45]. NMDA receptors (NR1 and NR2B) act as upstream molecules of JNK signaling and Akt signaling, inducing JNK activation and weakening Akt activation in ischemic brain injury [46]. The selective noncompetitive NMDA glutamate receptor antagonist MK-801 almost completely blocks glutamate- and NMDA-induced JNK activation [47]. NR2B antagonists have protective effects on LPS-induced JNK phosphorylation in the frontal lobe and hippocampus [48]. The activation of NMDAR, especially NMDAR containing NR2B, plays a key role in the phosphorylation of JNK in astrocytes [49]. In this study, we found that the activation of JNK during a cerebral ischemia-reperfusion injury was related to NR2B. However, it should be noted that the NR2B antagonist Ro25-6981 could not completely block the activation of JNK. Therefore, the activation of JNK in nerve cells does not completely depend on NR2B. Other factors, such as cytokines and proinflammatory cytokines, may also play a role in the JNK pathway in cerebral ischemia-reperfusion injury.

Previous studies have shown that moxibustion has a neuroprotective effect on cerebral ischemic injury [24]. In this study, the GV20 acupoint located in the head and the GV14 acupoint in the neck were selected. These two acupoints are commonly used in neuroprotection mechanisms [23]. This study showed that Ro25-6981 could significantly inhibit the protein expression of NR2B and downregulate JNK in ischemia/reperfusion rats. Moxibustion could also significantly downregulate the protein expression of NR2B and JNK in I/R rats.

In this study, our results show that moxibustion can reduce NDS, cerebral infarction rate, and neuronal apoptosis induced by cerebral I/R in rats. Moxibustion can upregulate the level of Bcl-2 protein and downregulate the levels of Bax, caspase-3, and JNK protein. Its effect is similar to that of NR2B antagonist Ro25-6981, suggesting that moxibustion may be an effective neuroprotective measure for the treatment of ischemic stroke. The study suggests that the neuroprotective mechanism of moxibustion is related to downregulating the expression of NR2B, in which the JNK signal pathway plays an important role. Moxibustion has a better effect of downregulating JNK than Ro25-6981, so the effect of downregulating JNK by moxibustion may not only be realized by downregulating NR2B, but we need to further explore in future research.

5. Conclusion

Moxibustion can improve neurological dysfunction and decrease infarction area and neuronal apoptosis caused by cerebral ischemia/reperfusion in rats. Its neuroprotective mechanism may be related to downregulating the expression of NR2B.

6. Ethics Approval

The animal study was reviewed and approved by the Institutional Animal Care and Use Committee of Zhejiang Chinese Medical University.

Data Availability

The raw data supporting the conclusions of this article will be made available by the authors, without undue reservation.

Conflicts of Interest

The authors declared no conflicts of interest.

Authors' Contributions

ZD conceived and designed the experiments. QG and QZ performed the experiments. ZD and QZ analyzed the data and drafted the manuscript. All authors contributed to the article and approved the submitted version.

Acknowledgments

This work was supported by the Natural Science Foundation of Zhejiang Province (Grant nos. LY17H270009 and LY18H270005); the National Natural Science Foundation of China (Grant no. 81503646); and the Science and Chinese Medicine Science and Technology Projects of Zhejiang Province (no. 2016ZQ020).

References

[1] M. Zhou, H. Wang, X. Zeng, P. Yin, J. Zhu, and W. Chen, "Mortality, morbidity, and risk factors in China and its provinces, 1990-2017: a systematic analysis for the Global Burden of Disease Study 2017," *Lancet*, vol. 394, no. 10204, pp. 1145–58, 2019.

[2] R. Lozano, M. Naghavi, K. Foreman, S. Lim, K. Shibuya, and V. Aboyans, "Global and regional mortality from 235 causes of death for 20 age groups in 1990 and 2010: a systematic analysis for the Global Burden of Disease Study 2010," *Lancet*, vol. 380, no. 9859, pp. 2095–128, 2012.

[3] V. L. Feigin, M. H. Forouzanfar, R. Krishnamurthi, G. A. Mensah, M. Connor, and D. A. Bennett, "Global and regional burden of stroke during 1990-2010: findings from the Global Burden of Disease Study 2010," *Lancet*, vol. 383, no. 9913, pp. 245–54, 2014.

[4] G. A. Donnan, M. Fisher, M. Macleod, and S. M. Davis, "Stroke," *Lancet*, vol. 371, no. 9624, pp. 1612–23, 2008.

[5] M. Y. Wu, G. T Yiang, W. T Liao, A. P. Tsai, Y. L. Cheng, and P. W. Cheng, "Current Mechanistic Concepts in Ischemia and Reperfusion Injury," *Cell Physiol Biochem*, vol. 46, no. 4, pp. 1650–67, 2018.

[6] D. Ma, Q. An, Z. Zhang, Q. Bian, Y. Li, and Y. Li, "Head Mild Hypothermia Exerts a Neuroprotective Role in Ischemia-Reperfusion Injury by Maintaining Glial Glutamate Transporter 1," *Ther Hypothermia Temp Manag*, vol. 32, 2020.

[7] S. A. Lipton, "Paradigm shift in neuroprotection by NMDA receptor blockade: memantine and beyond," *Nature Reviews Drug Discovery*, vol. 5, no. 2, pp. 160–170, 2006.

[8] S. Jiang, Q. A. Zhang, Q. Guo, and Z. Di, "The glutamatergic system and astrocytic impairment in rat hippocampus: a comparative study of underlying etiology and pathophysiology of depression," *Journal of Integrative Neuroscience*, vol. 18, no. 4, pp. 387–392, 2019.

[9] Y. Liu, T. P. Wong, M. Aarts et al., "NMDA receptor subunits have differential roles in mediating excitotoxic neuronal death both in vitro and in vivo," *Journal of Neuroscience*, vol. 27, no. 11, pp. 2846–2857, 2007.

[10] P. V. Massey, B. E. Johnson, P. R. Moult, Y. P. Auberson, M. W. Brown, and E. Molnar, "Differential roles of NR2A and NR2B-containing NMDA receptors in cortical long-term potentiation and long-term depression," *Journal of Neuroscience*, vol. 24, no. 36, pp. 7821–7828, 2004.

[11] M. Chen, T.-J. Lu, X.-J. Chen et al., "Differential roles of NMDA receptor subtypes in ischemic neuronal cell death and ischemic tolerance," *Stroke*, vol. 39, no. 11, pp. 3042–3048, 2008.

[12] G. Köhr, "NMDA receptor function: subunit composition versus spatial distribution," *Cell and Tissue Research*, vol. 326, no. 2, pp. 439–446, 2006.

[13] M. Farjam, F. B. Beigi Zarandi, S. Farjadian, B. Geramizadeh, A. R. Nikseresht, and M. R. Panjehshahin, "Inhibition of NR2B-containing N-methyl-D-Aspartate receptors (NMDARs) in experimental autoimmune encephalomyelitis, a model of multiple sclerosis," *Iranian Journal of Pharmaceutical Research: Iranian Journal of Pharmaceutical Research*, vol. 13, no. 2, pp. 695–705, 2014.

[14] G. Fischer, V. Mutel, G. Trube et al., "Ro 25-6981, a highly potent and selective blocker of N-methyl-D-aspartate receptors containing the NR2B subunit. Characterization in vitro," *Journal of Pharmacology and Experimental Therapeutics*, vol. 283, no. 3, pp. 1285–1292, 1997.

[15] W. Wang, X.-P. Mei, Y.-Y. Wei et al., "Neuronal NR2B-containing NMDA receptor mediates spinal astrocytic c-Jun N-terminal kinase activation in a rat model of neuropathic pain," *Brain, Behavior, and Immunity*, vol. 25, no. 7, pp. 1355–1366, 2011.

[16] F. Bu, H. Tian, S. Gong et al., "Phosphorylation of NR2B NMDA subunits by protein kinase C in arcuate nucleus contributes to inflammatory pain in rats," *Scientific Reports*, vol. 5, no. 1, p. 15945, 2015.

[17] H. Fan, X. Li, W. Wang et al., "Effects of NMDA-receptor antagonist on the expressions of bcl-2 and Bax in the subventricular zone of neonatal rats with hypoxia-ischemia brain damage," *Cell Biochemistry and Biophysics*, vol. 73, no. 2, pp. 323–330, 2015.

[18] S.-b. Liu and M.-g. Zhao, "Neuroprotective effect of estrogen: role of nonsynaptic NR2B-containing NMDA receptors," *Brain Research Bulletin*, vol. 93, pp. 27–31, 2013.

[19] X. K. Li, X. G. Liu, and S. Q. Yang, "Preliminary study on the mechanism of HO-1 protein mediated moxibustion pretreatment improving cerebral ischemia-reperfusion injury in rats," *Chinese Journal of basic medicine of traditional Chinese medicine*, vol. 22, no. 7, pp. 918–921, 2016.

[20] J. S. Hua, L. P. Li, and X. M. Zhu, "[Effects of moxibustion preconditioning on SOD and MDA in rats with global brain ischemia]," *Zhongguo Zhen Jiu*, vol. 26, no. 8, pp. 595–597, 2006.

[21] Z. R. Sun, Z. Y. Wang, and J. S. Hua, "Effect of moxibustion pretreatment on nitric oxide synthase activity in rat model of global cerebral ischemia-reperfusion," *Journal of acupuncture and moxibustion*, vol. 27, no. 01, pp. 52–54, 2011.

[22] A. J. Xiao, L. He, X. Ouyang, J. M. Liu, and M. R. Chen, "Comparison of the anti-apoptotic effects of 15- and 35-minute suspended moxibustion after focal cerebral ischemia/reperfusion injury," *Neural regeneration research*, vol. 13, no. 2, pp. 257–264, 2018.

[23] R.-X. Chen, Z.-M. Lv, M.-R. Chen, F. Yi, X. An, and D.-Y. Xie, "Stroke treatment in rats with tail temperature increase by 40-min moxibustion," *Neuroscience Letters*, vol. 503, no. 2, pp. 131–135, 2011.

[24] J.-S. Hua, L.-P. Li, and X.-M. Zhu, "Effects of moxibustion pretreating on SOD and MDA in the rat of global brain ischemia," *Journal of Traditional Chinese Medicine*, vol. 28, no. 4, pp. 289–292, 2008.

[25] L. Lu, H.-Q. Li, J.-H. Li, A.-J. Liu, and G.-Q. Zheng, "Neuroprotection of sanhua decoction against focal cerebral ischemia/reperfusion injury in rats through a mechanism targeting aquaporin 4," *Evidence-based Complementary and Alternative Medicine*, vol. 2015, pp. 1–7, 2015.

[26] E. Z. Longa, P. R. Weinstein, S. Carlson, and R. Cummins, "Reversible middle cerebral artery occlusion without craniectomy in rats," *Stroke*, vol. 20, no. 1, pp. 84–91, 1989.

[27] M. Shvedova, Y. Anfinogenova, E. N. Atochina-Vasserman, I. A. Schepetkin, and D. N. Atochin, "c-Jun N-terminal kinases (JNKs) in myocardial and cerebral ischemia/reperfusion injury," *Frontiers in Pharmacology*, vol. 9, p. 715, 2018.

[28] K. Y. Loh, Z. Wang, and P. Liao, "Oncotic cell death in stroke," *Reviews of Physiology, Biochemistry and Pharmacology*, vol. 176, pp. 37–64, 2019.

[29] J. Kocki, M. Ułamek-Kozioł, A. Bogucka-Kocka et al., "Dysregulation of amyloid-β protein precursor, β-secretase, presenilin 1 and 2 genes in the rat selectively vulnerable CA1 subfield of Hippocampus following transient global brain ischemia," *Journal of Alzheimer's Disease*, vol. 47, no. 4, pp. 1047–1056, 2015.

[30] A. Lau and M. Tymianski, "Glutamate receptors, neurotoxicity and neurodegeneration," *Pfluegers Archiv European Journal of Physiology*, vol. 460, no. 2, pp. 525–542, 2010.

[31] M. Kaniakova, K. Lichnerova, K. Skrenkova, L. Vyklicky, and M. Horak, "Biochemical and electrophysiological characterization of N- glycans on NMDA receptor subunits," *Journal of Neurochemistry*, vol. 138, no. 4, pp. 546–556, 2016.

[32] Y. Sun, L. Zhang, Y. Chen, L. Zhan, and Z. Gao, "Therapeutic targets for cerebral ischemia based on the signaling pathways of the GluN2B C terminus," *Stroke*, vol. 46, no. 8, pp. 2347–2353, 2015.

[33] K. Yashiro and B. D. Philpot, "Regulation of NMDA receptor subunit expression and its implications for LTD, LTP, and metaplasticity," *Neuropharmacology*, vol. 55, no. 7, pp. 1081–1094, 2008.

[34] M. Zhou and M. Baudry, "Developmental changes in NMDA neurotoxicity reflect developmental changes in subunit composition of NMDA receptors," *Journal of Neuroscience*, vol. 26, no. 11, pp. 2956–2963, 2006.

[35] P. Chazot, "The NMDA receptor NR2B subunit: a valid therapeutic target for multiple CNS pathologies," *Current Medicinal Chemistry*, vol. 11, no. 3, pp. 389–396, 2004.

[36] Z. H. Yang, Y. J. Lu, K. P. Gu, Z. Y. Xiang, and H. M. Huang, "Effect of ulinastatin on myocardial ischemia-reperfusion injury through JNK and P38 MAPK signaling pathways," *European Review for Medical and Pharmacological Sciences*, vol. 23, no. 19, pp. 8658–8664, 2019.

[37] Y. Shi, K. Li, K. Xu, and Q. H. Liu, "MiR-155-5p accelerates cerebral ischemia-reperfusion injury via targeting DUSP14 by regulating NF-kappaB and MAPKs signaling pathways," *European Review for Medical and Pharmacological Sciences*, vol. 24, no. 3, pp. 1408–1419, 2020.

[38] W. Hu, X. Wu, D. Yu et al., "Regulation of JNK signaling pathway and RIPK3/AIF in necroptosis-mediated global cerebral ischemia/reperfusion injury in rats," *Experimental Neurology*, vol. 331, Article ID 113374, 2020.

[39] C. Benakis, C. Bonny, and L. Hirt, "JNK inhibition and inflammation after cerebral ischemia," *Brain, Behavior, and Immunity*, vol. 24, no. 5, pp. 800–811, 2010.

[40] Q. H. Guan, D. S. Pei, T. L. Xu, and G. Y. Zhang, "Brain ischemia/reperfusion-induced expression of DP5 and its interaction with Bcl-2, thus freeing Bax from Bcl-2/Bax dimmers are mediated by c-Jun N-terminal kinase (JNK) pathway," *Neuroscience Letters*, vol. 393, no. 2-3, pp. 226–230, 2006.

[41] S. Banjara, C. D. Suraweera, M. G. Hinds, and M. Kvansakul, "The bcl-2 family: ancient origins, conserved structures, and divergent mechanisms," *Biomolecules*, vol. 10, no. 1, 2020.

[42] R. Singh, A. Letai, and K. Sarosiek, "Regulation of apoptosis in health and disease: the balancing act of BCL-2 family proteins," *Nature Reviews Molecular Cell Biology*, vol. 20, no. 3, pp. 175–193, 2019.

[43] T.-J. Fan, L.-H. Han, R.-S. Cong, and J. Liang, "Caspase family proteases and apoptosis," *Acta Biochimica et Biophysica Sinica*, vol. 37, no. 11, pp. 719–727, 2005.

[44] R. Nisticò, F. Florenzano, D. Mango et al., "Presynaptic c-Jun N-terminal Kinase 2 regulates NMDA receptor-dependent glutamate release," *Scientific Reports*, vol. 5, no. 1, p. 9035, 2015.

[45] R.-W. Chen, Z.-H. Qin, M. Ren et al., "Regulation of c-Jun N-terminal kinase, p38 kinase and AP-1 DNA binding in cultured brain neurons: roles in glutamate excitotoxicity and lithium neuroprotection," *Journal of Neurochemistry*, vol. 84, no. 3, pp. 566–575, 2003.

[46] H.-Y. Gong, F. Zheng, C. Zhang, X.-Y. Chen, J.-J. Liu, and X.-Q. Yue, "Propofol protects hippocampal neurons from apoptosis in ischemic brain injury by increasing GLT-1 expression and inhibiting the activation of NMDAR via the JNK/Akt signaling pathway," *International Journal of Molecular Medicine*, vol. 38, no. 3, pp. 943–950, 2016.

[47] M. A. Schwarzschild, R. L. Cole, and S. E. Hyman, "Glutamate, but not dopamine, stimulates stress-activated protein kinase and AP-1-mediated transcription in striatal neurons," *Journal of Neuroscience*, vol. 17, no. 10, pp. 3455–3466, 1997.

[48] Y. Song, X. Zhao, D. Wang et al., "Inhibition of LPS-induced brain injury by NR2B antagonists through reducing assembly of NR2B-CaMKII-PSD95 signal module," *Immunopharmacology and Immunotoxicology*, vol. 41, no. 1, pp. 86–94, 2019.

[49] W. Lin, Y. Zhao, B. Cheng et al., "NMDAR and JNK activation in the spinal trigeminal nucleus caudalis contributes to masseter hyperalgesia induced by stress," *Frontiers in Cellular Neuroscience*, vol. 13, p. 495, 2019.

Hindawi
Evidence-Based Complementary and Alternative Medicine
Volume 2021, Article ID 1399258, 6 pages
https://doi.org/10.1155/2021/1399258

Research Article

An Association Rule Analysis of the Acupressure Effect on Sleep Quality

Chih-Hung Lin,[1,2] **Ya-Hsuan Lin**,[3] **I-Shiang Tzeng**,[4,5] **and Chan-Yen Kuo**[4,6]

[1]*Respiratory Care and Chest Medicine, Department of Internal Medicine, Cathay General Hospital, Taipei, Taiwan*
[2]*School of Medicine, College of Medicine, Fu Jen Catholic University, New Taipei, Taiwan*
[3]*Department of Chinese Medicine, Taipei Tzu Chi Hospital, Buddhist Tzu Chi Medical Foundation, New Taipei, Taiwan*
[4]*Department of Research, Taipei Tzu Chi Hospital, Buddhist Tzu Chi Medical Foundation, New Taipei, Taiwan*
[5]*Department of Statistics, National Taipei University, Taipei, Taiwan*
[6]*Department of Nursing, Cardinal Tien College of Healthcare and Management, New Taipei, Taiwan*

Correspondence should be addressed to I-Shiang Tzeng; istzeng@gmail.com and Chan-Yen Kuo; cykuo863135@gmail.com

Received 2 July 2021; Accepted 9 September 2021; Published 29 September 2021

Academic Editor: Zhaohui Liang

Background. Sleep is recognized as an all-important physiological process, which also contributes to maintaining several bodily functions and systems. According to the Pittsburgh Sleep Quality Index (PSQI), also known as the most widely used tool in the field of subjective assessment of self-perceived sleep quality, a combination of acupoints could be more effective than single acupoint treatment in improving sleep quality. *Methods*. The present study was based on the extracted eligible studies rooted in a previous meta-analysis that worked on the basis of association rule mining and examined the potential kernel acupoint combinations for improving sleep quality. *Results*. Depending on the Apriori algorithm, we summarized 26 acupoints as binary data from the 32 eligible studies based on a previous meta-analysis and analyzed them. The top 10 most frequently selected acupoints were HT7, SP6, PC6, KI1, GV20, EM5, EX-HN3, EX-HN16, KI3, and MA-TF1. Furthermore, as deduced from 21 association rules, the primary relevant rules in the combination of acupoints are (EX-HN3, EX-HN16)=>(GV20) and (HT7, KI1)=>(PC6). *Conclusions*. In order to use acupuncture to improve sleep quality, integrating (EX-HN3, EX-HN16, GV20) with (HT7, KI1, PC6) acupoints could be deemed as the kernel acupoint combination.

1. Introduction

The essentiality of sleep as a vital and intricate physiological process in humans cannot be denied. Over the years, numerous studies [1, 2] have suggested that this process is affected by three elements, which are social, cultural, and environmental in nature. Nowadays, high levels of stress and poor sleep quality [3] result from the social and organizational demands experienced by individuals. Moreover, an increase in the number of diseases related to sleep quality [4] is an outcome of organic disorders. Driving accidents that cause over 2000 fatal crashes and 40,000 nonfatal injuries each year are two instantaneous consequences due to lack of sleep or poor quality of sleep in the US. Belated sequelae caused by sleep disorders are associated with the risk of many diseases such as metabolic disorders [5, 6], psychiatric conditions [7], cardiovascular diseases [8], and even cancers [4]. In addition, poor quality sleep and insomnia have a tight connection with emotions. Previous studies have observed the implications of loneliness, grief, hostility, impulsivity, stress, depression, and anxiety in terms of sleep [1, 9–11]. The close-knit relationship displayed between emotion and sleep is gradually being distinguished as a crucial area for research [12]. In order to understand the processes that can provide good quality sleep [13–16], recent studies have reported some mechanisms of sleep [17, 18] to comprehend its behavioral complexity and advancement beyond pathological descriptions.

In the last few years, the requirements on the estimation of the factors influencing the quality of sleep have increased. The necessity to understand these associations was motivated by the discovery that biological traits do not always have linkages with the perception of poor quality of sleep [19]. The Pittsburgh Sleep Quality Index (PSQI) is a method to investigate the subjective quality of sleep. This implementation provides an accurate picture of seven different circumstances of sleep: (a) sleep duration, (b) sleep disturbance, (c) sleep latency, (d) daytime dysfunction, (e) sleep efficiency, (f) subjective sleep quality, and (g) use of sleep medication [20]. Clinical practice is a better approach here rather than objective sleep measures [21, 22].

Applying pressure to specific points on the body is a traditional treatment known as acupressure. These specific points are referred to as acupoints, which correspond to different organs and systems in the human body. Traditional Chinese medicine (TCM) acupressure is the most empirically studied form of acupressure which is closely connected with TCM acupuncture. Nevertheless, instead of needles, practitioners of TCM acupuncture use fingers, knuckles, or dull. It has received much more attention on the grounds of its safe supplementary and alternative effects that overtly alleviate the symptoms of certain diseases. Therefore, acupressure could be a successful treatment for patients with sleep disorders in the near future. In clinical practice, poor sleep quality is a widely reported complaint. At the same time, it can also be identified as a significant symptom among various sleep and medical disorders [20, 23]. Frankly speaking, sleep quality can be considered as a combination of two conceptions, the quantitative aspects, such as sleep duration and sleep latency, and subjective perceptions of sleep, such as depth and restfulness [20]. In order to evaluate sleep quality [24, 25], subjective and objective assessments are applied as two prevalent, distinct, and complementary approaches in research as well as clinical settings.

As a matter of fact, based on a previous meta-analysis, it is claimed that acupuncture in conjunction with Chinese herbs is a tolerable and effective nonpharmacological treatment [26] for improving sleep quality of patients (i.e., PSQI). This meta-analysis included patients, clinicians, and decision makers with evidence-based advice in the healthcare system. In the meantime, further investigation through proper methodology is encouraged. Recent studies have discussed the relationship between acupuncture points and diseases. Data mining methods, which have been widely utilized in modern fields and Chinese medicine, are being employed to enhance the therapeutic effect of the treatment. A prior study supplied reference based data mining results with the selection and combination of acupuncture points for remedying various sleep disorders by means of clinical acupuncture therapy [27]. Some valuable suggestions about the selection and combination of acupuncture points for sleep disorders have also been contributed by another research [28]. As stated in the literature review, data mining has been used extensively on the scale of discovering potential acupuncture points and treating specific diseases effectively. Using a data mining approach [29], a study examined the selections and characteristics of acupuncture point principles for chronic kidney disease treatment. In reality, association rule mining (analysis) is generally used in the sphere of marketing to determine strong and frequent directional associations between jointly purchased items.

In this study, with the intention of determining the effect of acupuncture on sleep quality, we found the potential kernel combination of acupuncture points in accordance with acupoint data from a previous meta-analysis [26].

2. Materials and Methods

2.1. Data Sources. Based on a meta-analysis [26], acupoint data integrated acupuncture data that were interpreted by the content of the WHO Standard Acupuncture Point. This study was based on the previously reported meta-analysis study which reviewed 32 eligible studies. From a selection of 32 eligible studies that originated from the abovementioned study, there was an integration of 26 acupuncture point locations. All the included studies were required to use acupuncture-related methods, such as acupuncture, electroacupuncture (EA), abdomen acupuncture, eye acupuncture, ear acupuncture, or scalp acupuncture, and have precise outcome data on quality of sleep. We made a record of 26 acupuncture point locations involved in studies as binary data (Supplementary Table 1).

2.2. Risk of Bias Assessment. The Cochrane RoB 2.0 tool was used to assess quality the studies. The Cochrane RoB 2.0 tool investigated risk of selection bias, performance bias, detection bias, attrition bias, and reporting bias. Finally, the tool combined the above bias to assess the quality of 13 randomized controlled trials (RCTs) selected from 32 eligible studies based on a previous meta-analysis [26] (Supplementary Figure 1).

2.3. Data Analysis. On the basis of "arules" and "arulesViz" packages, association rule analysis (ARA) and plotting were performed with statistical software *R* (version 4.0.0). Cochrane RoB 2.0 tool was applied to evaluate the methodological quality of the studies included in this meta-analysis [26]. This tool uses seven domains to assess RoB and evaluates the overall quality of RCT after each domain is combined. The association rule learning algorithm is one of the widely used techniques to detect and analyze relations and useful information from transaction data. The association rule learning algorithm contains an antecedent and consequent sets, both of which are a set of items. In this study, support, confidence, expected confidence, and lift were kernel values involved with association rule analysis. First, support means the fraction of the total number of transactions in which the itemset occurs. And confidence defined the conditional probability of occurrence of consequent, given the antecedent. Next, expected confidence presents the probability of the consequent while consequent was independent of the antecedent. Final, lift expressed the ratio of joint antecedent and a consequent probability and product of each marginal probability.

Support and confidence factors are essential parameters in association rule learning. Support estimates the frequency of an acupoint appearing in the 32 formulas. On the other hand, confidence measures the frequency of acupoint appearing in the formulas, given that acupoint B appears simultaneously. Expected confidence is the number of formulas that include the consequent set of acupoints divided by the total number of formulas. During the exploration of the association rules, users need to test multiple combinations of the minimum values for support and confidence factors to discover the significant association rules. However, the selection of thresholds showed slight ambiguity and varied from case to case. If the parameter thresholds were set at extremely high values, then certain meaningful information would be discarded.

3. Results

3.1. Risk of Bias Assessment. The summary of 13 RCTs selected from 32 eligible studies based on a previous meta-analysis [26] and quality assessment with overall bias is presented in Supplementary Table 2. The results showed no serious risk of bias consisted with the previous study [26].

3.2. Acupoint Distribution. As stated by the antecedent meta-analysis, 26 acupoints were withdrawn from the 32 retrieved eligible studies. Therefore, taking Figure 1 as an example, a barplot was presented to sum up the acupoint frequency distribution. The following 10 acupoints were the most frequently selected among all the acupoints for best effects on sleep disorders and similar symptoms: HT7, SP6, PC6, KI1, GV20, EM5, EX-HN3, EX-HN16, KI3, and MA-TF1.

Data for 26 acupoints were recapitulated from acupoint combinations with reference to association rule analysis for the itemset (Table S1). The sporadic plot in Figure 2 demonstrates that all rules have excellent progress. The support/confidence border can be detected for the optimal rules (i.e., the most interesting rules) [30]. Amidst different acupuncture location points, the association rules are arranged by support. Moreover, the top 10 are listed in Table 1. Color or size is utilized by graph-based visualization to represent the itemset/rules. This plot has two advantages, namely, providing an exceedingly transparent demonstration of rules and enabling very tiny sets of rules to evade cluttered presentation. Subsequently, in Figure 3, the features are visually displayed on the basis of the grouped matrix of 10 associations. As stated in the evidence of the grouped matrix for 10 rules, we can perceive that (EX-HN3, EX-HN16)=>(GV20) and (HT7, KI1)=>(PC6) are interactively selected to uncover the rule's antecedent (LHS) and consequent (RHS) itemset. Through Table 1, we discovered that interactively selected association rules were composed of the No. 6 rule ((HT7, KI1) => (PC6)).

4. Discussion

Our results indicate that the core acupoint combinations for treating patients with sleep disorders were (EX-HN3, EX-HN16, GV20) and (HT7, KI1, PC6). With regard to the

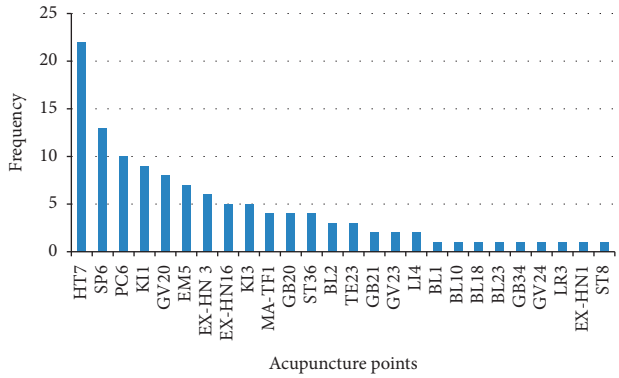

Figure 1: Acupoints distribution extracted from 32 eligible studies.

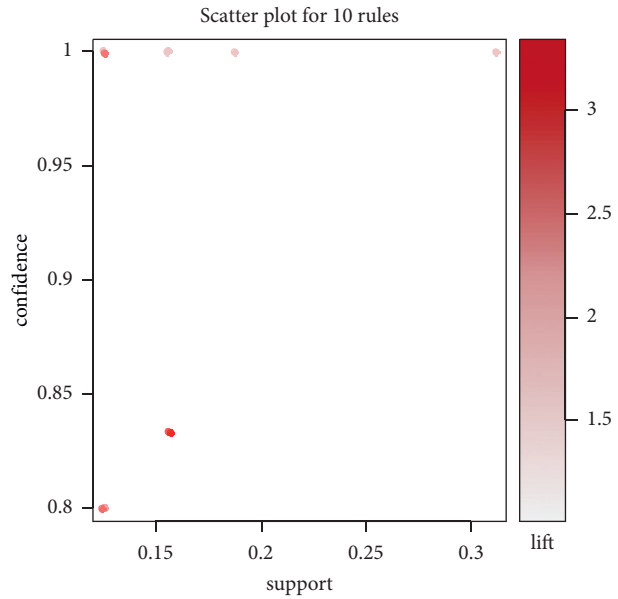

Figure 2: Top 10 association rules presented as a scatter plot.

preceding meta-analysis [26], these acupoint combinations contributed significantly towards the enhancement of PSQI patients under sleep medications with poor sleep quality. Their results demonstrated evidence-based strategies for acupoint selection in the forward therapy. As far as we are aware, this research is the first to point out the potential core acupoint combinations for treating patients with poor sleep quality in accordance with the consequences from a meta-analysis.

The current study corroborates that core acupoint combinations were salutary for patients with sleep disorders. Anti-inflammatory effects [31], improvement in neurologic conditions [32], improvement in hypertension [33], and improvement in exercise tolerance [34] were reported to be viable mechanisms to ameliorate sleep apnea by acupuncture.

Currently, complementary and alternative mediciness are being used worldwide to treat matters that poor sleep quality precipitate as a great public health concern [35–38]. Evaluation of the effects of acupressure on sleep quality can help public health practitioners, clinicians, and patients in

Table 1: Top 10 optimal acupuncture association rules.

No.	Association rules		Support	Confidence	Lift	Expected confidence
1	(PC6)	=> (HT7)	0.31250	1.0000000	1.454545	0.687500
2	(PC6, SP6)	=> (HT7)	0.18750	1.0000000	1.454545	0.687500
3	(EX-HN16)	=> (HT7)	0.15625	1.0000000	1.454545	0.687500
4	(EX-HN3)	=> (GV20)	0.15625	0.8333333	3.333333	0.250000
5	(KI1, PC6)	=> (HT7)	0.15625	1.0000000	1.454545	0.687500
6	(HT7, KI1)	=> (PC6)	0.15625	0.8333333	2.666667	0.312500
7	(ST36)	=> (SP6)	0.12500	1.0000000	2.461538	0.406250
8	(MA-TF1)	=> (HT7)	0.12500	1.0000000	1.454545	0.687500
9	(EX-HN16)	=> (PC6)	0.12500	0.8000000	2.560000	0.312500
10	(EX-HN16)	=> (SP6)	0.12500	0.8000000	1.969231	0.406250

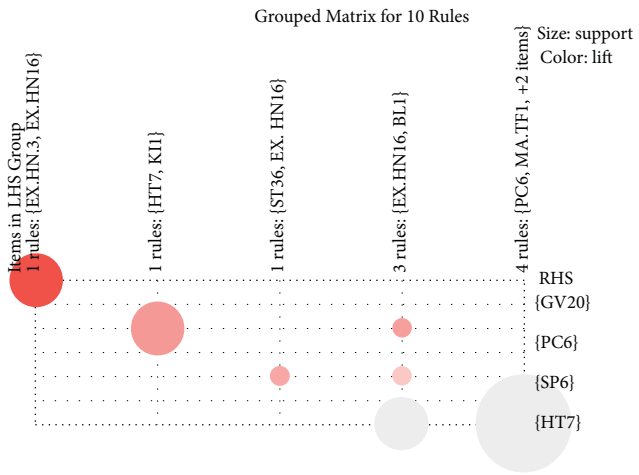

Figure 3: 10 association rules presented as grouped matrix.

making a decision to adopt it as a treatment modality. In developed countries, complementary and alternative medicine treatments are being included in national health insurance packages. On the contrary, acupressure usually remains excluded from these packages. This noninvasive procedure is easy to learn, execute, and is also incredibly convenient. With the help of medical staff, patients and their family members can be taught to implement acupressure on their own. Physicians may suggest acupressure as an incipient treatment to avoid the adverse effects of medications when confronted with recurrent requests from patients for sleeping pill prescriptions during their general practice [39].

Patients were associated with obstructive sleep apnea [40] owing to inflammation, as proved by Boyd et al. Acupuncture treatment may ameliorate both inflammation and sleep quality. A meta-analysis was conducted by Zhao et al. that stated that blood pressure [41] may be attenuated by acupuncture treatment. In addition, Simoncini et al. illustrated that acupuncture treatment with HT7 could boost the neurologic responses [42]. As far as clinical practice is concerned, acupuncture therapy typically provides treatment to patients with acupoint combinations, rather than a single acupoint. There was another suggestion stated by Chen et al. that indicated that acupuncture with multiple acupoints could enhance treatment for cervical spondylosis patients in two ways, namely, better symptomatic improvement and more decline in the regional homogeneity of pain in the matrix area of the brain [43]. Furthermore, as reported by Zhang et al., the acupoint combination of LR3 and KI3 could generate greater synergistic effects in patients with hypertension than that of a single acupoint (LR3 or KI3). The results of resting-state fMRI revealed that acupuncture from LR3 and KI3 could activate broader brain areas in comparison to single LR3 or KI3 [44]. In view of the two advantages of acupoint combination, it is important to ascertain the acupoint combination instead of the single acupoint. This combination could create advancements in the brain area as well as precipitate developments on other related areas of the brain. In addition, the acupoints selected may vary based on the differentiation of symptoms and diseases for the clinician. Meanwhile, TCM treatment is also usually prescribed based on the individual's model diagnosis. A literature review study focused the treatment of insomnia based on TCM pattern differentiation, treatment principle, and pattern-based treatment to investigate the constituency between TCM treatment and acupoints selection [45]. The results showed inconsistence between some differentiations of symptoms in the TCM treatment and acupoints selected. It may be attributed to the insufficient diagnosis process of extracted studies. More high-quality research studies are required to validate that relationship.

To our knowledge, the frequent pattern- (FP-) growth algorithm is the method of finding frequent patterns without candidate generation [46]. The FP-growth algorithm method constructed an FP-tree rather than Apriori using generates and inspects strategy. The FP growth algorithm method concentrated on fracturing the paths of the items and mining frequent patterns. We perform the FP growth algorithm method for sensitivity analysis in this study. We found that results under the FP growth algorithm method (Supplementary Table 3) were similar to Apriori algorithm-based association rule analysis (Table 1). For example, (PC6)=> (HT7) was Top 1 optimal acupuncture association rule determined for both Apriori algorithm and FP growth algorithm-based methods simultaneously. We may conserve the results under the Apriori algorithm method according to sensitivity analysis.

Despite the fact that we explained the core of the study with acupoint combinations, there were a few limitations to our study. First, the effects of acupuncture were affected by several considerations, including the depth of needling,

method of acupuncture on manipulation, time of retaining the needle, treatment frequency, and treatment course. However, in this analysis, we did not consider aforementioned factors. Second, this study did not address the roles of other acupuncture systems, such as scalp acupuncture, auricular acupuncture, and Tung's acupuncture. Third, the mechanisms of acupoint combinations remained vague. Owing to these reasons, it is necessary to conduct a thorough evaluation about the further fundamental and clinical studies.

5. Conclusions

(EX-HN3, EX-HN16, GV20) integrated with (HT7, KI1, PC6) is deemed as the kernel acupoint combination in the field of acupuncture therapies for sleep disorders. However, due to lack of reproducible verification hitherto, acupuncture is defined as a possible, but not dependable therapy. With reference to our analysis, this kernel acupoint combination was submitted for further verification including clinical trials, basic mechanism research, and treatment strategies.

Data Availability

The data used to support the findings of this study are included within the article.

Disclosure

CHL and YHL are the co-first authors.

Conflicts of Interest

The authors declare that they have no conflicts of interest.

Authors' Contributions

IST and CYK created the research idea, performed the analysis, wrote the results and discussion, and contributed to the literature review. CHL and YHL wrote the draft and helped revise the manuscript and contributed equally to this work. YHL, IST, and CYK supported the literature review and analysis. IST prepared the manuscript for submission. All authors read and approved the final manuscript. I-Shiang Tzeng and Chan-Yen Kuo contributed equally to this work.

Acknowledgments

This study was supported by grants CGH-MR-A10902 and 109CGH-TMU-06.

Supplementary Materials

Table 1: summary of 26 acupuncture point locations involved in studies as binary data. Table 2: quality assessment with overall bias. Figure 1: summary of risk of bias plot of 13 RCTs. (*Supplementary Materials*)

References

[1] M. de Zambotti, J. Trinder, A. Silvani, I. M. Colrain, and F. C. Baker, "Dynamic coupling between the central and autonomic nervous systems during sleep: a review," *Neuroscience & Biobehavioral Reviews*, vol. 90, pp. 84–103, 2018.

[2] R. Lopez, L. Barateau, and Y. Dauvilliers, "Organisation normale du sommeil et ses changements au cours de la vie [Normal organization of sleep and its changes during life," *Revue du Praticien*, vol. 69, no. 5, pp. 537–545, 2019.

[3] E. Ben Simon, R. Vallat, C. M. Barnes, and M. P. Walker, "Sleep loss and the socio-emotional brain," *Trends in Cognitive Sciences*, vol. 24, no. 6, pp. 435–450, 2020.

[4] R. T. H. Ho, T. C. T. Fong, C. K. P. Chan, and C. L. W. Chan, "The associations between diurnal cortisol patterns, self-perceived social support, and sleep behavior in Chinese breast cancer patients," *Psychoneuroendocrinology*, vol. 38, no. 10, pp. 2337–2342, 2013.

[5] F. S. Luyster, P. J. Strollo Jr, P. C. Zee, and J. K. Walsh, "Sleep: a health imperative," *Sleep*, vol. 35, no. 6, pp. 727–734, 2012.

[6] J. L. Poole and P. Siegel, "Effectiveness of occupational therapy interventions for adults with fibromyalgia: a systematic review," *American Journal of Occupational Therapy: Official Publication of the American Occupational Therapy Association*, vol. 71, no. 1, Article ID 7101180040p1, 2017.

[7] S. Baglioni, Nanovska, and W. Regen, "Sleep and mental disorders: a meta-analysis of polysomnographic research," *Psychological Bulletin Journal*, vol. 142, no. 9, pp. 969–990, 2016.

[8] H. Liu and A. Chen, "Roles of sleep deprivation in cardiovascular dysfunctions," *Life Sciences*, vol. 219, pp. 231–237, 2019.

[9] H. S. Cho, Y. W. Kim, H. W. Park et al., "The relationship between depressive symptoms among female workers and job stress and sleep quality," *Annals of Occupational and Environmental Medicine*, vol. 25, no. 1, p. 12, 2013.

[10] C. A. Feeley, M. Clougherty, L. Siminerio, D. Charron-Prochownik, A. L. Allende, and E. R. Chasens, "Sleep in caregivers of children with type 1 diabetes," *The Diabetes Educator*, vol. 45, no. 1, pp. 80–86, 2019.

[11] L. J. Silva-Perez, N. Gonzalez-Cardenas, and S. Surani, "Socioeconomic status in pregnant women and sleep quality during pregnancy," *Cureus*, vol. 11, no. 11, p. 9, 2019.

[12] G. Jia and P. Yuan, "The association between sleep quality and loneliness in rural older individuals: a cross-sectional study in Shandong Province, China," *BMC Geriatrics*, vol. 20, no. 1, p. 180, 2020.

[13] F. A. Etindele-Sosso, "Insomnia, excessive daytime sleepiness, anxiety, depression and socioeconomic status among customer service employees in Canada," *Sleep Science*, vol. 13, no. 1, pp. 54–64, 2020.

[14] R. I. B. Schnittger, C. D. Walsh, A.-M. Casey, J. P. Wherton, J. E. McHugh, and B. A. Lawlor, "Psychological distress as a key component of psychosocial functioning in community-dwelling older people," *Aging & Mental Health*, vol. 16, no. 2, pp. 199–207, 2012.

[15] A. Gadie, M. Shafto, and Y. Leng, "How are age-related differences in sleep quality associated with health outcomes? An epidemiological investigation in a UK cohort of 2406 adults," *BMJ Open*, vol. 7, no. 7, 13 pages, 2017.

[16] M. T. Caserta, "Sleep, quality of life, and intervention," *American Journal of Geriatric Psychiatry*, vol. 24, no. 10, pp. 855-856, 2016.

[17] M. E. Carter, J. Brill, P. Bonnavion, J. R Huguenard, R Huerta, and L de Lecea, "Mechanism for Hypocretin-mediated sleep-

to-wake transitions," *Proceedings of the National Academy of Sciences of the United States of America*, vol. 109, no. no39, pp. E2635–E2644, 2012.

[18] G. L. Sorensen, S. Knudsen, and P. Jennum, "Sleep transitions in hypocretin-deficient narcolepsy," *Sleep*, vol. 36, no. 8, pp. 1173–1177, 2013.

[19] M. Hayase, M. Shimada, and H. Seki, "Sleep quality and stress in women with pregnancy-induced hypertension and gestational diabetes mellitus," *Women and Birth*, vol. 27, no. 3, pp. 190–195, 2014.

[20] D. J. Buysse, C. F. Reynolds, T. H. Monk, S. R. Berman, and D. J. Kupfer, "The Pittsburgh Sleep Quality Index: a new instrument for psychiatric practice and research," *Psychiatry Research*, vol. 28, no. 2, pp. 193–213, 1989.

[21] M. Pavlova, "Circadian rhythm sleep-wake disorders," *Continuum: Lifelong Learning in Neurology*, vol. 23, pp. 1051–1063, 2017.

[22] J. E. McHugh, A.-M. Casey, and B. A. Lawlor, "Psychosocial correlates of aspects of sleep quality in community-dwelling Irish older adults," *Aging & Mental Health*, vol. 15, no. 6, pp. 749–755, 2011.

[23] D. J. Buysse, L. Yu, and D. E. Moul, "Development and validation of patient-reported outcome measures for sleep disturbance and sleep-related impairments," *Sleep*, vol. 33, no. 6, pp. 781–792, 2010.

[24] D. J. Buysse, S. Ancoli-Israel, J. D. Edinger, K. L. Lichstein, and C. M. Morin, "Recommendations for a standard research assessment of insomnia," *Sleep*, vol. 29, no. 9, pp. 1155–1173, 2006.

[25] S. Schutte-Rodin, L. Broch, and D. Buysse, "Clinical guideline for the evaluation and management of chronic insomnia in adults," *Journal of Clinical Sleep Medicine*, vol. 4, no. 5, pp. 487–504, 2008.

[26] A. Waits, Y.-R. Tang, H.-M. Cheng, C.-J. Tai, and L.-Y. Chien, "Acupressure effect on sleep quality: a systematic review and meta-analysis," *Sleep Medicine Reviews*, vol. 37, pp. 24–34, 2018.

[27] J. Sarris and G. J. Byrne, "A systematic review of insomnia and complementary medicine," *Sleep Medicine Reviews*, vol. 15, no. 2, pp. 99–106, 2011.

[28] P. Wu, C. Cheng, X. Song et al., "Acupoint combination effect of Shenmen (HT 7) and Sanyinjiao (SP 6) in treating insomnia: study protocol for a randomized controlled trial," *Trials*, vol. 21, no. 1, pp. 261–9, 2020.

[29] P. Xia, K. Gao, and J. Xie, "Data mining-based analysis of chinese medicinal herb formulae in chronic kidney disease treatment," *Evidence-Based Complementary and Alternative Medicine*, vol. 2020, Article ID 9719872, 14 pages, 2020.

[30] J. Roberto and R. A. Bayardo Jr., "Mining the most interesting rules," *In Proceedings of the Fifth ACM SIGKDD International Conference*, ACM Press, San Diego, CA, USA, 1999.

[31] J. M. Mullington, N. S. Simpson, H. K. Meier-Ewert, and M. Haack, "Sleep loss and inflammation," *Best Practice & Research Clinical Endocrinology & Metabolism*, vol. 24, no. 5, pp. 775–784, 2010.

[32] Y.-E. S. Ju, A. Videnovic, and B. V. Vaughn, "Comorbid sleep disturbances in neurologic disorders," *Continuum: Lifelong Learning in Neurology*, vol. 23, no. 4, pp. 1117–1131, 2017.

[33] E. Van Ryswyk, S. Mukherjee, and C. L. Chai-Coetzer, "Sleep disorders, including sleep apnea and hypertension," *American Journal of Hypertension*, vol. 31, no. 8, pp. 857–864, 2018.

[34] F. Quadri, E. Boni, L. Pini et al., "Exercise tolerance in obstructive sleep apnea-hypopnea (OSAH), before and after CPAP treatment: effects of autonomic dysfunction improvement," *Respiratory Physiology & Neurobiology*, vol. 236, pp. 51–56, 2017.

[35] C. M. Morin and D. C. Jarrin, "Epidemiology of insomnia," *Sleep Medicine Clinics*, vol. 8, no. 3, pp. 281–297, 2013.

[36] Y.-W. Hsu, C.-H. Ho, J.-J. Wang, K.-Y. Hsieh, S.-F. Weng, and M.-P. Wu, "Longitudinal trends of the healthcare-seeking prevalence and incidence of insomnia in Taiwan: an 8-year nationally representative study," *Sleep Medicine*, vol. 14, no. 9, pp. 843–849, 2013.

[37] S. Pallesen, B. Sivertsen, I. H. Nordhus, and B. Bjorvatn, "A 10-year trend of insomnia prevalence in the adult Norwegian population," *Sleep Medicine*, vol. 15, no. 2, pp. 173–179, 2014.

[38] M. Frass, R. P. Strassl, H. Friehs, M Müllner, M Kundi, and A. D Kaye, "Use and acceptance of complementary and alternative medicine among the general population and medical personnel: a systematic review," *The Ochsner Journal*, vol. 12, no. 1, pp. 45–56, 2012.

[39] D. Patel, J. Steinberg, and P. Patel, "Insomnia in the elderly: a review," *Journal of clinical sleep medicine: JCSM: official publication of the American Academy of Sleep Medicine*, vol. 14, no. 6, pp. 1017–1024, 2018.

[40] J. H. Boyd, B. J. Petrof, and Q. Hamid, "Upper airway muscle inflammation and denervation changes in obstructive sleep apnea," *American Journal of Respiratory and Critical Care Medicine*, vol. 170, no. 5, pp. pp541–546, 2004.

[41] Z. H. Zhao, Y. Zhou, and W. H. Li, "Auricular acupressure in patients with hypertension and insomnia: a systematic review and meta-analysis," *Evidence-Based Complementary and Alternative Medicine*, vol. 2020, Article ID 7279486, 11 pages, 2020.

[42] M. Simoncini, A. Gatti, and P. E. Quirico, "Acupressure in insomnia and other sleep disorders in elderly institutionalized patients suffering from Alzheimer's disease," *Aging Clinical and Experimental Research*, vol. 27, no. 1, pp. 37–42, 2012.

[43] W. Chen, X. Hou, and J. Chen, "MRI pain matrix regional homogeneity in cervical spondylosis of neck type treated with acupuncture at multiple acupoints," *Zhongguo Zhen Jiu*, vol. 35, no. 10, pp. 1005–1009, 2015.

[44] J. Zhang, X. Cai, and Y. Wang, "Different brain activation after acupuncture at combined acupoints and single acupoint in hypertension patients: an rs-fMRI study based on ReHo analysis," *Evidence-Based Complementary and Alternative Medicine*, vol. 2019, Article ID 5262896, 10 pages, 2019.

[45] W. F. Yeung, K. F. Chung, and M. M. Poon, "Prescription of Chinese herbal medicine and selection of acupoints in pattern-based traditional Chinese medicine treatment for insomnia: a systematic review," *Evidence-Based Complementary and Alternative Medicine*, vol. 2012, Article ID 902578, 16 pages, 2012.

[46] J. Han, H. Cheng, D. Xin, and X. Yan, "Frequent pattern mining: current status and future directions," *Data Mining and Knowledge Discovery*, vol. 15, no. 1, pp. 55–86, 2007.